UPPER JURASSIC TO UPPER CRETACEOUS STRATIGRAPHY AND SEDIMENTOLOGY OF THE QUEEN CHARLOTTE ISLANDS, BRITISH COLUMBIA

By

CHARLE ARTHUR GAMBA, B.Sc., M.Sc.

A Thesis

Submitted to the School of Graduate Studies

in Partial Fulfillment of the Requirements

for the Degree

Doctor of Philosophy

McMaster University

UPPER JURASSIC TO UPPER CRETACEOUS STRATIGRAPHY AND SEDIMENTOLOGY OF THE QUEEN CHARLOTTE ISLANDS, BRITISH COLUMBIA

DOCTOR OF PHILOSOPHY (1994) McMASTER UNIVERSITY

(Geology) Hamilton, Ontario

TITLE: Upper Jurassic to Upper Cretaceous Stratigraphy and Sedimentology of the Queen Charlotte Islands, British Columbia.

AUTHOR: Charle Arthur Gamba, B.Sc. (University of Toronto), M.Sc. (University of Ottawa)

SUPERVISOR: Professor R. G. Walker

NUMBER OF PAGES: 430, xxvii

ABSTRACT

The Late Jurassic to Late Cretaceous stratigraphy and sedimentology of the Queen Charlotte Islands (QCI) was studied on the outcrop scale in order to reconstruct the Late Mesozoic depositional history of the Queen Charlotte Basin. The newly defined Late Oxfordian to Tithonian White Point Formation consists of three gravelly fan delta successions up to 180 m thick. Each was deposited within a small fault bounded basin during a period of regional block faulting. The overlying Late Valanginian to Early Turonian Longarm, Haida, and Skidegate Formations were deposited within an expanded northwest-southeast trending, southwest-deepening basin. Eight depositional sequences 150 to 600 m thick and 1 to 17 Ma in duration are recognized within the three formations. The sequences consist of shallow shoreface, muddy offshore, slope and submarine fan deposits. Each sequence was deposited during a period of sea level fall and rise, and all progressively onlapped the northeastern margin of the basin over time.

The Late Turonian to Coniacian Honna Formation consists of up to 2500 m of gravelly submarine deposits. Two distinct submarine systems are recognized: a longitudinal

northwest - southeast trending braided channel complex, and transverse radial fans sourced from an uplifted and dissected magmatic arc to the east. Turbidity currents and debris flows within the channel complex flowed primarily from southeast to northwest, and were probably derived from the radial fans, one of which is preserved in the Skidegate Inlet region. The Honna is overlain by unnamed Late Coniacian to Maastrichtian volcanic and mudstone strata deposited within subaerial and muddy shelf environments respectively.

The Late Mesozoic succession exposed on the QCI accumulated within a continental forearc basin setting situated between an active magmatic arc to the northeast and a subduction zone to the southwest. Different tectonic mechanisms controlled deposition on both the small and large scale. Deposition of both the fan delta successions within the White Point Formation and the progradational shoreface successions within the Longarm and Haida Formations was influenced by local block faulting. The northwest-southeast paleocoastline trend also reflects an underlying structural control. The progressive eastward onlap of Late Oxfordian to Early Turonian strata exposed on the QCI tracked the progressive eastward migration of active magmatism within the Coast Plutonic Complex. Deposition of the Honna Formation was influenced by crustal thickening along the

northeast margin of the basin during a period of Late Cretaceous compression.

TABLE OF CONTENTS

LIST OF FIGURES

LIST OF TABLES

ACKNOWLEDGEMENTS

Logistical support for this project was provided by the Frontier Geoscience Program of the Geological Survey of Canada. I would like to thank Jim Haggart of the Cordilleran Division of the GSC both for arranging logistical support and for identifying macrofossil collections. Many of the ideas expressed in this thesis were formulated during discussions on the outcrop with Jim, with whom it was a pleasure to work.

Roger Walker patiently supervised the progress of the thesis, providing valuable insights and suggestions which are greatly appreciated. Through formal classes and informal seminars both Roger and Gerry Middleton fostered an excellent learning experience in clastic sedimentology and stratigraphy, for which I am grateful. Carolyn Eyles provided useful comments which improved the first draft of this thesis.

Jack Whorwood's amazing photographic skills and stout patience were frequently called upon during the course of my time at Mac. Thanks Jack. Imperial Oil Resources provided technical drafting services during the latter part of thesis preparation.

Then there are the host of friends one makes in the field and during ones passage through graduate school. Jarand Indelid, Jonny Hesthammer, and Susan Taite provided no end of good times on the Charlottes. Mark Hamilton provided excellent assistance and all around bonhomie in the field, not to mention a fairly respectable cup of coffee first thing in the morning. The Puterill family of Sandspit provided not only extraordinary expediting services, but also the warmth of their home on occassions too numerous to recall. Office mates Carlos Bruhn, Terry Wiseman, Richard Rouble and Bruce Ainsworth provided steadfast friendship which I shall never forget.

I would like to thank my folks Andre and Margaret Gamba for their support and for setting the example. Finally, I thank my wife Doris Chin Gamba for all of her love, support and understanding during the long drawn out course of this thesis, which included 12 months away in the field and countless late nights at the office.

CHAPTER 1. INTRODUCTION

1.1. SCIENTIFIC PROBLEM

This thesis involves a stratigraphic and sedimentological analysis of Late Jurassic to Late Cretaceous depositional systems exposed on the Queen Charlotte Islands (QCI) of western British Columbia. The position of the islands with respect to the remainder of the Canadian Cordillera provides a unique opportunity to study the Late Mesozoic evolution of subduction along the western margin of Canada. In essence, the main scientific problem addressed by this thesis concerns what the sedimentological and stratigraphic evolution of the Late Jurassic to Late Cretaceous succession exposed on the QCI can tell us about the Late Mesozoic tectonic evolution of the western Canadian Cordillera. There are currently three distinct models dealing with the evolution of the western Canadian Cordillera during this period (Yorath and Chase, 1981; Monger et al., 1982; and van der Hayden, 1989, 1992). An understanding of the Late Jurassic to Late Cretaceous evolution of depositional systems exposed on the QCI will constrain these models.

Throughout the Late Mesozoic, the QCI region was situated within a convergent margin setting. With the exception of a few other ancient examples, such as the Great Valley sequence of California, most convergent margin basins are destroyed or highly deformed during the final phases of the Wilson cycle. This makes study of the evolution of depositional systems within convergent margin basins particularly difficult. As a result, there is a distinct lack of understanding regarding the evolution of depositional systems within convergent margin basins. Instead, the majority of studies concerning the long term evolution of clastic depositional systems have involved successions deposited within tectonically less active foreland and passive margin basins. A sedimentological analysis of the Late Jurassic to Late Cretaceous succession exposed on the QCI therefore will provide some insight into the nature and evolution of depositional systems within a tectonically active convergent margin basin.

The final aim of this thesis will be to see how the Late Mesozoic stratigraphic and sedimentological evolution of the QCI region compares to other modern and ancient forearc basins.

1.2. STUDY AREA

The QCI comprise an archipelago of some 200 islands separated from the British Columbian mainland by Hecate Strait, a shallow epeiric sea (Fig. 1.1). In plan, the islands form a curved, crescent-shaped northwest-southeast oriented group approximately 150 km long and 60 km wide. Graham Island, the largest of the group, forms the northern half of the crescent, while Moresby Island, as well as the smaller Louise, Burnaby, and Kunghit Islands, form the tapering southern half of the crescent. Approximately 195 smaller islands and islets are scattered around the periphery and between these larger islands. Physiographically, the islands may be divided into three units: the Queen Charlotte Ranges, the Skidegate Plateau, and the Queen Charlotte Lowlands. The Queen Charlotte Ranges form the spine of Moresby Island, beginning at Kunghit Island in the south and ending at Rennell Sound on Graham Island in the north. The mountains of this range rise directly from the Pacific Ocean along the west coast of the islands to heights exceeding 1000 m. This sharp topography is related to the Queen Charlotte Fault, which is situated immediately off the west coast of the islands. This transcurrent fault accommodates motion between the Juan de Fuca spreading centre to the south and the Alaskan

Fig. 1.1 Location of the Queen Charlotte Islands (shaded) showing the main tectonostratigraphic elements of the Canadian Cordillera. The Queen Charlotte Islands are separated from mainland British Columbia to the east by Hecate Strait.

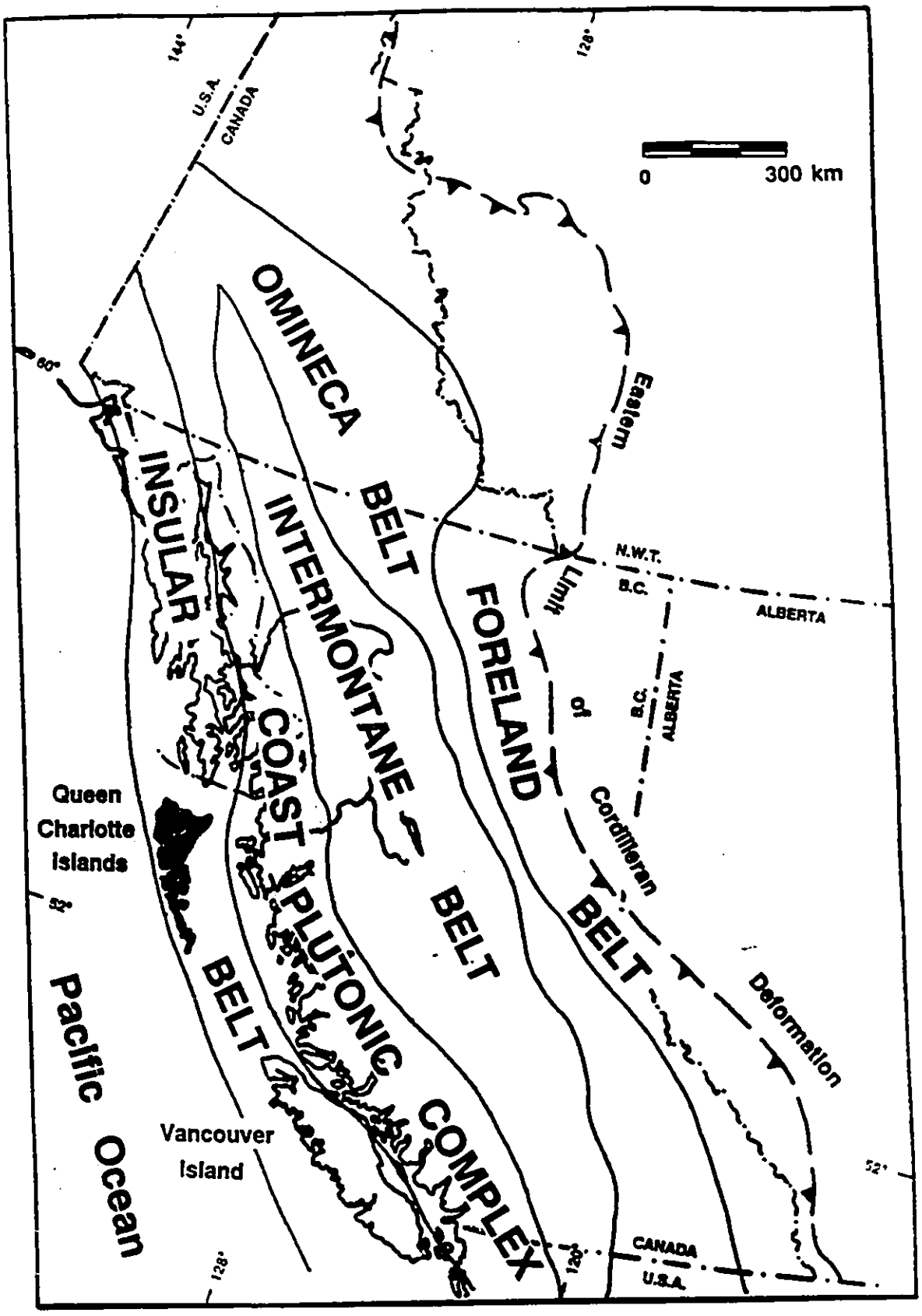
U.S.A.
CANADA
0
300 km
OMINECA BELT
INTERMONTANE BELT
FORELAND BELT
INSULAR BELT
COAST PLUTONIC COMPLEX
Eastern Limit of Cordilleran Deformation
N.W.T.
B.C.
ALBERTA
B.C.
ALBERTA
Queen Charlotte Islands
Vancouver Island
Pacific Ocean
CANADA
U.S.A.

subduction zone to the north. The fault also separates the North American and Pacific plates. To the northeast, the ranges are transitional into the Skidegate Plateau, which slopes gently to the northeast into the Queen Charlotte lowlands. The physiography of the islands, which includes hundreds of fjords, is the result of the last Pleistocene glaciation during which the islands were covered by the main Cordilleran ice sheet. The islands once boasted a luxurious west coast temperate rainforest which has been much reduced through logging activity. Untouched stands of first-growth forest do however still exist on the southern and northern tips of the archipelago.

1.3. GEOLOGICAL SETTING

The Canadian Cordilleran consists of 5 main tectonostratigraphic elements which, from west to east, include: the Insular Belt, the Coast Plutonic Complex, the Intermontane Belt, the Omineca Belt, and the Foreland Fold and Thrust Belt, marking the eastward limit of deformation (Fig. 1.1). The QCI form the northern portion of the Insular Belt, which includes all of Vancouver Island and a small sliver of the southwestern British Columbian mainland. The origin of the North American Cordillera has been the subject of considerable debate during the course of this

century. Early mobilistic views (eg. Daly, 1926) held that the Cordillera was somehow related to the westward movement of North America towards the Pacific Ocean, a process resulting in the opening of the Atlantic Ocean. Such early views were generally rejected by fixist geologists throughout the first half of the twentieth century until the recognition of large transcurrent displacements along various faults in California, Canada, and Alaska (eg. Hill and Dibble, 1953). The prospect that the northern Cordilleran was composed of allochthonous or "suspect" terranes plastered onto its western margin was first suggested by King (1958), and later substantiated by Dercourt (1970), Berg et al. (1972), and Monger et al. (1972). By the 1970's, the Mesozoic Cordillera was viewed as a mobile "Andean-type" orogen characterized by a western subductive margin and associated accretionary prism, a central magmatic arc, and an eastern fold and thrust belt. Today, the northern Cordillera is considered an "orogenic collage" (Hellwig, 1974) comprising an Andean-type orogen and numerous allochthonous terranes, all of which are overprinted by various phases of deformation and disrupted by large tangential displacements. There are currently three different models for the Mesozoic evolution of the western Canadian Cordillera. Each of these will be described in detail in chapter 6. The primary difference

between the various models involves the timing of terrane amalgamation and the timing of accretion of the amalgamated terranes to North America. Unravelling the evolution of the Late Jurassic to Late Cretaceous succession exposed on the QCI may help to determine which of the models is correct.

1.4. GEOLOGICAL HISTORY OF THE QUEEN CHARLOTTE ISLANDS

The geological history of the QCI has been recently summarized by Lewis et al. (1991) and Thompson et al. (1991). Late Paleozoic to Early Jurassic Wrangellian and Alexandrian strata on the QCI are unconformably overlain by a Middle to Late Jurassic volcanic and clastic succession. The Late Paleozoic to Early Jurassic strata were affected by regional southwest-vergent contractional deformation. Middle and Late Jurassic strata were affected by an episode of Late Jurassic block faulting. Cretaceous strata conformably overlie the Late Jurassic succession, and were affected by a second episode of Late Cretaceous regional contractional deformation. Throughout the Tertiary, the islands were affected by widespread volcanism and plutonism. Marine and nonmarine deposition within a number of extensional onshore and offshore basins coincided with this magmatic event.

1.5. LATE MESOZOIC STRATIGRAPHY OF THE QUEEN CHARLOTTE ISLANDS

Rocks exposed on the QCI range in age from Late Paleozoic to Recent, with the stratigraphic column being dominated by Early Triassic, Middle Jurassic, and Tertiary volcanics. The approximately 5000 m thick Late Jurassic to Late Cretaceous succession unconformably overlies Late Paleozoic to Middle Jurassic basement of the Wrangellia and Peninsula terranes. Late Jurassic to Late Cretaceous strata are exposed primarily within the core of the northwest-southeast trending Rennell Sound fold and fault belt which obliquely bisects northern Moresby and southern Graham Islands (Figs. 1.2 and 1.3). A secondary locus of Late Jurassic to Late Cretaceous strata is exposed on northwestern Graham and Langara Islands, separated from the main belt to the south by a wide swath of Tertiary volcanics. Scattered exposures of Late Jurassic and Early Cretaceous strata dot the small islands off the east coast of Moresby Island from Murchison Island in the north to Carpenter Bay in the south.

Late Jurassic to Late Cretaceous strata on the QCI have been affected by a period of Late Cretaceous compression and an episode of Tertiary plutonism. The Late Jurassic to Late Cretaceous stratigraphy is therefore

Fig. 1.2 Geological map of the Queen Charlotte Island region showing the distribution of the Late Jurassic to Late Cretaceous (Early Turonian) White Point Longarm, Haida, and Skidegate Formations. Based on Sutherland Brown (1968), Hesthammer and Indrelid (1991), Taite (1991), Thompson et al. (1991), and the authors own work.

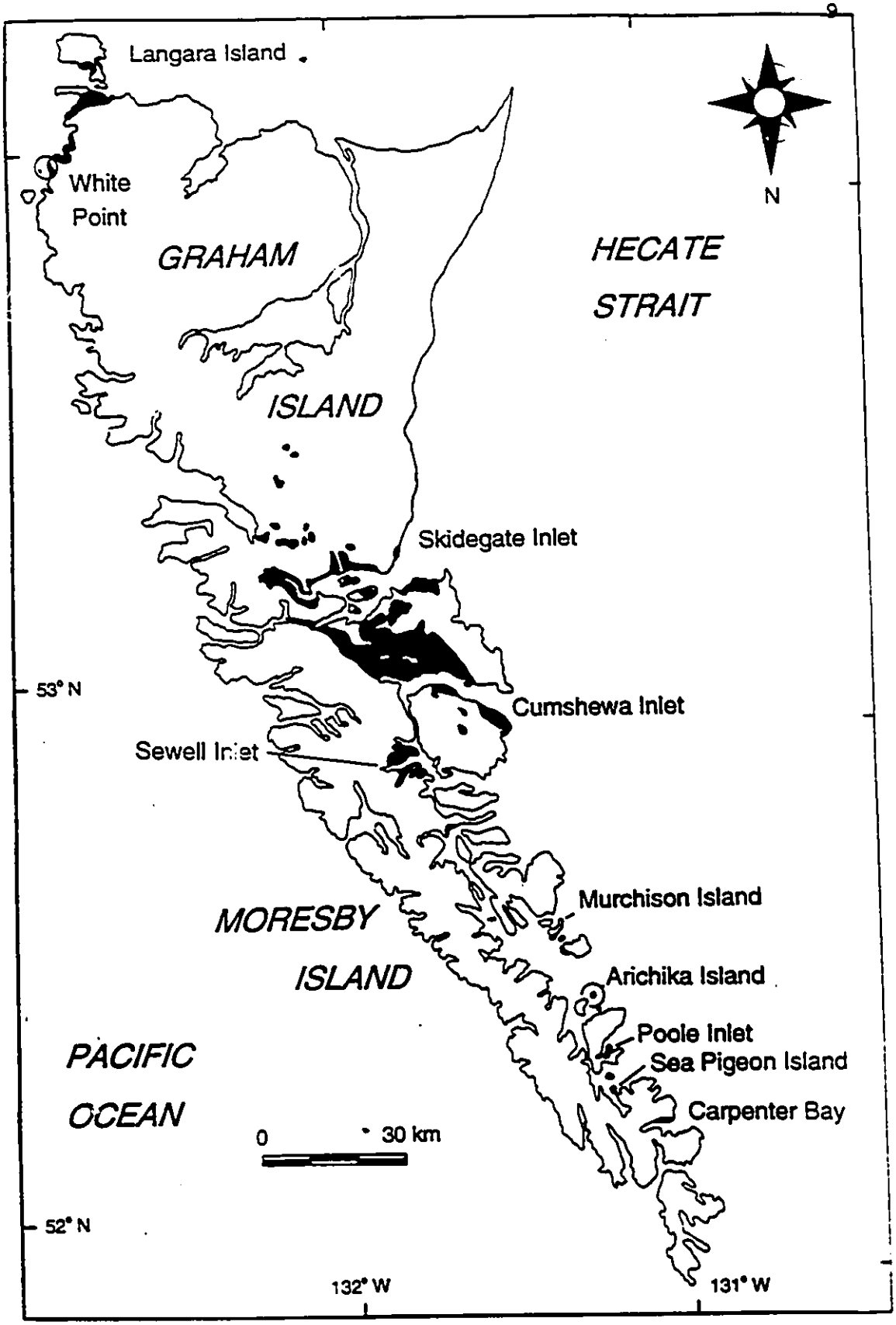
Langara Island
White Point
GRAHAM ISLAND
HECATE STRAIT
N
Skidegate Inlet
53° N
Cumshewa Inlet
Sewell Inlet
MORESBY ISLAND
Murchison Island
Arichika Island
Poole Inlet
Sea Pigeon Island
Carpenter Bay
PACIFIC OCEAN
0
30 km
52° N
132° W
131° W

Fig. 1.3 Geological map of the Queen Charlotte Island region showing the distribution of the Late Cretaceous (Late Turonian to Maastrichtian) Honna Formation and the unnamed volcanics and mudstones. Based on Sutherland Brown (1968), Hesthammer and Indrelid (1991), Taite (1991), Thompson et al. (1991), and the authors own work.

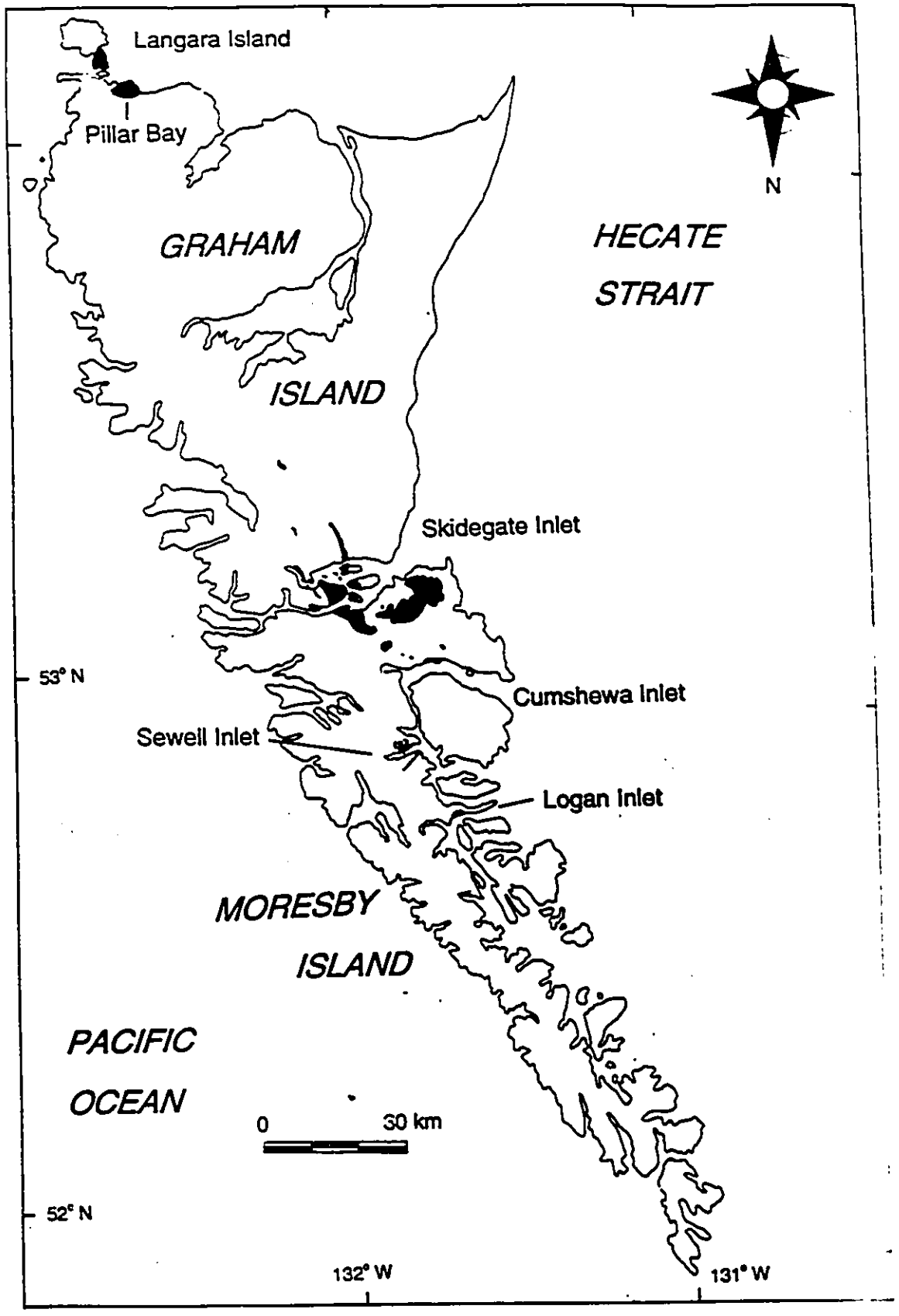
Langara Island
Pillar Bay
N
GRAHAM
ISLAND
HECATE
STRAIT
Skidegate Inlet
53° N
Cumshewa Inlet
Sewell Inlet
Logan Inlet
MORESBY
ISLAND
PACIFIC
OCEAN
0
30 km
52° N
132° W
131° W

complicated by high angle reverse and thrust faults, as well as associated folding. Strata situated close to Tertiary plutons, mainly in the southern archipelago, may also be intruded by dykes and sills.

Readers interested in the history of geological research and mineral exploration on the QCI are directed to a meticulous review by Woodsworth and Tercier (1991). In 1988, a regional 1:50 000 scale mapping project of the QCI1 was undertaken by the Frontier Geoscience Division of the Geological Survey of Canada. This Frontier Geoscience Project, still ongoing, is aimed primarily at evaluating the hydrocarbon potential of the onshore QCI and offshore Hecate Strait and Queen Charlotte Sound regions. An important outgrowth of this project is a revision of the Mesozoic and Cenozoic stratigraphy of these regions. The most up to date revision of the Late Jurassic and Cretaceous stratigraphy of the QCI are those of Thompson et al. (1991) and Haggart (1991) (Table 1.1).

Three main Late Jurassic to Late Cretaceous sedimentary packages are recognized: the Tithonian to Aptian Longarm Formation, the Albian to Coniacian Queen Charlotte Group (comprising, in ascending order, the Haida, Skidegate, and Honna Formations), and a Coniacian to Maastrichtian package of unnamed volcanic and sedimentary rocks (Thompson et al., 1991; Haggart, 1991). The Longarm Formation

Table 1.1. Late Mesozoic stratigraphy of the Queen Charlotte Islands

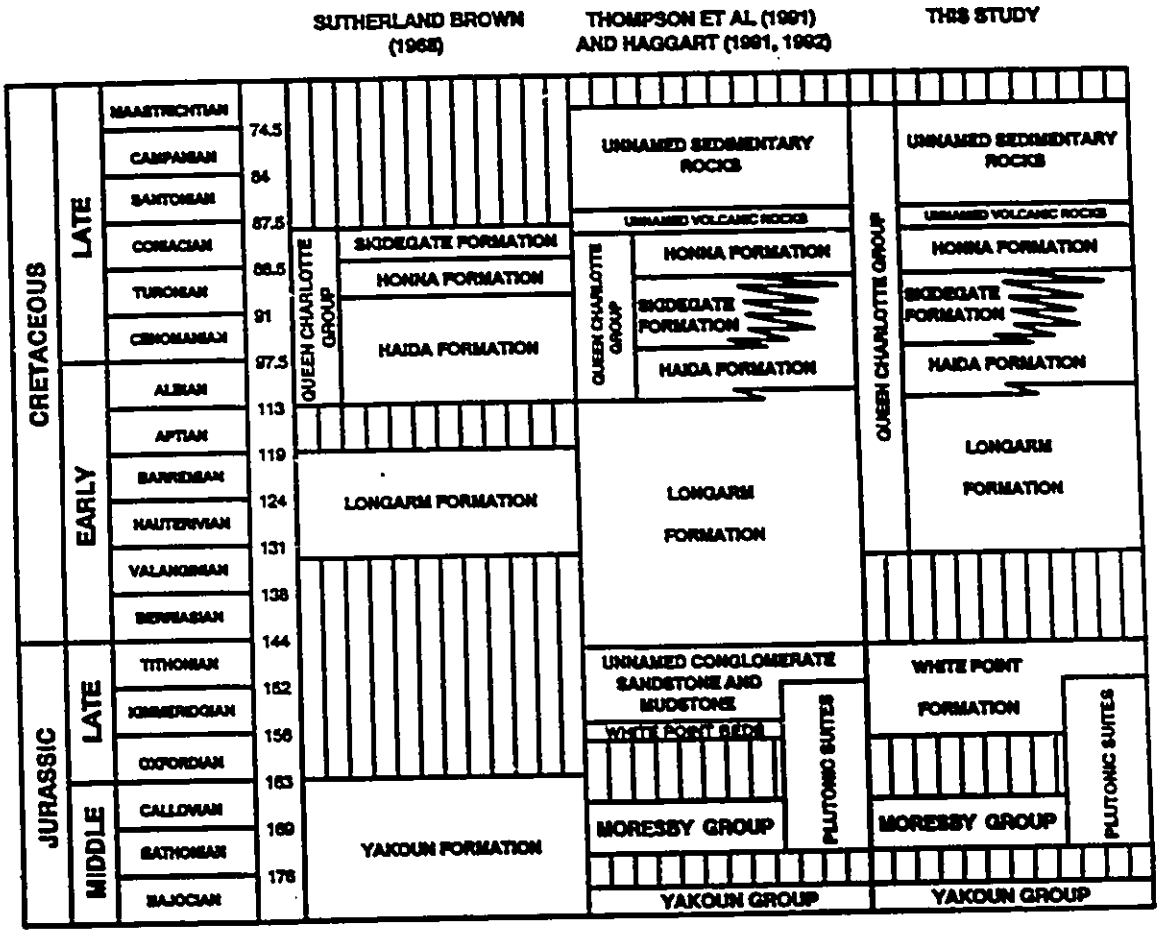

comprises a 740 m thick succession of sandstone, siltstone, mudstone, and minor conglomerate exposed in a narrow discontinous belt from northwestern Graham Island to Carpenter Bay in the southeast (Fig. 1.2). The Haida Formation comprises a 1550 m thick succession of sandstone, siltstone, and mudstone with very minor polymictic conglomerate. The Skidegate Formation comprises a 630 m thick succession of thinly bedded sandstone and mudstone. Both of these formations are exposed in a narrow discontinuous belt extening from Langara Island in the northwest to Sewell Inlet in the southeast. The Honna Formation comprises a 1600 m thick succession of polymictic conglomerate and minor interstratified mudstone and sandstone exposed in a discontinuous belt extending from Langara Island in the northwest to Logan Inlet in the southeast (Fig. 1.3). The unnamed volcanic rocks comprise a 390 m thick succession of andesite with minor interstratified sandstone exposed only in the western Skidegate Inlet region. The unnamed sedimentary rocks comprise a 45 m thick succession of mudstone exposed in the Skidegate Inlet and northwestern Graham Island regions.

Haggart (1989) expanded the Early Cretaceous Longarm Formation as originally defined by Sutherland Brown (1968) to include Tithonian strata exposed near White Point on northwestern Graham Island and probable Aptian strata

exposed near Dawson Cove in western Cumshewa Inlet. The occurrence of probable Aptian Longarm strata in Cumshewa Inlet led Haggart to suggest that the Longarm Formation was overlain conformably by Albian strata of the Haida Formation, and not unconformably as originally suggested by Sutherland Brown (1968). Haggart (1986, 1991), after McLearn (1972), assigned the Haida Formation an Early Albian to Early Turonian age. Haggart (1991), after Clapp (1914) recognized two informal members within the deposits of the Haida Formation: an Albian sandstone member and a gradationally overlying Cenomanian to Early Turonian mudstone member. The discovery of Early Turonian molluscs within the deposits of the Skidegate Formation in western Cumshewa Inlet led Haggart (1986, 1991) to suggest that the informal Haida mudstone and Skidegate Formation were partially correlative. This meant that the Skidegate Formation was considerably older than the Honna Formation, and not younger as originally suggested by Clapp (1914) and Sutherland Brown (1968).

The age of the Honna Formation is problematic due to a paucity of marine macrofossils. The few ammonites collected from the top of the Honna in western Skidegate Inlet indicate an Early Coniacian to Early Santonian age. In this area, conglomerates of the Honna Formation abruptly overlie Early Turonian deposits of the Haida and Skidegate

Formations. In Sewell Inlet and central Graham Island conglomerates at the base of the Honna are interstratified with thinly interbedded sandstones and mudstones considered part of the Skidegate Formation (Thompson and Thorkelson, 1989; Taite, 1991; Indrelid, 1991). On this basis, Haggart (1991) inferred that the Honna was conformable within the Cretaceous succession, and was of Late Turonian to Coniacian age.

In western Skidegate Inlet, sandstones of the Honna Formation are gradationally overlain by an unnamed volcanic unit comprising intermediate volcanic debris flows, massive flows, and scoria (Haggart et al., 1989). Haggart (1991) assigned a Turonian to Coniacian age to this unit based upon the relationship between the Honna and the underlying Skidegate and Haida Formations discussed above. At Pillar Bay, northwest Graham Island, and Langara Island, conglomerates of the Honna Formation are abruptly overlain by an unnamed unit of shale (Haggart and Higgs, 1989; Gamba, 1990). Haggart and Higgs (1989) recognized a similar shale unit in the Slatechuck Mountain area of western Skidegate Inlet situated stratigraphically above conglomerates of the Honna Formation. These authors assigned a Late Santonian to Early Campanian age to the shales of this unnamed unit, and suggested that they are conformably underlain by Coniacian deposits of the Honna Formation.

1.6. PREVIOUS WORK

The marine nature of the Late Jurassic to Late Cretaceous has long been inferred, based primarily upon the presence of marine macrofossils (eg. Dawson, 1889; Clapp, 1914). Only the deposits of the Honna Formation have received any serious sedimentological study (Yagishita, 1985 a and b; Higgs, 1990).

Sutherland Brown (1968) interpreted the Longarm Formation as a shallow to deep marine succession deposited within a faulted northwest-southeast trending "graben-like" trough. Yorath and Chase (1981) interpreted the Longarm formation as a nearshore to deep marine turbiditic succession deposited within a northwest-southeast trending fault-bounded "suture-type" basin. Sutherland Brown (1968) interpreted the unconformably overlying Haida Formation as a predominantly shallow marine succession deposited within a trough situated between a large island to the west and the remnants of a Middle Jurassic island arc to the east. Yagishita (1985 a and b), who undertook a petrographic examination of the Queen Charlotte Group, interpreted the Haida as a nearshore to deep marine submarine fan succession, with sediment derived from an easterly source. Fogarassy (1989) also undertook a petrographic and diagenetic study of the Queen Charlotte Group. Fogarassy

and Barnes (1991) interpreted the Haida Formation as a transgressive nonmarine to deep marine succession, and proposed that sediment was supplied to the basin from a source located to the south.

The deposits of the Honna Formation have been the object of detailed sedimentological analysis. Sutherland Brown (1968) interpreted the Honna Formation as a marine succession deposited within several small fault-bounded basins. Based upon clast imbrication measurements, Sutherland Brown (1968) inferred a western source of sediment supply. Yagishita (1985 a and b) interpreted the Honna Formation as a canyon-fed submarine fan succession. On the basis of clast imbrication and sandstone petrography, Yagishita suggested that the Honna was derived from a dissected Andean-type magmatic arc source located to the east (Fig. 1.4 a). Higgs (1988, 1990) interpreted the Honna as a deep-water fan delta succession deposited within a foreland basin setting (Fig. 1.4 b). Clast imbrication measurements confirmed the eastern provenance of the Honna, although Higgs (1990) suggested that post-depositional block rotation complicated paleogeographic reconstructions. Haggart et al. (1989) interpreted the unnamed volcanics overlying the Honna Formation in western Skidegate Inlet as a subaerial succession. Haggart and Higgs (1989) interpreted the unnamed shale unit overlying the Honna at

Fig. 1.4. Proposed depositional models for various Cretaceous Formations exposed on the Queen Charlotte Islands. a) Depositional model of Yagishita (1985 a and b) for the Haida (Cenonamian to Early Turonian) and Honna and Skidegate Formations (Late Turonian to Coniacian). b) Deep-water fan delta model for the Honna Formation proposed by Higgs (1991), c) Early to mid Cretaceous depositional model of the Queen Charlotte Group by Haggart (1991).

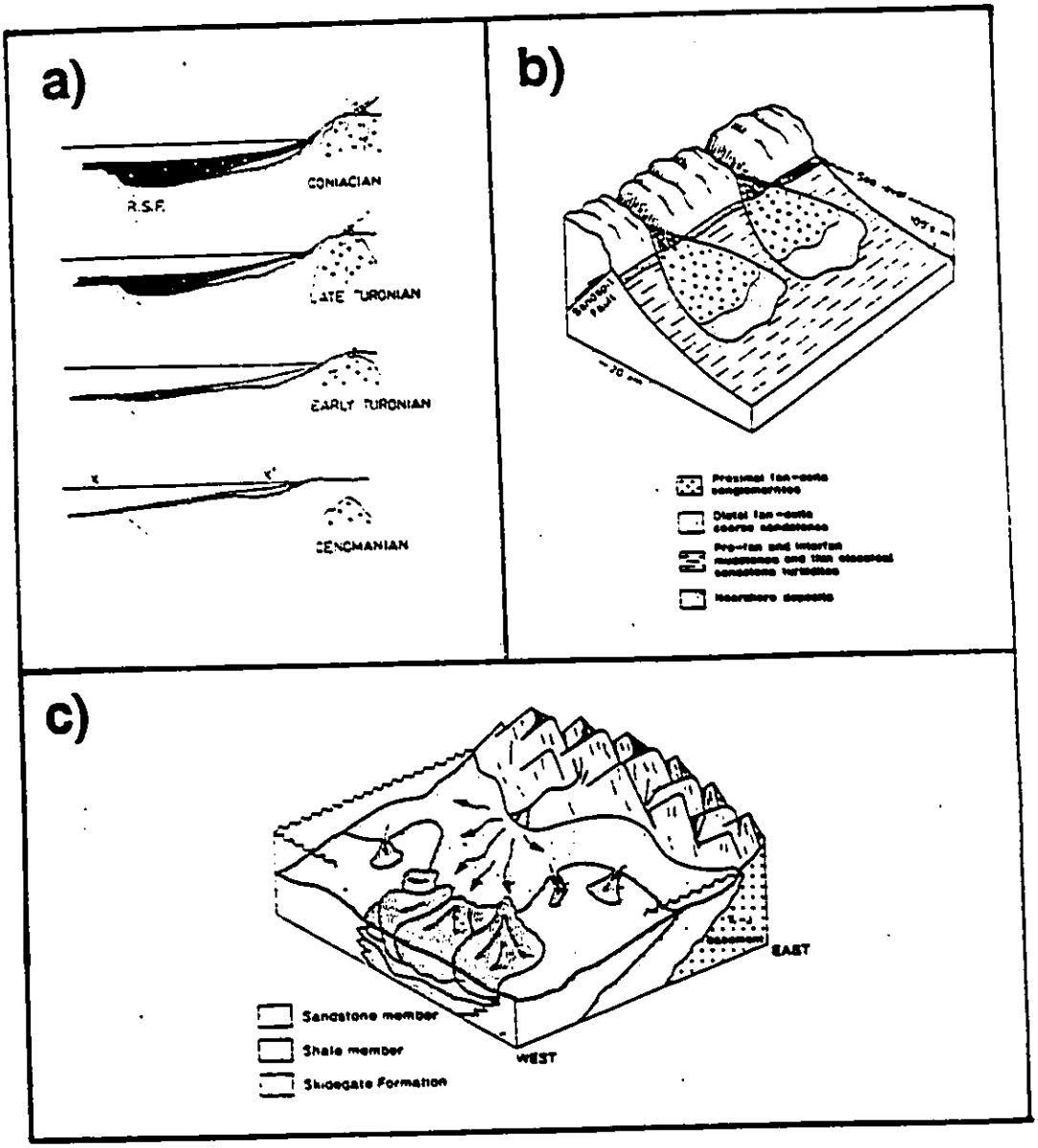
a)
CONIACIAN
R.S.F.
LATE TURONIAN
EARLY TURONIAN
CENOMANIAN
b)
Bounding Fault
Sandstone member
Shale member
Shoreface Formation
WEST
EAST

Slatechuck Mountain as a muddy outer shelf succession.

Haggart (1991) provided the latest depositional synthesis of the Late Jurassic to Late Cretaceous succession. He recognized two large scale fining-upward packages. The first comprises the Late Jurassic to mid Cretaceous Longarm, Haida, and Skidegate Formations, which Haggart (1991) suggested formed a single, uninterrupted transgressive shallow to deep marine succession deposited within a westward-deepening basin under a regime of steadily rising sea level (Fig. 1.4 c). Transgression was interrupted in Middle to Late Turonian time by a eustatic sea level fall, resulting in progradation of gravelly submarine fans of the Honna Formation into the basin from the east. The Honna and overlying unnamed shales and volcanics form the second fining-upward transgressive succession. Haggart (1991) suggested that no significant hiatus separated the transgressive successions. He concluded (Haggart, 1991: p. 253) that "the correlation of the local sea level curve for the islands with independently-produced eustatic curves is striking" and that "earlier models invoking large-scale tectonic processes for the development of the Cretaceous sequence in the islands appears unnecessary."

1.7. METHODS

Three field seasons totalling 39 weeks were spent on the islands during the summers of 1989, 1990, and 1991. During the 1989 season, all exposures of Late Jurassic to Late Cretaceous strata mapped by Sutherland Brown (1968) and various other members of the Geological Survey of Canada during the course of the Frontier Geoscience Project were visited. During the 1989 - 1991 field seasons, 122 sections varying between 30 and 1600 m thick were logged. These included exposures mapped by Sutherland Brown (1968), other members of the Geological Survey of Canada, and new sections discovered during the course of mapping by the author. Coastal exposures were the most suitable for logging due to the density of rainforest cover, however quarries blasted by the logging industry did provide some suitable sections inland. Coastal exposures were accessed by a combination of zodiac inflatable, fixed-wing aircraft, and helicopter, while inland exposures were accessed by truck. Late Jurassic to Late Cretaceous strata have a pronounced structural dip generally not exceeding 90°. These strata may also be faulted, particularly within the core of the Rennell Sound fold and fault belt. Displacement is generally minimal, with beds being easily traced across small faults in outcrop. In the southern archipelago, Late

Jurassic to Early Cretaceous strata may be extensively intruded by a variety of Tertiary dikes and sills. Exposures which were pervasively faulted and/or intruded were not logged.

The logging procedure involved the measurement and description of facies in a vertical and lateral context. Fossil and lithological samples collected from the sections were tied into the logs. All paleocurrent measurements were subsequently rotated to correct for structural tilts in excess of 25 degrees. Macro and microfossil samples collected by the author were submitted to J. Haggart of the Geological Survey of Canada in Vancouver. Molluscan samples were dated by J. Haggart in a number of fossil reports, while any, nannofossil, and radiolarian samples were dated by various consultants. Geochron samples collected from the Honna Formation were dated by R. Parrish at the U - Pb Geochron Lab of the Geological Survey of Canada in Ottawa. Photographs of trace fossils were submitted for identification to J. MacEachern at the University of Alberta.

1.8. PLAN OF THESIS

In Chapter 2, the Late Jurassic to Late Cretaceous stratigraphy of the QCI is formally revised. This revision

facilitates a logical and coherent sedimentological analysis of this succession. Chapters 3, 4 and 5 concern the sedimentology of the White Point Formation, Longarm - Haida - Skidegate Formations, and the Honna Formation respectively. In Chapter 6, the depositional history of the Late Jurassic to Late Cretaceous succession will be synthesized and compared to the various models proposed for the Late Mesozoic evolution of the Canadian Cordilleran. The results and conclusions of the thesis are stated in Chapter 7.

CHAPTER 2. REVISION OF LATE MESOZOIC STRATIGRAPHY

2.1. CHAPTER SUMMARY

A new formal stratigraphic unit, the White Point Formation, is introduced for a succession of Late Oxfordian to Tithonian conglomeratic and mudstone strata exposed on northwestern Graham Island. Based upon new biostratigraphic evidence, Late Valanginian to Aptian strata of the Longarm Formation are incorporated into the Queen Charlotte Group. Based upon lithostratigraphic relations, unnamed Late Coniacian/Santonian to Maastrichtian successions of volcanic and sedimentary rocks are also incorported into the Queen Charlotte Group. The newly defined Queen Charlotte Group therefore comprises a lithologically diverse suite of Late Valanginian to Maastrichtian strata which are unconformably underlain by the newly defined Late Jurassic White Point Formation and unconformably overlain by unnamed nonmarine Tertiary volcanic and clastic strata.

2.2. INTRODUCTION

Based upon field work conducted by the author during

the 1989 through 1991 field seasons (Gamba et al., 1990; Haggart and Gamba, 1990; Gamba, 1991, 1992, 1993), as well as recent and current work by Haggart (1986, 1989, 1991, 1992, 1993), enough data now exists to attempt a formal revision of the Late Jurassic to Late Cretaceous stratigraphy of the Queen Charlotte Islands (QCI).

Proposed revisions to the Late Jurassic to Late Cretaceous stratigraphic schemes recently advanced by Thompson et al. (1991) and Haggart (1992) include: 1) recognition of a new formal stratigraphic unit, the White Point Formation, for a succession of Late Oxfordian to Tithonian conglomeratic and mudstone strata, 2) incorporation of the Late Valanginian to Aptian Longarm Formation into the Queen Charlotte Group (QCG), and 3) incorporation of the Late Coniacian to Maastrichtian unnamed volcanic and sedimentary rocks into the QCG (Table 1.1).

2.3. LATE JURASSIC WHITE POINT FORMATION

The newly defined White Point Formation comprises a 300 m thick succession of conglomerate and mudstone strata exposed to the south of White Point on northwest Graham Island (Fig. 2.1). The largest exposure of this formation occurs upon a wide tidal bench located 1 to 2.2 km south of White Point in the vicinity of Otter Creek. Conglomeratic

Fig. 2.1 Geological map of the Klaht Islet - Otter Creek area of northwest Graham Island showing the distribution of the White Point Formation (based on mapping by the author).

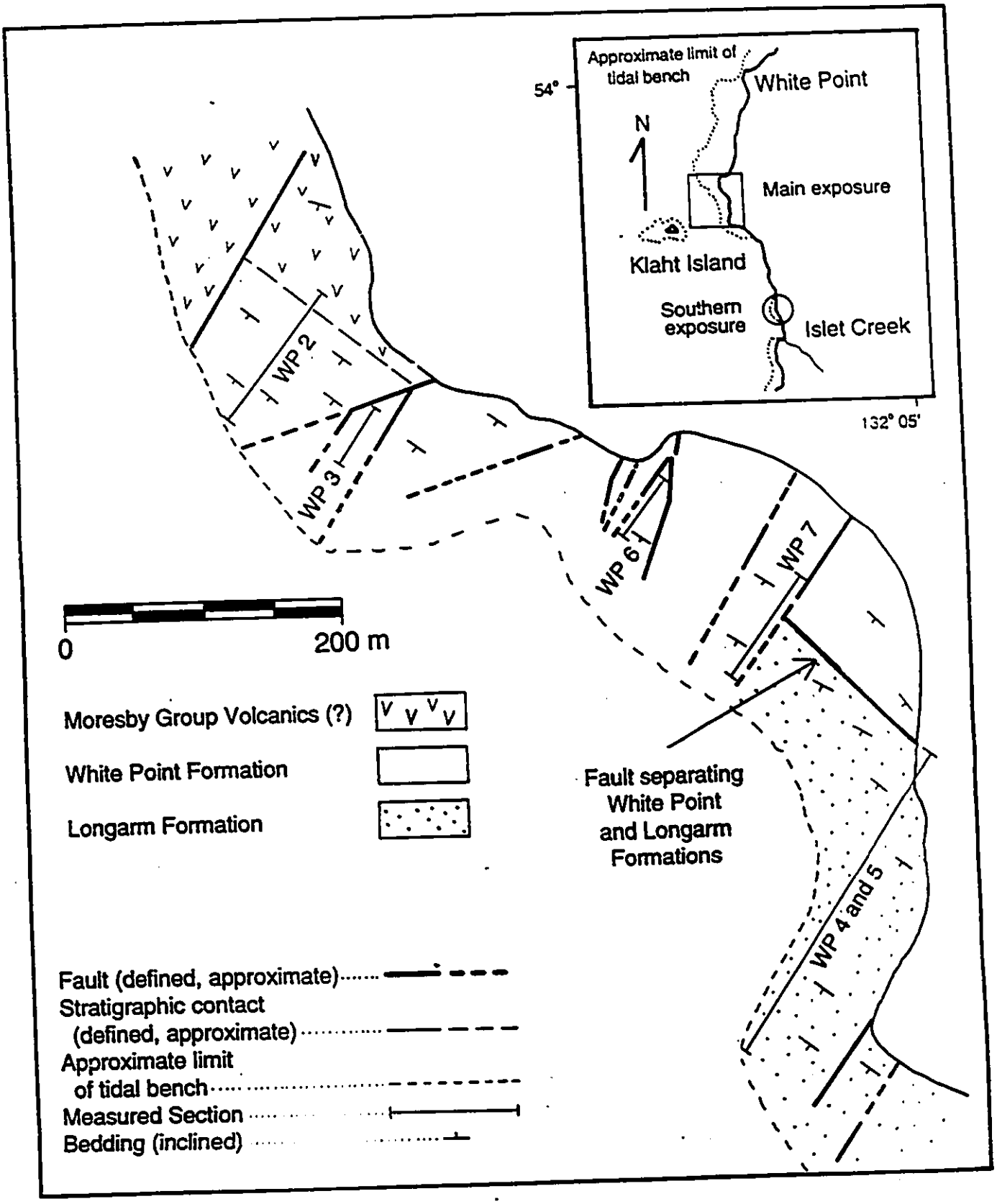
Approximate limit of tidal bench
White Point
54°
N
Main exposure
Klaht Island
Southern exposure
Islet Creek
132° 05'
WP 2
WP 3
WP 6
WP 7
WP 4 and 5
0
200 m
Moresby Group Volcanics (?)
White Point Formation
Longarm Formation
Fault separating White Point and Longarm Formations
Fault (defined, approximate)
Stratigraphic contact (defined, approximate)
Approximate limit of tidal bench
Measured Section
Bedding (inclined)

strata are also exposed on Klaht Islet, situated approximately 500 m offshore to the west of the main coastal exposure. Two small exposures of conglomerate and mudstone also occur along the coast approximately 1 km south of the main exposure and 300 m north of Islet Creek. Strata within the northernmost exposure dip steeply to the west-southwest, and are cut by numerous steeply dipping normal faults. Most of the larger faults trend northeast-southwest at approximately 040°. These faults are cut at almost right angles by a second set of faults trending northwest-southeast at approximately 300°. Strata may be easily traced across individual faults, with displacement generally not exceeding 100 m.

Despite the structural complexity of the main coastal exposure, a 300 m thick composite section composed of poorly sorted polymictic conglomerate and lesser interstratified mudstone can be constructed. The section is separated from underlying andesitic basement by a 14 m covered interval. The age of the volcanic basement is poorly constrained, although Haggart (1992) suggested a Late Jurassic age. The andesites exposed at this location may therefore be equivalent to andesites of the Late Jurassic Moresby Group exposed to the south in the Skidegate Inlet region. Jeletzky (in Sutherland Brown, 1968) and Jeletsky (1984) assigned a Late Jurassic (Tithonian) age to the

conglomeratic strata exposed on Klaht Islet. These strata are correlative with the lower part of the conglomeratic succession exposed on the mainland (Gamba, 1991, 1993). Haggart (1992) assigned a revised Late Oxfordian to Tithonian age to these same conglomerates based on new macrofossils collected from both the mainland and Klaht Islet exposures. The Late Jurassic strata exposed on the mainland south of White Point are overlain by Late Valanginian to Hauterivian strata of the Longarm Formation (Haggart, 1989; Gamba, 1991). Haggart (1989, 1992) suggested that the contact between the Late Jurassic strata and the Longarm strata was gradational, and that both represented a continuous section spanning the Jurassic - Cretaceous boundary. This implies that transitional Berriasian and Early Valanginian strata should occur at this location. Detailed mapping of Late Jurassic and Early Cretaceous strata exposed at this location by Gamba (1991, 1993) however revealed that strata of the Late Jurassic succession are separated from strata of the overlying Longarm Formation by a prominent southeast-northwest (121° - 301°) trending fault (Fig. 2.1). This fault cuts out the upper part of the underlying Late Jurassic succession, superimposing Late Valanginian Longarm strata directly upon the Late Jurassic strata. In addition, no Berriasian to Early Valanginian faunas have been reported from these or

any other strata exposed on the QCI. The faulted relationship exposed at this location, coupled with the absence of linking Berriasian to Early Valanginian strata here and elsewhere on the QCI, indicates that the Late Jurassic and Early Cretaceous strata are separated by an unconformity marked by a significant temporal hiatus (Table 1.1).

The distinctive lithology and well defined lower and upper boundaries of the Late Jurassic strata favour its elevation to formational status. The lithology of the succession is certainly mappable on a regional extent, thereby fulfilling one of the main criteria of a formation. The faulted and unconformable relationship with strata of the overlying Late Valanginian Longarm Formation does not lend support to Haggart's (1989, 1991, 1992) suggestion that the Late Jurassic strata be considered an earlier phase of Longarm deposition.

The Late Jurassic strata exposed south of White Point, northwest Graham Island, as well as the Late Jurassic strata exposed on Klaht Islet, are therefore formally assigned to the newly erected White Point Formation. The succession exposed on the wide tidal bench in the vicinity of Otter Creek on the coast of northwest Graham Island south of White Point serves as the type section of this formation (Fig. 2.1). The White Point Formation therefore comprises

300 m of Late Oxfordian to Tithonian polymictic conglomerate and mudstone strata. The formation is underlain, with uncertain stratigraphic relation, by Late Jurassic andesites of the Moresby Group (?), and is unconformably overlain by Late Valanginian to Hauterivian strata of the Longarm Formation (Table 1.1).

2.4. THE QUEEN CHARLOTTE GROUP

The Queen Charlotte Group (QCG), as formally defined by Clapp (1914) and recently modified by Thompson et al. (1991) and Haggart (1991, 1992), is expanded to include both the Late Valanginian to Aptian Longarm Formation and the unnamed Coniacian to Maastrichtian volcanic and sedimentary rocks (Table 1.1).

2.4.1. Longarm Formation

Sutherland Brown (1968) suggested that Late Valanginian to Barremian strata of the Longarm Formation were separated from Albian strata of the overlying Haida Formation by an unconformity. This interpretation was based upon a biostratigraphic argument, because the actual contact between the two formations was not observed. Accordingly, Sutherland Brown (1968) excluded the Longarm Formation from the QCG (Table 1.1). Haggart (1989) suggested that the

uppermost strata of the Longarm Formation exposed in western Skidegate Inlet may contain Early Aptian ammonites. Haggart (1991) recovered the Aptian ammonites Shastoceras sp., Lytoceras (Gabbioceras) sp., Shasticrioceras sp., and Tropaeum sp. from upper Longarm strata exposed in Dawson Cove, western Cumshewa Inlet. The presence of Aptian strata within the Longarm Formation in both western Skidegate and western Cumshewa Inlets (Haggart and Gamba, 1990; Haggart, 1991, 1992) suggests that no lengthy temporal hiatus separates the two formations (Table 1.1). Haggart (1991) furthermore suggested that Aptian Longarm strata exposed in Dawson Cove, western Cumshewa Inlet, are conformable and gradational into Early Albian strata of the Haida Formation exposed to the east.

In terms of lithofacies and vertical facies succession, strata of the Longarm and Haida Formations are very similar. This will be obvious when the sedimentology of these two formations is described in chapter 4. This has traditionally made differentiation of the two formations in the field difficult, particularly in the absence of marine macrofossils (see Haggart et al., 1991).

Two factors support the inclusion of the Longarm Formation into the QCG. These are 1) the absence of a prominent nonconformity marking a significant hiatus between Aptian and Albian strata of the Longarm and Haida

Formations, and 2) the remarkable lithological similarity of the two formations.

2.2.2. Stratigraphy of the Longarm, Haida, and Skidegate Formations

The Longarm, Haida, and Skidegate Formations are composed of a 2000 m thick package of sandstones, mudstones, and minor conglomerates (Sutherland Brown, 1968). The sandstones and mudstones form thick successions which are interstratified with one another. Strata of the Longarm are Late Valanginian to Aptian in age, while the conformably overlying strata of the Haida and Skidegate Formations are Albian to Early Turonian in age. Strata of the three formations are exposed within a discontinuous belt extending from Langara Island in the northwest to Carpenter Bay in the southwest (Fig. 1.2). In general, the deposits of the Longarm and Skidegate Formations are exposed within the southwest part of this belt, while the deposits of the Haida Formation are exposed mainly within the northeast part of the belt. No post Aptian age strata of the Haida, Skidegate, or Honna Formations are observed south of Logan Inlet on Moresby Island. Strata of the Longarm Formation are not observed north of White Point on northwestern Graham Island.

The three formations can be divided into a number of

sequences (sensu Vail et al., 1977 and Posamentier et al. 1988), each separated by erosional surfaces of regional significance. A detailed description of the internal stratigraphy of these three formations will be presented in Chapter 4. Early Turonian strata of the Haida and Skidegate Formation are abruptly though conformably overlain by Late Turonian strata of the Honna Formation.

2.2.3. Unnamed volcanic and sedimentary rocks

At Gust Island in western Skidegate Inlet, sandstone and conglomeratic strata of the Honna Formation are conformably overlain by massive mafic flows of an unnamed volcanic unit (see Haggart et al. 1989). Haggart (1991, 1992) suggested that strata of the volcanic unit be included within the Honna Formation, although Thompson et al. (1991) excluded the strata from the Honna Formation and the QCG in general. The distinct lithology of the unnamed volcanics, which may be mapped on a regional basis, favours elevating the unit to formational status. In order to keep the formal Late Cretaceous stratigraphy of the QCI as simple as possible however, such a formal revision will not be undertaken in this study.

Santonian to Maastrichtian strata of an unnamed sedimentary unit exposed both in the western Skidegate Inlet area (Haggart and Higgs, 1990) and in eastern Pillar Bay

(Gamba, 1991) are separated from conglomeratic strata of the Honna Formation by covered intervals. At Pillar Bay, the covered interval is 62 m wide (see Fig. 10 of Gamba, 1991). The shale strata at this location are concordant with underlying conglomeratic strata of the Honna Formation, thus suggesting a conformable contact. Furthermore, two 40 and 120 m thick mudstone units of similar lithology to the unnamed shale unit are interstratified lower down within the 1600 m thick succession of Honna Formation exposed at Pillar Bay (see Fig. 10 of Gamba, 1991). Based partly upon this interstratification and the concordant relationship between strata of the Honna Formation and the unnamed shales at Pillar Bay, the unnamed sedimentary unit is incorporated into the QCG.

In order to facilitate a sedimentological analysis, the Late Jurassic to Late Cretaceous stratigraphy exposed on the QCI is divided into three packages: the Late Jurassic White Point Formation; the Early to mid Cretaceous Longarm, Haida, and Skidegate Formations, and the Late Cretaceous Honna Formation and unnamed units. The sedimentology of the Late Jurassic White Point Formation will be addressed in Chapter 3. The stratigraphy and sedimentology of the Longarm, Haida, and Skidegate Formations will be addressed in Chapter 4. The sedimentology of the Honna Formation and the unnamed units will be addressed in Chapter 5.

CHAPTER 3. SEDIMENTOLOGY OF THE LATE JURASSIC WHITE POINT FORMATION

3.1. CHAPTER SUMMARY

Three gravelly fan delta successions, each up to 180 m thick, occur within the newly defined Late Jurassic White Point Formation. The sequences are separated from one another by erosional surfaces which separate finer-grained deposits below from conglomerates above. The lower part of each sequence consists of poorly sorted boulder to pebble conglomerates deposited by high density turbidity currents and debris flows within a marine slope environment situated above storm wave base (less than 200 m water depth). Paleocurrent measurements from clast imbrication indicate that the flows originated from a source to the east. Clast size decreases from boulders at the base to cobbles and pebbles at the top of the sequences. The gravelly slope deposits are abruptly overlain by either high energy sandy shoreface or storm dominated muddy offshore deposits. The sandy shoreface deposits of one sequence are overlain by gravelly distributary channel deposits, indicating that the sequence is progradational.

The White Point Formation was deposited within a small fault bounded basin during a period of Late Jurassic regional block faulting. Each sequence was deposited in response to an episode of block faulting which led to rapid basin subsidence. Shallow marine gravelly fan delta systems prograded westwards into the basin away from the uplifted margins. The large scale fining-upward trend within each sequence reflects the gradual erosional decrease in the relief of uplifted basin margin over time.

3.2. STRATIGRAPHY OF THE WHITE POINT FORMATION

Strata of the White Point Formation exposed on the tidal bench are cut by a series of southwest - northeast and southeast - northwest trending high-angle faults (Haggart, 1989; Hickson and Lewis, 1990). Displacement across the faults is generally quite small, so that despite the structural complexity, a 300 m thick composite section can be reconstructed (Fig. 3.1). Two other sections exposed on Klaht Island were also measured (Fig. 3.2). Three sequences (1, 2 and 3), are recognized within the main succession exposed on Graham Island (Fig. 3.1). Each exhibits an abrupt scoured basal contact overlain by poorly sorted boulder conglomerates. Sequence 1 is 180 m thick and overlies Middle to Late Jurassic andesites of the Moresby

Fig. 3.1 Composite stratigraphic section of the White Point Formation exposed along the tidal bench on northwestern Graham Island. Location of measured sections (WP 2, 3, 6, and 7) used to build the composite are illustrated in Fig. 2.1.

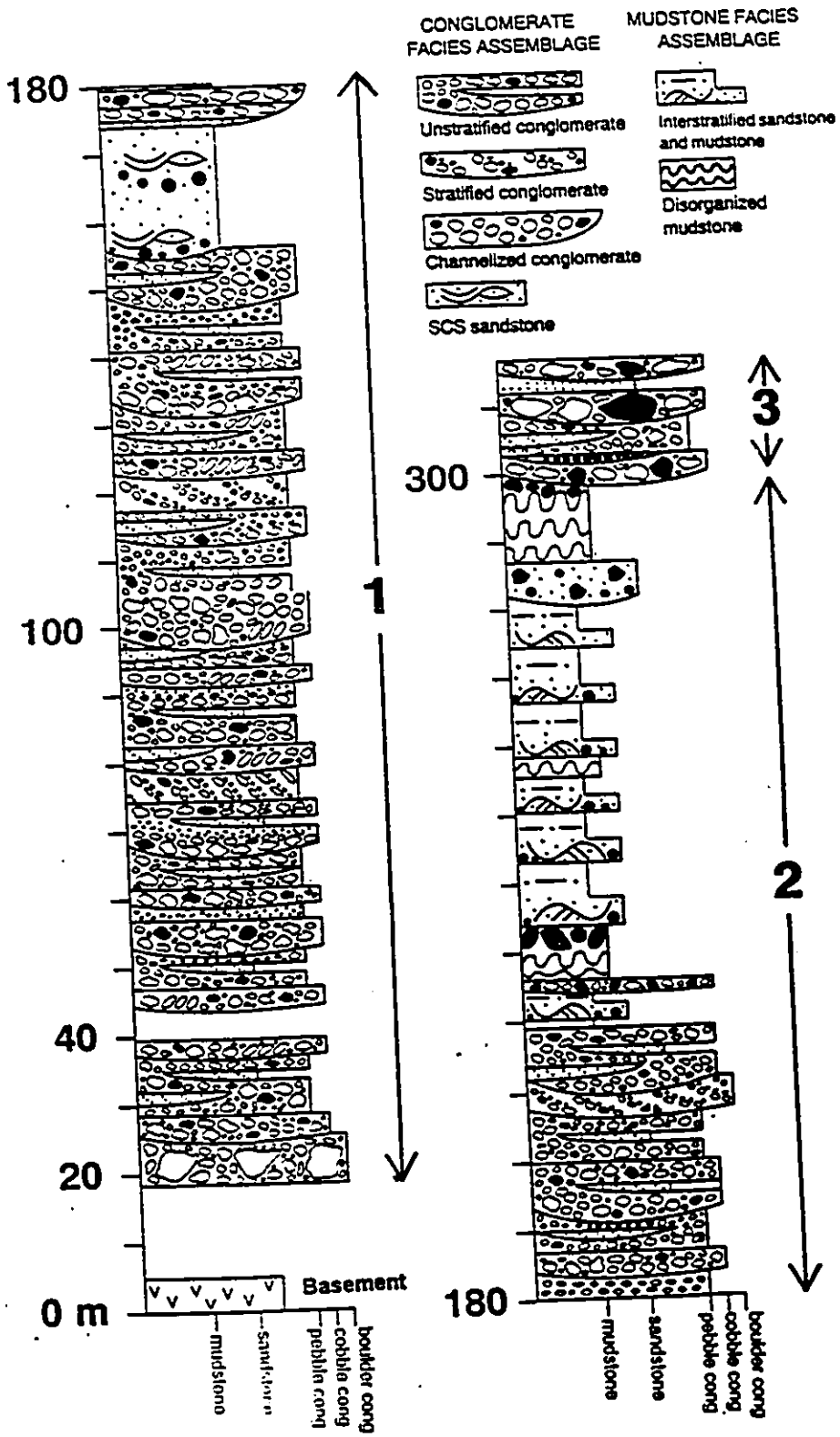
CONGLOMERATE FACIES ASSEMBLAGE
MUDSTONE FACIES ASSEMBLAGE
Unstratified conglomerate
Stratified conglomerate
Channelized conglomerate
SCS sandstone
Interstratified sandstone and mudstone
Disorganized mudstone
180
100
40
20
0 m
300
180
1
2
3
Basement
mudstone
sandstone
pebble cong
cobble cong
boulder cong

Fig. 3.2 Measured sections from Klaht Island a) near top and b) near middle of sequence 1.

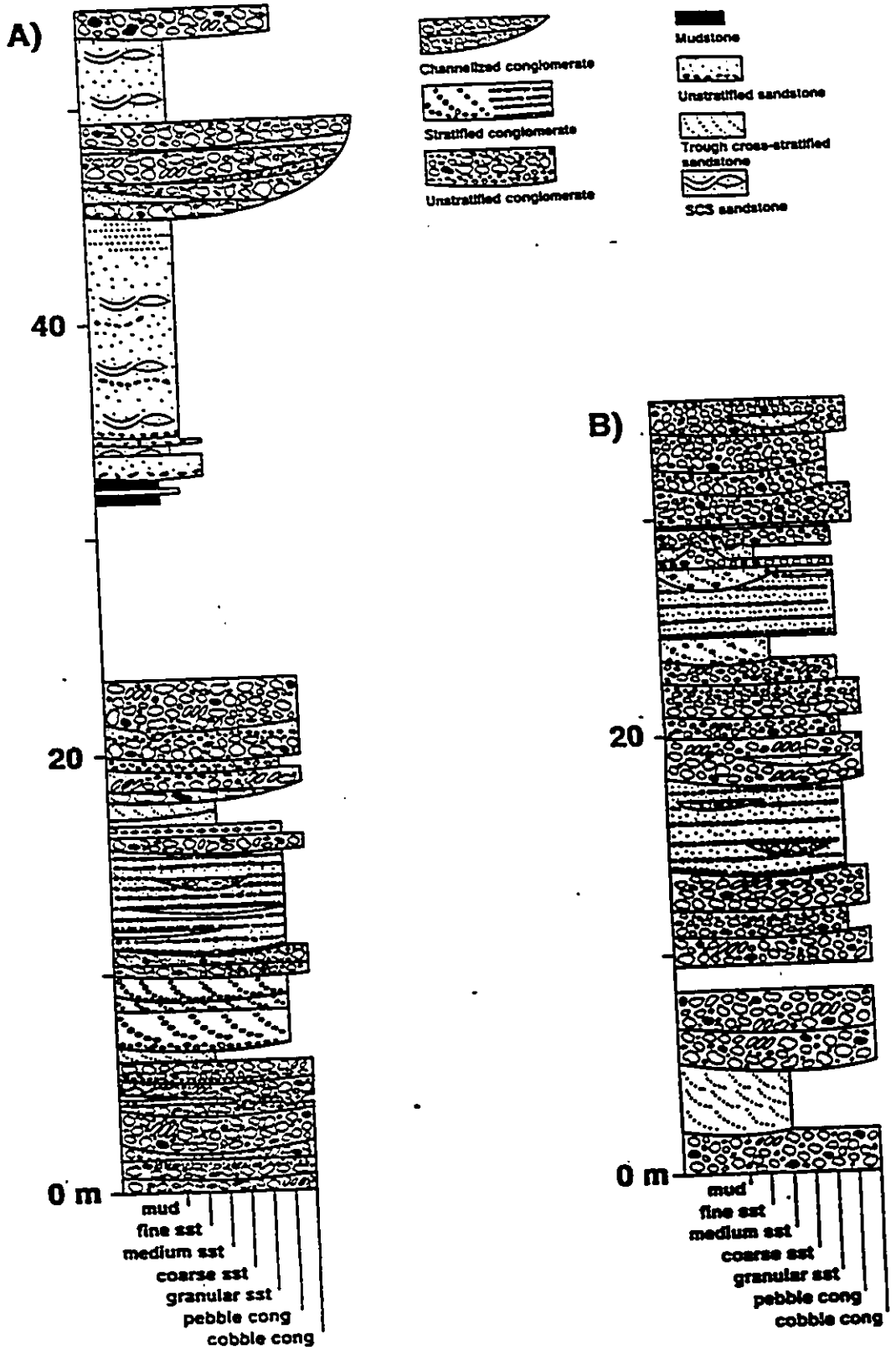
A)
40
20
0 m
mud
fine sst
medium sst
coarse sst
granular sst
pebble cong
cobble cong
Channelized conglomerate
Stratified conglomerate
Unstratified conglomerate
Mudstone
Unstratified sandstone
Trough cross-stratified sandstone
SCS sandstone
B)
20
0 m
mud
fine sst
medium sst
coarse sst
granular sst
pebble cong
cobble cong

Group. The lower part of the sequence consists primarily of conglomerates, while the upper part consists primarily of sandstones. Sections A and B exposed on Klaht Island (Fig. 3.2 a and b) are correlative with sequence 1 exposed on the mainland, as they are both located in proximity to underlying andesites of the Moresby Group.

Sequence 2 is 120 m thick and abruptly overlies the sandstones of sequence 1. The lower 40 m of the sequence consists of conglomerate, while the overlying 80 m of the sequence consists primarily of mudstone. The deposits of sequence 3 abruptly overlie those of sequence 2 on the mainland, and consist of 16 m of conglomerate.

3.3. FACIES DESCRIPTIONS AND INTERPRETATIONS

3.3.1. Unstratified conglomerate facies

Description

This facies is composed of massive and graded poorly sorted pebble to boulder conglomerate. The massive conglomerates predominate, and are clast-supported, poorly sorted, unstratified, and ungraded (Fig. 3.3 a). The massive beds are between 0.2 and 2.7 m thick, and exhibit deeply scoured basal contacts (Fig. 3.3 b). Clasts exhibit a disorganized fabric, and no preferred orientation.

The graded conglomerates are clast-supported, poorly

Fig. 3.3 a) Amalgamated beds of the unstratified massive conglomerate facies with minor interbedded sandstone. Stick 1.4 m.

b) Bed of the massive conglomerate facies. Note the massive texture and relief along the basal contact to left of stick. The conglomerate is overlain by a bed of trough cross-stratified sandstone, with forsets dipping to left. Stick 1.4 m.

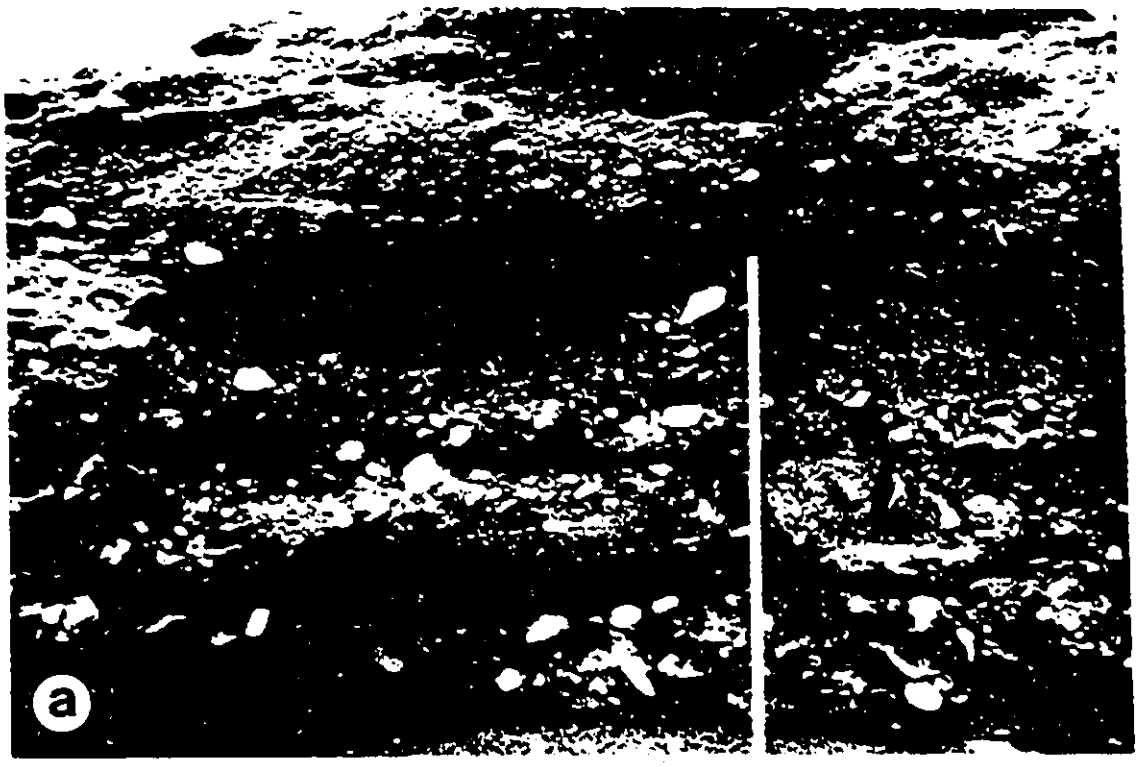
a

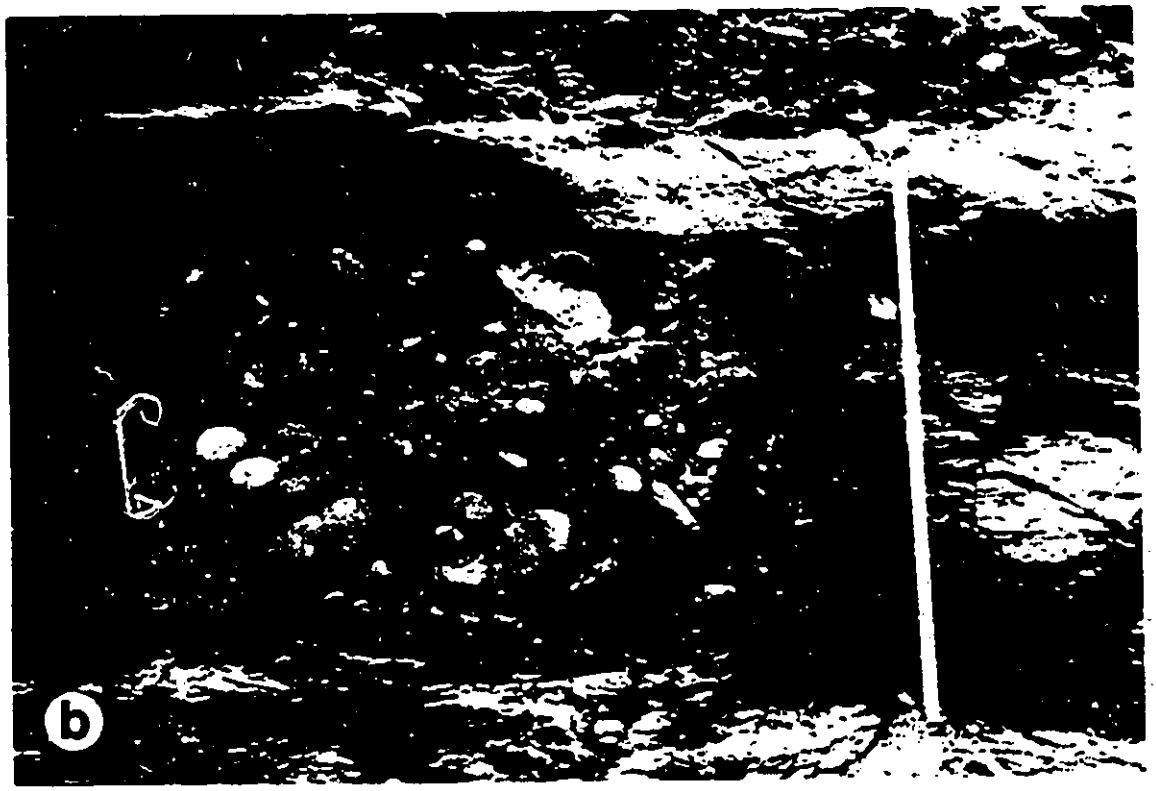
b

to moderately well sorted, unstratified, and exhibit normal or inverse to normal grading (Fig. 3.4 a). Graded beds are between 0.1 and 3.0 m thick, and exhibit planar to scoured basal contacts. Some conglomerates grade normally into poorly sorted fine to medium grained massive pebbly sandstone. Clasts exhibit a well developed a(p) a(i) fabric (Fig. 3.4 b).

Both massive and graded conglomerates contain a poorly sorted sandstone matrix. Abundant Buchia bivalves and belemnite fragments occur within the matrix of both types of conglomerate and within the interstratified sandstones (Fig. 3.5). Contacts between beds of conglomerate are often difficult to discern, particularly in the absence of interstratified sandstone or where the clasts within adjacent beds are of similar size. Clasts are composed primarily of olive green andesite, identical in composition to the underlying Late Jurassic Moresby Group. Less abundant lithologies include black argillite and grey limestone clasts derived from the Late Triassic - Early Jurassic Kunga Group and minor granodioritic clasts derived from the Late Jurassic Moresby Group. Calcareous mudstone intraclasts also form a significant component of some conglomerate beds. Extraformational clasts are well rounded to subangular, while intraformational clasts are subangular to angular. Angular boulders of olive green andesite up to

Fig. 3.4 a) Inverse to normally graded bed of the unstratified graded conglomerate facies. The conglomerate is abruptly overlain by a thin bed of trough cross-stratified medium-grained sandstone.

b) Close up of the graded conglomerate facies. Note the poor sorting and the well developed a(p) a(i) clast fabric. Paleoflow from right to left.

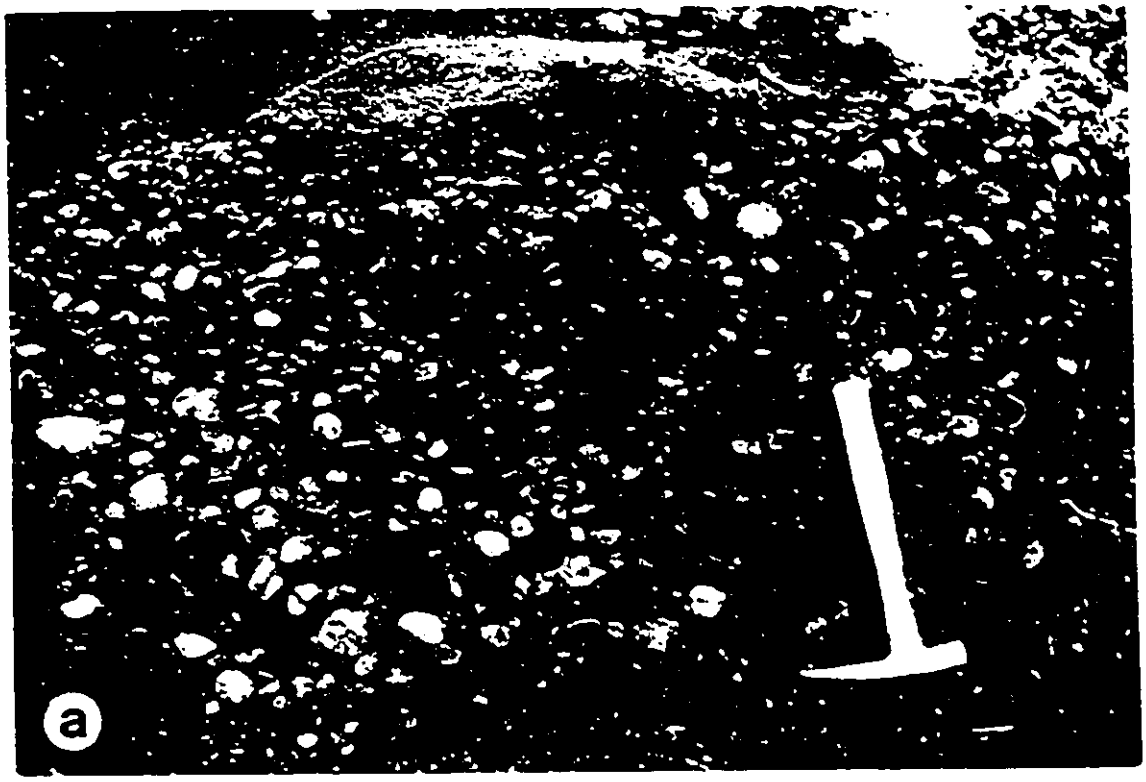
a

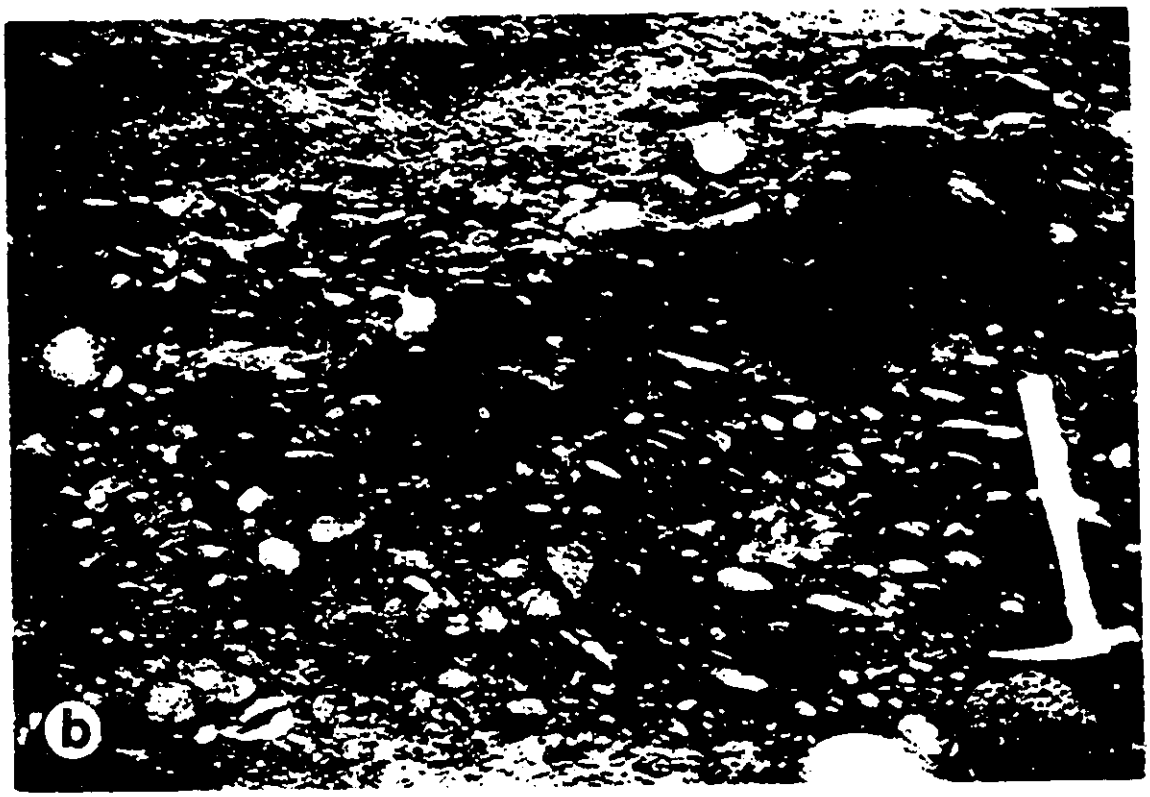
b

Fig. 3.5 Typical bed of massive sandstone interstratified with beds of the conglomerate facies. This particular bed contains abundant bivalve fragments that appear to define a poorly developed inverse to normal grading within the bed. Note the large articulate bivalve immediately to left of hammer. Note also the bivalve fragments (arrows) within the sandy matrix of the underlying bed of massive pebble conglomerate.

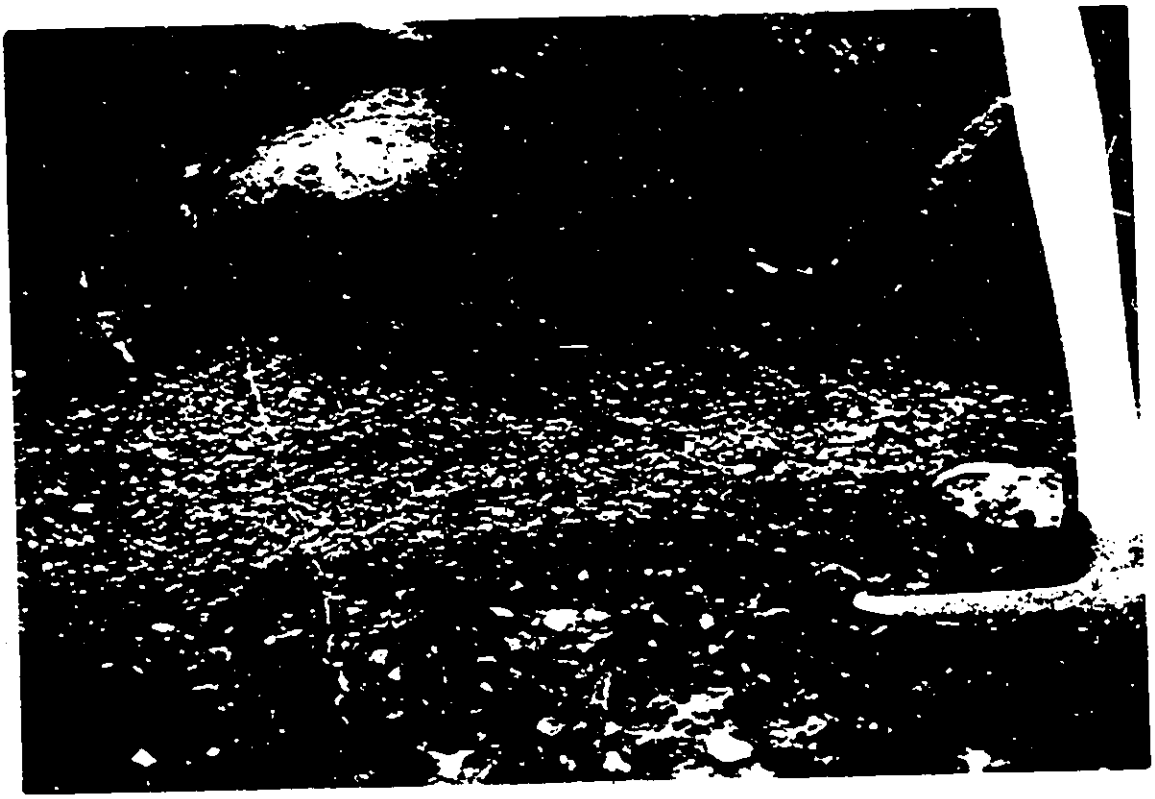

2.7 m in diameter occur within the conglomerates at the base of sequence 1 (Fig. 3.6), while large angular sandstone intraclasts up to 3.4 m in diameter occur within the conglomerates at the base of sequence 3 (Fig. 3.1). A large 4.0 by 2.5 m angular block of calcareous mudstone encased in amalgamated beds of unstratified conglomerate occurs within sequence 1 exposed on Klaht Island (Fig. 3.7). Imbricate clasts within several different beds of this facies dip towards the north-northwest and south-south-east, implying flow generally towards the west (Fig. 3.8).

Lenticular beds of pebbly sandstone between 0.1 and 3.0 m thick are interstratified with the conglomerates of this facies (Figs. 3.2, 3.3 b, 3.5, and 3.7). The sandstones are fine to medium grained and, in order of decreasing abundance, are structureless and normally graded, hummocky cross-stratified, wave rippled, and trough cross-stratified. A single 0.2 m thick lenticular bed of calcareous mudstone was observed interstratified with the conglomerate near the top of sequence 1 exposed on Klaht Island (Fig. 3.2 b).

Interpretation

The graded and massive conglomerates are interpreted as the deposits of gravelly high density turbidity currents and subaqueous debris flows respectively. The occurrence of

Fig. 3.6 Angular boulder of andesite within massive conglomerates near the base of sequence 1 exposed on northwestern Graham Island. Bedding within the conglomerate dips towards the left.

Fig. 3.7 Recessively weathering boulder of calcareous mudstone (arrow) surrounded by beds of the unstratified conglomerate facies within the lower part of sequence 1 exposed on Klaht Island (section B). The boulder is approximately 2.5 by 3 m in size. Bedding within the surrounding conglomerates dips gently towards upper right. Note squatting biostratigrapher (lower right) desperately looking for ammonites with which to date section and dispel sedimentological model.

Fig. 3.8 Rose diagram illustrating inferred paleoflow direction derived from imbricated clasts within 14 different beds of unstratified conglomerate in sequence 1. Each petal represents an average obtained from the measurement of 25 clast per bed. Rose petals are equal area.

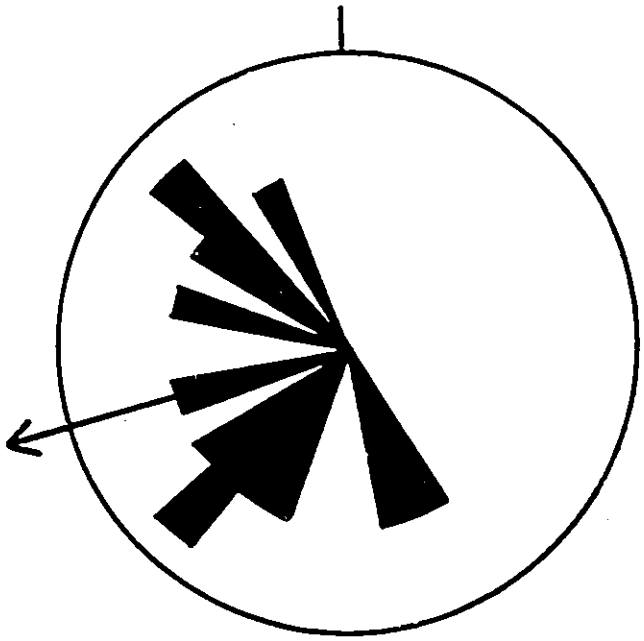

$\bar{x} = 256°$

N = 14

bivalve fragments within the conglomerates and interstratified sandstones clearly indicates that the conglomerates were deposited within a marine environment. The normal grading within beds of the graded conglomerate reflects deposition from decelerating gravelly high density turbidity currents, where successively smaller clasts were deposited directly from suspension (Walker, 1975 a and b, 1977; Lowe, 1982). The a(p) a(i) clast fabric indicates that clasts were deposited directly from turbulent suspension without rolling on the bed (Walker, 1975 a, 1975 b). The inverse grading at the base of some of the beds reflects the freezing of a concentrated traction carpet at the base of the turbidity current. Clasts within the carpet are supported primarily by dispersive grain pressure, where larger clasts are buoyed towards the top. Deposition occurs instantly when the velocity of the turbidity current drops below that necessary to maintain the dispersive pressure in the traction carpet (Walker, 1975 a, 1975 b; Lowe, 1982), resulting in an inversely graded texture.

The disorganized clast fabric and lack of grading within beds of the massive conglomerate indicates that they were emplaced by subaqueous debris flows. In true cohesive debris flows, clasts are supported above the bed by the cohesiveness of a sediment-water matrix (Middleton and Hampton 1973, 1976; Lowe, 1976, 1982). Deposition occurs en

masse when the shear strength of the matrix exceeds the shear stress imposed on the flow, with the resulting deposit typically exhibiting a matrix-supported framework (Lowe, 1976, 1982). However, in some debris flows, clasts may remain in contact with one another while the flow is proceeding downslope, with the resulting deposit typically exhibiting a clast-supported framework (Lowe, 1982).

The interstratified structureless and normally graded sandstones resemble the Ta division of Bouma (1962), and are interpreted as the deposits of sandy turbidity currents. Some of these beds were subsequently reworked into HCS or wave ripples by storm generated oscillatory currents. The trough cross-stratified sandstones represent the deposits of three dimensional dunes formed by unidirectional tractional currents. The hummocky cross-stratified and wave rippled sandstone beds interstratified with the conglomerates indicates that this facies was deposited within an environment situated between storm and fairweather wave base (< 200 m water depth; Dott and Bourgeois, 1982; Walker et al. 1983; Walker, 1985; Duke, 1985).

3.3.2. Stratified conglomerates

Description

This facies is much less common than the previous facies, and consists of horizontally- to low angle-

stratified and trough cross-stratified pebble to cobble conglomerate and pebbly sandstone. The horizontally- to low angle-stratified pebble and cobble conglomerates form tabular, sharp-based beds 1.5 to 5.6 m thick (Fig. 3.9 a). Strata within the bed are 0.1 to 0.3 m thick, clast-supported, moderately well sorted, and are normally or inverse to normally graded. Adjacent strata vary greatly in clast size and shape sorting, and clasts may exhibit a poorly developed a(t) b(i) fabric. Fragments of bivalve shells are scattered throughout the matrix of some beds.

The trough cross-stratified facies consists of clast-supported conglomerate or pebbly sandstone, forming sharp based sets 0.4 and 1.7 m thick (Fig. 3.9 b). Cross-stratification is defined by alternating layers of conglomerate and pebbly sandstone comprising differing grain sizes. Sets are generally solitary, although they may be grouped into cosets up to 3.5 m thick.

Interpretation

The presence of bivalve fragments within beds of this facies is indicative of deposition within a marine environment. The grading within the horizontal to low angle- stratified conglomerates reflects deposition from high density turbidity currents. The inverse to normal grading reflects frictional freezing of a concentrated

Fig. 3.9 a) Beds of the horizontally- to low angle cross-stratified conglomerate facies within sequence 1. Note the well sorted nature of the conglomerate. Stick approximately 1 m long.

b) End on view of trough cross-stratified pebbly sandstone bed (T). The cross-stratified set of pebbly sandstone is overlain by a bed of horizontally-stratified (H) pebble conglomerate.


a

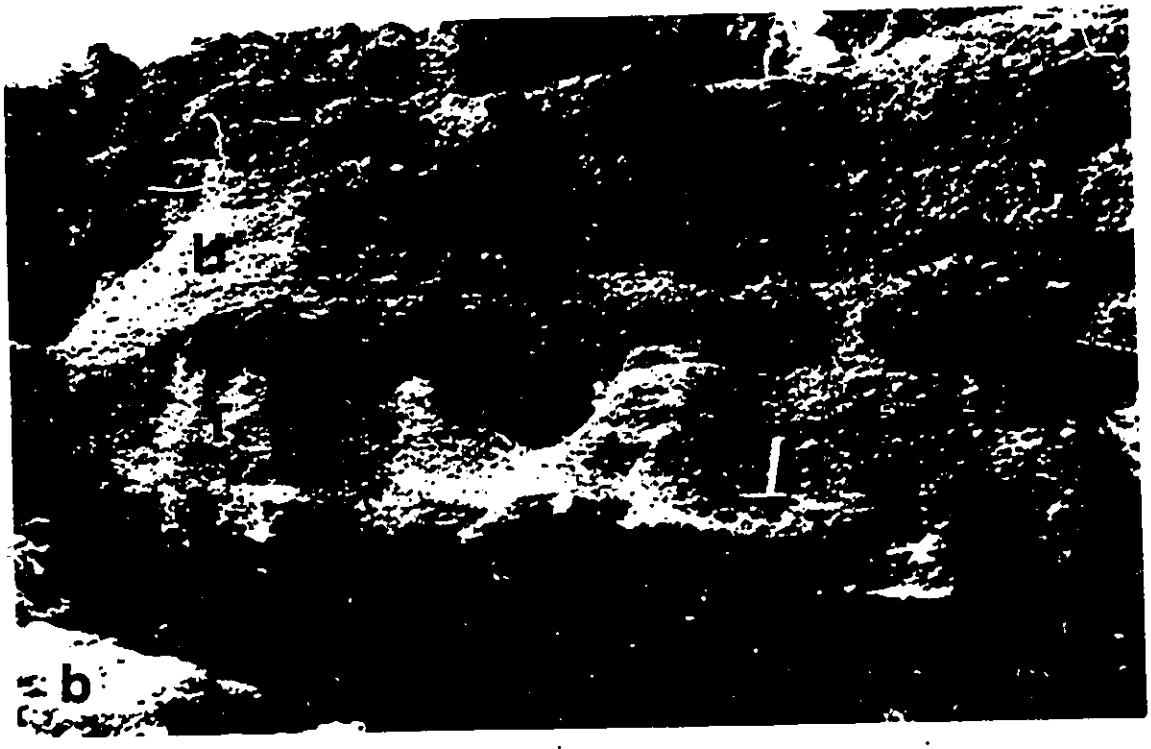
b

traction carpet followed by the deposition of gravel directly from suspension as the turbidity current decelerated (Walker, 1975 a, 1977; Lowe, 1982). The weakly developed a(t) b(i) clast fabric indicates that clasts rolled along the bed in traction prior to deposition (Rust, 1968; Walker, 1975 a). The low angle inclined nature of stratification within some of the conglomerate beds suggests that gravel was emplaced upon an inclined slope or perhaps upon the flank of a large barform. The trough cross-stratified conglomerates and pebbly sandstones represent gravelly three dimensional dunes deposited under the influence of unidirectional currents. The association of the trough cross-stratified conglomerates with beds of unstratified conglomerate suggests that they too were deposited by gravelly high density turbidity currents.

3.3.3. Swaley cross-stratified sandstone facies

Description

These deposits abruptly cap the conglomerates forming the lower part of sequence 1, and consist primarily of 5 to 18 m of well sorted fine to medium grained swaley cross-stratified (SCS) sandstone. The sandstones exhibit broad intersecting sets of concave-up (swaley) laminae interstratified with sets of subparallel undulating laminae and minor sets of convex-up (hummocky) laminae (Fig. 3.10).

Fig. 3.10 Bed of well sorted fine to medium grained swaley cross-stratified sandstone. Note the low angle concave-up swales (arrow) near the base and middle of the bed.

Fig. 3.11 Bed of the channelized conglomerate facies deeply incised into swaley cross-stratified sandstone (SCS) near the top of sequence 1 exposed at section A on Klaht Island. Relief along channel margin is approximately 2 m in this photo. Note the poorly sorted nature of the conglomerate infilling the channel, and the cross-stratified sandstones near the top of the frame.

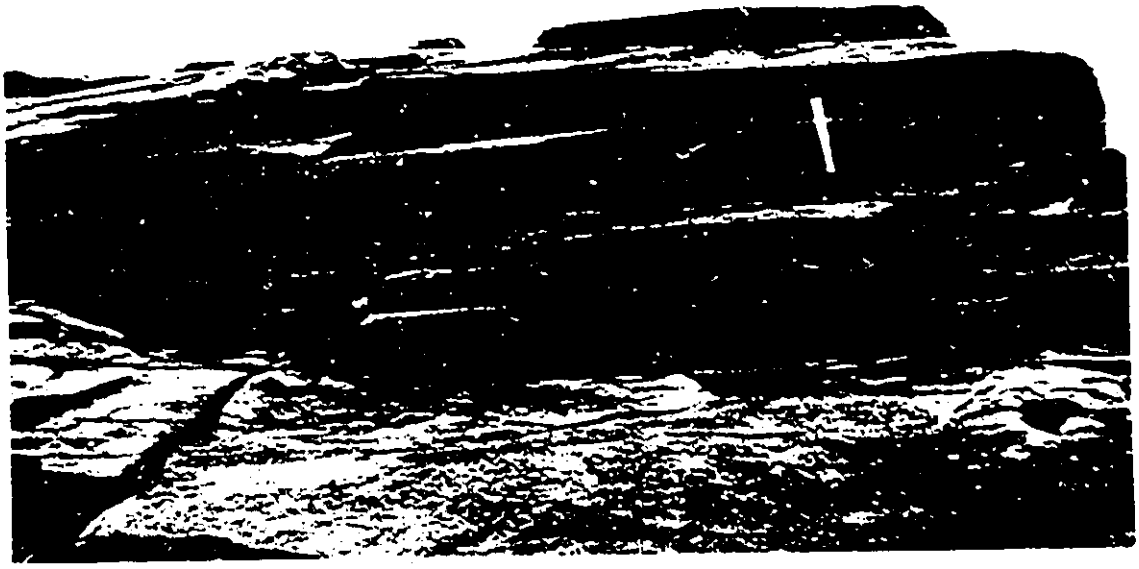

In good three dimensional exposure, the swaley laminae dip and intersect at very low angles regardless of orientation. The base of some SCS sandstone beds exhibit thin intraclast lags. Minor lenticular beds of mudstone and siltstone are interstratified with the SCS sandstones.

On Klaht Island, 5 m of SCS sandstones abruptly overlie 2.4 m of thinly interstratified fine grained sandstone and mudstone (Fig. 3.2 a). Sandstone beds within this unit are wave-rippled or massive. Interstratified near the top of the same SCS sandstones is a 0.2 m thick bed of well sorted fine grained horizontally- to low angle planar-stratified sandstone.

Interpretation

SCS is believed to be formed by oscillatory currents within a high energy wave dominated shoreface environment (Leckie and Walker, 1982; Walker, 1985; Rosenthal and Walker, 1987). The symmetrically rippled sandstones interstratified with the mudstones near the base of the SCS sandstone succession exposed on Klaht Island were deposited by oscillatory, wave generated currents. The interstratified mudstones represent background deposition from hemipelagic suspension. The interstratified sandstones and mudstones were therefore probably deposited within an offshore environment situated between storm and fairweather

environment. The horizontally- to low angle planar-stratified nature of the sandstone bed near the top of the SCS succession is typical of beach lamination, which is inclined gently seawards (Reineck and Singh, 1980). The coarsening-upward sandstone succession capping sequence 1 on Klaht Island therefore represents the progradation of a wave dominated shoreface into a muddy transitional offshore environment.

3.3.4. Channelized conglomerate facies

Description

This facies consists of clast-supported conglomerates which infill broad channels incised into the SCS sandstones near the top of sequence 1 exposed on Graham Island (Fig. 3.1) and upon Klaht Island (Figs. 3.2 a and 3.11). The channel on Klaht Island exhibits a maximum depth of 4.7 m and a minimum width of 45 m. The axis of the channel exposed on Klaht Island trends approximately 060-240°, while the other channel, exposed half a kilometre to the northeast on Graham Island, trends approximately 082-262°.

The channels are infilled with amalgamated beds of massive (i.e. unstratified and ungraded) pebble to boulder conglomerate and sandstone (Fig. 3.11). The conglomerates are very poorly sorted and contain a poorly sorted sandstone matrix. Beds exhibit scoured basal contacts and are 0.3 to

1.0 m thick. Pebble and cobble clasts within the conglomerates exhibit a weakly developed a(t) b(i) imbricate fabric. Bivalve fragments and other marine macrofossils are lacking within the conglomerates and sandstones of this facies.

The massive conglomerates are interstratified with medium grained trough cross-stratified pebbly sandstones (Fig. 3.11). Sets are solitary and between 0.3 and 0.6 m thick. Beds of poorly sorted matrix-supported intraclast breccia are also interstratified with the conglomerates infilling the channels. The breccias reach a maximum thickness of 1.4 m near the channel margins and pinch out towards the channel axis.

Interpretation

The channel fill nature of these conglomerates and the association of this facies with the swaley cross-stratified sandstone facies into which it is incised indicates deposition within a coastal distributary environment. The very poorly sorted texture and weakly developed a(t) b(i) fabric of these conglomerates are indicative of rapid deposition from unidirectional tractional currents. The massive conglomerates are similar in character to those deposited as channel lags or longitudinal bars within gravelly braided fluvial systems

(Nemec and Steel, 1984).

The trough cross-stratified pebbly sandstones represent the deposits of three dimensional dunes which migrated along the channel floor under the influence of unidirectional currents. The matrix-supported nature of the intraclast breccias indicates that the clasts were supported by the buoyancy and cohesiveness of a mud-water matrix. The debris flows were probably generated by slumping of the oversteepened channel margins. Deposition of the beds occurred en masse when the shear strength of the matrix exceeded the shear stress of the flow (Middleton and Hampton, 1976; Lowe, 1979, 1982). The complex nature of the channel fill indicates that the channels do not represent a simple cut and fill structure related to a single erosional/depositional event.

3.3.5. Interstratified sandstone and mudstone facies

Description

This facies forms most of the upper part of sequence 2 and consists of sandstone and bioturbated sandy mudstone (Fig. 3.12 a). Sandstone beds are sharp based and tabular, and are, in order of decreasing abundance; hummocky cross-stratified (HCS), wave-rippled, parallel-laminated, massive, or normally graded. A typical HCS sandstone bed is 0.1 to 0.8 m thick and exhibits a thin intraclast pebble breccia

Fig. 3.12 a) Interstratified sandstone and mudstone facies. This photo shows several sharp based beds of hummocky cross-stratified fine grained sandstone (H) gradationally overlain by beds of sandy mudstone (M).

b) A typical bed of hummocky cross-stratified sandstone. The bed exhibits an abrupt scoured basal contact overlain by coarse grained massive sandstone which is abruptly overlain by a thin unit of hummocky cross-stratified sandstone. The bed is capped by a bed of wave rippled sandstone. Irregular white dots on photo are barnacles. Scale 9 cm long.

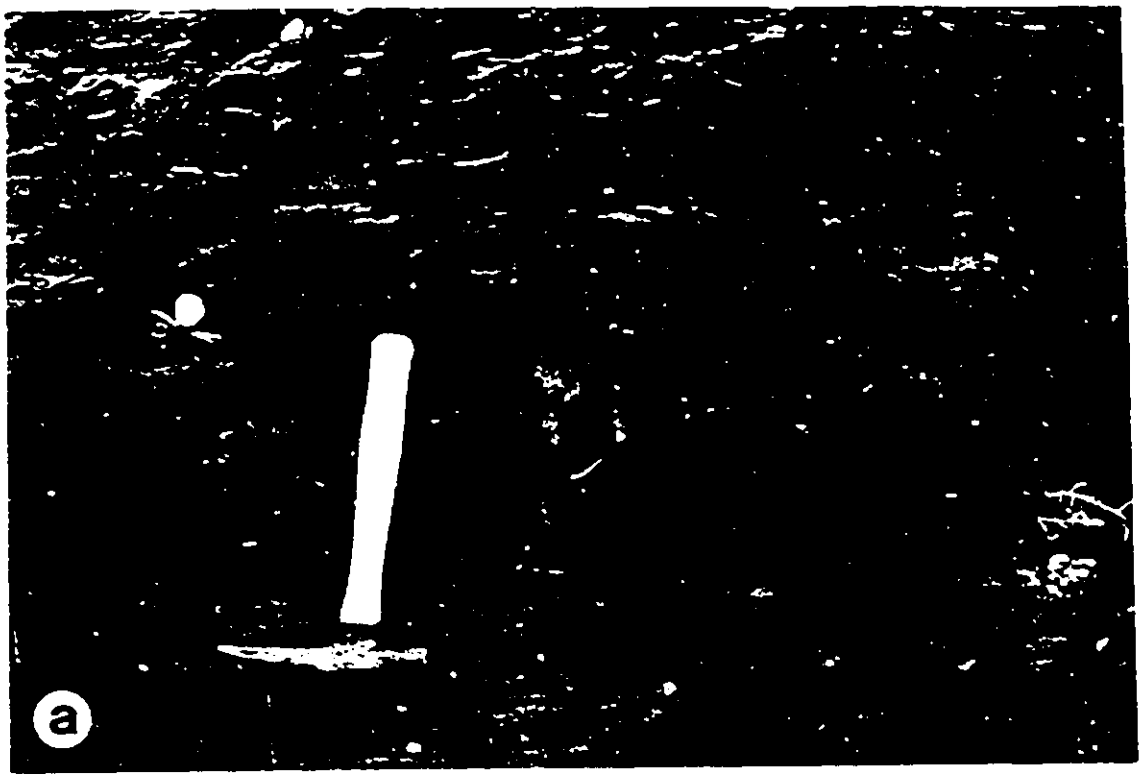
a


b

lag one clast to 0.1 m thick. The lag may be overlain by a thin bed of massive to horizontally-laminated medium to coarse grained sandstone, which in turn is overlain by HCS sandstone. The HCS sandstone within some beds grade into wave rippled fine grained sandstone (Fig. 3.12 b).

The unstratified sandstone beds are 0.2 and 5.6 m thick and exhibit a scoured basal contact overlain by angular pebble to cobble intraclasts forming a clast-supported breccia lag up to 0.45 m thick. The lag grades into unstratified, poorly sorted medium grained sandstone which may exhibit normal grading. The sandstones are interstratified with beds of bioturbated sandy mudstone 0.8 to 4 m thick (Fig. 3.12 a). Within the sandy mudstones there are thin (<3 cm) fine to very fine grained sandstones that are either mottled and structureless or wave or current rippled. Abundant in situ Buchia bivalves and resistant weathering calcareous mudstone beds and concretions occur within the sandy mudstones.

Interpretation

The vertical sequence of sedimentary structures within a typical sharp based HCS sandstone bed is indicative of deposition during waning storms (Dott and Bourgeois, 1982; Walker et al. 1983; Duke, 1985). Both the massive and normally graded sandstones correspond to the T_a division of

Bouma (1962), and are interpreted as the deposits of sandy turbidity currents. The paucity of turbidites within this facies indicates that most were reworked into HCS or wave ripples by storm generated oscillatory currents. The interstratified bioturbated sandy mudstones reflect normal background deposition of mud from hemipelagic suspension. This facies was therefore deposited within a muddy offshore environment situated between storm and fair weather wave base.

3.3.6. Disorganized mudstone facies

Description

This facies also occurs only within the upper part of sequence 2 and consists of tabular beds of disorganized mudstone 2.9 to 13.2 m thick (Fig. 3.1). The disorganized mudstones are matrix-supported and consist of discontinuous highly deformed strata of the interstratified sandstone and mudstone facies, angular pebble to boulder size mudstone and sandstone intraclasts, randomly oriented calcareous mudstone concretions, and minor well rounded extraformational pebbles and cobbles. The matrix consists of poorly sorted sandy mudstone. Beds are structureless, ungraded, and exhibit planar basal contacts. Boulder to cobble size calcareous mudstone concretions and angular mudstone and sandstone intraclasts are concentrated near the tops of some beds

where they protrude into the overlying deposits.

Interpretation

The muddy matrix-supported framework, massive texture, and disorganized clast fabric of these beds indicates that they were emplaced by cohesive muddy debris flows (Middleton and Hampton, 1976; Enos, 1977; Lowe, 1979, 1982). The presence of large angular mudstone intraclasts within some beds indicates that the flows did not travel far from source. If they had, the relatively soft mudstone intraclasts would have been broken into smaller pieces. This fact, and the composition of the beds, indicates that slumping of nearby strata of the interstratified sandstone and mudstone facies (described previously) provided most of the sediment to the debris flows. The occurrence of well rounded extraformational pebbles and cobbles within the debris flows suggests that conglomeratic deposits also contributed sediment to the debris flows.

3.4. FACIES SUCCESSIONS

3.4.1. Sequence 1

Sequence 1 is 180 m thick and rests unconformably upon Late Jurassic andesites of the Moresby Group. The lower 155 m of the sequence is composed primarily of

amalgamated beds of the unstratified conglomerate facies, with minor solitary beds of the stratified conglomerate facies. The conglomeratic succession within this sequence exhibits a gross fining-upward trend, from boulder conglomerate at the base to pebble and cobble conglomerate above. Included within these conglomerates in section B on Flaht Island is a large angular block of mudstone (Fig. 3.7). These conglomerates were emplaced primarily by high density turbidity currents and debris flows within a marine environment situated above storm wave base. The conglomerates are overlain by a 20 m thick progradational wave dominated shoreface succession. This succession is overlain by 5 m of channelized conglomerates which were deposited within a coastal distributary environment.

The vertical arrangement of facies within sequence 1 therefore reflects a shoaling trend, from gravels emplaced mainly by sediment gravity flows within an environment situated above storm wave base, to sandstones deposited within a wave dominated shoreface environment, to channelized conglomerates deposited within a coastal distributary environment. The conglomerates forming the lower part of the sequence were probably deposited upon the subaqueous slope of a gravelly deltaic system (Fig. 3.13). Sediment was supplied to the slope by a network of gravelly distributary channels. The gravity flows responsible for

Fig. 3.13 Schematic diagram illustrating the depositional environments inferred from the White Point Formation. Deposition upon the subaqueous delta slope was dominated by gravelly high density turbidity currents and debris flows probably triggered by the slumping of mouth bars. Between these events, the slope was blanked by hemipelagic mud deposited from suspension. The delta distributaries were transitional laterally into wave dominated shoreface and offshore environments. Eposodic slumping in this region led to the emplacement of beds of the pebbly muddstone facies.

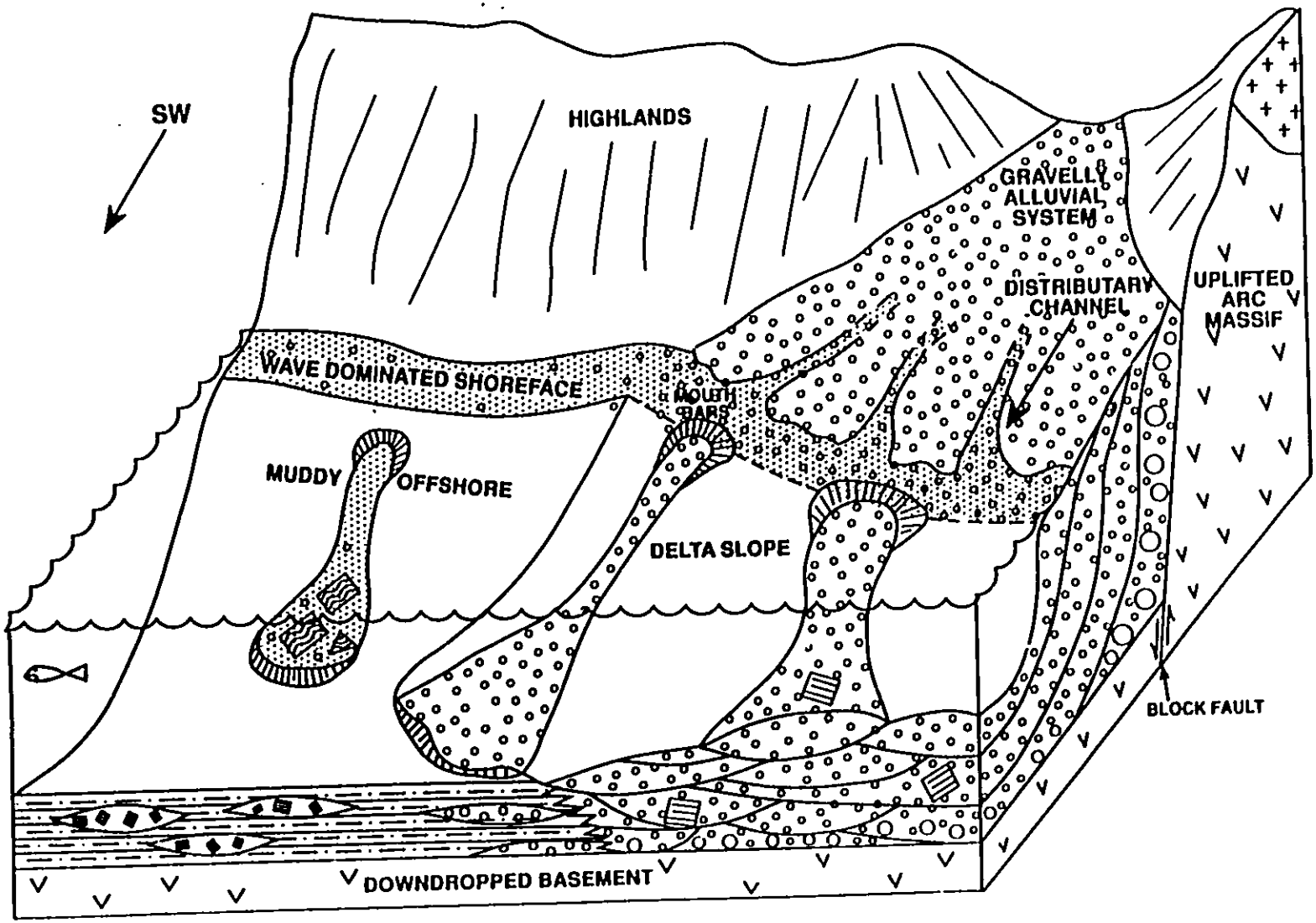
SW
HIGHLANDS
GRAVELLY ALLUVIAL SYSTEM
DISTRIBUTARY CHANNEL
UPLIFTED ARC MASSIF
WAVE DOMINATED SHOREFACE
MOUTH BARS
MUDDY OFFSHORE
DELTA SLOPE
BLOCK FAULT
DOWNDROPPED BASEMENT

emplacing gravel upon the slope may have been generated by flood events affecting the fluvial system, or by slumping of oversteepened delta front deposits. The presence of a large block of mudstone within the slope conglomerates exposed on Klaht Island (Fig. 3.7) indicates that slumping of muddy offshore strata may also have contributed sediment to the slope.

Clast imbrication measured from graded conglomerate beds indicate that the high density turbidity currents generally flowed down the slope from east to west (Fig. 3.8). The axis of the distributary channels exposed on Graham Island (Fig. 3.1) and on Klaht Island (Figs. 3.2 a and 3.11) trend approximately east - west, which is consistent with the eastern provenance inferred from clast imbrication. It is therefore probable that the deltaic system or systems supplying sediment to the basin during sequence 1 time were situated to the east. The vertical arrangement of facies within sequence 1 therefore reflects the progradation of a gravelly deltaic system.

3.4.2. Sequences 2 and 3

The shoreface and distributary channel deposits of sequence 1 are abruptly overlain by the deposits of sequence 2. The lower 40 m of this sequence is composed primarily of amalgamated beds of the unstratified and stratified

conglomerate facies. The conglomerates are abruptly overlain by 80 m of the mudstone and sandstone facies containing minor interstratified beds of the disorganized mudstone facies. Sequence 2 is capped by a 13.2 m thick bed of the disorganized pebbly mudstone facies, which in turn is abruptly overlain by the unstratified boulder conglomerates forming sequence 3.

Like those of sequence 1, the amalgamated beds of unstratified and stratified conglomerate forming the lower part of sequence 2 and all of sequence 3 were also deposited within a subaqueous deltaic slope environment. The overlying mudstones and sandstones were deposited within an offshore environment situated between storm and fairweather wave base. Deposition within this environment was dominated primarily by storm and mass flow events. The mass flows may have been triggered by a variety of mechanisms including seismic shocks, oversteepening, rapid rates of sedimentation, or cyclic wave loading during storm events (Nardin et al., 1979; Allen, 1980). These finer grained facies probably represent background depositional conditions in the absence of the influx of gravelly density modified grain flows and high density turbidity currents. Within the gravelly delta slope successions of both sequences 1 and 2, these finer grained background deposits were constantly eroded and incorporated into the gravelly turbidity currents

and debris flows. This may explain the abundance of mudstone intraclasts within beds of the unstratified and stratified conglomerate facies.

Unlike sequence 1, the vertical arrangement of facies within sequence 2 therefore do not appear to document a shoaling trend. Gravelly deposition upon the slope appears to have been abandoned abruptly and replaced by the deposition of finer grained sediment within an offshore environment.

Widespread failure of the offshore environment at the end of sequence 2 time appears to have preceded the resumption of gravelly delta slope deposition, represented by the boulder conglomerates at the base of sequence 3 (Fig. 3.1). Evidence of such failure includes the 16 m thick bed of disorganized pebbly mudstone capping sequence 2. The presence of such large intraclast boulders within the overlying conglomerates of sequence 3 may be related to reintrenchment of the slope by a new gravelly delta system, which resulted in the widespread erosion of the deposits of the underlying sequence.

3.5. CONTROLS ON DEPOSITION

The sequences preserved within the White Point Fm are similar in character to the subaqueous component of the

coarse-grained alluvial deltas described by Ethridge and Wescott (1984), McPherson et al. (1987, 1988), and Nemec (1990). These types of delta form where a coarse-grained fluvial system, usually an alluvial fan or a braidplain, discharges into a standing body of water. Deposition within the subaqueous environments of these systems is dominated by gravelly sediment gravity flows triggered by the failure of oversteepened distributary mouth bars. The coarse-grained nature of the alluvial deltas usually reflects proximity to a faulted or otherwise elevated highland.

Because no fluvial deposits are preserved within the White Point Fm, the exact nature of the subaerial system supplying the delta cannot be ascertained. The gravelly nature of the deposits however indicate that the subaerial systems supplying sediment to the deltas were alluvial fans or braided streams situated to the east. The predominance of andesite clasts within the conglomerates of the three sequences indicates that the fluvial system drained an uplifted volcanic arc consisting primarily of Late Jurassic Moresby Group andesites. The occurrence of granodioritic clasts within the conglomerates indicates that the uplifted arc had, by latest Jurassic time, been partially dissected.

The QCI region was affected by a prolonged period of block faulting throughout Late Jurassic time (Thompson et al., 1990; Lewis et al., 1991). This faulting occurred

along a network of north-northwest - south-southeast trending high angle faults, which were later reactivated during Late Cretaceous and Tertiary time. Sutherland Brown (1968) and Hickson and Lewis (1990) mapped several north-northwest - south-southeast trending faults at Cun'nin Bay 2 km to the northeast of where the White Point Fm is exposed on Graham Island. Although these faults cut Tertiary strata, Lewis et al. (1991) suggested that these and most other Cenozoic high-angle faults were likely reactivated Late Mesozoic structures. It is therefore probable that these faults and others like them controlled deposition of the White Point Fm within this area during Late Jurassic time.

3.6. DEPOSITIONAL HISTORY

Deposition of each of the sequences was probably controlled by the episodes of block faulting affecting the QCI region during Late Jurassic time. Evidence of this may be inferred from the vertical facies trend within each sequence. The coarse-grained deltaic slope deposits of each sequence display a gross fining-upwards trend, from poorly sorted boulder conglomerate at the base to pebble and cobble conglomerate above, and hence into finer grained sandstones and/or mudstones. This fining-upward trend probably

reflects the gradual decrease in relief of the uplifted basin margin following each episode of block faulting. The large extraformational boulders within the conglomerates at the base of sequences 1 and 3 were probably derived by avalanching off an adjacent fault scarp during the initial period following faulting when relief along the basin margin was high. During this stage, the subaerial component of the alluvial delta was very small, and coarse talus avalanching off the fault scarp was deposited directly at the base of the slope. As the highlands were eroded and the alluvial component of the system prograded and enlarged, a conical subaqueous delta slope was constructed. Instead of being transported directly to the delta front, the coarsest faction of the sediment load shed from the adjacent highland was trapped within the most proximal reaches of the fluvial system as the alluvial system grew. Progressively finer grained sediment was supplied to the delta front and slope by the fluvial system over time as relief along the basin margin decreased. This resulted in the deposition of progressively finer grained sediment over time, and hence the gross fining-upward trend observed within the deposits of the sequences within the White Point Fm.

Emplacement of the 13 m thick bed of pebbly mudstone capping sequence 2 is probably related to a renewed episode of fault activity and margin uplift. The accompanying

seismic activity resulted in widespread failure of the offshore environment, and eventually the establishment of a new gravelly deltaic system along the basin margin, represented by the slope boulder conglomerates of sequence 3. If this interpretation is correct, then the QCI region was affected by at least three separate episodes of block faulting during Late Oxfordian to Tithonian time.

Busby - Spera and Boles (1986) and Busby - Spera (1988) documented a similar fining-upwards trend within subaqueous fan delta deposits of the Early Cretaceous Asuncion Formation exposed in Baja California. These fans were deposited within small faulted half grabens situated in an extensional forearc setting. Each fan delta system deposited a single, 200 m thick fining-upwards sequence characterized by fault talus breccias containing angular boulders 2 to 6 m in size at the base. The breccias within each sequence are transitional upward into pebble and cobble conglomerates, interpreted by Busby - Spera and Boles (1986) as high density turbidites and debris flows. These in turn are transitional upwards into finer grained turbidites. Busby - Spera and Boles (1986) and Busby - Spera (1988) suggested that the gross fining-upward trend recorded a single phase of rapid down-dropping of the half grabens. Deposition of the fault talus breccias at the base of each deltaic succession occurred during the initial period when

basin margin relief was high. Gradual erosion of the uplifted horst block resulted in the deposition of an upward fining infill within each half graben.

Prior and Bornhold (1990) and Bornhold and Prior (1990) suggested that progradation of Holocene side wall fjord fan deltas in British Columbia would also generate an overall fining-upward facies succession. The authors suggested that this trend reflects the gradual decrease in the relief of the deglaciated basin margins over time. During the initial period of high basin margin relief, deposition upon the subaqueous portion of the delta is dominated by debris avalanching, gravelly grainflows, and high density turbidity currents (unsteady-state delta growth). It is during this period that the coarsest sediment is deposited within the marine environment, as the subaerial component of the alluvial delta is small and the steepness of the slope is high. River-borne sediments eroded from the adjacent highland bypass the nearshore zone and accumulate at the base of the slope. Over time, a cone shaped body of sediment is constructed against the slope. Deposition during this phase is dominated by gravelly high density turbidity currents. Subsequent deposition, when the subaerial delta plain is large and the subaqueous cone is less steep, is dominated by finer grained turbidites and by hemipelagic mud from suspension, which blankets inactive

portions of the subaqueous delta. The finer grained subaqueous deltaic deposits capping the succession are abruptly overlain by coarse alluvial deposits, as the subaerial component of the system progrades basinwards.

The fining-upward trend within both the Early Cretaceous Asuncion Formation of California and the subaqueous deposits of Prior and Bornhold's (1990) and Bornhold and Prior's (1990) idealized model reflect the gradual decrease in the relief of the basin margins over time. The fining-upward trend observed within the sequences preserved within the White Point Formation may be attributed to a similar cause.

CHAPTER 4. STRATIGRAPHY AND SEDIMENTOLOGY OF THE EARLY TO EARLY LATE CRETACEOUS LONGARM, HAIDA, AND SKIDEGATE FORMATIONS

4.1. CHAPTER SUMMARY

The deposits of the Longarm, Haida, and Skidegate Formations were deposited within a much enlarged northwest - southeast trending, southwest deepening marine basin. Twelve distinct facies are recognized within the deposits of the three formations. The facies are grouped into a sandstone facies assemblage (SFA), a mudstone facies assemblage (MFA), a disorganized facies assemblage (DFA), and a turbidite facies assemblage (TFA). The facies of the SFA were deposited within high energy shoreface to transitional sandy offshore environments. The facies of the MFA were deposited within storm dominated muddy offshore environments. The facies of the DFA were deposited within a mass flow dominated slope environment. The facies of the TFA were deposited within a sandy submarine fan environment.

Eight depositional sequences are observed within the three formations. Each is bound by erosional surfaces of regional significance marking a basinward change in facies.

An idealized sequence represents a complete cycle of long term (1 to 17 Ma) sea level fall and rise, and consists of the deposits of all four facies assemblages. The DFA and TFA represent contemporaneous slope and submarine fan deposits which were emplaced to the southwest during periods of relative sea level fall. The SFA and MFA represent contemporaneous shoreface and offshore deposits emplaced during the ensuing period of relative sea level rise.

The SFA and MFA of an idealized sequence consist of numerous progradational sandy shoreface and/or gravelly mouth bar successions. The progradational successions are stacked into a retrogradational set deposited during a long term relative rise in sea level. The progradational successions were therefore deposited during smaller scale periods of relative sea level fall or stillstand superimposed upon the long term rise in relative sea level. The shoreface successions were deposited along northwest - southeast trending paleocoastline characterized by irregular headlands and bays, fed at intervals by coarse grained deltas. Paleocurrent measurements from the TFA indicate that turbidity currents flowed towards the northwest, parallel to the basin axis.

The eight sequences progressively onlap the basin margin to the northeast throughout Late Valanginian to Early Turonian time. This accounts for the over-representation of

Late Valanginian to Late Albian shallow marine deposits and Cenomanian to Early Turonian deep water deposits exposed on the Queen Charlotte Islands.

4.2. INTRODUCTION

The Longarm, Haida, and Skidegate Formations are composed of approximately 2000 m of Late Valanginian to Early Turonian clastic strata. The strata are exposed in a 20 km wide outcrop belt which extends 250 km from Carpenter Bay in the southeast to Langara Island in the northwest (Fig. 1.2). Four different types of facies succession are recognized within the deposits of these three formations (Fig. 4.1): a sandstone facies assemblage (SFA), a mudstone facies assemblage (MFA), a disorganized facies assemblage (DFA), and a turbidite facies assemblage (TFA). Each assemblage consists of a group of genetically related facies (Table 4.1), each defined on the basis of lithology, physical sedimentary structures, and biogenic sedimentary structures. What follows is a description of each of the facies within each assemblage. The descriptions will be followed by a brief interpretation, which will be expanded in a later section within this chapter, when the vertical facies successions are discussed.

Fig. 4.1 Strike section oriented northwest - southeast illustrating the general stratigraphy of the Longarm, Haida, and Skidegate Formations. Note the interstratification of the various different facies assemblages.

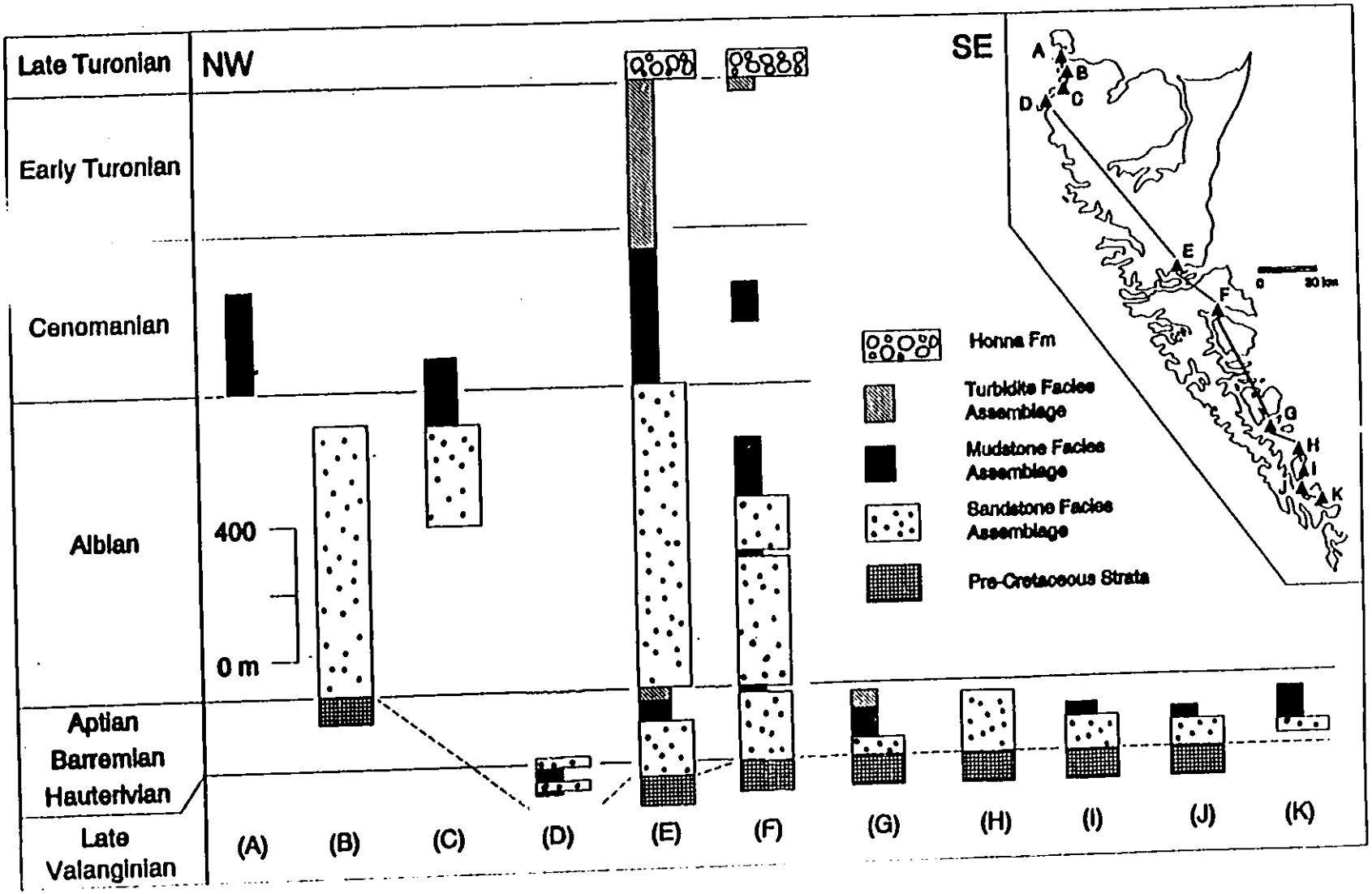
Late Turonian
Early Turonian
Cenomanian
Albian
Aptian
Barremian
Hauterivian
Late Valanginian
NW
SE
400
0 m
(A)
(B)
(C)
(D)
(E)
(F)
(G)
(H)
(I)
(J)
(K)
A
B
C
D
E
F
G
H
I
K
0
30 km
Honna Fm
Turbidite Facies Assemblage
Mudstone Facies Assemblage
Sandstone Facies Assemblage
Pre-Cretaceous Strata

Table 4.1 Component facies of the four assemblages recognized within the deposits of the Longarm, Haida, and Skidegate Formations.

FACIES ASSEMBLAGE	FACIES
Sandstone Facies Assemblage	Basal Transgressive Facies Conglomerate Facies Trough and Planar Tabular Cross-Stratified Sandstone Facies Swaley Cross-Stratified Sandstone Facies Structureless Bioturbated Sandstone Facies
Mudstone Facies Assemblage	Shale and Silty Mudstone Facies Mudstone and Thin-Bedded Sandstone Facies Hummocky Cross-Stratified Sandstone and Sandy Mudstone Facies Solitary Thick-Bedded Sandstone Facies
Disorganized Facies Assemblage	Pebbly Mudstone Facies Intraclast Breccia Facies
Turbidite Facies Assemblage	Classical Turbidite Facies Thick Bedded Sandy Turbidite Facies

4.3. DESCRIPTION OF THE SANDSTONE FACIES ASSEMBLAGE

4.3.1. Basal transgressive facies

Description

The unconformities and disconformities bounding each of the sequences are overlain by a poorly sorted conglomerate, breccia, or pebbly sandstone. This facies is coarsest and best developed where associated with the unconformities separating the deposits of the sandstone facies assemblage of each sequence from the pre-Cretaceous basement. Where associated with the disconformities separating stratigraphically stacked sequences, this facies is finer grained and less well developed.

The basal conglomerates and breccias which directly overlie the unconformity with the pre-Cretaceous basement are clast-supported and very poorly sorted, forming irregular beds between 0.4 and 15.4 m thick. Beds are massive and have a poorly sorted sandstone matrix containing oyster shell fragments (Fig. 4.2). Clasts are well-rounded to angular, depending upon their lithology, and exhibit no organized fabric. The conglomerate overlying the unconformity on Arichika Island contains irregular outsized boulders (Fig. 4.3) of Yakoun andesite, one 15 m in diameter. The lithology of the clasts generally reflects that of the underlying basement, although rounded clasts of

Fig. 4.2 Exhumed boulders of granodiorite within the transgressive conglomerate of the Longarm Formation exposed at Poole Inlet. Note the very poor sorting of the conglomerate and the rounding of the clasts. Scale is 9 cm long.

Fig. 4.3 Well rounded boulder (arrow) of Early Jurassic Yakoun andesite within the basal transgressive conglomerate of the Longarm Formation overlying the unconformity exposed on Arichika Island. The boulder is 3 m in diameter.

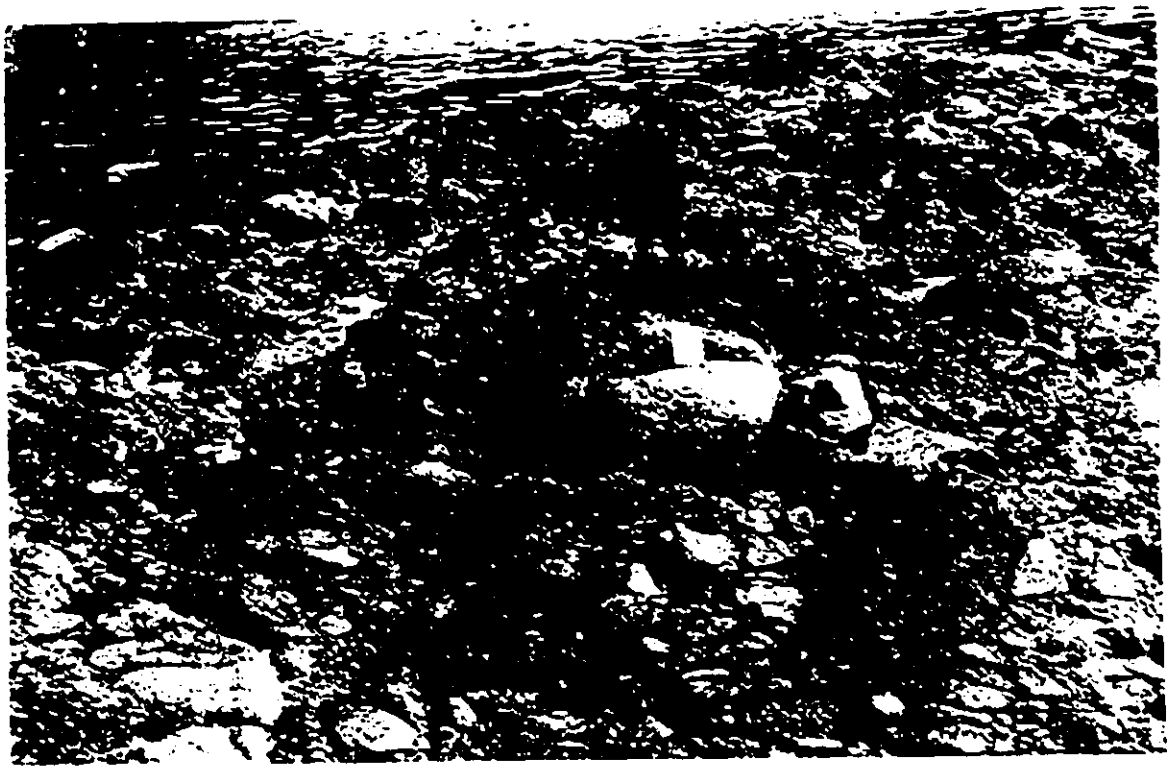

olive green andesite from the Yakoun Group are ubiquitous.

The disconformities separating the sequences are overlain by a poorly sorted medium grained sandstone or pebble conglomerate between 0.5 and 40 cm thick. Clasts are composed of well rounded extraformational pebbles, sandy and muddy carbonate concretions, and abundant wood debris (Figs. 4.4 and 4.5). Some of the calcareous sandstone and mudstone concretions within the lag are sideritized.

Interpretation

The conglomerates and breccias overlying the unconformities are interpreted as transgressive lags. The occurrence of bivalve fragments within the matrix of these conglomerates and breccias indicates that they were deposited within a marine environment. The occurrence of boulders up to 15 m in diameter within the lag exposed on Arichika Island and Poole Inlet indicates that the lag accumulated adjacent to a coastal cliff of high relief. The well rounded nature of the clasts within the conglomerates may be attributed to wave-related clast collisions within the high energy surf zone. Rounding by this process is particularly effective within the surf zone of modern high energy cobble beaches (Bluck, 1968).

The conglomerates and pebbly sandstones overlying the disconformities are also interpreted as transgressive lags.

Fig. 4.4 Transgressive pebbly sandstone overlying a disconformity within the Haida Formation exposed at Lauder Point, northwestern Graham Island. Note the well rounded nature of the light coloured calcareous sandstone concretions (C) as well as the smaller, dark-coloured extraformational pebbles. Scale is 9 cm long.

Fig. 4.5 Transgressive lag within the Haida Formation overlying the disconformity exposed on McLelland Island, eastern Cumshewa Inlet. Note the light coloured sideritized calcareous mudstone concretions (C) protruding from the recessively weathering mudstones into the overlying resistantly weathering sandstones.

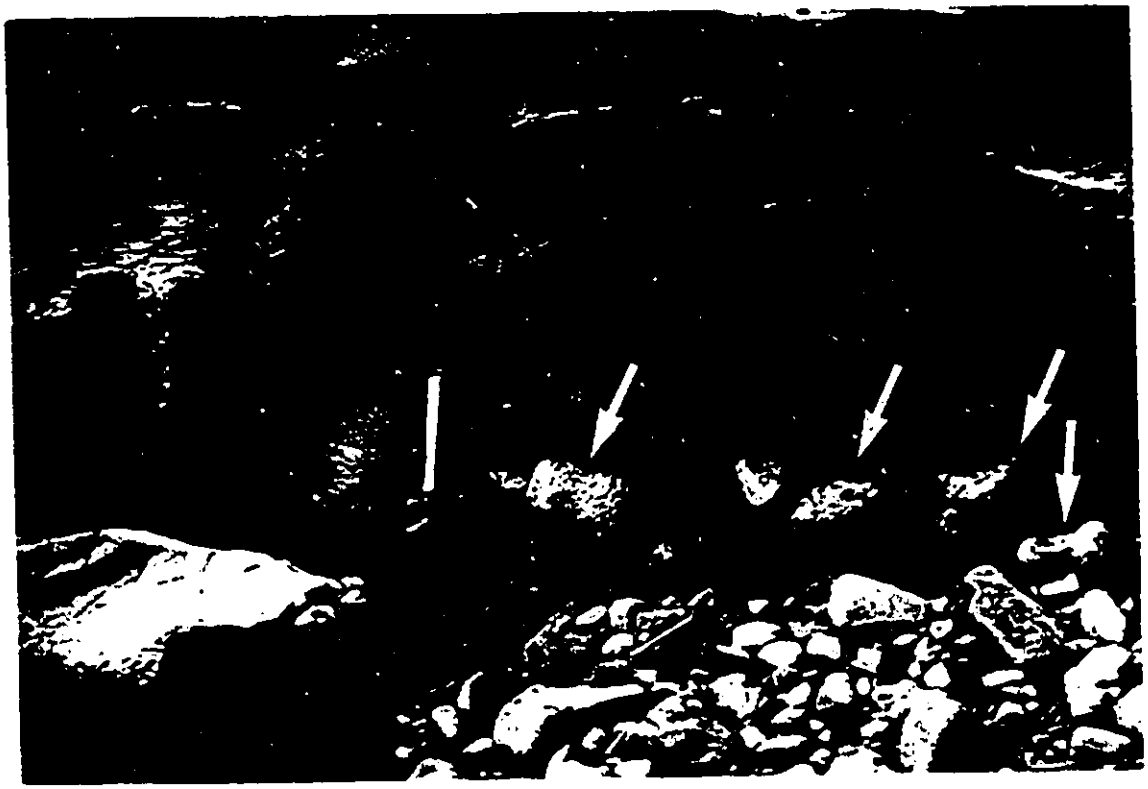

The finer grained nature of the conglomerates and pebbly sandstones indicates that they accumulated within an environment situated adjacent to coastlines of lower relief.

4.3.2. Trough and planar cross-stratified sandstone facies

Description

This facies consists of trough and planar-tabular cross-stratified fine to very coarse grained pebbly sandstone forming small to large scale sets 0.2 to 1.4 m thick (Figs. 4.6). The sets are typically grouped into cosets 1.9 to 46.2 m thick. The sandstones are well sorted, although coarser sets tend to be less well sorted and pebbly. The base of some sets is overlain by a thin, poorly sorted lenticular pebble lag. The trough and planar-tabular cross-stratified sandstones may be interbedded with minor wave rippled and hummocky cross-stratified fine grained sandstones.

Fragments of Inoceramid and oyster shells, as well as whole ammonites and belemnites, are common within the cross-stratified sandstones. Traces include, in order of decreasing abundance, Ophiomorpha nodosa, Skolithos, Macaronichnus simplicatus, Conichnus conicus and Siphonichnus / Polycylindrichnus (J. MacEachern and I. Raychaudhuri, pers. comm. 1992). A rather peculiar though prolific trace occurs within the cross-stratified sandstones

Fig. 4.6 Cosets of small and medium scale trough cross-stratified fine to medium grained sandstone within the Longarm Formation exposed at Arichika Island. Scale is 9 cm long.

Fig. 4.7 Radiating traces exposed along the upper bedding plane of a set of trough cross-stratified sandstone within the Longarm Formation exposed on Arichika Island. Note the Y-shaped branch (arrow).

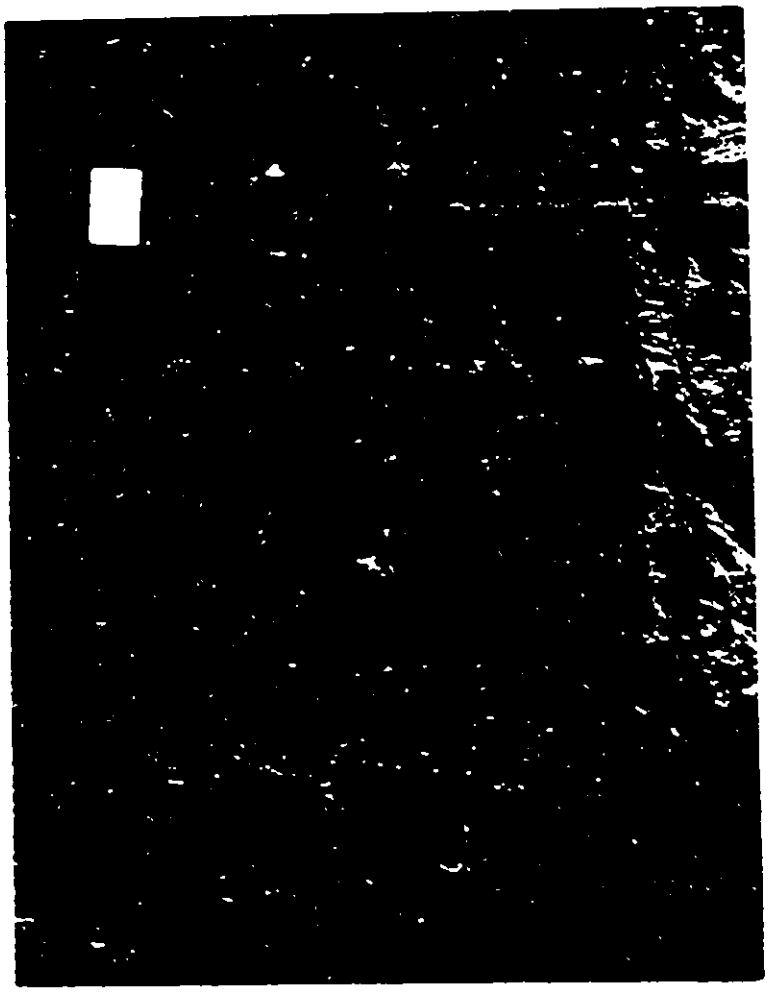

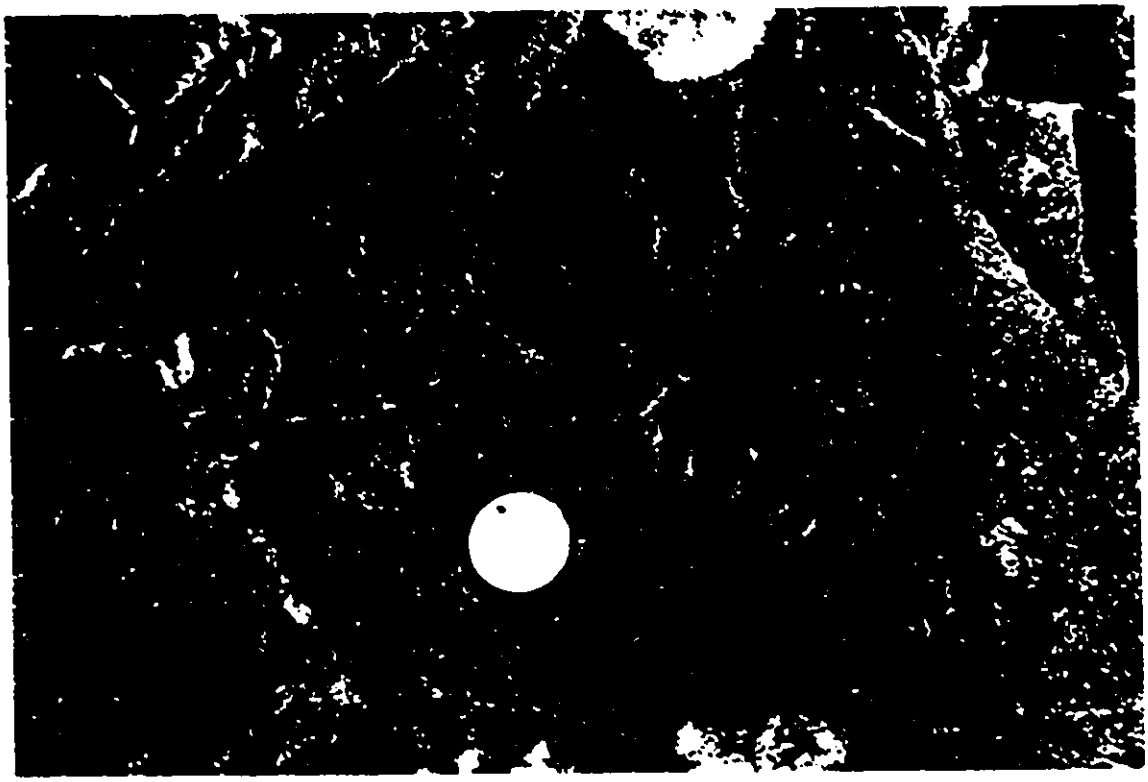

exposed on Arichika Island (Fig. 4.7).

Interpretation

The planar tabular and trough cross-stratified sandstones are interpreted as the deposits of two and three dimensional dunes respectively. The traces common to this facies belong to the Skolithos ichnofacies of Pemberton et al. (1984, 1992). This ichnofacies is characteristic of relatively moderate to high energy lower littoral to infralittoral substrates (Pemberton et al., 1984, 1992). The marine fauna, Skolithos ichnofacies, absence of interstratified mud, and the scale of cross-stratification indicates that the dunes migrated within a shallow marine shoreface environment.

4.3.3. Conglomerate facies

Description

Three types of conglomerate are recognized: trough cross-stratified, low angle cross-stratified, and structureless. All of these conglomerates are interstratified with beds of the trough and planar-tabular cross-stratified sandstone facies described above.

The trough cross-stratified conglomerates are poorly sorted and form sharp based sets 0.1 to 2 m thick (Fig. 4.8). Sets are generally solitary, although they may be

Fig. 4.8 Trough cross-stratified bed of pebble conglomerate within the Longarm Formation exposed on Arichika Island. Note that the cross-stratified conglomerate abruptly overlies a bed of structureless pebble conglomerate. Another sharp based bed of structureless pebble conglomerate occurs at the top of the photo. Scale is 9 cm long.

Fig. 4.9 Symmetrically-rippled pebble conglomerate capping bed of trough cross-stratified pebble conglomerate within the Longarm Formation exposed on Arichika Island.

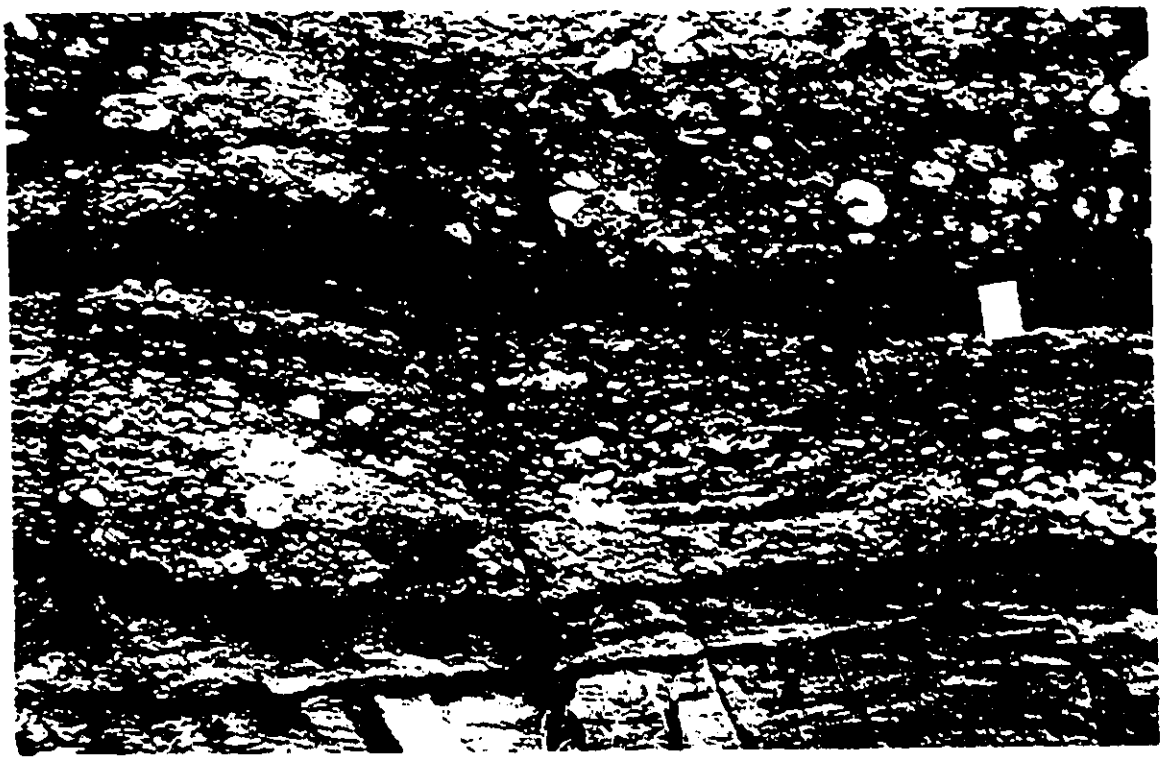

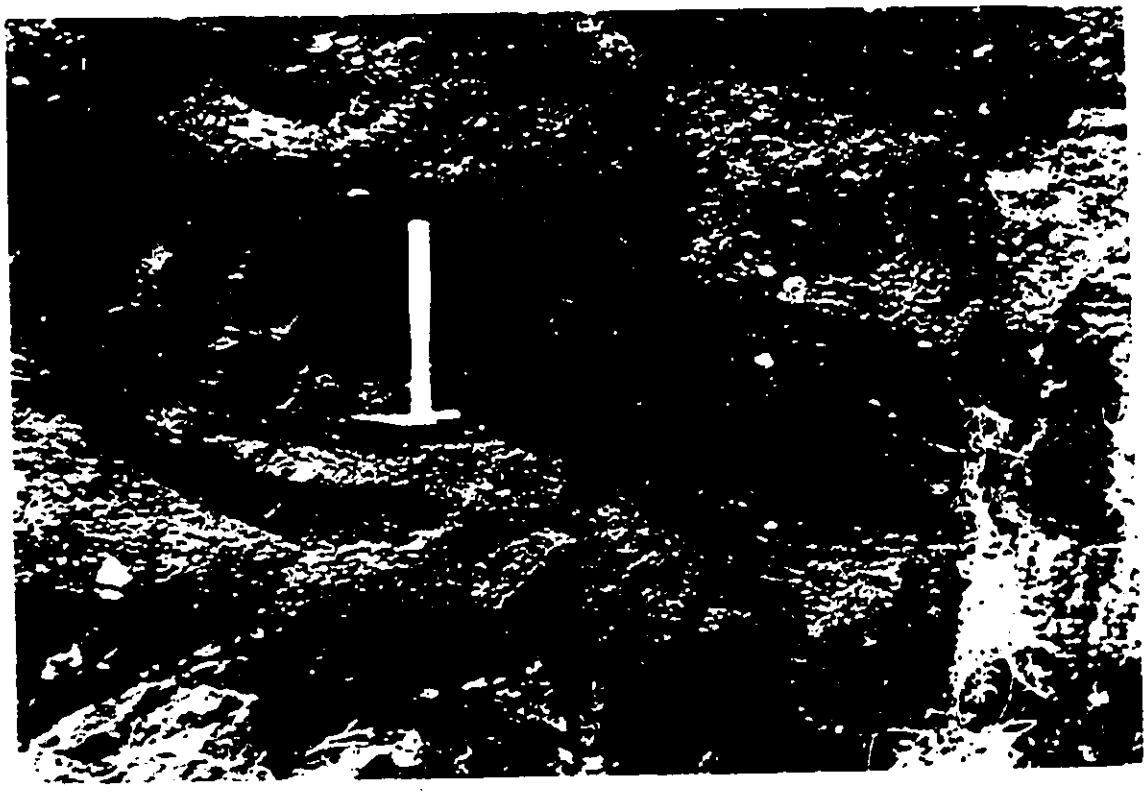

grouped into cosets up to 4 m thick. The tops of some sets are reworked into pebbly symmetrical ripples (Fig. 4.9).

The structureless pebble and cobble conglomerates form sharp based tabular beds 0.4 to 2 m thick. The conglomerates are poorly sorted and clast-supported, and are either massive or normally graded (Figs. 4.10 and 4.11). The matrix is medium grained and poorly sorted, and clasts exhibit no well developed fabric. Large disarticulated Inoceramid valves aligned parallel to stratification occur within many of the conglomerates. Some beds of structureless conglomerates are transitional upwards into horizontally-stratified conglomerate and sandstone (Fig. 4.11). Some beds of structureless conglomerate are abruptly overlain by a set of trough cross-stratified conglomerate (Fig. 4.9).

The low angle cross-stratified conglomerates form sharp based tabular beds 2 to 7 m thick (Fig. 4.12). Individual strata within the beds are 5 to 30 cm thick and are composed of clast-supported, poorly to moderately well sorted pebble to cobble conglomerate containing a well sorted sandstone matrix. Strata are inversely graded or massive and are inclined at a low angle (Fig. 4.13). Adjacent strata may vary greatly in clast size, although clasts do not exhibit any well developed fabric. Some strata are separated by thin lenticular beds of wave rippled

Fig. 4.10 Crudely graded bed of the structureless pebble conglomerate facies within the Longarm Formation exposed on Arichika Island. Scale is 9 cm long.

Fig. 4.11 Bed of the structureless pebble conglomerate facies within the Longarm Formation exposed on Arichika Island. Note the recessively weathering concave-up disarticulated Inoceramid valves within the conglomerate (arrow). Also note the upward transition into horizontally to low angle stratified conglomerate and sandstone. Another sharp based bed of structureless conglomerate occurs at the top of the photo. Scale is 9 cm long.

Fig. 4.12 Bed of the low-angle cross-stratified facies within the Longarm Formation exposed on Arichika Island. Stick is approximately 1.3 m long.

Fig. 4.13 Inversely graded cross-strata (arrows) within the low angle cross-stratified conglomerate facies within the Longarm Formation exposed on Arichika Island. 10 cm bars on stick to right.

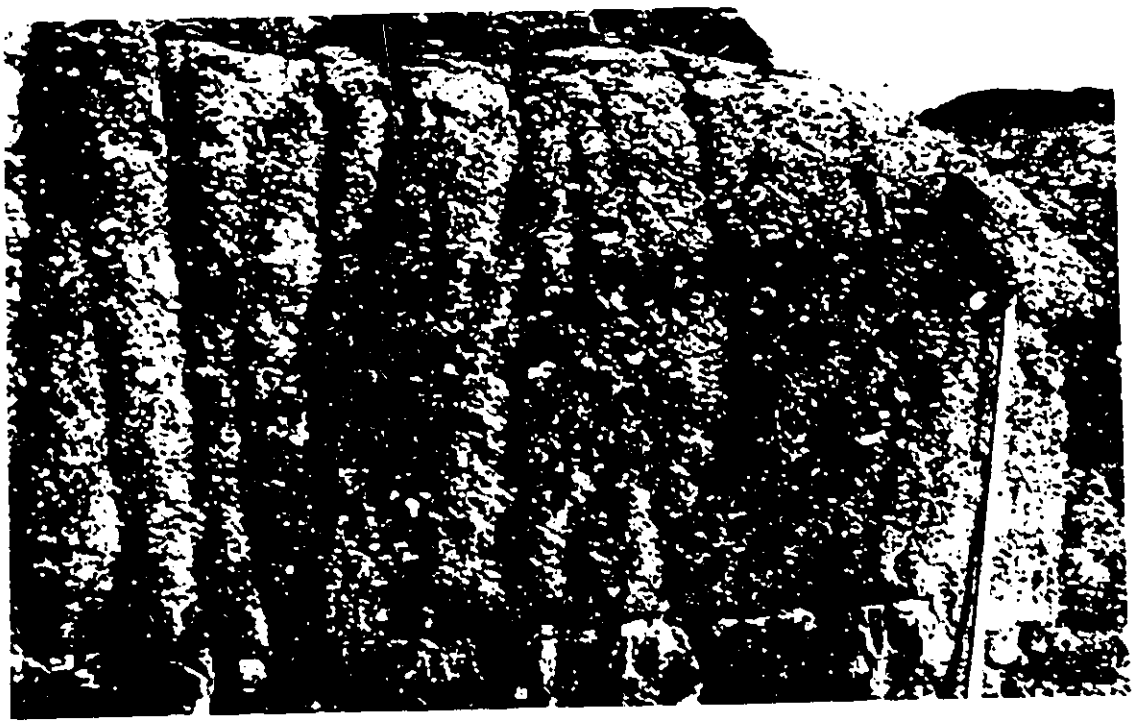

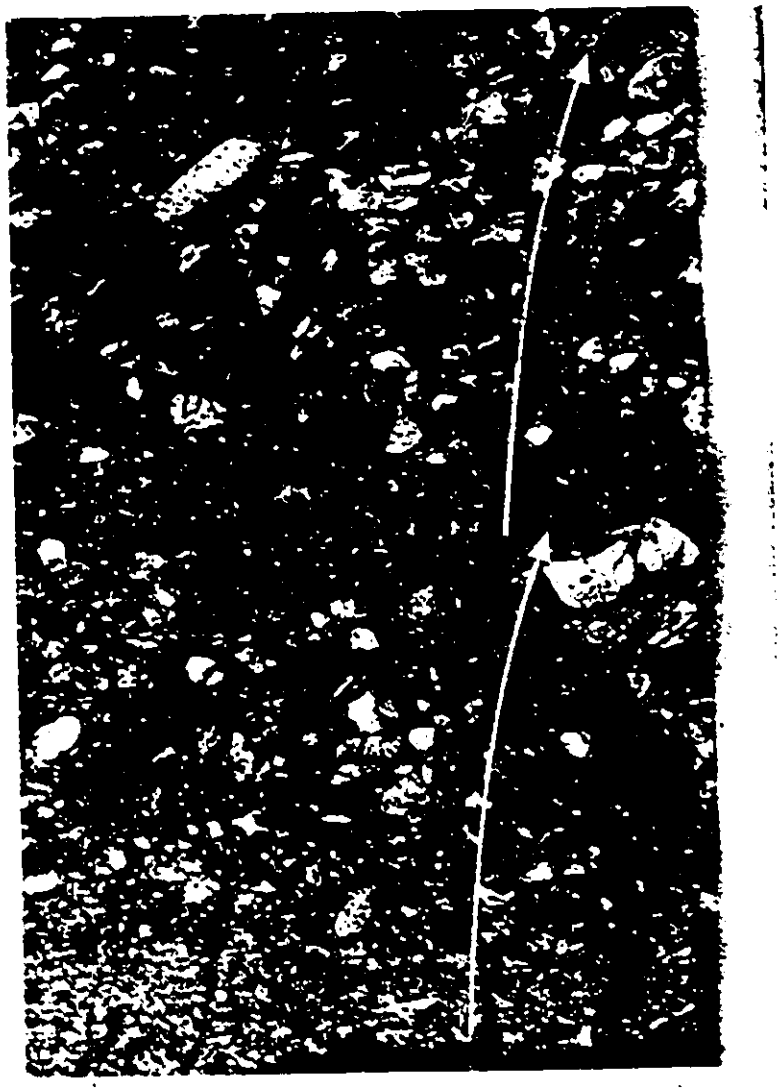

fine grained sandstone.

Interpretation

The association of these conglomerates with the cross-stratified sandstones described above indicate that the conglomerates were deposited within a shoreface environment. The presence of Inoceramid bivalve fragments within each of the conglomerate facies also reflects deposition in a marine environment. The trough cross-stratified conglomerates represent the deposits of gravelly three dimensional dunes which migrated under the influence of unidirectional currents. The tops of some sets were subsequently reworked into symmetrical ripples by wave generated oscillatory currents.

The sharp-based and graded nature of the beds of structureless conglomerate probably reflects episodic deposition from waning currents. The upwards transition to horizontally-stratified conglomerate and sandstone within some of the beds may represent deposition of thin gravelly and sandy traction carpets during the waning phases of the current.

The inverse grading of strata within the low angle cross-stratified conglomerate facies is typical of deposition from grain flows. In these types of flow, clasts are maintained above the bed by a combination of the

dispersive pressure arising from grain collisions, and by the buoyant lift force imparted by a dense sediment-water matrix (Middle and Hampton, 1973, 1976; Lowe, 1976, 1982). Deposition occurs by frictional freezing, with the beds usually exhibiting an inversely graded texture. This reflects the relatively high dispersive pressure between the large clasts in the flow. The maintenance of such flows requires slopes approaching the static angle of repose, which is generally between 18 and 28° (Middleton and Hampton, 1973, 1976). This suggests that the strata were deposited toesets of steep bars, which would account for the low angle inclination of stratification within beds of this facies.

4.3.4. Swaley cross-stratified sandstone facies

Description

This facies consists of moderately to well sorted fine to medium grained swaley cross-stratified (SCS) sandstones 10 to 110 m thick. The sandstones exhibit broad intersecting sets of concave-up (swaley) laminae interstratified with sets of subparallel undulating laminae and minor sets of convex-up (hummocky) laminae (Fig. 4.14). In good, three dimensional exposure, the swaley laminae dip and intersect at very low angles regardless of orientation. Minor sets of trough cross-stratified sandstone and rare

Fig. 4.14 Swaley cross-stratified fine grained sandstones within the Haida Formation exposed at Onward Point, Skidegate Inlet. Note the predominance of low angle concave-up and undulating laminations, as well as the low angle at which swales intersect. Scale is 9 cm long.

Fig. 4.15 Massive lenticular bed of conglomerate (arrow) interstratified with swaley cross-stratified sandstones within the Haida Formation exposed at Onward Point, eastern Skidegate Inlet.

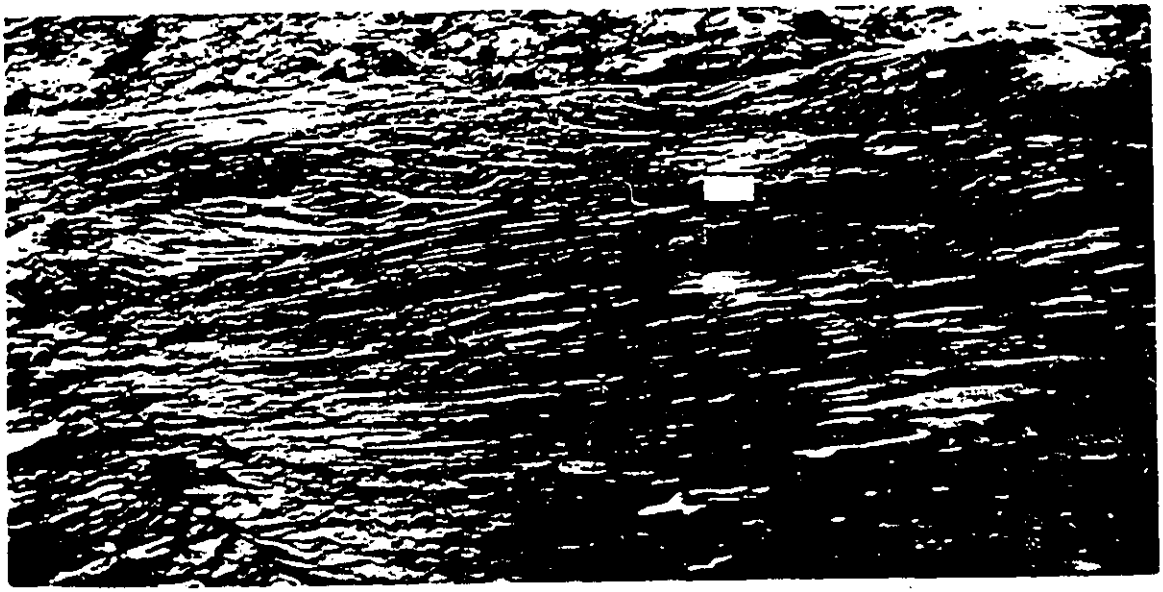

lenses of wave rippled fine grained silty sandstone and mudstone are interbedded with the SCS sandstones.

Shell fragment-rich and fragment-poor varieties of SCS sandstone were observed within the deposits of the SFA exposed near White Point. In the shell fragment-rich variety, abundant platy Inoceramid fragments occur along the low angle convex-up swaley laminae and concave-up hummocky laminae. The shell fragments oriented parallel to bedding are particularly abundant along laminae near the base of SCS sandstone beds, and become less abundant upwards throughout the bed. Lenticular beds of clast-supported Inoceramid shell breccia up to 0.6 m thick were also observed. The fragment-rich variety of SCS sandstone forms beds up to 6.8 m thick which are interstratified with beds of the fragment-poor variety. The latter variety contains only rare Inoceramid fragments, and forms beds up to 4.2 m thick.

Poorly sorted beds of clast-supported pebble conglomerates are interstratified with this facies at sections DaC 1 and OnP 4. The conglomerates are massive to normally graded, and form sharp based tabular to lenticular beds 0.06 to 1.2 m thick (Fig. 4.15). The bases of some conglomerate beds may exhibit gutters. Clasts are well-rounded to subangular and include abundant disarticulate Trigonid bivalve shells. Clast-supported beds of Inoceramid and Trigonid bivalve conglomerate are also interstratified

with the SCS sandstone at some locations. Valves within these conglomerates are usually intact and unabraded.

Traces within the SCS sandstones include Ophiomorpha nodosa, Arenicolites, Diplocraterion habichi, Skolithos, and Conichnus conicus. There are also elongate cylindrical well sorted sand-filled traces up to 5 mm in diameter that may possibly be Macaronichnus simplicatus (J.A. MacEachern and I. Raychaudhuri, pers. comm. 1992).

Interpretation

Swaley cross-stratification is believed to be formed by storm-generated oscillatory currents within a high energy wave-dominated shoreface environment (Leckie and Walker, 1982; Walker, 1985; Rosenthal and Walker, 1987). The lenticular nature of the Inoceramid shell-fragment breccias and pebble conglomerates interbedded with the SCS sandstones suggests that they were deposited within shallow scours or perhaps rip channels upon the shoreface. The traces observed within this facies belong to the Skolithos ichnofacies of Pemberton et al. (1992), which is typically indicative of high energy shoreface settings.

4.3.5. Structureless bioturbated silty sandstone facies

Description

This facies is composed of structureless, pervasively

bioturbated silty sandstone forming successions 80 to 600 m thick. Despite this great thickness, there appear to be no smaller-scale facies trends within the successions, although the successions tend to become increasingly silty and more thoroughly bioturbated upwards. The successions consist of poorly sorted fine grained organic rich silty sandstone. There are very few bedding surfaces preserved; those present define beds up to 2.5 m thick (Fig. 4.16). Bedding surfaces are defined by thin highly carbonaceous fine grained silty laminae which may exhibit a crude parallel lamination (Fig. 4.17). Thin (< 30 cm) lenses of fine grained hummocky cross-stratified sandstone occur at the base of some of structureless sandstone beds (Fig. 4.18). These hummocky cross-stratified sandstone beds grade upwards into structureless bioturbated sandstone. Beds of vaguely parallel and cross-laminated silty sandstone are also observed within the otherwise structureless sandstone beds.

Numerous petrified logs up to 20 cm in diameter and 5 m long as well as smaller wood fragments occur within the sandstones of this facies. Most petrified logs and wood fragments are pervasively bored by Teredolites. The sandstones are thoroughly bioturbated and include, in order of decreasing abundance, Planolites montanus, P. beverlyensis, Thalassinoides, Ophiomorpha, Paleophycus herberti, Schaubcylindrichnus, Siphonichnus /

Fig. 4.16 Meter scale tabular bedding within the structureless bioturbated sandstone facies of the Haida Formation exposed near Queen Charlotte City, Skidegate Inlet. Person in photo is approximately 1.6 m in height.

Fig. 4.17 Structureless bioturbated sandstone facies. Note the carbonaceous rich recessively weathering laminae defining the crude tabular bedding within this facies (arrows). Note also the virtually structureless and thoroughly bioturbated nature of this facies. Scale is 9 cm long.

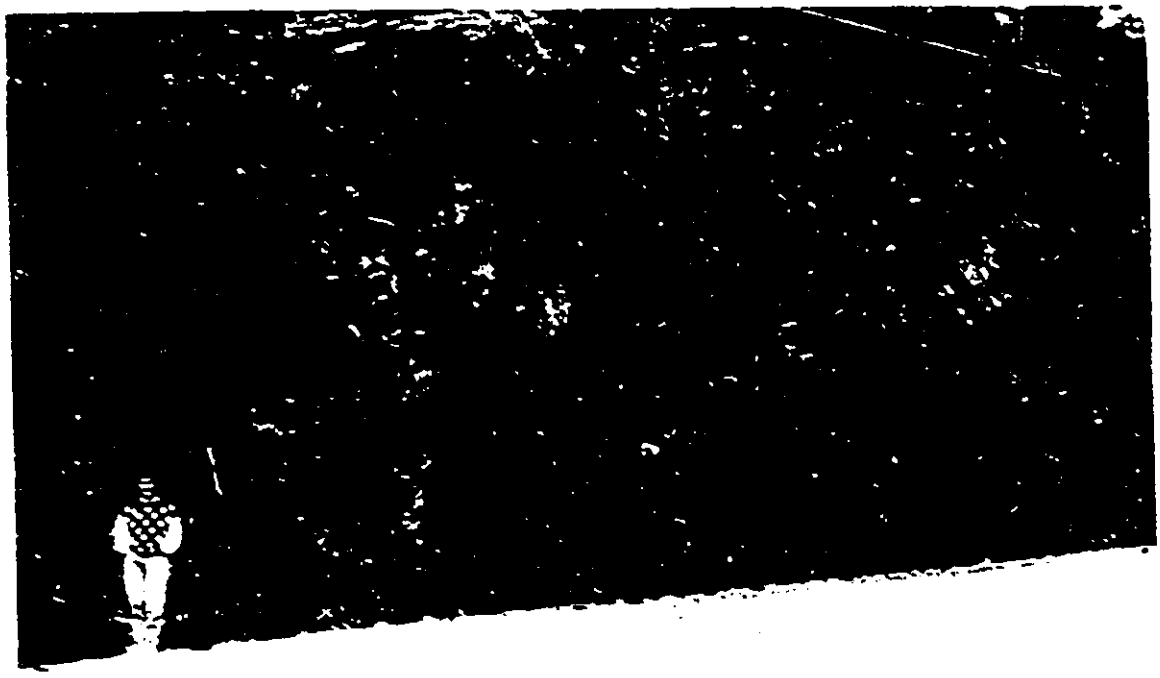

Polycylindrichnus, and Terebellina (J.A. MacEchearn and I. Raychaudhuri, pers. comm. 1992). Mud-lined P. montanus, P. beverlyensis, and Thalassinoides traces are by far the most common (Fig. 4.19). Abundant ammonites and articulate Buchia and Inoceramid bivalves as well as rare Mausosaur bones also occur within this facies. Resistantly weathering calcareous concretions of every conceivable size and shape also abound within this facies. Two very broad categories of concretion were observed: spherical to ellipsoidal concretions and concretionary burrows. Spherical to ellipsoidal concretions are most common, and vary between 0.02 to 2 m in diameter. Internally, the concretions may exhibit ring-like calcium carbonate cementation fronts. In plan view, the concretions are circular, potato shaped, or highly irregular. Flattened ellipsoidal concretions may coalesce laterally, forming irregular "beds" which extend 10's to 100's of meters along strike.

Concretionary burrows are generally highly elongated, with the a-axis oriented parallel or obliquely to bedding. In transverse cross-section, the concretions are generally circular and between 0.5 and 6 cm in diameter. In plan view, the concretions are straight to curved and up to 4 m in length. The concretions tend to coincide within the tunnels of robust traces, such as Ophiomorpha. Internally, the concretions are composed of massive, moderately well

Fig. 4.18 Lenticular bed of fine grained hummocky cross-stratified sandstone (arrow) within the structureless bioturbated sandstone facies. Stick is 1.5 m long.

Fig. 4.19 Prolific P. montanus and P. beverlyensis traces within the structureless bioturbated sandstone facies. Scale is 9 cm long.

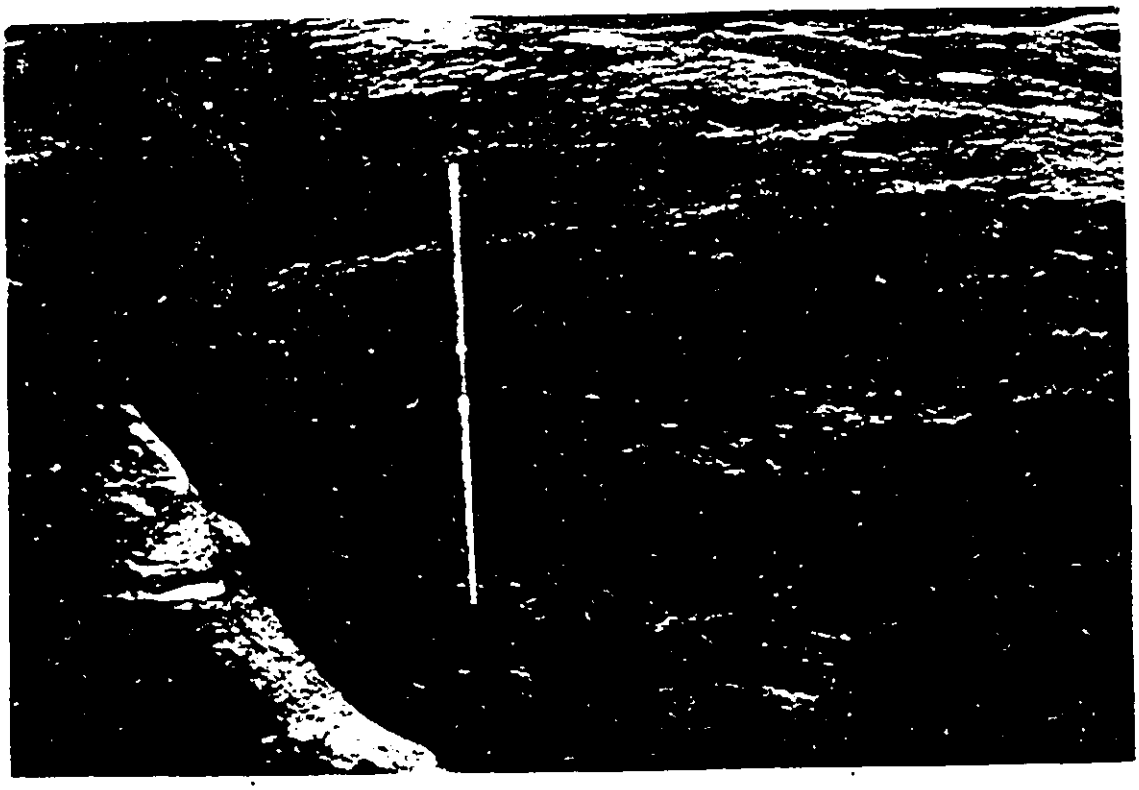

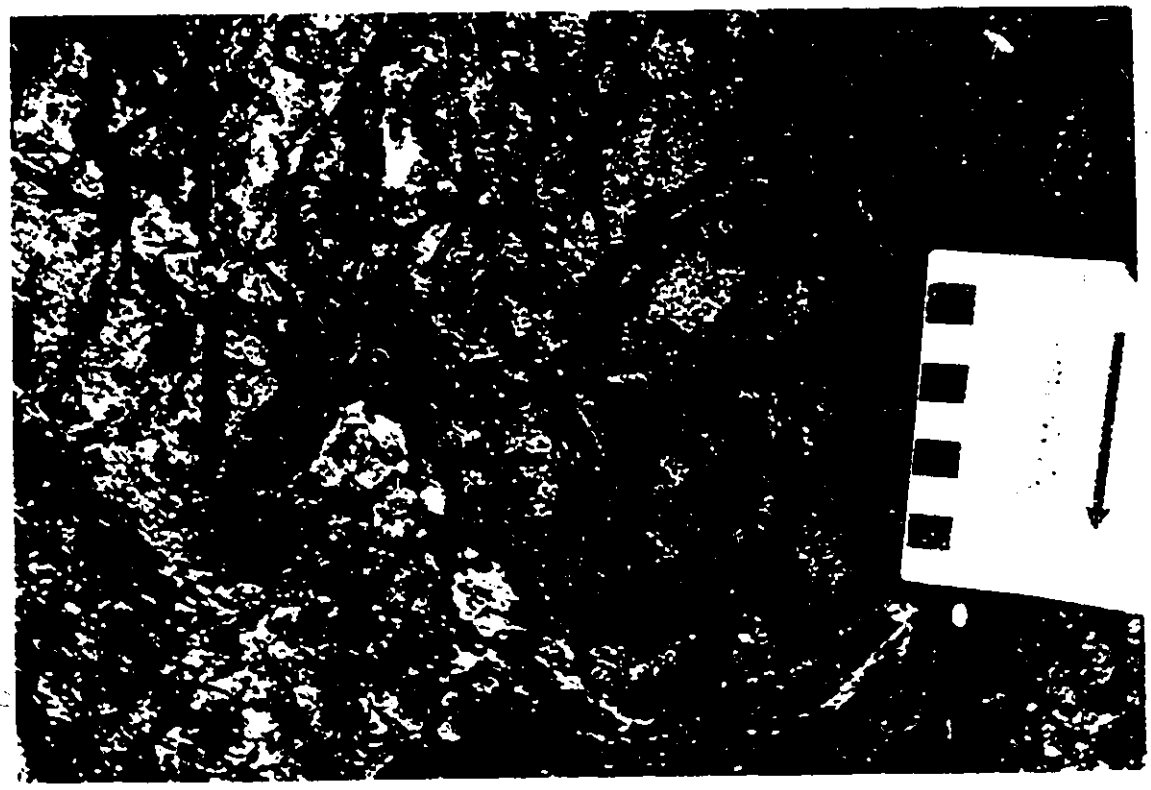

sorted fine grained sandstone lacking finer grained silt or mud.

Interpretation

The occurrence HCS sandstone lenses within this facies indicates that much of the sand may have been emplaced during storm events. Finer grained siltstones may have been deposited by other processes between storm events. These finer grained deposits, along with the storm emplaced sandstones, were subsequently reworked by a variety of benthic marine organisms, resulting in the complete destruction of sedimentary structures. The traces common to this facies belong to the Cruziana ichnofacies, and are characteristic of relatively moderate to low energy infralittoral to shallow circalittoral substrates situated between fairweather and storm wave base (Pemberton et al., 1984, 1992).

The circular cross section of the spherical concretions reflects a precompactional origin, whereas the flattened elliptical cross-section of the ellipsoidal concretions reflects a post compactional origin (Raiswell, 1971; Wetzel and Aigner, 1986). The laterally linked concretionary "beds" may reflect changes in the rate of sedimentation, which can affect cementation rates within the sediments beneath the sea floor (Raiswell, 1987; Pirrie and

Marshal, 1991). The circular transverse cross section of the concretionary burrows indicate that they are precompactional. The mud and silt free nature of the concretions probably facilitated the rapid cementation of the burrow infill.

4.4. DESCRIPTION OF THE MUDSTONE FACIES ASSEMBLAGE

4.4.1. Shale and silty mudstone facies

Description

This facies consists of interbedded shales and silty mudstones forming successions up to 124 m thick. The shales contain abundant grey-coloured elliptical calcareous and septarian concretions. The silty mudstones consist of thin, normally graded siltstones and mudstones (descriptively similar to T_{ae} beds in Bouma's 1962 scheme for turbidites) arranged in siltstone-mudstone couplets between 0.2 and 3.0 cm thick (Fig. 4.20). There are also thin (< 2 cm), rare, sharp based very fine to fine grained structureless (T_{ae}) or current rippled (T_{ce}) sandstones. The sandstones contain Rhizocorallium, Chondrites, Muensteria, and Planolites traces. Fossils are fairly common within this facies, and include ammonites and thin shelled in-situ Inoceramid bivalves.

Fig. 4.20 Graded siltstone-mudstone couplets (between arrows) within the shale and silty mudstone facies. Pencil is 14 cm long.

Fig. 4.21 Symmetrically rippled beds of sandstone (arrows) within the mudstone and thin bedded sandstone facies. Scale is 9 cm long.

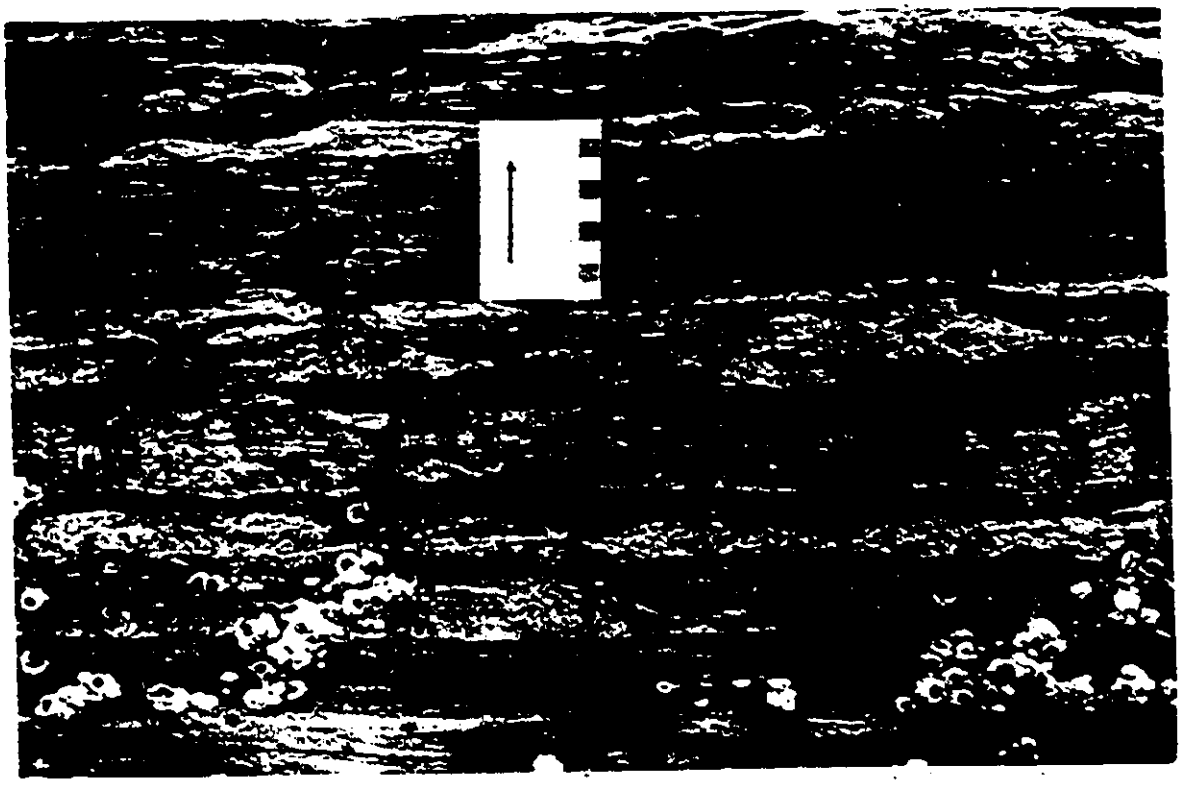

Interpretation

The mud forming the bulk of this facies was deposited from hemipelagic suspension within a quiet, low energy marine environment. The traces associated with the deposits of this facies indicate that the environment was fully marine. The graded siltstone at the base of the siltstone-mudstone couplets was probably deposited by waning currents. The normal grading of the siltstones may reflect deposition from low density turbidity currents. The overlying mudstones within each couplet represents deposition from background hemipelagic suspension. The similarity of the structureless and current rippled sandstone beds to the T_{bc} and T_{ce} divisions by Bouma (1962) suggests that they were deposited by low density turbidity currents (Lowe, 1976, 1982). The absence of oscillatory current formed sedimentary structures within the sandstone beds of this facies indicates that the depositional environment was not affected by wave generated oscillatory currents. The environment was therefore situated below storm wave base (> 200 m water depth).

4.4.2. Mudstone and thin bedded sandstone facies

Description

This facies consists of interbedded black silty mudstones and glauconitic sandstones forming successions up

to 133 m thick. The mudstones contain in situ Inoceramid bivalves. The sandstones are very fine to fine grained, and comprise 5 to 60 percent of the succession. Most sandstone beds are 1 to 5 cm thick and are structureless and mottled, parallel laminated, or symmetrically rippled (Fig. 4.21). Rare beds of hummocky cross-stratified (HCS) sandstone less than 10 cm thick also occur within this facies. Some sandstone beds exhibit thin basal lags of Inoceramid bivalve fragments or rip-up clasts. Intraclast breccia beds up to 3 cm thick also occur within this facies.

Traces include Rhizocorallium, Taenidium, Helminthopsis, Teichichnus, Chondrites, Planolites, Muensteria, Zoophycos and possible Scolecia (J.A. MacEchearn and I. Raychaudhuri, pers. comm., 1992).

Interpretation

The wave rippled and HCS sandstone beds were deposited under the influence of wave generated oscillatory currents (Walker et al., 1983; Duke, 1985). HCS is believed to be deposited within an environment situated between storm and fairweather wave base by purely oscillatory or combined currents (Dott and Bourgeois, 1980; Walker et al., 1983; Duke, 1985; Southard et al., 1990). The Inoceramid lags and intraclast breccia beds are interpreted as storm winnowed lags. The interstratified sandy mudstones were deposited

primarily from hemipelagic background suspension. The environment was therefore normally a quiet and low energy one. This quiet was interrupted by the occasional storm, which deposited HCS and wave rippled beds of sandstone. The traces are typical of the Cruziana and Zoophycos ichnofacies of Pemberton et al. (1984, 1992). These ichnofacies are characteristic of relatively moderate to low energy sublittoral to bathyal substrates.

4.4.3. Hummocky cross-stratified sandstone and sandy mudstone facies

Description

This facies consists of well sorted fine grained hummocky cross-stratified (HCS) or symmetrically rippled sandstone and interbedded sandy mudstone forming successions up to 236 m thick. The HCS sandstone beds are tabular, 0.1 to 1.9 m thick, and form up to 12 percent of the successions (Fig. 4.22). A typical sharp based bed begins with a basal breccia or conglomeratic lag overlain by massive to parallel-laminated fine to medium grained sandstone. This in turn is overlain by HCS sand, which grades upwards into rippled sandstone or bioturbated sandy mudstone (Fig. 4.23). The HCS may exhibit some soft sediment deformation. Beds of HCS may be underlain by a sharp based clast-supported lag composed of articulated Buchia bivalve shells, oriented

Fig. 4.22 Typical exposure of the hummocky cross-stratified (HCS) and sandy mudstone facies. HCS sandstones form tabular, resistantly-weathering beds, while sandy mudstone weather recessively. Stick is 1.5 m long.

Fig. 4.23 Thick bed of resistantly weathering hummocky cross-stratified sandstone exhibiting convex-up hummocks and concave-up swales. The HCS sandstone is overlain by recessively weathering sandy mudstone.

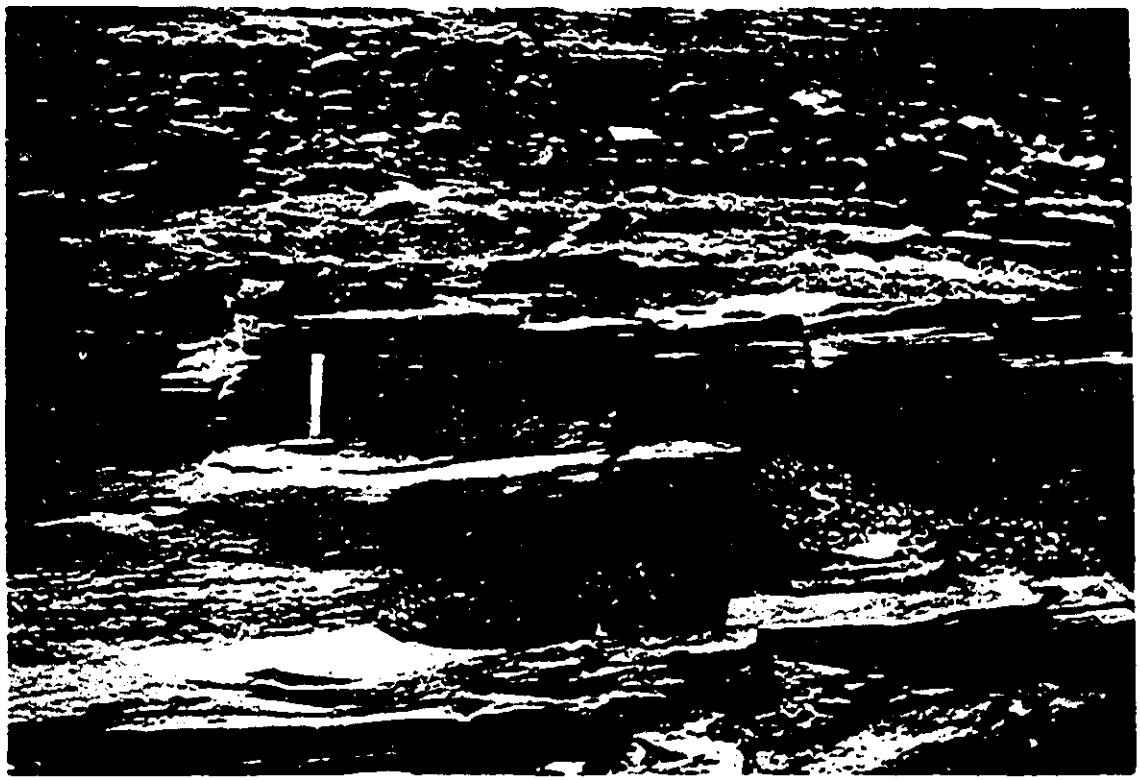

belemnites, and mudstone rip-up clasts 0.02 to 0.25 m thick. Similarly, some beds of HCS may be underlain by a clast-supported extraformational conglomerate lag up to 0.2 m thick. Laminations within the overlying HCS may exhibit parting lineation. The HCS in turn grades up into symmetrically rippled fine grained sandstone, and finally into sandy mudstone. Within the Skidegate Inlet region, some HCS sandstone beds infill broad concave-up scours 2 m deep and 30 m wide. Traces in the sandstones include Rhizocorallium, Zoophycos, Muensteria, Thalassinoides, and Planolites.

The bioturbated sandy mudstones form beds 0.8 to 12 m thick, and occur as thin partings between the HCS sandstones. Within the sandy mudstones there are thin (<3 cm) fine- to very fine grained sandstones that are either mottled and structureless, or rippled (symmetrical or asymmetrical). The sandy mudstones contain in situ Inoceramid bivalves. Groups of sandy mudstone beds 0.3 to 0.8 m thick are, in places, coherently deformed into overturned folds (Fig. 4.24).

Interpretation

The HCS sandstone beds within this facies were emplaced during waning storms by oscillatory or combined currents within an environment situated between storm and

Fig. 4.24 Coherently deformed bed of thinly interstratified sandstone and mudstone within a succession of the HCS sandstone facies of the Haida Formation exposed in Bearskin Bay, Skidegate Inlet. Note that most of the folds are overturned towards the right. Scale is 15 cm long.

fairweather wave base (Dott and Bourgeois, 1982; Walker et al. 1983; Duke, 1985; Southard et al., 1990). The sandy mudstones represent background deposition within a muddy offshore environment. The Buchia bivalve and extraformational conglomerates underlying some beds the HCS sandstone are interpreted as storm winnowed lags. The predominance of articulated Buchia bivalves within these lags, and the abundance of in situ Buchia bivalves within the interbedded sandy mudstones, indicates that the shell lags are parautochthonous (Brenner and Davies, 1973; Aigner, 1982; Brenchley, 1985). The traces are typical of the Cruziana and Zoophycos ichnofacies of Pemberton et al. (1992), which are characteristic of moderate to relatively low energy sublittoral to bathyal environments.

The deformation within the coherently deformed beds of sandstone and mudstone is attributed to submarine sliding and rotational slumping. This probably involved the collapse and downslope movement of partially lithified superficial deposits as semi-rigid and coherent sheets sliding along a basal glide plane (Nardin et al., 1979; Allen, 1980). The association of slide deposits abruptly overlain by beds of HCS sandstone indicates that sliding occurred within an environment situated above storm wave base. The deep concave-up scours infilled by HCS sandstones in the Skidegate Inlet region could have formed by wave

scouring during the storms. Alternatively, the presence of slumps and slides indicates that the concave-up scours could represent slump scars which were subsequently infilled by HCS sandstones during storm events.

4.4.4. Solitary thick bedded sandstone facies

Description

This facies consists of thick, solitary beds of buff-weathering sandstone interstratified with deposits of the mudstone and thin bedded sandstone facies and the hummocky cross-stratified sandstone and sandy mudstone facies. The beds are tabular to broadly lenticular, 0.3 to 1.9 m thick, and exhibit a channelized basal contact (Figs. 4.25 and 4.26). Lenticular beds 1.7 m thick were observed to pinch out 26 m along strike. Internally, the beds exhibit a characteristic vertical arrangement of sedimentary structures and a decrease in grain size. Two types of solitary thick bedded sandstone were identified (Fig. 4.27). In the first type, the basal contact is overlain by a massive intraclast breccia 0.05 to 0.1 m thick (Fig. 4.27 a). The subcircular platy intraclasts forming the breccias exhibit and imbricate fabric. The breccia is overlain by a unit of medium to very coarse grained horizontally-laminated sandstone or granular conglomerate 0.2 to 0.8 m thick (Figs. 4.25, 4.26, 4.27 a). The horizontally-stratified sandstones

Fig. 4.25 1.7 m thick bed of the solitary sandstone facies within the Haida Formation exposed in Cumshewa Inlet. Note the deeply channelized basal contact. This bed pinches out 26 m along strike (towards the upper right of the photo). Stick 1.5 m long.

Fig. 4.26 1.9 m thick bed of the solitary sandstone facies within the deposits of the Haida Formation exposed in Bearskin Bay. This bed is composed primarily of horizontally-stratified medium to very coarse grained pebbly sandstone overlain by a single set of trough cross-stratified sandstone. Bed is 1.5 m thick. House perched precariously close to edge of the bed is inhabited by local midgets, who are quite friendly.

are 3 to 4 cm thick and are normally graded, from coarse grained and granular at the base to fine or medium grained at the top (Fig. 4.27 a). The horizontally-stratified sandstones thin and fine upwards, and are abruptly overlain by a single set or rarely, grouped sets, of trough cross-stratified medium- to coarse grained sandstone 0.1 to 0.6 m thick (Figs. 4.25, 4.26, 4.27 a, 4.28). In some sets, stratification is completely deformed. In other sets, laminations are thrown into simple or complicated folds which are not overturned. In one set, the angle of cross-stratification was observed to decrease steadily towards the top of the bed (Fig. 4.28). The above described foresets are undulatory and symmetrically-rippled. Symmetrically-rippled fine grained sandstone caps most beds (Figs. 4.27 a and 4.28).

The second type of solitary thick bedded sandstone also exhibit a channelized basal contact overlain by an intraclast lag (Fig. 4.27 b). The lag is overlain by horizontally-laminated medium to very coarse grained pebbly sandstone. Stratification within the coarse pebbly sandstones near the base of some beds are inclined at a very low angle. Some laminations however were observed to form low angle convex-up hummocks and concave-up swales which intersect at low angles (Fig. 4.29). The horizontally laminated sandstones are abruptly overlain by a single set

Fig. 4.27 Vertical profiles of two solitary thick bedded sandstones within the Haida Formation exposed at a) Cumshewa Inlet, and b) Bearskin Bay, Skidegate Inlet.

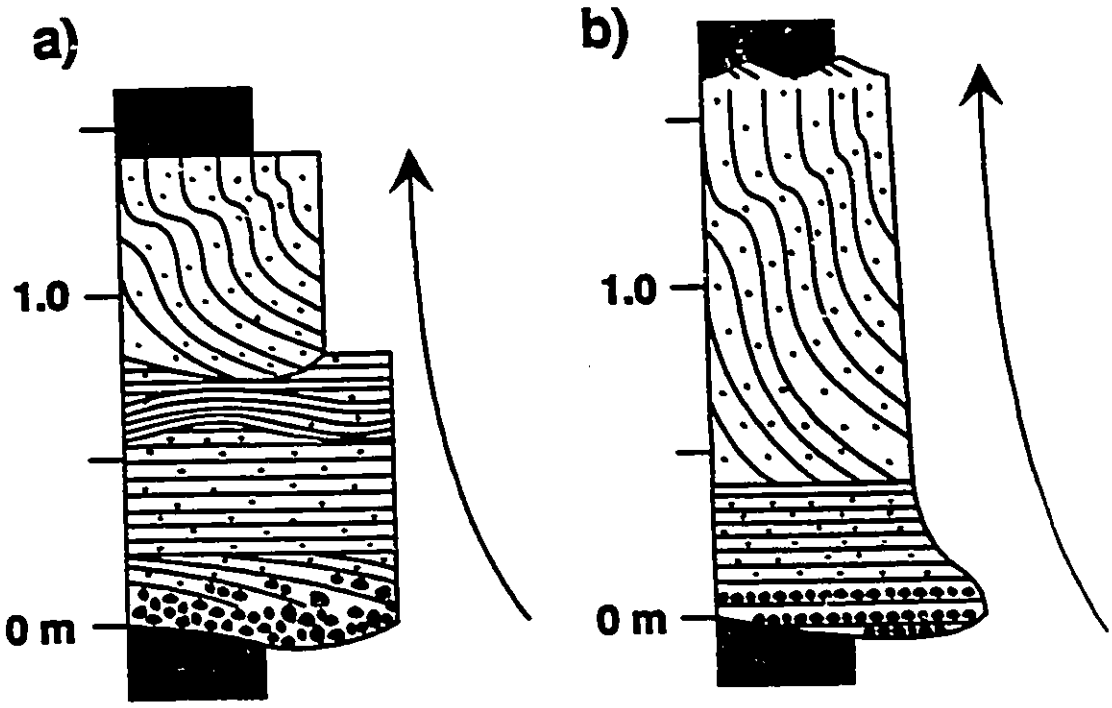
a)
1.0
0 m
b)
1.0
0 m

Fig. 4.28 Cross-stratified fine grained sandstone capping the thick solitary sandstone bed in Fig. 4.25. Cross-stratification within the bed immediately below and to the left of hammer has been completely deformed, yielding a massive weathering sandstone. Foresets above and to the right of the hammer are thrown into gentle, undulating folds. The angle at which the foresets within this bed are inclined decreases steadily upwards. The cross-stratified sandstone is capped by a bed of wave rippled sandstone.

Fig. 4.29 Convex-up hummock within the predominantly horizontally-laminated sandstones of the second type of thick bedded solitary sandstone. Scale is 9 cm long.

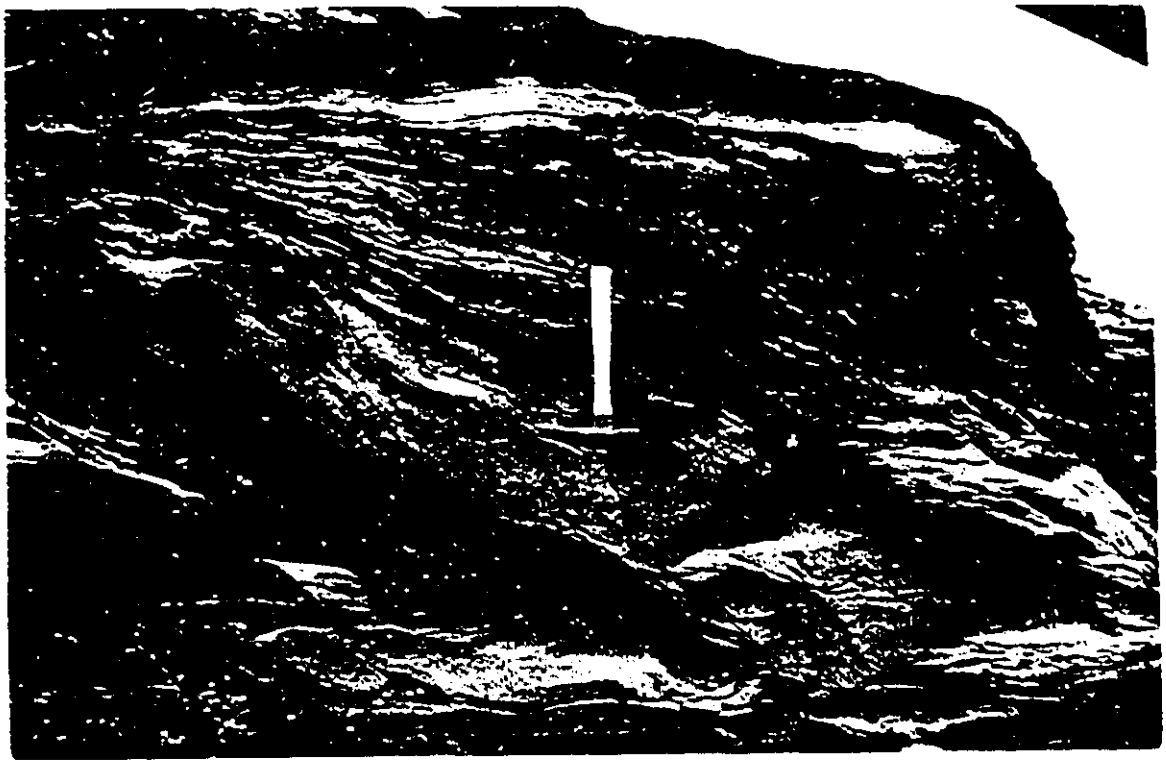

of trough cross-stratified sandstone (Figs. 4.26, 4.27 b).

Interpretation

The vertical decrease in grain size and the arrangement of sedimentary structures within each bed indicates that they were deposited under waning flow conditions. The velocity of the flow was initially sufficient to incise 2 m deep channels or scours into the seafloor. The intraclasts within the breccia at the base of each bed were derived by erosion of the seafloor prior to deposition. The channel or scour was subsequently infilled under waning flow conditions. In the case of the first type of thick bedded sandstone, deposition initially commenced under upper flow regime flat bed conditions, resulting in the accumulation of horizontally stratified sandstones. This was followed by the deposition of a single set of trough cross-stratified sandstone under lower flow regime conditions as current velocity decreased. Deposition of the first type of sandstone therefore appears to have occurred under purely unidirectional current conditions.

The presence of HCS within the lower part of the second type of thick bedded sandstone indicates that deposition occurred under combined or oscillatory current conditions. The presence of a single set of trough cross-stratified sandstone over the lower HCS portion of the bed

indicates that deposition during the final phase was dominated by unidirectional currents.

The presence of HCS and wave-ripples within both types of sandstone bed, and the occurrence of these beds with the deposits of the HCS sandstone and sandy mudstone facies (described previously), indicates that the beds were deposited within an environment situated between storm and fairweather wave base. The deformation observed within the cross-stratified sandstones capping both types of bed indicates that deposition was rapid, resulting in relatively elevated pore fluid pressure and subsequent failure (Allen, 1980).

4.5. DESCRIPTION OF THE DISORGANIZED FACIES ASSEMBLAGE

4.5.1. Pebbly mudstone facies

Description

This facies consists of matrix-supported pebbly mudstones forming beds 0.2 to 17.2 m thick. The clasts within the mudstones consist of deformed blocks of the mudstone and thin bedded sandstone facies; angular pebble to boulder sized mudstone and sandstone intraclasts; chaotically oriented calcareous concretions; and rare well rounded extraformational clasts (Fig. 4.30). Pebbly mudstone beds are sharp based, massive and ungraded. Large

calcareous concretions, intraclasts, and extraformational clasts may in places be concentrated near the tops of beds, where they protrude into the overlying deposits (Fig. 4.31). Well-rounded granitic and andesitic boulder up to 2 m in diameter also occur near the top of some pebbly mudstone beds. Beds of pebbly mudstone generally exhibit planar basal contacts. Some thick beds may however have very irregular and stepped basal contacts exhibiting up to 15 m of relief. Pebbly mudstone beds are typically amalgamated, forming successions up to 25 m thick.

Solitary beds of pebbly mudstone occur interstratified with the HCS sandstone and sandy mudstone facies of the MFA described above. These solitary beds are typically overlain by a bed of HCS sandstone.

Interpretation

The matrix-supported texture of the pebble mudstones is indicative of emplacement by subaqueous cohesive debris flows (Middleton and Hampton, 1973, 1976; Lowe, 1982; Nemec and Steel, 1984). Clasts within these flows are supported by the cohesive strength of a muddy matrix. These flows originated by the slumping of a muddy substrate. Deposition occurred en masse when the shear strength of the matrix exceeds the shear stress imposed on the flow, resulting in the matrix-supported texture. The

Fig. 4.30 Typical bed of the disorganized pebbly mudstone facies within the Haida Formation exposed on western Lina Island, Skidegate Inlet. Note the large rotated blocks of deformed interstratified sandstone and mudstone.

Fig. 4.31 Rafted concretions of light coloured calcareous mudstone at the top of a thick bed of disorganized pebbly mudstone within the Longarm Formation exposed near White Point, northwestern Graham Island. The resistantly weathering concretions rest within a recessively weathering mudstone matrix, which in this photo has been colonized by seaweed. The rafted clasts within the pebbly mudstone are abruptly overlain by a sharp based bed of HCS sandstone.

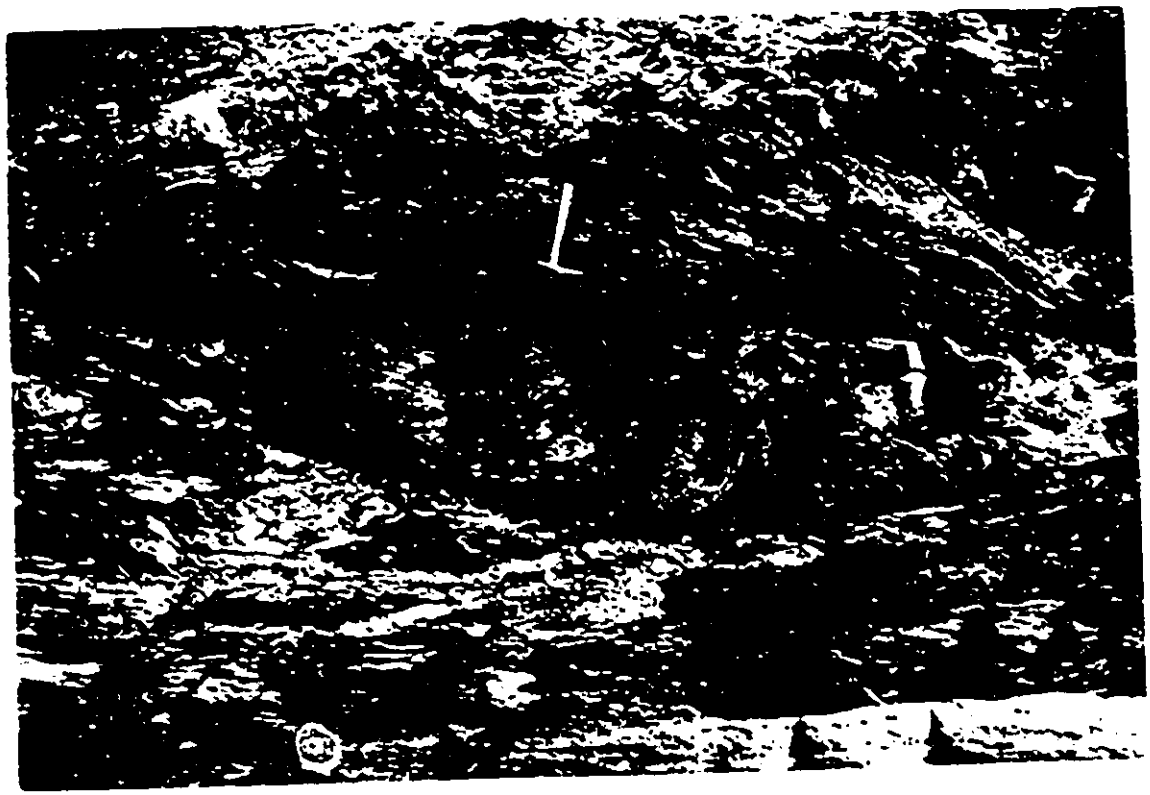

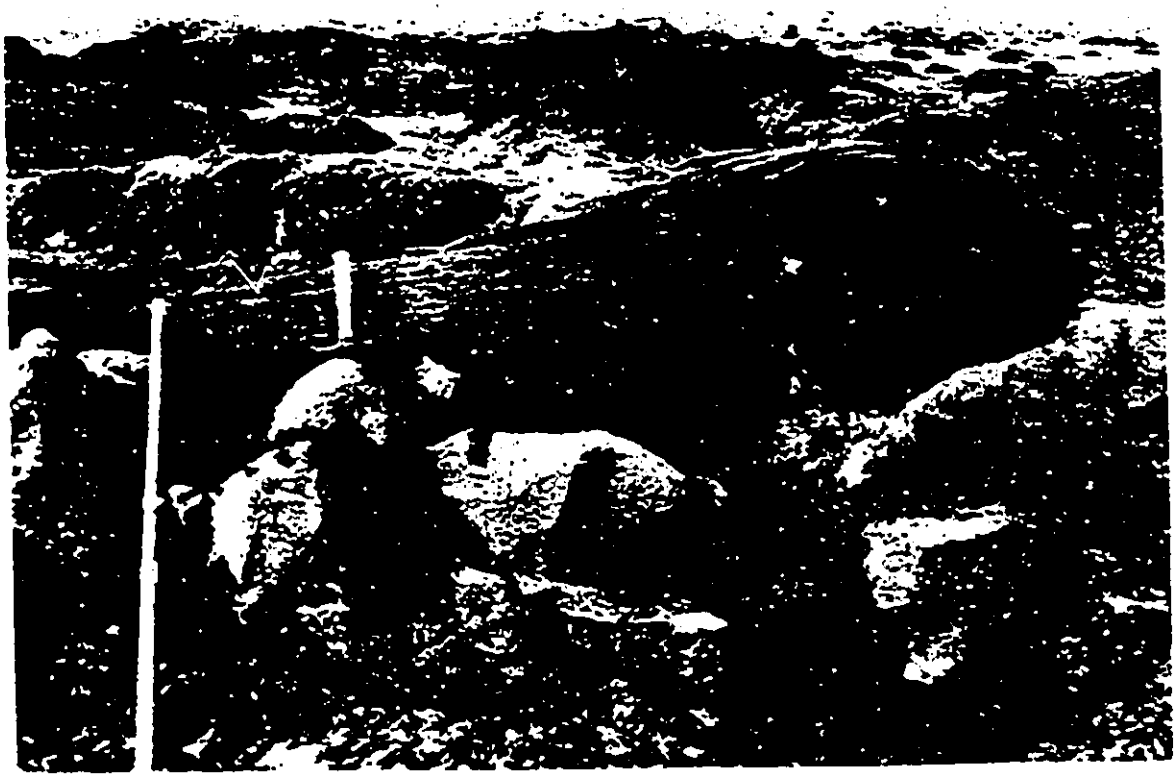

rafted clasts represent plugs carried at the top of the flows. The presence of large, relatively undeformed mudstone intraclasts indicates that the flows could not have travelled far from their origin. If they had, these large intraclasts would have been broken into much smaller pieces.

4.5.2. Intraclast breccia facies

Description

This facies consists of clast- to matrix-supported conglomerate or breccia forming sharp based beds between 0.1 and 2.5 m thick. Clasts consist of angular to rounded pebbles to boulders of deformed sandstone and mudstone; angular to rounded calcareous mudstone concretions; and rounded extraformational granitic and volcanic cobbles and boulders (Fig. 4.32). The conglomerates also contain abundant wood fragments, coprolites, ammonites, shark teeth, reptilian bones, and thick-shelled bivalves. The matrix consists of very poorly sorted sandy mudstone. Beds exhibit planar basal contacts and are massive or inversely graded. Rafted boulders occur along the tops of some conglomerate beds and protrude into overlying strata. The conglomerates are interstratified with beds of the pebbly mudstone facies. A 15 by 20 m olistolith of the structureless bioturbated sandstone facies occurs within the Haida Formation exposed on western McLelland Island in Cumshewa Inlet.

Fig. 4.32 Well rounded siltstone and mudstone intraclasts within a bed of clast supported intraclast conglomerate facies.

Fig. 4.33 Typical exposure of the thin bedded classical turbidite facies dipping towards upper left of photo. Note hammer in middle of photo.

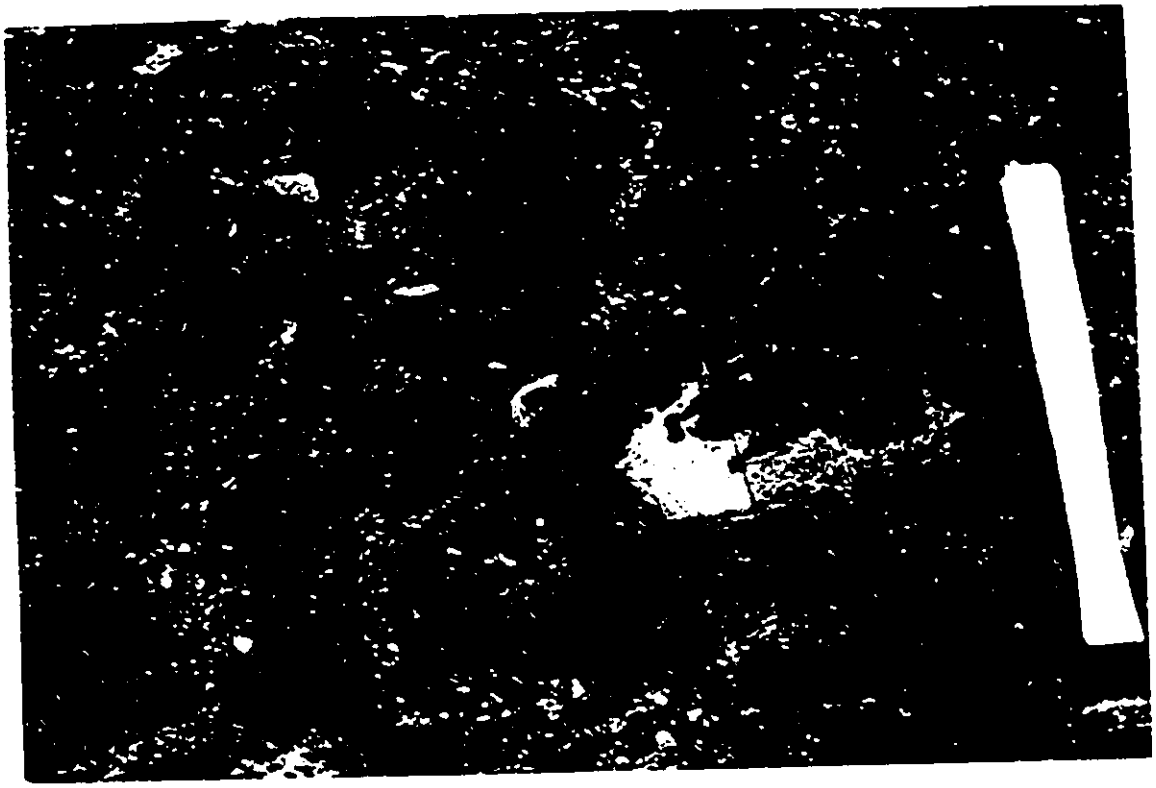

Interpretation

The matrix-supported texture of the breccias indicates that these beds, like the pebbly mudstones with which they are associated, were also emplaced by subaqueous debris flows. The composition of the breccias indicates that they originated the slumping of a siltstone dominated substrate, unlike the pebbly mudstones, which were derived by the failure of a muddy substrate. The presence of blocks of the bioturbated silty sandstone facies and a resedimented shallow water fauna within successions of this facies indicates that much of the sediment was probably derived from a nearshore environment. The small and well rounded nature of the majority of the intraclasts within the breccia beds indicates that they travelled relatively long distances prior to deposition.

4.6. DESCRIPTION OF THE TURBIDITE FACIES ASSEMBLAGE

4.6.1. Classical turbidite facies

Description

This facies consists of interbedded mudstone and sandstone forming successions up to 240 m thick. Sandstones beds are sharp based, non-amalgamated, and are thin (< 10 cm) to thick (2 m) bedded (Figs. 4.33). The sandstones are very fine to fine grained, and exhibit a vertical

arrangement of sedimentary structures which may be described in terms of Bouma's (1962) scheme for turbidite facies. Some thin bedded sandstones may exhibit a basal pebble lag composed of intra- or extraformational clasts. The T_c divisions of some thin bedded sandstones may be convolute. Thick bedded sandstones typically contain muddy rip-ups and are convoluted. Common traces within the sandstone beds include Chondrites, Rhizocorallium, Cosmorhaphe, Planolites, Muensteria, and Helminthopsis. The interbedded shales and bioturbated silty mudstones form between 50 and 95 % of a typical unit.

Solitary beds of the disorganized pebbly mudstone facies 0.5 to 11 m thick occur interstratified within successions of this facies.

Interpretation

The sandstones correspond to the pelitic-arenaceous I turbidite facies of Mutti and Ricci Lucchi (1972), and the thin- and thick bedded classical turbidite facies of Walker (1978). The disorganized pebbly mudstone beds interstratified with the turbidites are interpreted as muddy debris flows.

4.6.2. Thick bedded sandy turbidite facies

Description

This facies consists of amalgamated sandy beds forming successions ranging from 8 to 30 m thick. Sandstone beds exhibit sharp, convex-up basal contacts and are 0.2 to 2.1 m thick (Fig. 4.34). The sandstones are moderately well sorted, fine to coarse grained, and are massive (T_a) or parallel-laminated (T_b). The T_b division of many thick bedded sandstones exhibits parting lineation. Some thick bedded sandstones are underlain by clast-supported poorly sorted pebble and cobble rip-up breccias 0.1 to 1.7 m thick.

Interpretation

This facies corresponds to the arenaceous turbidite facies of Mutti and Ricci Lucchi (1972) and the massive sandstone facies of Walker (1978), which are believed to deposited by high density sandy turbidity currents (Lowe, 1977, 1982). The intraclast breccias underlying some thick bedded sandstones are interpreted as erosive lags.

4.7. FACIES SUCCESSIONS WITHIN THE SFA AND THE MFA

In this section, the various facies successions observed within the deposits of the SFA and MFA of the Longarm, Haida and Skidegate Formations will be described

Fig. 4.34 Amalgamated beds of the thick bedded sandy turbidite facies. Note the scoured basal contact of the bed immediately above the hammer. Most of the beds within the photo display the T_b division of Bouma (1968).

and interpreted. Two scales of cyclicity are observed. On the smaller scale are coarsening-upward successions between 5 and 140 m thick. These successions are bound above and below by flooding surfaces. The small scale successions are stacked vertically to form larger scale fining-upward successions up to 600 m thick. These larger scale entities are bound by erosional surfaces which may be correlated on a regional basis, unlike the flooding surfaces bounding the smaller scale coarsening-upward successions, which may be correlated only on a local basis. Finally, the legend for all of the following measured sections is presented in Table 4.2.

4.7.1. Small scale sandy coarsening-upward successions

Description

Three coarsening-upward successions 16 to 150 m thick are observed within the Late Valanginian to Hauterivian (Haggart, 1992; Gamba, 1993) deposits of the Longarm Formation exposed south of White Point on northwest Graham Island (Fig. 4.35). Each succession exhibits an upward increase in grain size and a characteristic vertical arrangement of facies. The lower part of each succession is composed of the deposits of the DFA and/or MFA, while the upper part is composed of the deposits if the SFA.

Only the uppermost succession contains deposits of

Table 4.2 Legend of the various facies used to construct the following stratigraphic sections.

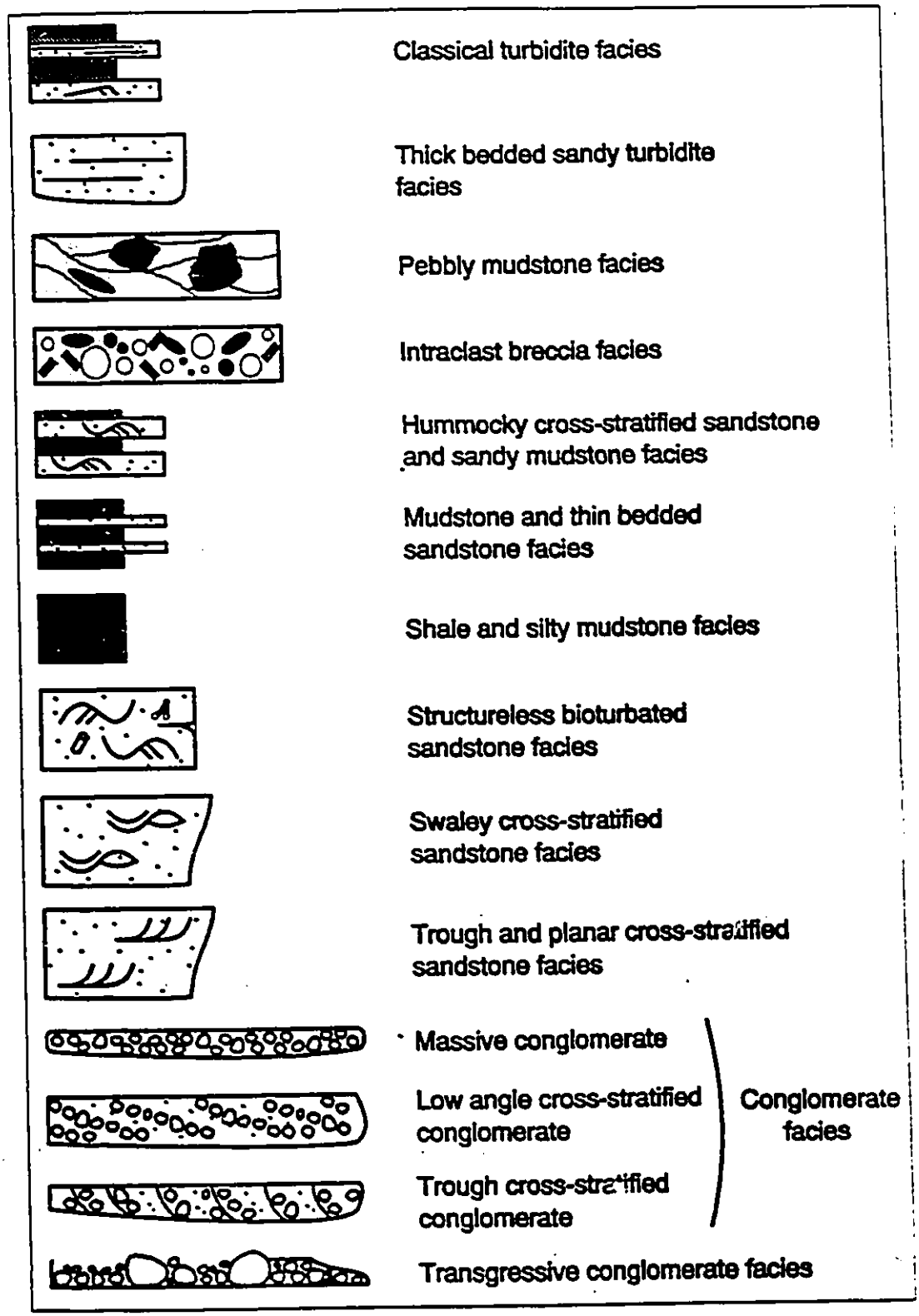
Classical turbidite facies
Thick bedded sandy turbidite facies
Pebbly mudstone facies
Intraclast breccia facies
Hummocky cross-stratified sandstone and sandy mudstone facies
Mudstone and thin bedded sandstone facies
Shale and silty mudstone facies
Structureless bioturbated sandstone facies
Swaley cross-stratified sandstone facies
Trough and planar cross-stratified sandstone facies
Massive conglomerate
Low angle cross-stratified conglomerate
Trough cross-stratified conglomerate
Conglomerate facies
Transgressive conglomerate facies

Fig. 4.35 Section through the Longarm Formation exposed south of White Point, northwestern Graham Island (see Fig. 2.1 for location). Note the three coarsening-upward successions. MFA - mudstone facies assemblage, SFA - sandstone facies assemblage, DFA - disorganized facies assemblage.

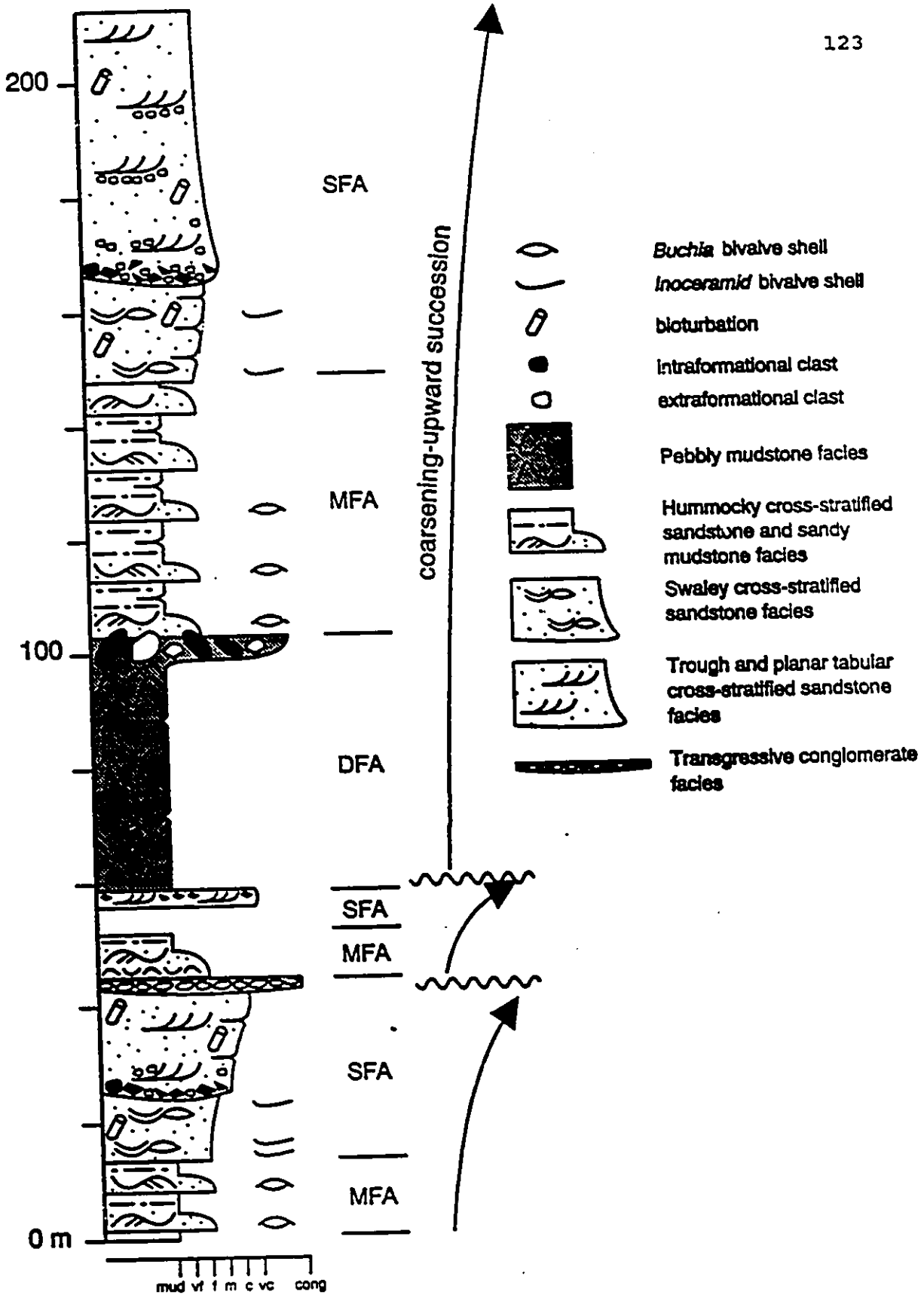
200
100
0 m
SFA
MFA
DFA
SFA
MFA
SFA
MFA
coarsening-upward succession
mud vf f m c vc cong
Buchia bivalve shell
Inoceramid bivalve shell
bioturbation
intraformational clast
extraformational clast
Pebbly mudstone facies
Hummocky cross-stratified sandstone and sandy mudstone facies
Swaley cross-stratified sandstone facies
Trough and planar tabular cross-stratified sandstone facies
Transgressive conglomerate facies

DFA, which form the lower 42 m of the succession. These deposits consist of amalgamated beds of the pebbly mudstone facies. Large well rounded boulders of andesite and granodiorite up to 2 m in diameter, as well a angular mudstone intraclasts, occur at the top of the DFA within this succession. The deposits of the DFA are overlain by 45 m of the MFA. Similar deposits also form the lower part of the two older successions. The deposits of the MFA within all three successions are composed primarily of the HCS sandstone and sandy mudstone facies. The number and thickness of HCS fine grained sandstone beds tends to increase upwards within each succession. This trend is accompanied by an increased tendency towards amalgamation of the HCS sandstone beds. HCS sandstone beds within the lower part of these successions exhibit well developed Buchia bivalve shell lags. The thickness and abundance of these lags decreases upwards within each succession.

The deposits of the MFA within each succession are abruptly overlain by those of the SFA, which varies between 3 and 65 m thick. The contact between the two assemblages is erosional. The lower part of each of the SFA's is composed of the SCS sandstone facies, while the upper part is composed of the trough cross-stratified sandstone facies. The SCS sandstones are fine grained, while the overlying trough cross-stratified sandstones are medium to coarse

grained. The SCS sandstones at the base of the SFA within the lower- and uppermost successions are 13 and 18 m thick respectively. Some SCS sandstone beds contain abundant Inoceramid fragments, both within basal lags and scattered along laminae.

The SCS fine grained sandstones are abruptly overlain by 18 and 44 m respectively of trough and planar-tabular cross-stratified medium grained pebbly sandstone. The contact between the two within the lower- and uppermost successions is erosive, and is overlain by a thin breccia composed of angular pebbles and boulders of the underlying Inoceramid fragment-rich SCS sandstone (Fig. 4.36). The breccia also contains well rounded cobbles of granodiorite and andesitic.

The trough and planar-tabular cross-stratified sandstones of the lowermost succession are abruptly overlain by a clast-supported pebble conglomerate. This conglomerate contains abundant articulated Buchia and Trigonid bivalves (Fig. 4.37). The conglomerate is in turn overlain by sandy mudstones of the overlying succession.

Interpretation

The pebbly mudstones forming the DFA of the uppermost succession are interpreted as the deposits of cohesive muddy debris flows. The debris flows may have been triggered by a

Fig. 4.36 Irregular erosional contact between light coloured Inoceramid fragment-rich SCS fine grained sandstones and darker coloured trough cross-stratified coarse grained pebbly sandstones within lowermost coarsening-upward succession exposed near White Point. Approximately 1.2 m of erosional relief along this particular contact. Angular pebbles and cobbles of the SCS sandstones occur within the overlying trough cross-stratified sandstones.

Fig. 4.37 Bed of massive conglomerate capping the lowermost coarsening-upward succession within the Longarm Formation exposed near White Point. Note the thin shelled articulate bivalves within the matrix of the conglomerate. Scale is 9 cm long.

variety of mechanisms including seismic shocks, oversteepening, rapid rates of sedimentation, or cyclic wave loading during storm events (Nardin et al., 1979; Myrow and Hiscott, 1991). The presence of large extraformational boulders within some of the disorganized beds indicates that the flows may have been derived by the slumping of proximal nearshore or fluvial deposits. The occurrence of a bed of HCS sandstone immediately overlying the debris flow at the top of the DFA (Fig. 4.31) indicates that the flows were emplaced within an environment situated between storm and fairweather wave base.

The MFA's of each succession were deposited within a wave-dominated offshore environment. This is inferred from the fact that most of the sandstone beds within each of the successions were deposited under oscillatory current conditions. The Buchia bivalve lags underlying many of the HCS sandstone beds are interpreted as parauthochthonous shell lags formed by winnowing of the sea floor during storm events (Kriesa, 1981; Aigner, 1982; Kriesa and Bambach, 1982).

The interbedded sandy mudstones separating HCS sandstone beds were deposited primarily from hemipelagic suspension between storm events. The presence of traces belonging to the Cruziana and Zoophycos ichnofacies within these deposits is indicative of deposition within a moderate

to relatively low energy sublittoral to bathyal environment (Pemberton et al., 1992).

The upward increase in the thickness and tendency towards amalgamation of HCS sandstone beds within the MFA's of the lowermost and uppermost successions reflects a shoaling trend. The amalgamation of HCS sandstone beds is attributed to deposition within relatively more energetic environments (Duke, 1985). The increasing thickness of HCS sandstone beds upwards is accompanied by a gradual disappearance of in situ Buchia bivalves within the interstratified sandy mudstones. This indicates that the Buchia bivalves could not tolerate the increase in current strength which accompanied shoaling.

The SCS sandstones of the overlying SFA within each succession were deposited within a wave dominated shallow shoreface environment situated below fairweather wave base (Walker et al., 1983; Walker and Plint, 1992). The fragmented nature of the Inoceramid valves within the shell lags indicates that they are allochthonous, unlike the parautochthonous Buchia lags underlying the HCS sandstones.

The prevalence of trough cross-stratification within the overlying medium grained sandstones suggests that they were deposited within the zone of breaking waves in a shoreface environment situated above fairweather wave base. Clifton et al. (1971), Davidson Arnott and Greenwood (1976),

Hunter et al. (1979), Howard and Reineck (1981), and Short (1984) documented similar sedimentary structures upon modern barred and nonbarred high energy shorefaces which are dominated by small and medium scale dunes. The dunes upon these shorefaces were observed to migrate either onshore under the influence of storm-generated unidirectional currents or alongshore under the influence of longshore currents. The absence of wave-generated oscillatory current formed sedimentary structures within these uppermost sandstones may be attributed to reworking by fairweather wave processes. The occurrence of traces belonging to the Skolithos ichnofacies within the trough cross-stratified sandstone is indicative of deposition within an energetic shoreface environment (Pemberton et al., 1992).

The upward coarsening trend in grain size, the vertical arrangement of facies, and the distribution of trace fossils within each of the three successions reflects a shoaling trend. This shoaling trend reflects the progradation of a high energy sandy shoreface into a muddy storm dominated offshore environment. The erosional contact separating the muddy offshore deposits of the MFA and the SCS shoreface sandstones of the SFA within the lower and uppermost successions may be attributed to shoreface erosion by fairweather wave scour during the course of shoreface progradation (Plint, 1988, 1991).

There are two possible explanations regarding the origin of the erosional contact between the SCS and trough cross-stratified sandstones of the lower and uppermost successions (Fig. 4.36). The first is that the SCS sandstones and the overlying trough cross-stratified sandstones represent two different stacked shorefaces; the lower wave dominated, the upper longshore current dominated. The erosive contact between the SCS and trough cross-stratified sandstones may therefore be attributed to shoreface progradation in response to an abrupt drop in relative sea level (a "forced regression" of Plint, 1991). An abrupt drop of relative sea level would have resulted in wave scouring of the underlying SCS deposits in front of the prograding shoreface. Early cementation of the underlying SCS sandstones provided a firm substrate which was scoured and brecciated during shoreface progradation. A sudden drop in relative sea level would also account for the change in grain size and the introduction of extraformational pebbles within the overlying trough and planar-tabular cross-stratified sandstones.

Alternatively, the erosional contact between the SCS sandstones and the trough cross-stratified sandstones may be attributed to the progradation of a barred shoreface. Hunter et al. (1979) suggested that the progradation of a longshore trough would superimpose trough cross-stratified

upper shoreface sandstones over lower shoreface and offshore deposits. The erosive contact separating the deposits of the two environments would represent an erosional lag concentrated at the base of the longshore trough. The SCS sandstones within the lower and uppermost successions would therefore represent lower shoreface deposits which were truncated by the base of a longshore trough as the shoreface prograded. In this context, the SCS and trough cross-stratified sandstones would represent the deposits of a single progradational shoreface.

The thin bed of poorly sorted cobble conglomerate separating the shoreface sandstones of the lowermost succession from the overlying muddy offshore deposits of the middle succession is interpreted as a winnowed lag. This lag is composed of gravelly shoreface and nonmarine deposits which once capped the underlying succession, and were subsequently reworked during the course of marine transgression. The abundance of calcareous fossils within the transgressive lag is typical of condensed beds deposited during periods of marine transgression (van Wagoner et al., 1989; Kidwell, 1991).

Each of the successions therefore represents the progradation of a high energy sandy shoreface into a storm dominated muddy offshore or slope environment during a period of sea level fall or stillstand. The possibility

that the SFA's of the lower- and uppermost successions each contain two stacked shorefaces indicates that sea level may have fallen abruptly at some point during progradation. Shoreface progradation was terminated by a relative rise in sea level, which was accompanied by the incision of a transgressive ravinement surface and a return to deposition within a muddy offshore environment.

The occurrence of debris flow deposits at the base of the lowermost succession suggests that progradation of the shoreface may have coincided with widespread failure of the muddy offshore environment. The presence of granitic and andesitic boulders within the debris flows is puzzling, given the lack of such coarse sediment within the overlying shoreface succession. This may suggest that the shoreface was bypassed in places, resulting in coarse sediment being supplied directly to the offshore where it was subsequently resedimented in the form of debris flows.

4.7.2. Small scale gravelly coarsening-upward successions

Description

Five successions between 5 and 40 m thick are observed within the deposits of the SFA of the Longarm Formation on Arichika Island (Fig. 4.38). Each succession exhibits a coarsening-upwards trend in grain size and a characteristic vertical arrangement of sedimentary

Fig. 4.38 Measured section through the SFA of the Longarm Formation exposed at Arichika Island. Note the five coarsening-upward successions, and the fining-upward succession at the top.

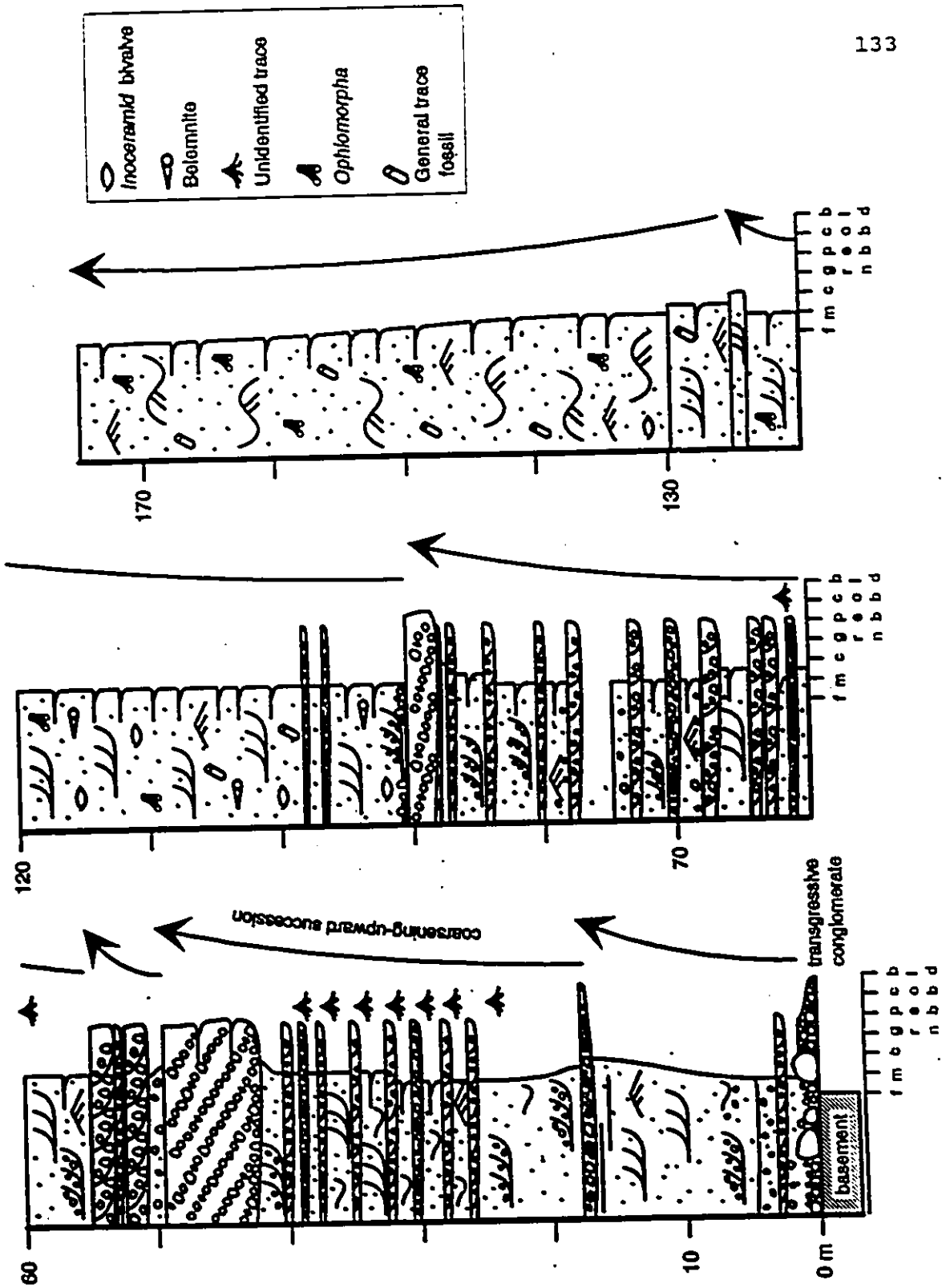
Inoceramid bivalve
Belemnite
Unidentified trace
Ophiomorpha
General trace fossil
170
130
120
70
80
10
0 m
basement
transgressive conglomerate
coarsening-upward succession
f m c g p c b
r e o l
n b b d

structures (Fig. 4.39). The successions are separated from the underlying Late Triassic Peril Formation by an angular unconformity (Fig. 4.3). The unconformity is overlain by a massive bed of very poorly sorted clast-supported boulder conglomerate 1.5 to 15.4 m thick. Clasts within the conglomerate are well-rounded to angular, depending upon their lithology, and exhibit no organized fabric. The conglomerate contains a rounded boulder of Yakoun andesite 15 m in diameter. The sandstone matrix is poorly-sorted and contains oyster shell fragments.

The lower part of each succession consists of 2 to 35 m of the trough and planar-tabular cross-stratified sandstone facies (Figs. 4.38 and 4.39). The grain size within the sandstones increases from fine or medium grained at the base to medium or coarse grained and pebbly at the top. The sandstones contain abundant Inoceramid bivalve shells, both articulate and disarticulate, and exhibit a variety of traces belonging to the Skolithos ichnofacies of Pemberton et al. (1992) including Skolithos, Macronichnus, Ophiomorpha, and an unidentified trace (Fig. 4.7). Tabular beds of trough cross-stratified (Fig. 4.8) or structureless pebble conglomerate (Fig. 4.11 and 4.12) and minor beds of HCS sandstone are interstratified with the sandstones. The conglomerate beds become more common upward within each succession.

Fig. 4.39 Schematic model of a gravelly coarsening-upward succession within the Longarm Formation based on three measured sections from Arichika Island (one of which is illustrated in Fig. 4.38).

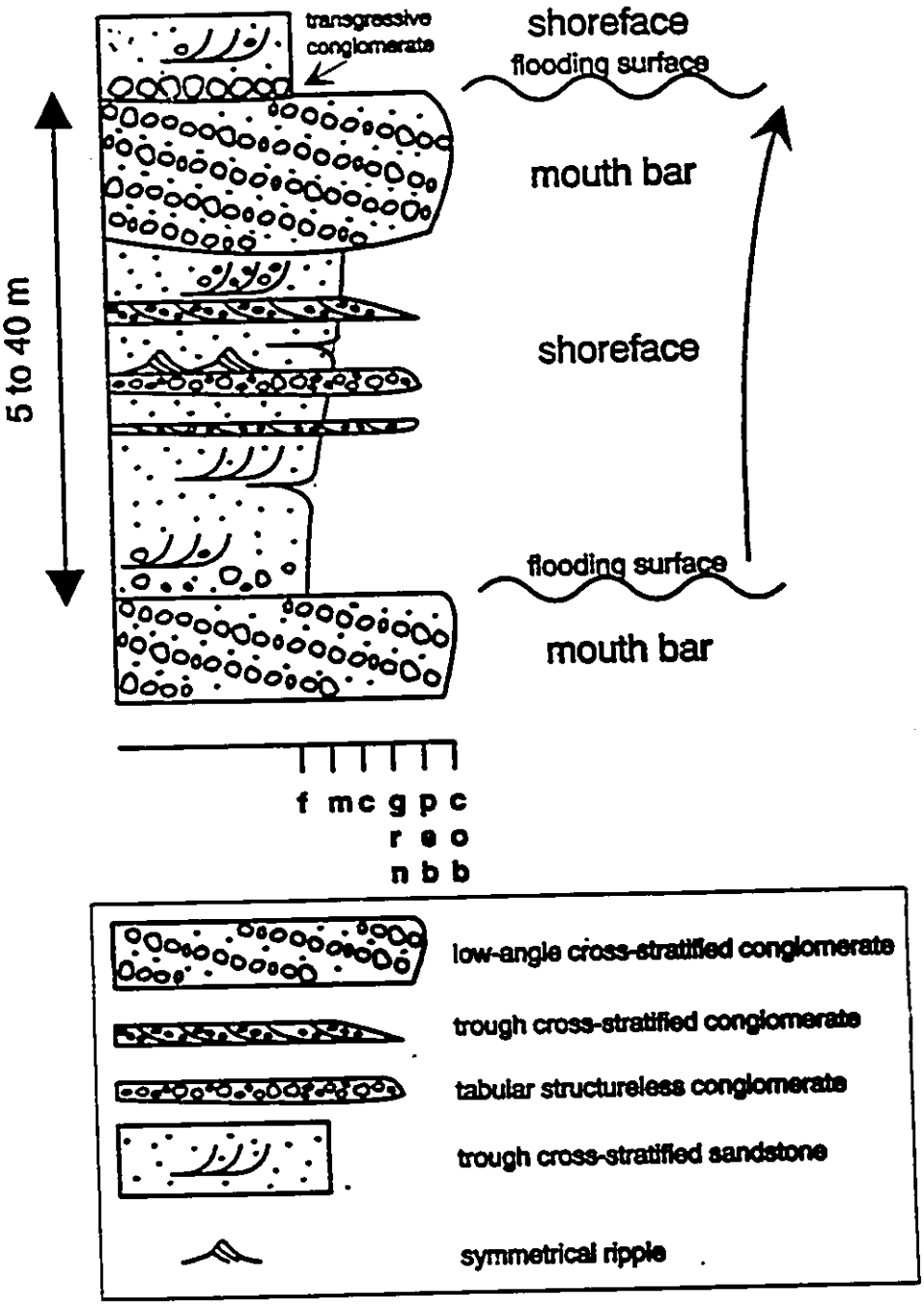
transgressive conglomerate
shoreface
flooding surface
mouth bar
shoreface
flooding surface
mouth bar
5 to 40 m
f
m
c
g
p
c
r
e
o
n
b
b
low-angle cross-stratified conglomerate
trough cross-stratified conglomerate
tabular structureless conglomerate
trough cross-stratified sandstone
symmetrical ripple

The cross-stratified sandstones within each succession are abruptly overlain by 1 to 7 m of the low-angle to cross-stratified conglomerate facies (Fig. 4.13). The conglomerates within many of the successions are capped by a thin bed of poorly sorted cobble lag. The lags are clast-supported and contain a well sorted medium to coarse grained sandstone matrix containing bivalve fragments, and are abruptly overlain by the cross-stratified sandstones of the next succession.

The five successions are overlain by a 40 m succession of the trough and planar tabular cross-stratified sandstone facies. The grain size within this succession changes from fine grained at the base to medium and coarse grained at the top. This succession is in turn overlain by 55 m of the structureless bioturbated sandstone facies.

Somewhat similar coarsening-upward successions are observed within Early Albian deposits of the Haida Formation exposed to the east of Onward Point (Fig. 4.40). Three fully or partially preserved coarsening-upwards successions up to 36 m thick occur at this location. The lower part of a typical succession consists of the fine grained structureless bioturbated sandstone facies. This facies contains abundant well developed beds of HCS sandstones which become amalgamated upward. The HCS sandstones are abruptly overlain by beds of medium grained SCS sandstone

Fig. 4.40 Measured section of the Haida Formation exposed to east of Onward Point in Skidegate Inlet. Note the gravelly coarsening-upward successions.

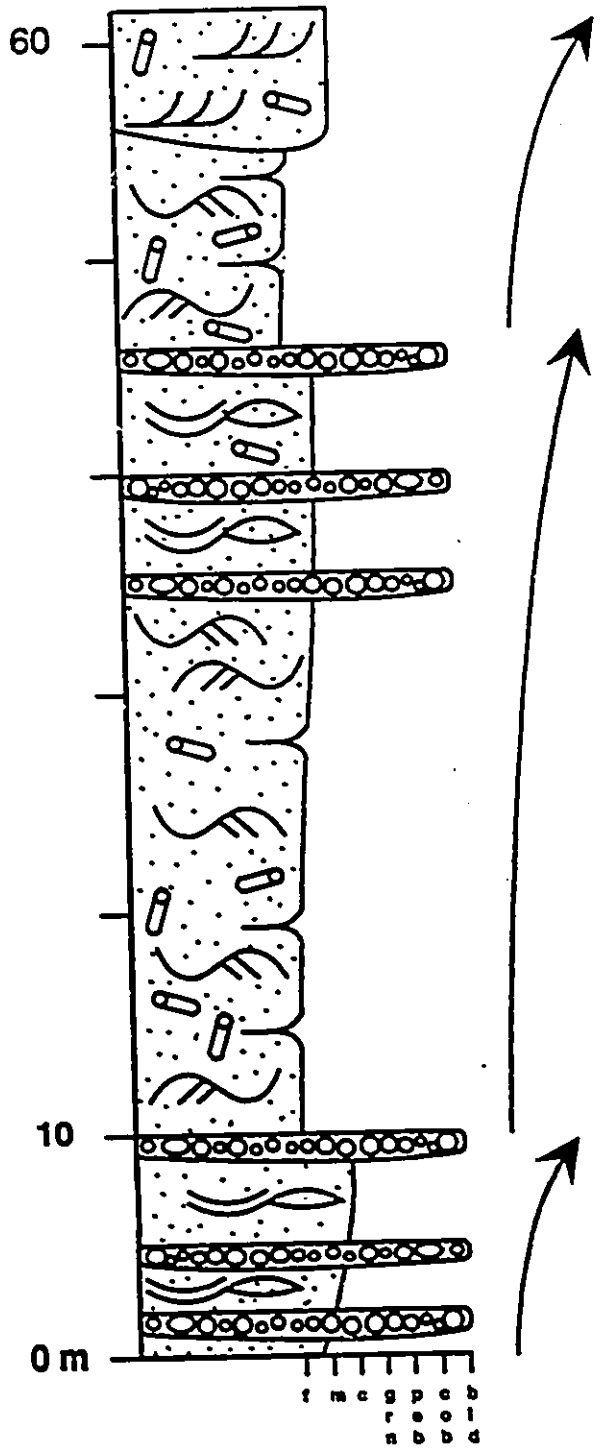
60
10
0 m
f
m
c
g r a n
p e b
c o b
b l d

and interstratified massive pebble conglomerate or beds of coarse grained trough and planar tabular cross-stratified sandstone. The coarser grained deposits are abruptly overlain by the finer grained structureless bioturbated sandstones of the overlying succession.

Interpretation

The basal conglomerate underlying the succession exposed on Arichika Island is interpreted as a transgressive lag deposited within a high energy foreshore environment situated adjacent to a rocky headland. The oyster fragments within the matrix of the conglomerate indicate that it was deposited in a marine or marginal marine environment. The clasts were derived directly from an adjacent coastal cliff. Following emplacement, the smaller pebble and cobble clasts were rounded within the swash zone. Rounding within this zone is particularly effective on modern cobble beaches (Bluck, 1968). The 15 m boulder probably avalanched directly off of the cliff into the surf zone. This particular boulder was too large to have been moved landwards by the normal velocity asymmetry of the oscillatory bottom currents operating in the surf zone (Kumar, 1976), so it remained where it fell. The rounded nature of this particular boulder may be attributed to the abrasive action of smaller clasts and sand being tossed

about in the surf zone.

Each of the five overlying successions is interpreted as the deposits of a progradational shoreface/mouth bar (Fig. 4.41). The cross-stratified sandstones forming the bulk of each succession were deposited within a high energy shoreface environment. The predominance of trough and planar cross-stratification within these sandstones indicates that deposition occurred mainly under the influence of unidirectional currents within an environment situated above fairweather wave base. The scarcity of interstratified HCS sandstone beds indicates that storm generated sedimentary structures formed within this environment were subsequently reworked by unidirectional fairweather currents. The occurrence of traces belonging to the Skolithos ichnofacies is indicative of deposition within a high energy shoreface environment (Pemberton et al., 1992).

The cross-stratified conglomerates interbedded within the shoreface sandstones represent the deposits of three dimensional dunes which migrated under the influence of unidirectional currents. Gravel may have originally been emplaced in the nearshore as mouth bar deposits and subsequently transported onto the shoreface by rip currents. These gravels were then redistributed upon the shoreface by unidirectional currents, resulting in the deposition of the

Fig. 4.41 Depositional model of a progradational gravelly mouth bar / shoreface succession based on successions exposed at Arichika Island.

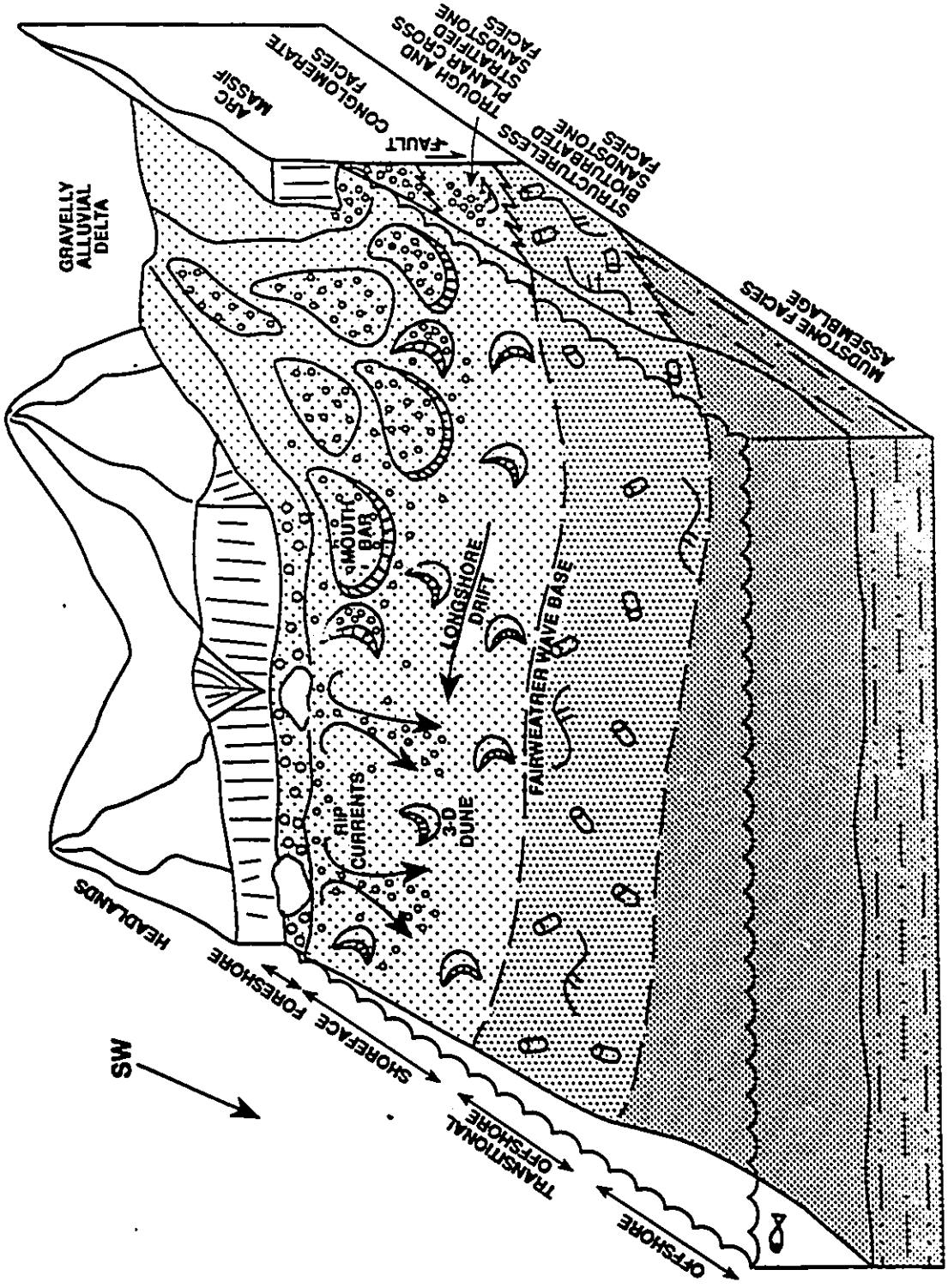
GRAVELLY ALLUVIAL DELTA
ARC MASSIF
CONGLOMERATE FACIES
FAULT
TROUGH AND PLANAR CROSS STRATIFIED SANDSTONE FACIES
STRUCTURELESS BIOTURBATED SANDSTONE FACIES
MUDSTONE FACIES ASSEMBLAGE
MOUTH BAR
LONGSHORE DRIFT
FAIRWEATHER WAVE BASE
RIP CURRENTS
3-D DUNE
HEADLANDS
FORESHORE
SHOREFACE
TRANSITIONAL OFFSHORE
OFFSHORE
SW

cross-stratified conglomerates. The tops of some cross-stratified sets were subsequently reworked into symmetrical wave ripples by oscillatory wave-generated currents (Fig. 4.9).

The beds of structureless conglomerate interstratified with the shoreface sandstones are interpreted as storm winnowed lags. The crude normal grading within these conglomerates is indicative of deposition from waning currents. The abundance of Inoceramid valves within many of these beds indicates that the clasts were derived by the reworking of gravels within the shoreface. The tops of some of these conglomerates were subsequently reworked into pebbly symmetrical ripples by oscillatory wave-generated currents. Kumar and Sanders (1976) documented similar normally graded conglomerates in cores from the shoreface off of Long Island, New York. Gravel within these lags was emplaced upon the shoreface by rip currents and subsequently reworked into a normally graded lag during the waning phases of a storm event. Similar storm emplaced beds of normally graded conglomerate interstratified with sandy shoreface deposits have also been identified from the Pleistocene of Monterey Bay, California (Dupre et al., 1980), the Miocene of the Caliente Range, southern California (Clifton, 1981), the Cretaceous Moosebar - Lower Gates interval of British Columbia (Leckie and

Walker, 1982), and the Miocene of Floras Lake (Leithold and Bourgeois, 1984).

The thick amalgamated beds of trough cross-stratified conglomerate capping some of the successions are interpreted as gravelly dunes deposited near the mouths of distributary channels under the influence of unidirectional currents. The low angle cross-stratified conglomerates capping many of the successions are interpreted as toeset deposits emplaced on the lee side of large gravelly mouth bars. The inverse grading within most of the low angle inclined strata indicate that they were deposited by density modified grainflows. The grainflows were probably initiated by the avalanching of fluvially deposited gravels emplaced on top of the bar. The occurrence of thin wave rippled sandstones interstratified with some of the gravelly toesets indicates that some of the grainflow deposits were subsequently reworked by oscillatory currents.

Leckie and Walker (1982) and Leithold and Bourgeois (1984) described similar low angle cross-stratified conglomerates from the Cretaceous Moosebar - Lower Gates Interval of British Columbia and the Miocene of Floras Lake respectively. These authors interpreted the conglomerates as the deposits of low amplitude bars deposited within a lower shoreface environment. The authors suggested that the bars migrated onshore under the influence of storm generated

currents. The main difference between the conglomerates described by Leckie and Walker (1981) and Leithold and Bourgeois (1984) and those exposed on Arichika Island is that the former were deposited within a lower shoreface environment, while the latter were deposited within an upper shoreface environment.

Each succession therefore reflects the progradation of a gravelly shoreface/mouth bar complex into a high energy sandy shoreface environment. The progradational nature of each succession is reflected by the upward increase in grain size and the vertical arrangement of sedimentary structures. The poorly sorted cobble conglomerates capping the mouth bar deposits of some of the successions are interpreted as transgressive lags deposited along ravinement surfaces. Stratigraphically, these lags separate the underlying gravelly mouth bar deposits of the succession below from the shoreface sandstones of the overlying succession. Cobbles within the lags were reworked from the underlying mouth bar and possible nonmarine deposits capping the succession during the course of transgression.

The 40 m thick coarsening-upward succession of cross-stratified sandstones overlying the uppermost progradational mouth bar succession is very similar in character to the lower parts of the underlying successions, and represent the deposits of a progradational high energy sandy shoreface.

The main difference is that it is not capped by gravelly mouth bar deposits. The overlying 55 m of bioturbated sandy siltstone were deposited within a relatively quite water transitional sandy offshore environment characterized by intense biological activity. This resulted in the complete destruction of all primary stratification. The intensity of biological activity within this facies indicates that it was deposited within a well oxygenated and relatively stable marine environment.

The coarsening-upward successions exposed within the Haida Formation east of Onward Point (Fig. 4.40) are interpreted as progradational wave dominated shoreface successions. This may be inferred from the vertical arrangement of sedimentary structures and ichnofacies within each succession.

4.7.3. Large scale fining-upward successions

Many large scale fining-upward successions 40 to 600 m thick are observed within the deposits of the Longarm and Haida Formations. Each succession exhibits a characteristic vertical arrangement of facies, a vertical decrease in grain size, and a vertical increase in the degree of bioturbation. This trend is observed within the Hauterivian to Aptian deposits of the Longarm Formation exposed at Sea Pigeon Island (Fig. 4.42 a), Poole Inlet (Fig. 4.42 b), Murchison

Island (Fig. 4.42 c), and Dawson Cove (Fig. 4.42 d). Fining-upward successions are also preserved within Albian to Cenomanian deposits of the Haida Formation exposed at Lauder Point (Fig. 4.43 a) and Beresford Bay (Fig. 4.43 b), and within the Skidegate Inlet (Fig. 4.44) and Cumshewa Inlet (Fig. 4.45) regions.

Description

All of the fining-upward successions within the Longarm Formation unconformably overlie pre-Cretaceous basement. The unconformity is overlain by a bed of the transgressive conglomerate facies. At Poole Inlet (Fig. 4.42 d) this bed is 16 m thick and consists of poorly sorted boulder conglomerate (Fig. 4.2). The largest boulders are well rounded and consist of quartz diorite derived directly from an underlying Late Jurassic Moresby Group pluton. Oyster shell fragments are scattered throughout the poorly sorted sandstone matrix of the conglomerate. The transgressive conglomerates at Poole Inlet are overlain by 90 m of the trough and planar cross-stratified sandstone facies (Fig. 4.42 d). The lowermost sandstones are medium to coarse grained and pebbly, which grade upward into well sorted fine-grained sandstone. The sandstones contain scattered Inoceramid bivalves and traces belonging to the Skolithos ichnofacies. The cross-stratified sandstones are

Fig. 4.42 Measured section of the Longarm Formation exposed in the southern archipelago at a) Dawson Cove b) Murchison Island, c) Sea Pigeon Island, and d) Poole Inlet. Note the upward-fining trend in grain size within each succession, the lower part of each composed of deposits belonging to the SFA, which grade upwards into deposits of the MFA.

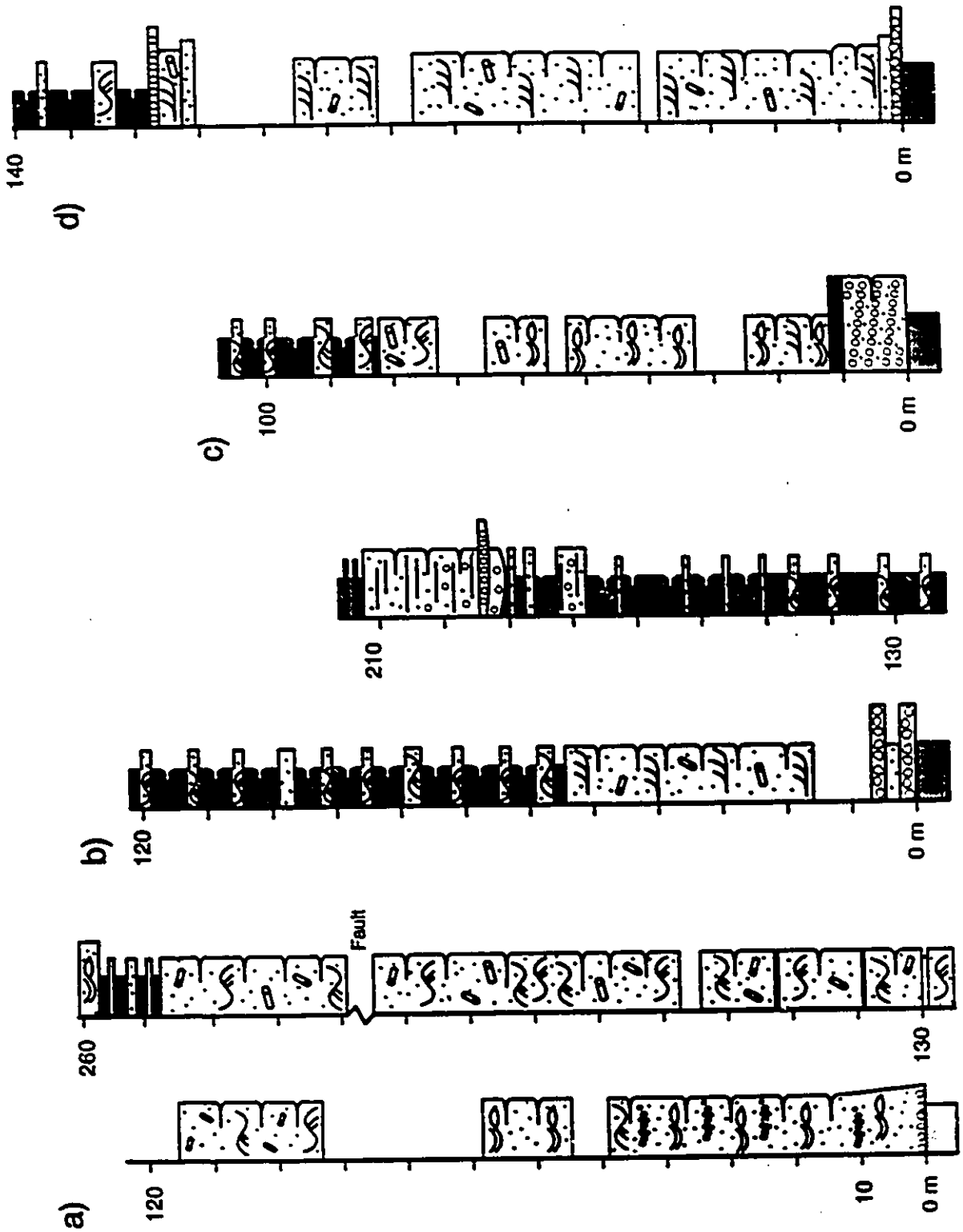
d)
140
0 m
c)
100
0 m
210
130
b)
120
0 m
Fault
260
130
a)
120
10
0 m

Fig. 4.43 Measured sections of the Haida Formation exposed on northwestern Graham Island at a) Lauder Point (Early to Late Albian) and b) northern Beresford Bay (Late Albian), and southern Beresford Bay (Late Albian).

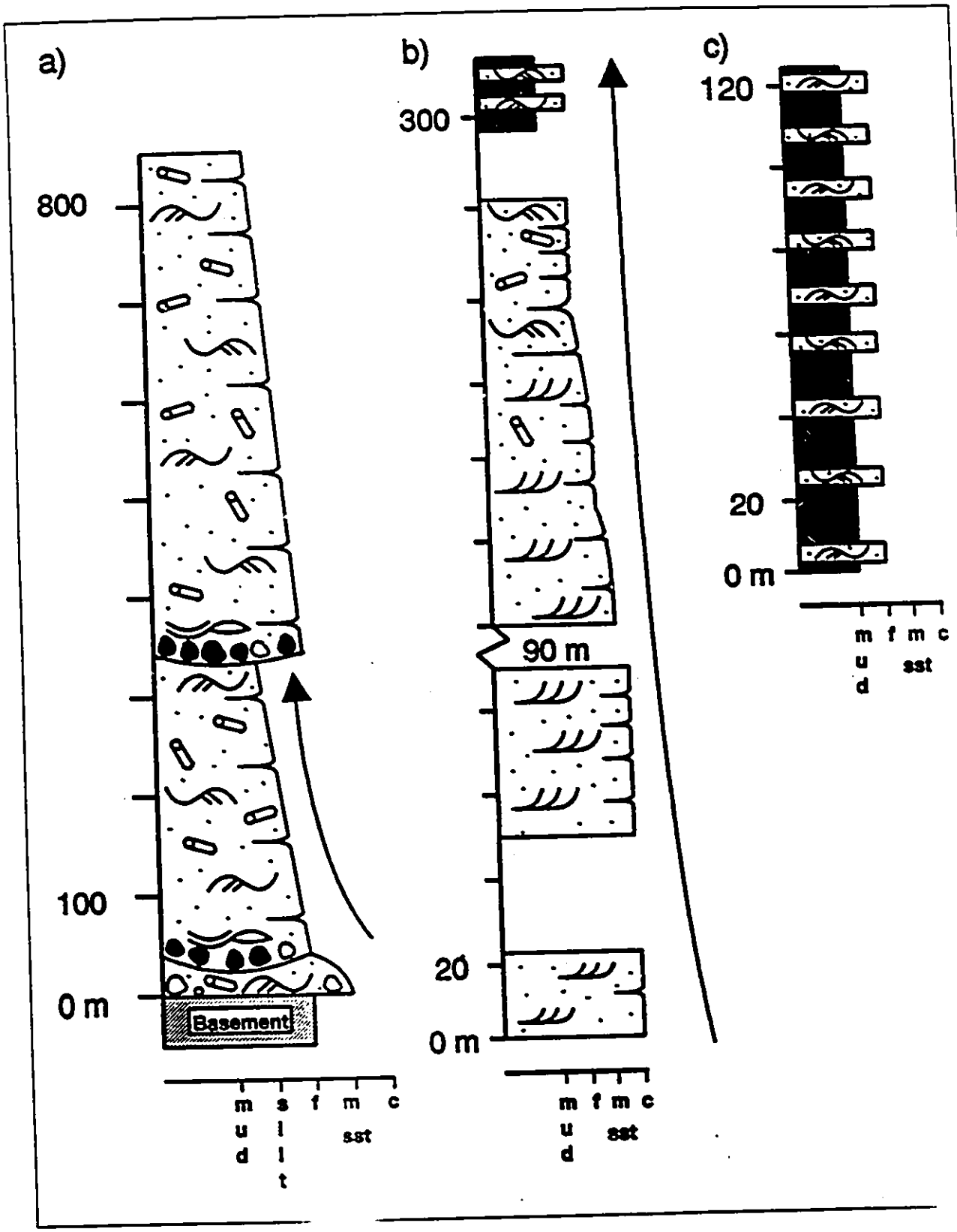
a)
800
100
0 m
Basement
m u d
s l l t
f
m sst
c
b)
300
90 m
20
0 m
m u d
f
m sst
c
c)
120
20
0 m
m u d
f
m sst
c

Fig. 4.44 Measured sections of the Albian to Cenomanian Haida Formation exposed in Skidegate Inlet at a) Bearskin Bay, b) Lina Island, c) Maude Island, d) Gooden Island, e) west of Onward Point, f) at Onward Point, and g) east of Onward Point. Biostratigraphic zonation of McLearn (1972), with ages of sections from Sutherland Brown (1968) and McLearn (1972).

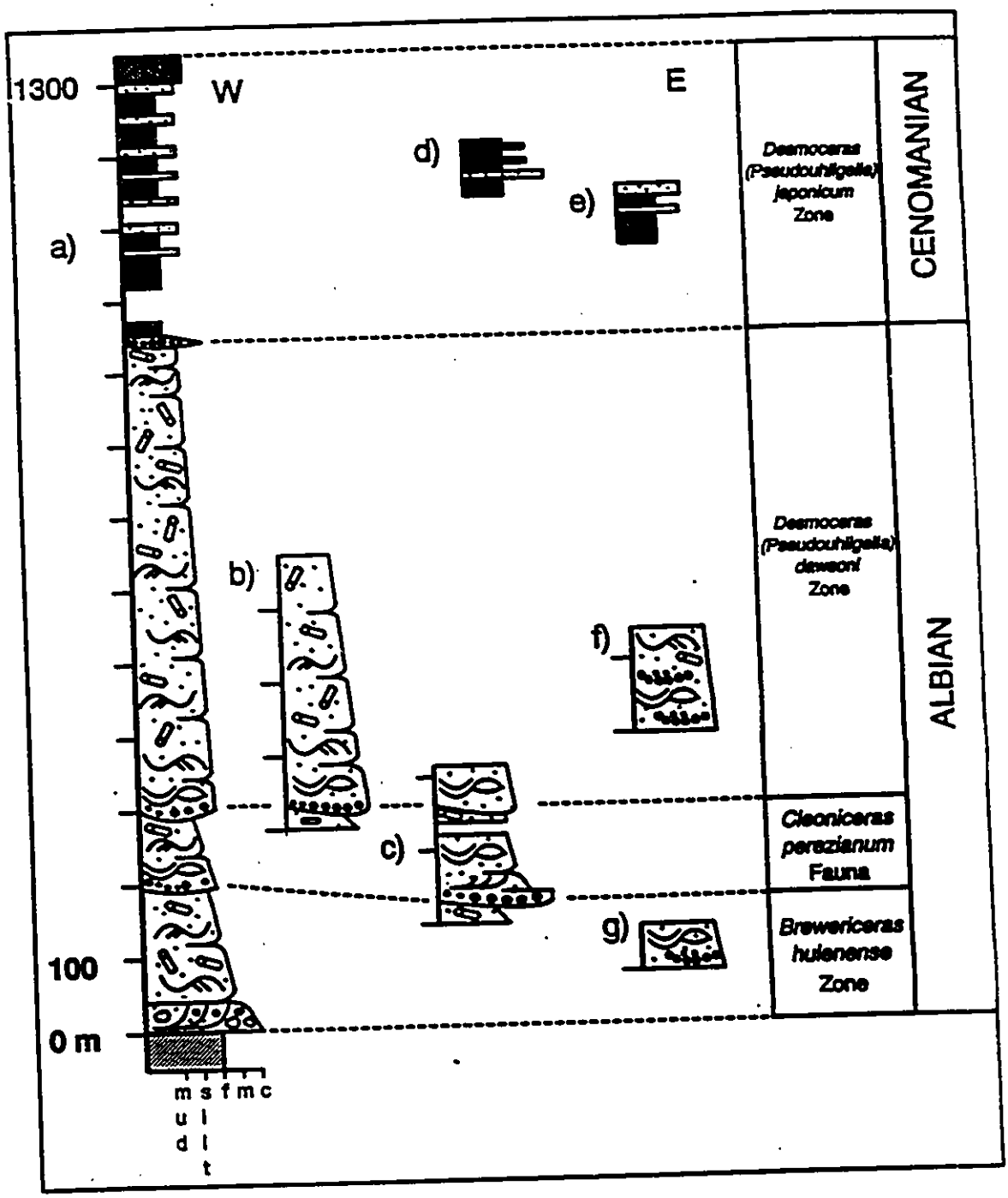
1300
W
E
a)
d)
e)
b)
f)
c)
g)
100
0 m
m s f m c
u l l
d t
Desmoceras (Pseudouhligella) japonicum Zone
Desmoceras (Pseudouhligella) dawsoni Zone
Cleoniceras perezianum Fauna
Brewericeras hulenense Zone
CENOMANIAN
ALBIAN

Fig. 4.45 Measured sections of the Haida Formation exposed in Cumshewa Inlet at a) eastern Dawson Cove (Early to Middle Albian), b) east of Conglomerate Point (Cenomanian), and c) McLelland Island (Late Albian to Cenomanian).

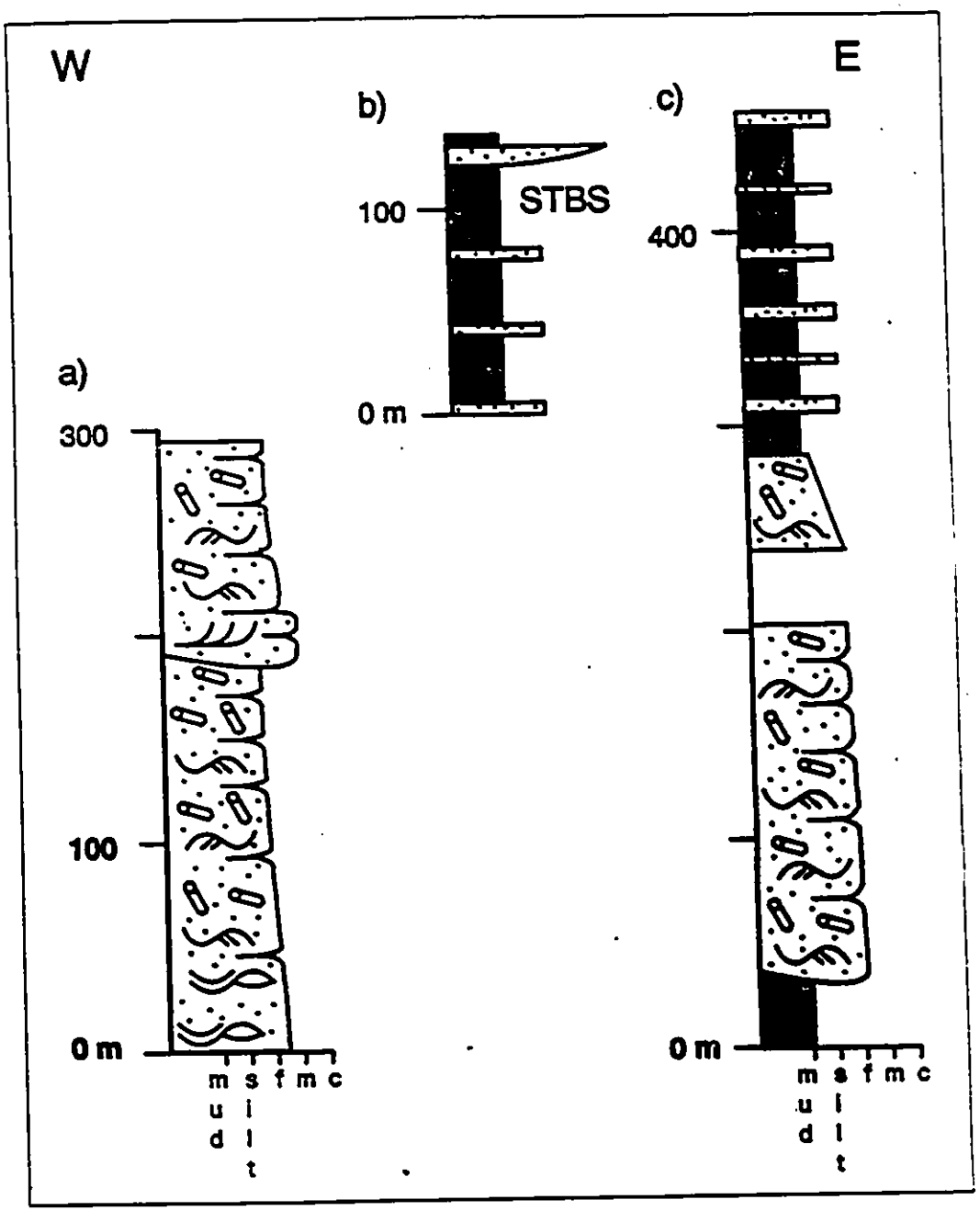
W
E
a)
b)
c)
STBS
300
100
0 m
100
400
0 m
0 m
m
u
d
s
i
l
t
f
m
c
m
u
d
s
i
l
t
f
m
c

abruptly overlain by 23 m of the black silty mudstone facies which contain abundant in situ Inoceramid bivalves and traces belonging to the Zoophycos ichnofacies. The mudstones also contain minor beds of HCS fine grained glauconitic sandstone.

At Murchison Island, the unconformity is overlain by a 7 m thick bed of the transgressive pebble conglomerate facies (Fig. 4.42 b). The conglomerate is overlain by 40 m of the trough and planar tabular cross-stratified sandstone facies identical in character to those at Poole Inlet. The cross-stratified sandstones are abruptly overlain by 90 m of the HCS sandstone and interstratified sandy mudstone facies which grade upward into 30 m of the silty mudstone facies. Sandstone beds within these facies contain traces belonging to the Zoophycos ichnofacies. The mudstones are abruptly overlain by deposits of the TFA, which will be described in a later section.

At Dawson Cove, the unconformity is overlain by 0.5 m of the transgressive pebble conglomerate facies (Fig. 4.42 a). The conglomerate is overlain by 80 m of the SCS sandstone facies, the lowermost sandstones being medium grained and pebbly. Lenticular beds of poorly sorted and massive pebble conglomerate are interstratified with the sandstones in the lower 50 m of the succession. The sandstones become progressively finer grained upwards, and

contain abundant Trigonid bivalves as well as traces belonging to the Skolithos ichnofacies. The SCS sandstones are overlain by 90 m of the structureless bioturbated fine grained sandstone facies which contains abundant ammonites and traces belonging to the Cruziana ichnofacies. The bioturbated sandstones are overlain by approximately 10 m of the HCS sandstone and interstratified sandy mudstone facies. These mudstones are abruptly overlain by SCS sandstones of the Albian Haida Formation.

At Sea Pigeon Island (Fig. 4.42 c), the unconformity is overlain by a massive 1 m thick bed of the transgressive pebble conglomerate facies. The conglomerate is overlain by 10 m of horizontally to low angle-stratified pebble conglomerate facies. Strata within the conglomerate are well sorted, and form well defined sets which are gently inclined. The conglomerates are in turn overlain by 2 m of cross-stratified pebble conglomerate and interbedded cross-stratified medium grained sandstone. These are overlain by 55 m of the fine grained SCS sandstone facies containing scattered Trigonid bivalves and traces belonging to the Skolithos ichnofacies. These sandstones are gradationally overlain by 9 m of the structureless bioturbated fine grained sandstone facies containing traces belonging to the Cruziana ichnofacies. These sandstones are abruptly overlain by 25 m of the HCS sandstone and interbedded sandy

mudstone facies.

Three fining-upward successions 40 to 510 m thick are observed within the Albian deposits of the Haida Formation exposed at Lauder Point (Fig. 4.43 a). The strata exposed here unconformably overlie Late Triassic basement of the arc massif. A typical succession exhibits an abrupt scoured basal contact overlain by a thin bed of the transgressive pebble conglomerate facies. The conglomerates are very poorly sorted and contain a very poorly sorted medium to coarse grained sandstone matrix (Fig. 4.4). Clasts within the conglomerate are composed primarily of sandstone concretions, with lesser granite and andesite. The conglomerates also contain abundant wood fragments. The conglomerates are overlain by medium grained SCS sandstones 3 to 10 m thick. This bed is gradationally overlain by up to 500 m of the fine grained structureless bioturbated silty sandstone facies. Beds of this facies contain abundant ammonites and traces belonging to the Cruziana ichnofacies. This facies becomes increasingly siltier and finer grained up section, and is abruptly overlain by the transgressive pebble conglomerates of the overlying succession.

A 310 m thick fining-upward succession of Late Albian age is exposed at Beresford Bay (Fig. 4.43 b). The lower 250 m of the succession consists of poorly sorted granular to medium grained trough and planar tabular cross-stratified

sandstone. The cross-stratified sandstones are gradationally overlain by 30 m of the fine grained structureless bioturbated sandstone facies. The succession is capped by 15 m of the HCS sandstone and sandy mudstone facies. A correlative 150 m thick succession of HCS sandstone and sandy mudstone is exposed 5 km to the south (Fig. 4.43 c).

Fining-upward successions of identical character are observed within the Albian to Cenomanian deposits of the Haida and Skidegate Formations exposed in the Skidegate Inlet region. At least three such successions 100 and 600 m thick are observed within the Albian sections exposed at Bearskin Bay (Fig. 4.44 a) and the correlative sections exposed on Lina and Maude Islands (Fig. 4.44 b and c respectively) immediately to the south. The successions exposed on Lina and Maude Islands are composed primarily of the SCS sandstone facies, unlike those exposed a Bearskin Bay, which are composed primarily of the structureless bioturbated sandstone facies.

The three successions exposed at Bearskin Bay are abruptly overlain by a fining-upward succession of Cenomanian age. The lower part of the succession consists of a 5 m thick bed of massive matrix-supported pebble conglomerate. The conglomerate contains a poorly sorted medium to coarse grained sandstone matrix. The conglomerate

is abruptly overlain by approximately 80 m of the shale and silty mudstone facies, which grades upwards into 240 m of the HCS sandstone and interstratified sandy mudstone facies. This facies contains numerous beds of coherently deformed mudstone and sandstone and pebbly mudstone. The abundance and thickness of interstratified sandstone beds within this succession increases gradually upwards. A bed of the thick bedded solitary sandstone facies is interstratified both within correlatives of the HCS sandstone and interstratified sandy mudstone and the shale and silty mudstone facies exposed on Gooden Island (Fig. 4.44 d). The deposits of the MFA exposed at section Bearskin Bay are abruptly overlain by the deposits of the DFA (Fig. 4.44 a), which will be described in a subsequent section.

Correlatives of the Albian successions exposed at Bearskin Bay, Lina, and Maude Islands are exposed to the east near Onward Point (Fig. 4.44 e, f, g). The succession exposed at Onward Point (Fig. 4.44 f) exhibits the same fining-upward trend in grain size as does its counterpart to the west. This succession consist of 100 m of the SCS sandstone facies overlain by 20 m of the structureless bioturbated sandstone facies, which is abruptly overlain by a 5 m thick bed composed of the trough and planar cross-stratified coarse grained sandstone facies.

Fining-upward successions similar to those exposed at

Lauder Point and Skidegate Inlet are also observed within the Albian to Cenomanian deposits of the Haida and Skidegate Formations exposed in Cumshewa Inlet (Fig. 4.45). Two well developed Albian aged fining-upward successions are observed in western Cumshewa Inlet (Fig. 4.45 a). A 450 m thick fining-upward succession is observed on McLelland Island in eastern Cumshewa Inlet (Fig. 4.45 c). This succession abruptly overlies the MFA of an early Albian succession. The lower part of the succession consists of 280 m of the SFA, which grade upward into 170 m of the MFA. Correlatives of the MFA exposed 10 km to the west (Fig. 4.45 b) contain beds of the solitary thick bedded sandstone facies up to 1.7 m thick.

Interpretation

The vertical decrease in grain size, arrangement of facies, and arrangement of ichnofacies within each of the fining-upward successions is indicative of deposition within progressively deeper and lower energy marine environments. The poorly sorted conglomerate or pebbly sandstone at the base of each of the successions were deposited within a high energy foreshore environment. This may be inferred from the fact that the conglomerates contain thick shelled oyster fragments and because the conglomerates are overlain by trough or SCS sandstones deposited within a shoreface

environment. The 16 m thick bed of massive conglomerate at the base of the Longarm Formation exposed at Poole Inlet (Fig. 4.42 d) may represent the deposits of a small coastal alluvial fan. These conglomerates may originally have been emplaced as debris flows shed from an adjacent coastal highland and subsequently reworked within a high energy rocky foreshore environment.

The horizontally- to low angle-stratified pebble conglomerates within the Longarm Formation exposed on Sea Pigeon Island (Fig. 4.42 c) are also interpreted as high energy foreshore deposits. The style of stratification within the conglomerates is typical of modern beach environments, where strata are inclined gently towards the sea (Allen, 1980). In addition, the well sorted nature of the strata may be indicative of deposition upon a beach (Bluck, 1968). The stratigraphic position of the conglomerates is also indicative of deposition within a foreshore or very shallow marine environment.

The trough and planar tabular cross-stratified sandstones overlying the basal conglomerates at Murchison Island and Poole Inlet (Figs. 4.42 b and d), Bearskin Bay (Fig. 4.44 a), and forming most of the section exposed at Beresford Bay (Fig. 4.43 b) were deposited within a high energy shoreface environment situated above fairweather wave base. The SCS sandstones overlying the foreshore

conglomerates at Dawson Cove (Fig. 4.42 a), Sea Pigeon Island (Fig. 4.42 c), Lauder Point (Fig. 4.43 a), and Onwards Point (Fig. 4.44 f and g), and the trough cross-stratified sandstones at Bearskin Bay (Fig. 4.44 a) were deposited within a wave dominated shoreface environment situated between storm and fairweather wave base. The lenticular beds of pebble conglomerate interstratified with the SCS sandstones at Dawson Cove (Fig. 4.42 a) and Onward Point (Fig. 4.44 f and g) are interpreted as rip channel deposits or storm winnowed lags.

The overlying structureless bioturbated sandstones forming the bulk of the successions exposed at Bearskin Bay (Fig. 4.44 a) and Lauder Point (Fig. 4.43 a), as well as the upper part of the successions exposed at Dawson Cove (Fig. 4.42 a), Arichika Island (Fig. 4.38), Beresford Bay (Fig. 4.43 b), McLelland Island (Fig. 4.45 c) and Onward Point (Fig. 4.44 f) were deposited in a relatively low energy transitional sandy offshore environment characterized by thorough reworking of the sediments by a variety of burrowing organisms.

The HCS sandstones and sandy mudstones overlying the deposits of the SFA at Dawson Cove, Murchison Island, Sea Pigeon Island (Fig. 4.42 a, b, c), Beresford Bay (Fig. 4.43 b and c), Bearskin Bay (Fig. 4.44 a), and McLelland Island (Fig. 4.45 c) were deposited within a wave-dominated

offshore environment situated between storm and fairweather wave base. The same is true of the silty Inoceramid rich mudstones capping the successions exposed at Poole Inlet and Murchison Island. The thick solitary beds of sandstone within the MFA's of some sequences (eg. 4.44 d and 4.45 b) were probably emplaced during exceptionally large scale storm events. The debris flow and slide deposits interbedded within the MFA of the uppermost succession exposed at Bearskin Bay (Fig. 4.44 a) indicate that this environment, apart from being subject to frequent storm events, was also subject to episodic failure. Failure may have been induced by a variety of mechanisms including seismic shocks, oversteepening, rapid rates of sedimentation, and cyclic wave loading during storm events (Nardin et al., 1979; Myrow and Hiscott, 1991). Sediment failure is typical of environments characterized by high rates of sedimentation, such as river dominated prodeltas (Martinson, 1989; Bhattacharya and Walker, 1992). It is therefore quite probable that some of the facies of the MFA, such as the HCS sandstone and sandy mudstone facies, were deposited within prodeltaic environments.

The vertical arrangement of facies and the gross fining-upward nature of each of the successions is indicative of deposition within progressively deeper and lower energy marine environments. The distribution of

traces within many of the successions: Skolithos and Cruziana within the deposits of the SFA, Zoophycos within the overlying deposits of the MFA, is also indicative of deposition within progressively deeper and lower energy marine environments (Pemberton et al., 1992).

The fining-upward successions probably represent the deposits of several stacked smaller scale progradational successions (Fig. 4.46). At least 7 shoreface / mouthbar successions are observed within the Hauterivian to Barremian deposits of the SFA of the Longarm Formation exposed on Arichika Island (Figs. 4.38). The coarsening-upward successions are stacked into a larger scale grossly fining-upward succession. The basal conglomerate was deposited within a rocky foreshore environment. The five overlying successions were deposited within progradational sandy shoreface / gravelly mouth bar environments, while the upper two successions were deposited in a sandy shoreface and finally a transitional sandy offshore environment respectively. The large scale succession therefore is characterized by a net upward decrease in grain size reflecting a shift towards deposition in progressively deeper environments. The similarity between this transgressive succession and the correlative fining-upward successions exposed in the Longarm Formation elsewhere (Fig. 4.42) indicate that they too are composed of several smaller

Fig. 4.46 Schematic stratigraphic model demonstrating how the large scale fining-upward successions are composed of smaller scale progradational coarsening-upward successions. This particular model is based upon exposures of the Longarm Formation. SFA - sandstone facies assemblage, MFA - mudstone facies assemblage, TFA - turbidite facies assemblage.

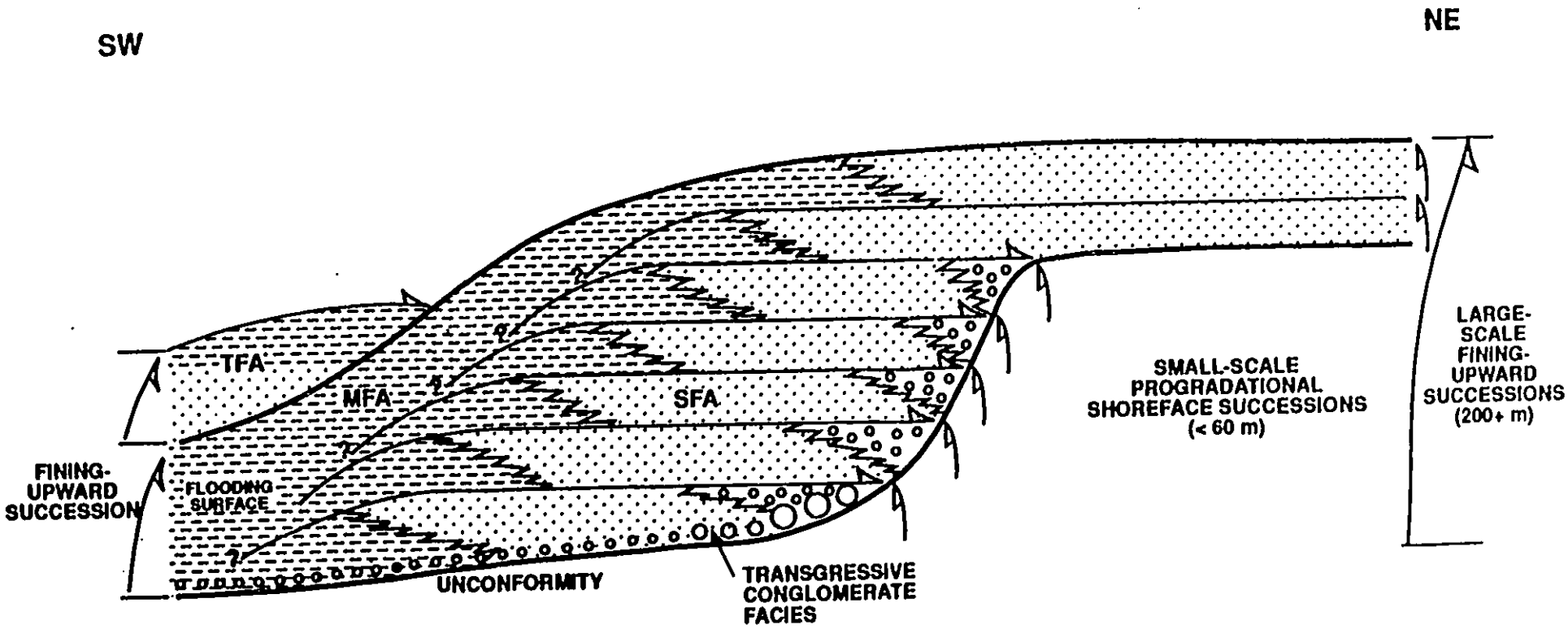
SW
NE
TFA
MFA
SFA
FINING-
UPWARD
SUCCESSION
FLOODING
SURFACE
UNCONFORMITY
TRANSGRESSIVE
CONGLOMERATE
FACIES
SMALL-SCALE
PROGRADATIONAL
SHOREFACE SUCCESSIONS
(< 60 m)
LARGE-
SCALE
FINING-
UPWARD
SUCCESSIONS
(200+ m)

scale progradational successions.

The fining-upward successions are therefore composed of a number of progradational packages which progressively backstepped the basin margin over time (Fig. 4.46). This indicates that the bulk of these successions were therefore deposited during minor periods of relative sea level fall or stillstand superimposed upon a larger scale overall transgression.

The smaller scale progradational successions are developed only within the more proximal and coarser grained shoreface deposits (ie. those exposed at Arichika Island in Fig. 4.38 and Onward Point in Fig. 4.40), where the effects of relative sea level fluctuation upon sedimentation would be more pronounced. Within deeper transitional offshore deposits, where the effects of relative sea level fluctuation upon sedimentation would be less pronounced, smaller scale progradational successions are not well developed. In these successions, only the larger scale transgression has a significant effect upon deposition, resulting in a progressive net decrease in grain size accompanying a shift towards deposition within increasingly deeper shelf environments.

4.8. FACIES SUCCESSIONS WITHIN THE DEPOSITS OF THE DFA

Description

The deposits of the DFA exposed on Rodderick Island (Fig. 4.47 a) abruptly overlie the deposits of the MFA forming the uppermost fining-upward succession at Bearskin Bay (Fig. 4.44 a). The succession is 20 m thick and consists primarily of interstratified beds of the pebbly mudstone and breccia facies. Individual beds are 0.5 to 3 m thick and are interstratified with beds of the thin bedded classical turbidite facies. The succession is overlain by 10 m of the classical turbidite facies. A similar 40 m thick succession of the DFA is exposed to the south at McLelland Island in Cumshewa Inlet, where it abruptly overlies a succession composed of the MFA (Fig. 4.47 b). The succession consists of interstratified beds of the pebbly mudstone and breccia facies. Beds range in thickness from 0.3 to 16 m, and are interstratified with beds of the classical turbidite facies. A 15 by 20 m angular olistolith consisting of the structureless bioturbated sandstone facies is encased by beds of pebbly mudstone within the lower part of the succession. The disorganized beds are overlain by 12 m of the classical turbidite facies.

A single 12 m thick bed of the pebbly mudstone facies is exposed in eastern Skidegate Inlet west of Onward Point

Fig. 4.47 Measured sections of the disorganized facies assemblage within the Haida Formation exposed at a) Roderick Island, Skidegate Inlet, b) McLelland Island, Cumshewa Inlet, and c) west of Onward Point, Skidegate Inlet.

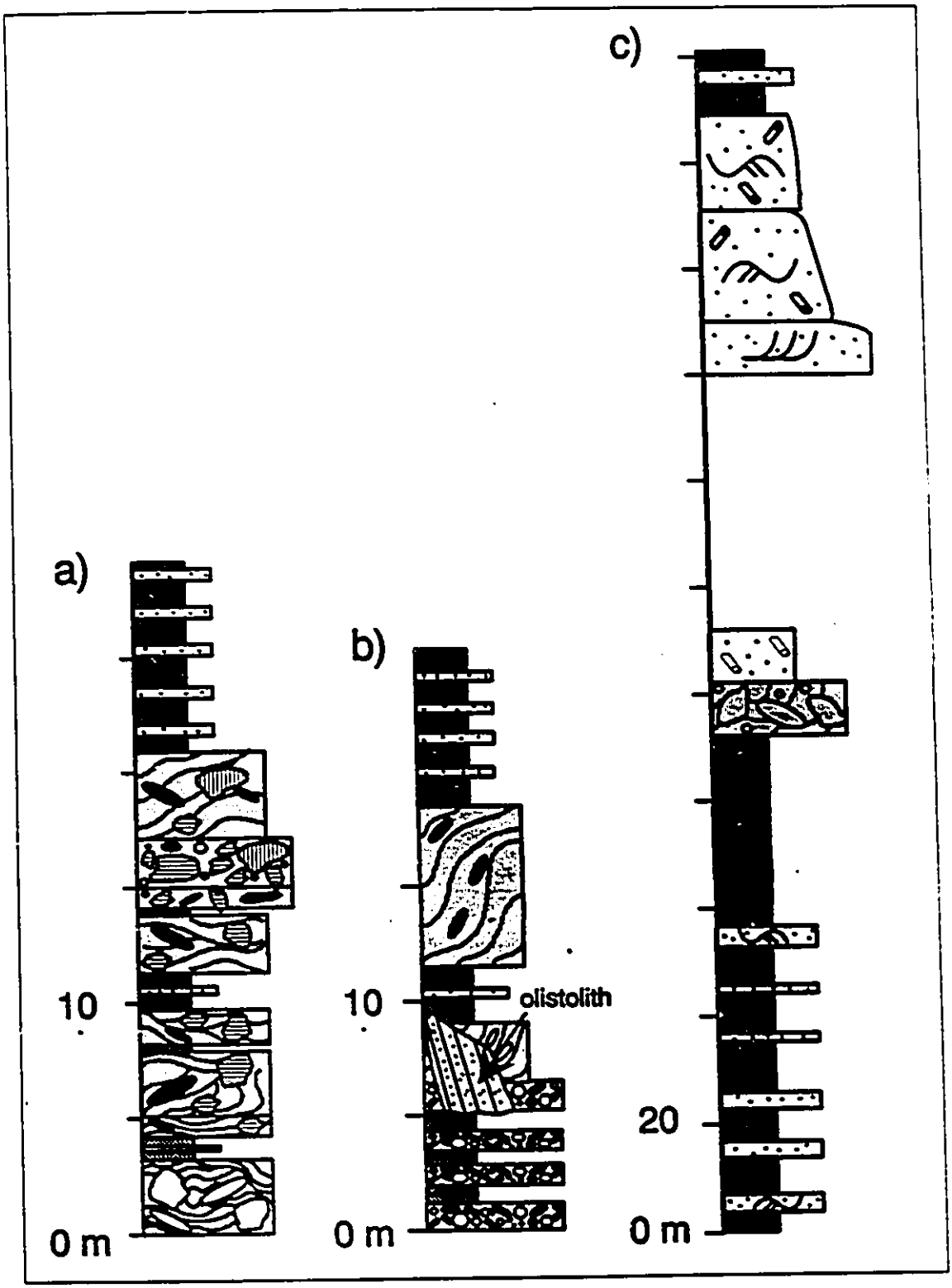
a)
b)
c)
olistolith
10
10
20
0 m
0 m
0 m

(Fig. 4.47 c). The bed abruptly overlies deposits of the MFA, and is abruptly overlain by the deposits of the SFA, which consists of a 50 m thick fining-upward succession.

Interpretation

Both the pebbly mudstone and breccia facies are interpreted as the deposits of subaqueous debris flows. The large olistolith of the SFA, the well rounded granitic boulders, and the nearshore fauna associated with the breccia facies suggests derivation from a sandy shallow marine environment. The pebbly mudstones are very similar to the breccias, except that they are muddy matrix-supported. It is therefore possible that debris flows similar to those that formed the breccias moved into an area of poorly consolidated wet mud and mixed with it to form the pebbly mudstone facies (Crowell, 1957 for the formation of pebbly mudstones in California). Alternatively, the pebbly mudstones may represent the deposits of debris flows derived from a muddy offshore area. The presence of large angular stratified blocks within some of the beds indicates that the slumps did not travel very far from source. If they had, the unlithified blocks would have broken into smaller pieces (Walker, 1985).

The absence of wave formed sedimentary structures within these successions indicates that they were emplaced

within an environment situated below storm wave base. The occurrence of interbedded turbidites within successions of this assemblage, as well as the mass flow dominated nature of the environment, suggests that the debris flows were emplaced at the base of a slope. The debris flows may have been triggered by a variety of mechanisms including seismic shocks, oversteepening, rapid rates of sedimentation, and cyclic wave loading during storm events (Nardin et al., 1979; Myrow and Hiscott, 1991). Similar successions composed of muddy and gravelly debris flows containing large olistoliths of shallower water deposits have been described from many ancient deep marine slope successions, particularly those associated with active continental margins (Winn and Dott, 1977; Pickering et al., 1989).

4.9. FACIES SUCCESSIONS WITHIN THE DEPOSITS OF THE TFA

Description

The fining-upward succession of the SFA and MFA within the Longarm Formation exposed on Murchison Island (Fig. 4.42 b) is overlain by deposits of the TFA. The contact separating the deposits of the two assemblages is erosional. The deposits of the TFA consist of 5 m of the thick bedded sandy turbidite facies overlain by 8 m of the thin bedded classical turbidite facies. The classical

turbidites are abruptly overlain by 22 m of the thick bedded sandy turbidite facies, which in turn are overlain by 6 m of the classical turbidite facies. The thick bedded sandstones are medium grained and pebbly and occur in massive to parallel laminated beds up to 1.3 m thick. Interstratified near the base of each thick bedded succession are beds of massive clast supported cobble conglomerate 0.5 to 1.5 m thick.

The deposits of the TFA are better developed within the Cenomanian to Early Turonian strata of the Skidegate Formation exposed in Saltspring Bay and Kagan Bay in Skidegate Inlet (Fig. 4.48). These successions are very similar to the TFA exposed on Murchison Island to the south (Fig. 4.42 b). The best exposed occur in the western Skidegate Inlet region near Saltspring Bay (Fig. 4.48 a). The deposits of the TFA at this location abruptly overlie those of the MFA. The contact is deeply scoured (Fig. 4.49) and is overlain by 13 m of the thick bedded sandy turbidite facies. The thick bedded sandy turbidites are abruptly overlain by 4 m of the thinly bedded classical turbidite facies, which in turn are abruptly overlain by 8 m of the thick bedded sandy turbidite facies. These sandy turbidites are gradationally overlain by approximately 300 m of the thin bedded classical turbidite facies. Sandstone beds become progressively thinner and siltier upwards within this

Fig. 4.48 Measured sections of the turbidite facies assemblage exposed in Skidegate Inlet at a) Saltspring Bay and b) Kagan Bay.

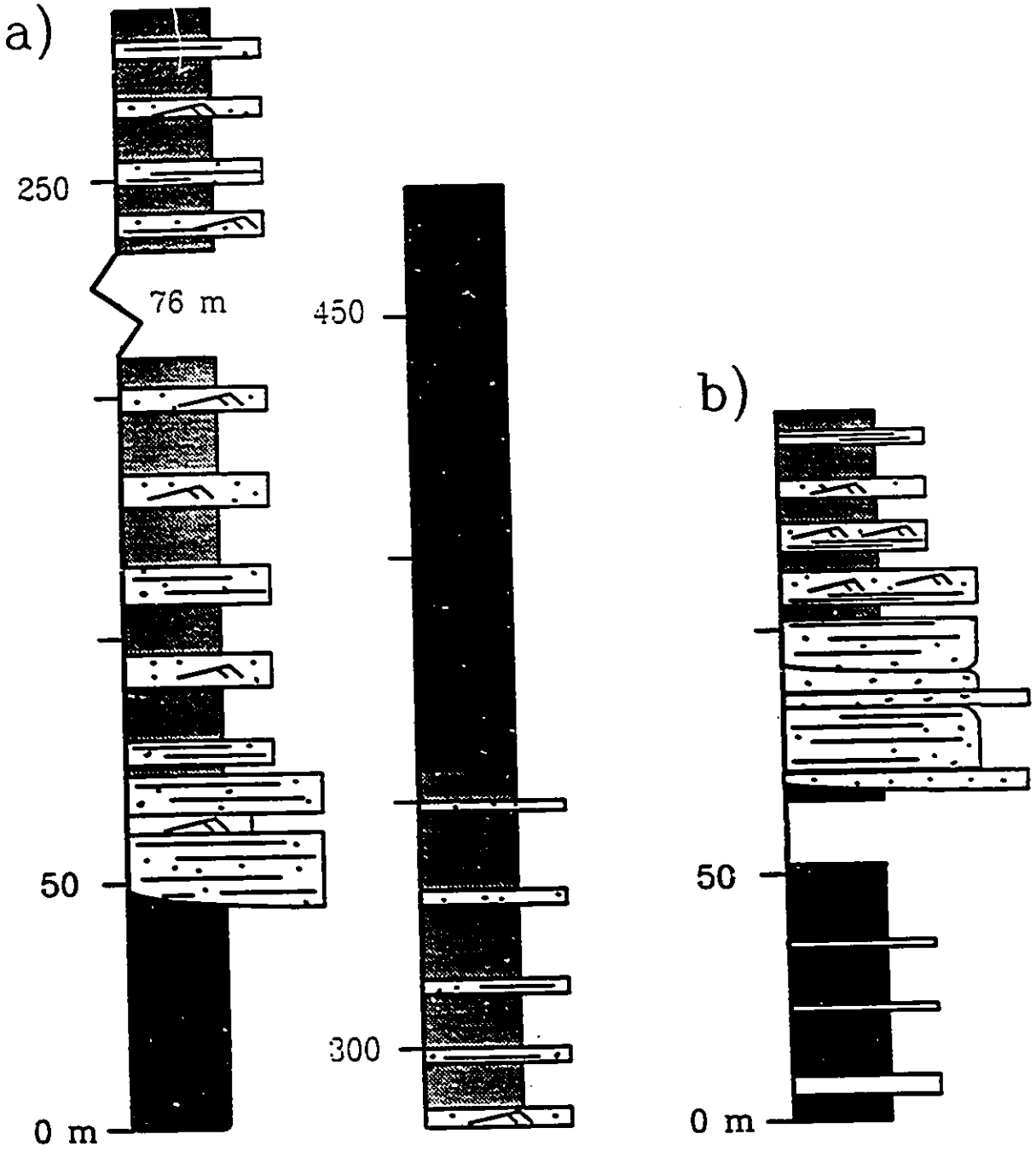
a)
250
76 m
450
50
300
0 m
b)
50
0 m

Fig. 4.49 Deeply scoured basal contact at the base of a succession of thick bedded sandy turbidites exposed at Saltspring Bay (Fig. 4.48 a) in western Skidegate Inlet. The turbidites are underlain by recessively weathering shales of the mudstone facies assemblage.

thick succession. The classical turbidites grade upwards into approximately 150 m of the shale and silty mudstone facies. A similar though somewhat thinner succession is observed within the deposits of the TFA exposed near Kagan Bay to the east (Fig. 4.48 b).

Interpretation

The sandstone beds within the TFA successions were emplaced by turbidity currents within a submarine fan setting. The sand rich and amalgamated nature of the thick bedded sandy turbidites forming the lower part of each succession indicates that they were deposited upon a more proximal part of the fan by relatively energetic turbidity currents, perhaps within channels. The presence of interstratified conglomerates within the lower part of the succession exposed on Murchison Island is almost certainly indicative of deposition within a submarine channel from relatively energetic high density turbidity currents. The overlying thinner bedded and finer grained classical turbidites were deposited by relatively less energetic turbidity currents, perhaps upon levees or within a more distal lower fan environment.

The vertical arrangement of facies and the fining-upward grain size trend of the two packages within these successions reflect a net decrease in the level of

depositional energy over time. This may be attributed to gradual infilling of a channel or to the lateral shifting of a depositional lobe. The fining-upward motif within the successions is reminiscent of the positive megasequence described by Mutti and Ricci Lucchi (1972), which these authors attributed to the gradual infilling of submarine fan channels. The nature of the exposure upon precludes the recognition of broad, deeply incised channels. In the case of the succession exposed at Saltspring Bay (Fig. 4.48 a), the inactive submarine fan lobe was blanketed by deep basinal shales and mudstones of the MFA.

4.10. GENERIC DEPOSITIONAL SEQUENCE

The aim of this section is to develop a generic model of a depositional sequence. This model will be used to erect a stratigraphic framework for the deposits of the Longarm, Haida, and Skidegate Formations. The reasoning behind this is that on the outcrop scale the relationship between the various types of assemblages is not clear. This is due partly to the poor nature of the exposure, and also to the poorly developed biostratigraphic framework. The model will therefore be based primarily upon the vertical and lateral relationships observed between the various facies assemblages. In the following section (4.11), the

model will be used to delineate the number and types of depositional sequences within the three formations.

4.10.1. Relationship between the SFA and MFA

The vertical and lateral relationships observed between the deposits of the MFA and SFA indicate that they represent contemporaneous offshore and shoreface deposits respectively. Such a relationship is obvious in the progradational offshore / shoreface successions of the Late Valanginian to Hauterivian deposits of the Longarm Formation exposed near White Point (Fig. 4.35). A similar lateral relationship is observed between Hauterivian to Aptian aged deposits of the MFA exposed on Murchison Island, Sea Pigeon Island, and Carpenter Bay and correlative deposits of the SFA exposed at Dawson Cove, Arichika Island, and Poole Inlet (Fig. 4.50). A similar lateral relationship is observed between Late Albian deposits of the SFA of the Haida Formation exposed at Bearskin Bay and correlative deposits of the MFA exposed 110 km to the northwest at Beresford Bay (Figs. 4.44 a and 4.43 b and c).

4.10.2. Paleocurrent analysis of the SFA and MFA

A large amount of paleocurrent data was collected from the various facies of the Longarm, Haida, and Skidegate Formations. This data is grouped according to class and

Fig. 4.50 Southeast - northwest oriented strike section through the Longarm Formation exposed in the southern archipelago. Based on measured sections at a) White Point, b) western Dawson Cove, c) Murchison Island, d) Arichika Island, e and f) Poole Inlet, g) Sea Pigeon Island, and h) Carpenter Bay.

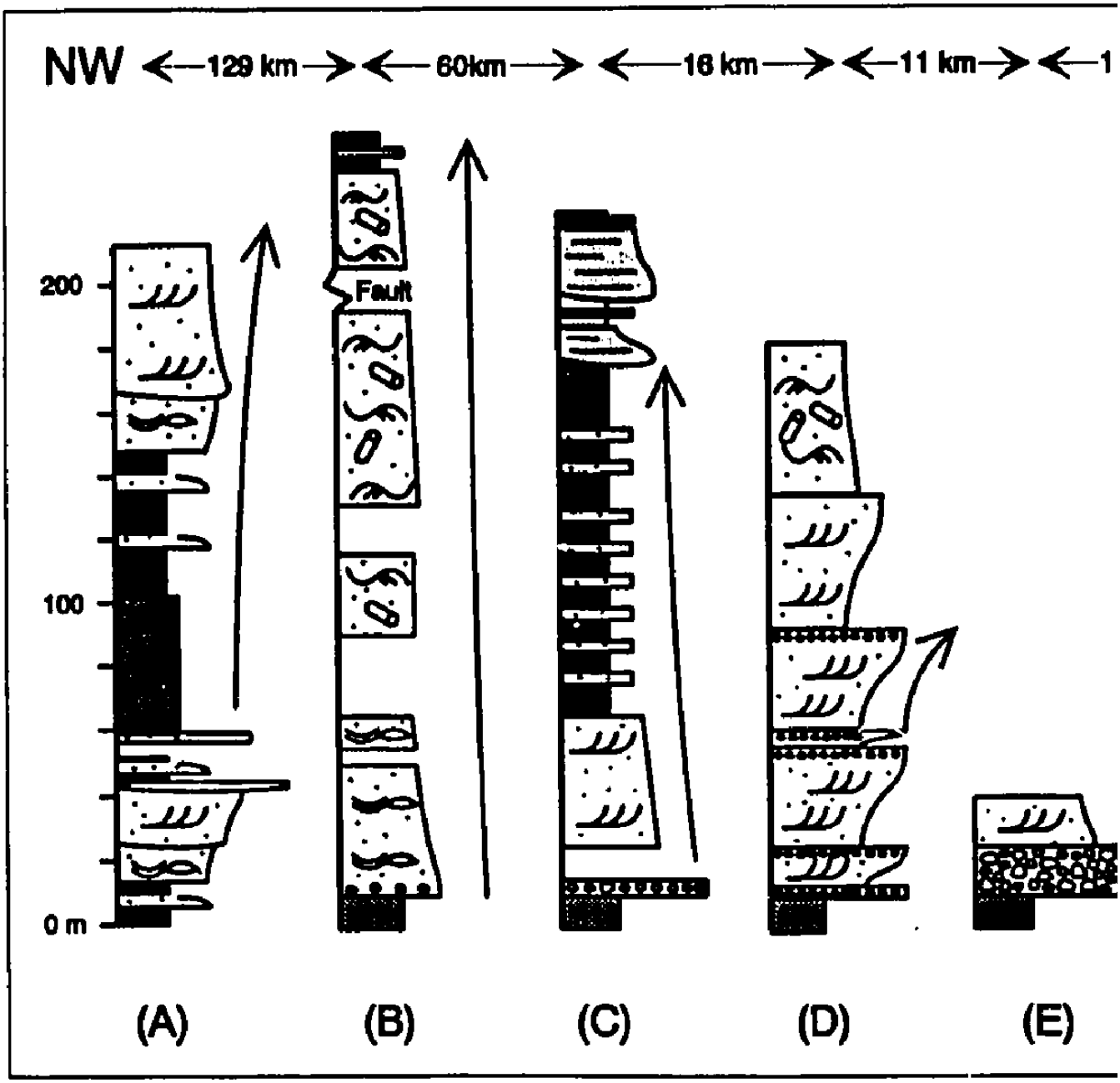
NW
129 km
60km
16 km
11 km
1
200
100
0 m
Fault
(A)
(B)
(C)
(D)
(E)

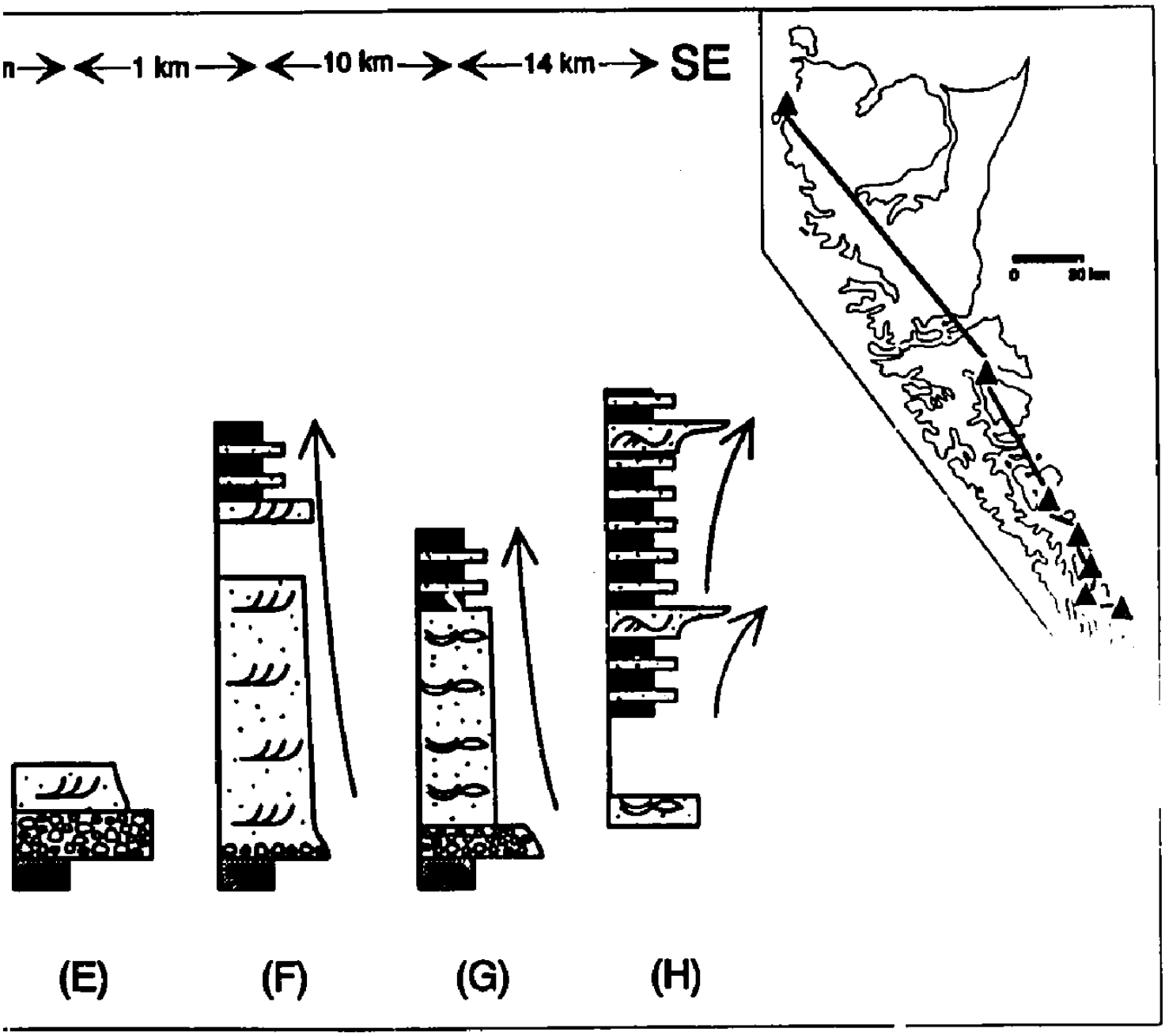
n
1 km
10 km
14 km
SE
0
(E)
(F)
(G)
(H)

location and is presented in a series of rose diagrams (Fig. 4.51). When considered collectively, these paleocurrent trends may be used to determine the approximate geometry of the depositional systems represented by correlative successions of the SFA and MFA. The data collected from the Longarm (Fig. 4.51) will be analyzed first, followed by that collected from the Haida and Skidegate Formations.

The long axes of the belmnites within the MFA of the Longarm exposed at Carpenter Bay and Murchison Island are oriented southwest - northeast (Fig. 4.51 a and b), while those at White Point are oriented east - west (Fig. 4.51 c). The orientation of conical cylindrical fossils under oscillatory current conditions was examined experimentally by Nagle (1967). In these experiments, Turritella gastropod shells aligned themselves transversely with respect to the direction of wave propagation (i.e. parallel to shoreline), with apices pointed in equal numbers to either side. This suggests that the axes of elongate conical fossils should be oriented parallel to paleoshoreline within ancient shelf successions. The axes of elongate fossils within many ancient siliciclastic and carbonate shelf and platform successions however are typically oriented perpendicular to the inferred paleoshoreline trend (Leckie and Krystinik , 1990). This shore normal orientation of elongate fossils parallels that of the sole marks associated with some storm

Fig. 4.51 Rose diagrams (equal area) illustrating paleocurrent data collected from the Longarm, Haida, and Skidegate Formations. a, b, c) Orientation of the long axes of belemnites from the Longarm Fm exposed at White Point, Murchison Island, and Carpenter Bay. d) Orientation of the long axes of symmetrical pebbly wave ripples from the Longarm Fm at Arichika Island. e, f) Direction of inclination from sets of trough and planar tabular cross-stratified sandstones or conglomerates from the Longarm Fm at Arichika Island. g, h, i) Same from White Point, Poole Inlet, and within the Haida Formation exposed at Girand Point and McLelland Island (eastern Cumshewa Inlet), and Bearskin Bay and Maude Island (central Skidegate Inlet). j) Orientation of the long axes of logs within the structureless bioturbated sandstone facies of the Haida Fm exposed at Lauder Point. k) Direction of inclination of sets of trough cross-stratified sandstone from the solitary thick bedded sandstone facies of the Haida Fm exposed at Gooden Island, Bearskin Bay, and Lina Island in Skidegate Inlet, and east of Conglomerate Point in Cumshewa Inlet. l) Orientation of the axes of coherently deformed beds of sandy mudstone within the HCS sandstone and interbedded sandy mudstone facies of the Haida Fm exposed at Bearskin Bay in Skidegate Inlet. m) Orientation of parting lineation form the sandy turbidite facies exposed in Kagan Bay, Skidegate Inlet. f) Direction of inclination of sets within cross-laminated current ripples from the thin bedded classical turbidite facies exposed in Kagan Bay, Skidegate Inlet.

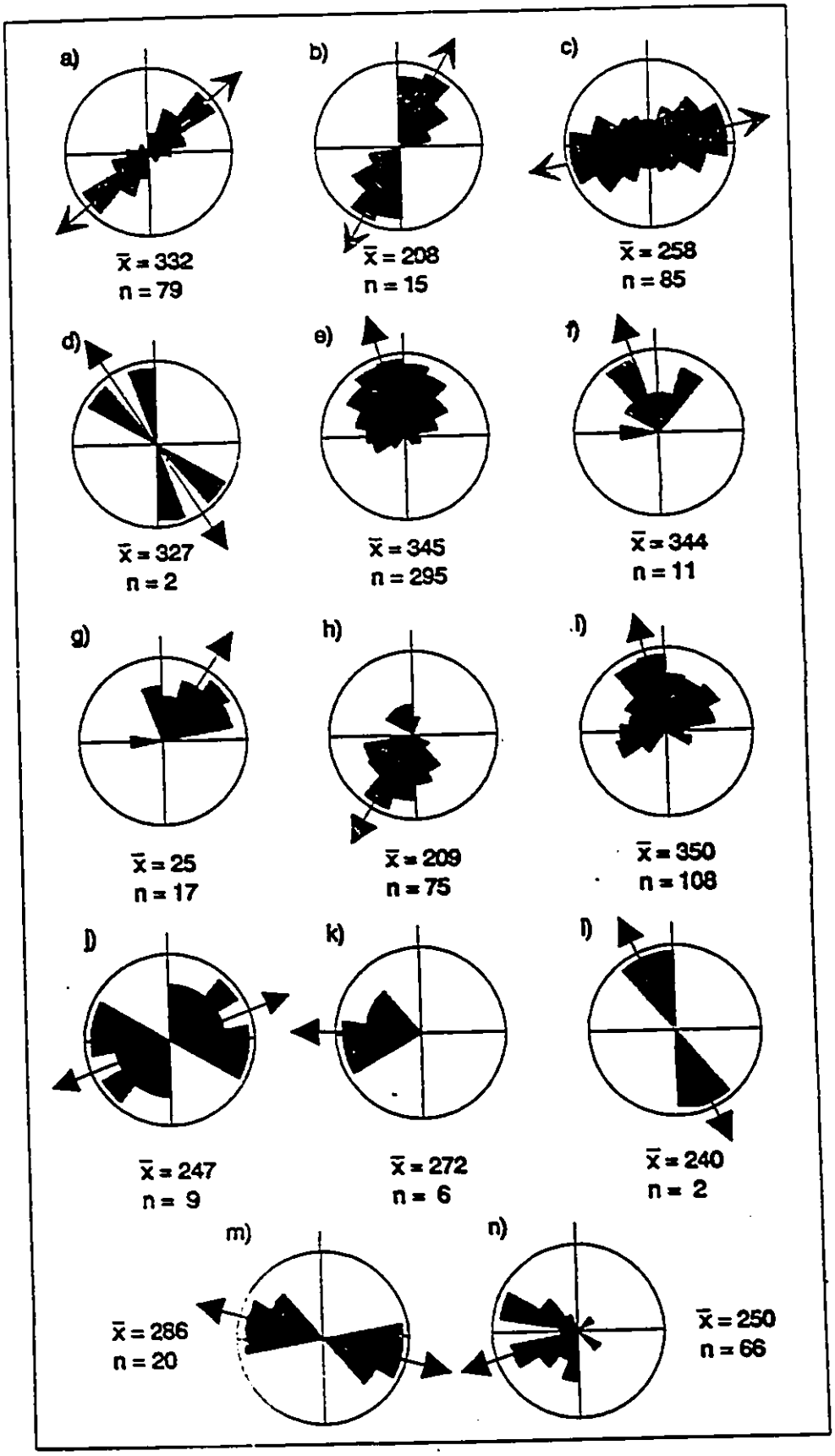
a)
x̄ = 332
n = 79
b)
x̄ = 208
n = 15
c)
x̄ = 258
n = 85
d)
x̄ = 327
n = 2
e)
x̄ = 345
n = 295
f)
x̄ = 344
n = 11
g)
x̄ = 25
n = 17
h)
x̄ = 209
n = 75
i)
x̄ = 350
n = 108
j)
x̄ = 247
n = 9
k)
x̄ = 272
n = 6
l)
x̄ = 240
n = 2
m)
x̄ = 286
n = 20
n)
x̄ = 250
n = 66

deposits. Such sole marks typically indicate that the flows were directed offshore, normal to the paleoshoreline (Leckie and Krystinik , 1989; Duke, 1990). Like tool marks, the orientation of elongate fossils may be the result of instantaneous flow conditions very near the bed, and may not reflect time averaged flow conditions (Duke, 1990). If this is the case, then the paleoshoreline in the vicinity of Carpenter Bay and Murchison Island during Late Valanginian to Aptian time was oriented approximately northwest - southeast. Near White Point, the coeval paleoshoreline was oriented approximately north - south.

The axes of two coarse-grained wave ripples exposed in plan view within the SFA exposed on Arichika Island trend northwest - southeast (Fig. 4.51 d). The axes of these types of wave ripples are generally believed to be oriented parallel with respect to paleoshoreline (Leckie and Krystinik , 1990). This suggests that the paleoshoreline in the vicinity of Arichika Island was oriented northwest - southeast. Both the oriented belemnites and wave ripples therefore seem to indicate that the paleoshoreline during Longarm time was oriented roughly northwest - southeast.

The predominate north-northwestward dipping inclination of cross-stratification within the shoreface sandstones and conglomerates of the SFA exposed on Arichika Island is oriented parallel with respect to this

paleoshoreline trend (Fig. 4.51 e and f). This suggests that most of the sediment was transport along the shoreface by longshore currents. Subordinate oblique onshore (northeast) and offshore (northwest) components of transport are also observed. The average trend of cross-stratification at White Point is oriented northeast (Fig. 4.51 g), which is indicative of net onshore migration of dunes with respect to the north - south trend of the paleoshoreline at this location. The predominate scuthwestward direction of transport evident at Poole Inlet is oriented almost directly offshore with respect to the inferred northwest - southeast trend of the paleoshoreline in this area (Fig. 4.51 h).

Assuming that the majority of cross-stratified beds within the SFA's of the Haida and Skidegate Formations are inclined alongshore (as was the case in Longarm Formation), then the paleoshoreline during Albian to Early Turonian time was also oriented roughly northwest - southeast. This is demonstrated by measurements collected from the cross-stratified shoreface sandstones of the SFA's of the Haida exposed at Girand Point, McLelland Island, Bearskin Bay, and Maude Island (Fig. 4.51 i). The measurements display a wide spread from northeast to southwest, with most clustered in the northwest sector. The minor northeast and southwest trends reflect subordinate components of onshore and

offshore migration respectively. The long axes of logs within the structureless bioturbated sandstone facies are oriented perpendicular to this paleoshoreline trend (Fig. 4.51 j). This situation is reminiscent of the oriented belemnites within the MFA of the Longarm Formation (Fig. 4.51 a to c), which were also oriented normal to paleoshoreline.

The cross-stratification within thick bedded solitary sandstones is oriented obliquely offshore towards the west-southwest with respect to the paleoshoreline trend (Fig. 4.51 k). This suggests that the storm related currents responsible for emplacing these beds within the offshore flowed obliquely offshore. This obliquity may be related to the Coriolis affect, which deflects offshore flowing currents to the right in the northern hemisphere. The axes of the two slumped beds are oriented parallel with respect to paleoshoreline trend (Fig. 4.51 l). In addition, the folds are overturned downslope towards the southwest.

4.10.3. Depositional model of the SFA and MFA

From this data a clear picture of the nature and orientation of the depositional system represented by correlative successions of the SFA and MFA within the three formations emerges. The deposits of the SFA and MFA are particularly well exposed within the Longarm Formation,

which makes it possible to reconstruct the paleogeography during Late Valanginian to Aptian time.

The foreshore conglomerates at the base of the Longarm vary greatly in thickness along strike, from 16 m at Poole Inlet to less than 1 m at Arichika Island to 0.5 m at Dawson Cove (Fig. 4.50). This variation probably reflects local changes in the relief of the paleocoastline. The thickest and coarsest accumulations of conglomerate were probably deposited adjacent to coastal headlands of high relief, while the thinner and finer accumulations of conglomerate were deposited adjacent to headlands of low relief. The relief of the coastline was probably related to basement lithology. The Late Jurassic pluton underlying the 16 m thick basal conglomerate exposed at Poole Inlet no doubt formed a resistantly weathering headland of relatively high relief.

Similar along strike variations in the thickness of the SFA are also observed. The deposits of the SFA are thickest and coarsest in the Arichika Island (175 m) - Poole Inlet (100 m) area in the southeast and the Dawson Cove (215 m) area in the northwest (Fig. 4.50). At points between, Murchison Island for example, the SFA is markedly thinner (40 m) and finer grained. The shoreface deposits exposed in the Arichika Island - Poole Inlet area are also transitional along strike both to the southwest and northwest into time

equivalent offshore deposits at Sea Pigeon Island and Ramsay Island.

These variations may be used to delineate the location of the major depocenters, which were presumably situated close to a deltaic source. The thickest and coarsest accumulations of the SFA should be situated relatively close to a deltaic source. In contrast, the thinnest and finest accumulations of the SFA, as well as the thickest accumulations of the MFA, should be situated in a relatively distal location with respect to source. In light of this, two main loci of sediment input may be identified; one in Poole Inlet - Arichika Island area, the other in the vicinity of Dawson Cove. The abundance of conglomerate within the deposits of the SFA at these two locations also denotes proximity to a major source of coarse grained sediment. In contrast, the Murchison Island, Ramsay Island, and Carpenter Bay areas were situated within relatively distal locations with respect to source. The great thickness of the shoreface sandstones exposed at White Point is also indicative of deposition close to a major source of sediment input into the basin.

The irregular nature of the coastline and the point source nature of sediment supply may account for the along strike variation in the type of shoreface. For example, the deposits of the SFA exposed at Arichika Island and Poole

Inlet consist primarily of trough and planar tabular cross-stratified sandstones deposited within high energy mouthbar and shoreface environments. Those exposed to the southeast at Huston Point and Sea Pigeon Island however consist of SCS sandstones deposited within a wave dominated shoreface environment. The SFA exposed at Dawson Cove to the northeast also consist primarily of sandstones deposited within wave dominated shoreface environments.

The SFA's and MFA's within the younger Haida and Skidegate Formations were also deposited within a similar setting. It is quite apparent from the paleocurrent analysis of these formations that the general northwest - southeast orientation of the paleoshoreline remained relatively constant throughout Early and Late Cretaceous time. This no doubt reflects the long term nature of the tectonic controls influencing the geometry of the forearc basin.

4.10.4. Relationships between the DFA and TFA

The deposits of the DFA and TFA are interstratified at several locations (Fig. 4.47), indicating that deposition of these two assemblages was contemporaneous. The deposits of these two assemblages are not interstratified with those of the SFA and MFA anywhere on the QCI's, which suggests that deposition of these four assemblages was not

contemporaneous. The deposits of the DFA and TFA abruptly overlie those of the MFA (Figs. 4.44 a and 4.47 a). The contact between the deposits of the MFA and those of the TFA/DFA at these locations is erosional. These relationships clearly demonstrate an abrupt change in depositional environments, from muddy offshore (MFA) to slope (DFA) and submarine fan (TFA). For example, the deposits of the DFA exposed west of Onward Point in Skidegate Inlet are abruptly overlain by those of the SFA (Fig. 4.44 e). This relationship clearly demonstrates an abrupt change in depositional environment (from slope to shoreface), marking a basinward shift in facies.

The orientation of parting lineation and current ripples within the deposits of the TFA indicate that the turbidity currents flowed towards the west-northwest (Figs. 4.52 e and f). Apparently the turbidites flowed almost parallel with respect to paleoshoreline. It is probable that the turbidity currents flowed parallel to the longitudinal axis of the basin, which may have been oriented northwest - southeast.

4.10.5. Erosional surfaces

The large scale fining-upward successions formed by the deposits of the SFA/MFA and the TFA are bound by erosional surfaces which represent distinct breaks in

deposition (Fig. 4.43 a, 4.44 a, and 4.45 a). Where the surfaces separate deposits of the SFA from the underlying pre-Cretaceous basement (Fig. 4.42 and 4.50), they are referred to as unconformities. Strata upon either side of the unconformity exhibit a marked angular discordance. Where the surfaces separate the deposits of the large scale fining-upward successions, they are referred to as disconformities. Strata upon either side of the disconformity do not generally display an angular discordance. Both the unconformities and disconformities may be correlated on a regional basis.

Description

The nature of the unconformity is dependant upon the lithology and paleoweathering style of the underlying pre-Cretaceous strata. At Arichika Island, the unconformity separating the deposits of the SFA from the underlying Late Triassic Peril Formation is jagged and irregular (Fig. 4.3). At Poole Inlet, the unconformity separating the deposits of the same SFA from the underlying Late Jurassic quartz diorites of the Burnaby Island Plutonic Suite is smooth and rounded. Near Conglomerate Point in Cumshewa Inlet the unconformity separating the Middle Albian deposits of SFA from heavily intruded strata of the Late Triassic Peril Formation features blocky protrusions and downward tapering

fissures (Fig. 4.52). Shallow circular burrows up to 1.5 cm deep of the Trypanites ichnofacies of Pemberton et al. (1992) are incised into dykes intruding strata of the Peril Formation beneath the unconformity (Fig. 4.53).

Four disconformities are evident within the section exposed in Bearskin Bay (Fig. 4.44 a). Three are evident within the section exposed at Lauder Point (Fig. 4.43 a). The disconformities are generally associated with a distinct change in facies, grain size, and weathering style (Fig. 4.54). Up to 3 m of erosional relief was observed along the disconformity separating the middle and uppermost fining-upward succession exposed at Lauder Point. These disconformities separate finer grained facies of the SFA or MFA below from coarser grained facies of the SFA above. In addition, the surfaces are overlain by transgressive lags. The disconformities typically exhibit traces belonging to the Glossifungities ichnofacies of Pemberton et al. (1992), including dense Rhizocorallium (Fig. 4.55 and 4.56).

Interpretation

The paleoweathering features associated with the unconformities indicate that they represent exhumed rocky paleoshorelines. The Trypanites ichnofacies along the unconformities is typically associated with erosive omission surfaces or hardgrounds formed in a high energy marine

Fig. 4.52 Unconformity separating Early Albian sandstones of the Haida Formation (light grey) from heavily intruded strata of the Late Triassic Peril Formation (dark) at Conglomerate Point, Cumshewa Inlet. The swaley cross-stratified sandstones dip toward the southeast (upper left). Note how the sandstones infill fissures and surround blocky protrusions of the underlying Peril Formation strata.

Fig. 4.53 Shallow circular burrows of the Trypanities ichnofacies (arrows) incised into Jurassic dyke intruding strata of the Late Triassic Peril Formation along the unconformity exposed at Conglomerate Point, Cumshewa Inlet. Note also the sandstones infilling paleojoint within the underlying dyke. Scale is in centimetres. This photo was taken immediately above the hammer in Fig. 4.52.

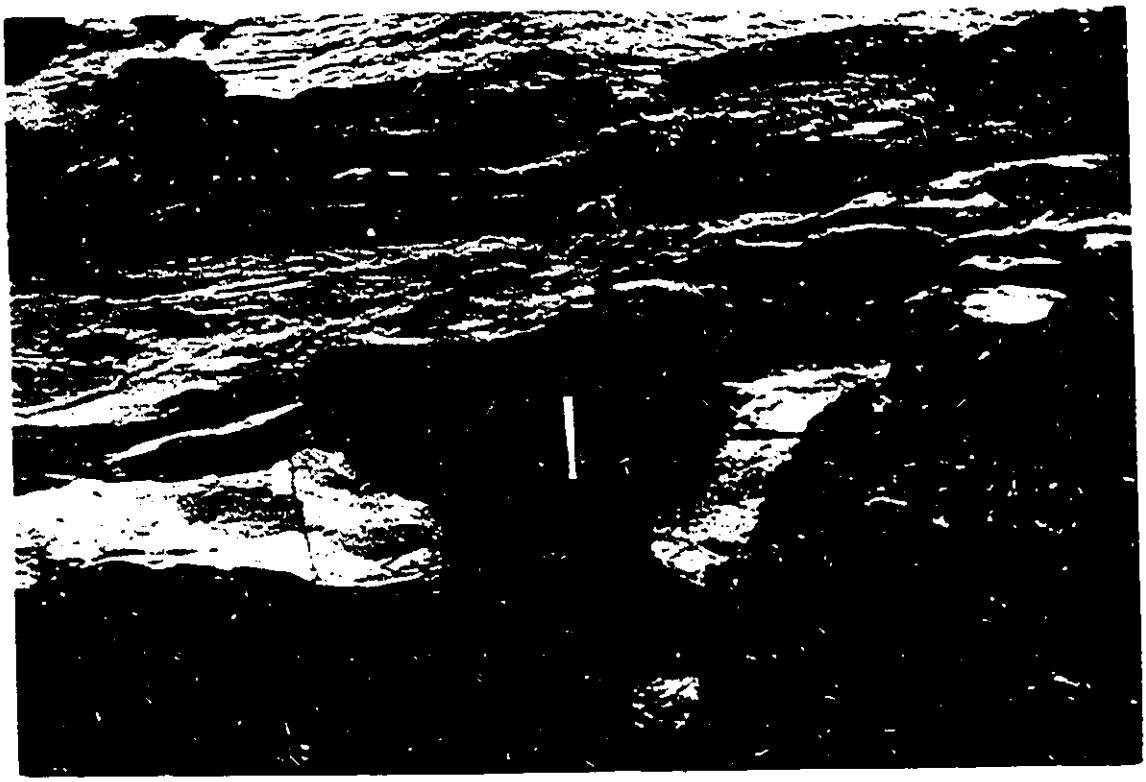

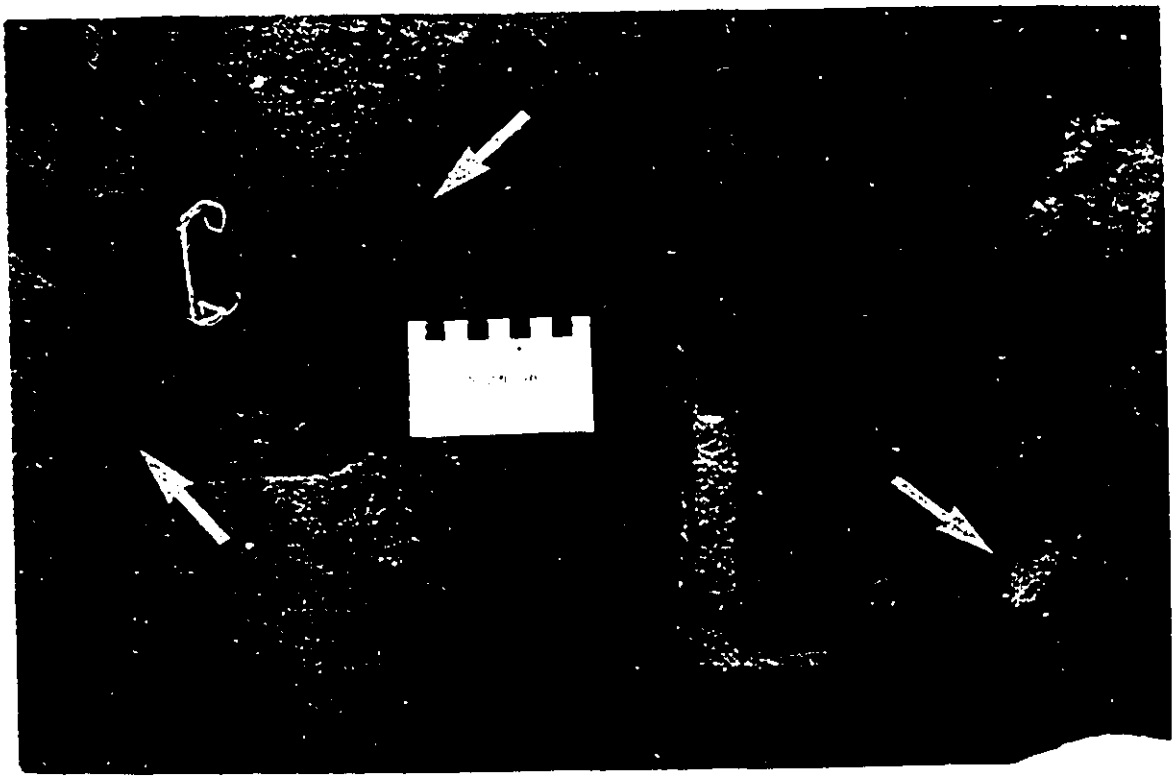

Fig. 4.54 Disconformity (arrow) separating recessively weathering fine grained silty sandstones capping the top of one fining-upward succession from the resistantly weathering coarse grained cross-stratified sandstones at the base of an overlying fining-upward succession within the Albian deposits of Haida Formation exposed at Maude Island in Skidegate Inlet. Resistantly weathering blocky sandstone is approximately 6 m thick.

Fig. 4.55 Rhizocorallium of the Glossifungities ichnofacies along the disconformity separating Aptian muddy offshore deposits of the Longarm Formation from Early Albian shoreface sandstones of the Haida Formation exposed at eastern Dawson Cove in Cumshewa Inlet.

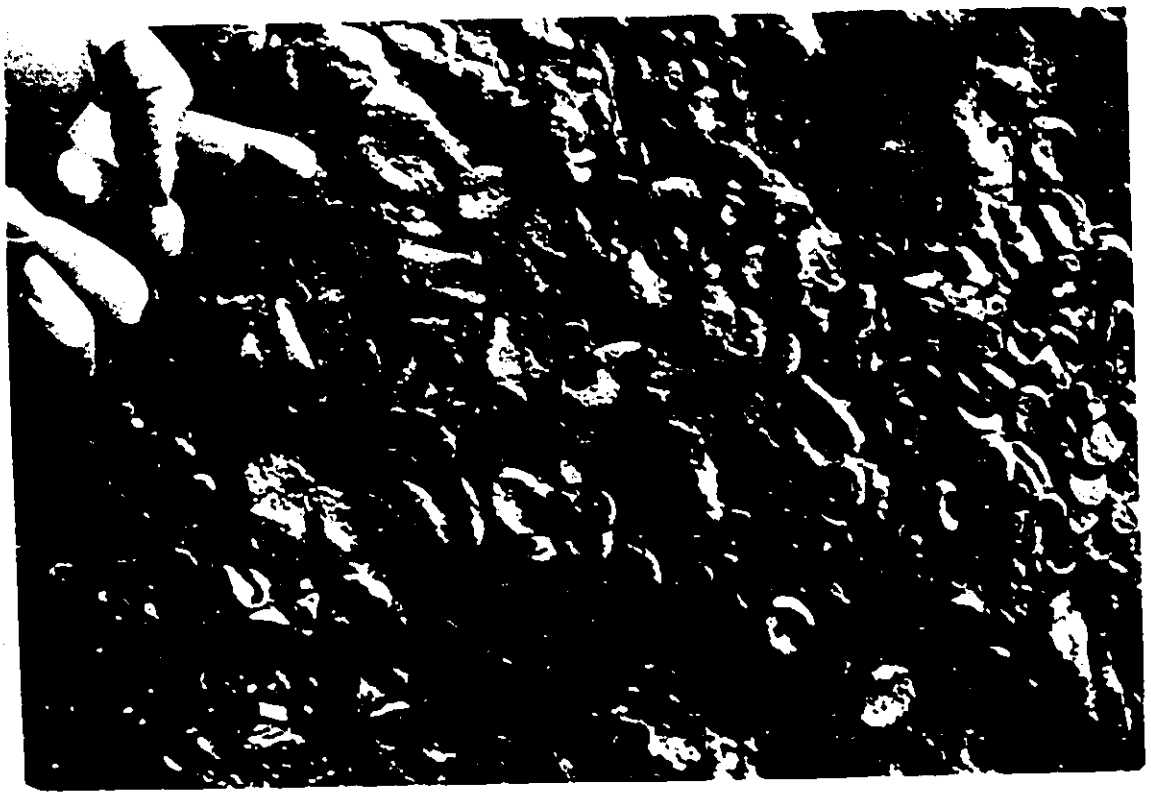

Fig. 5.56 Rhizocorallium of the Glossifungities ichnofacies along the disconformity separating structureless bioturbated fine grained silty sandstones below from cross-stratified coarse grained sandstones of an overlying fining-upward succession above within the Haida Formation exposed at Maude Island in Skidegate Inlet. This photo was taken at the contact shown in Fig. 4.54.

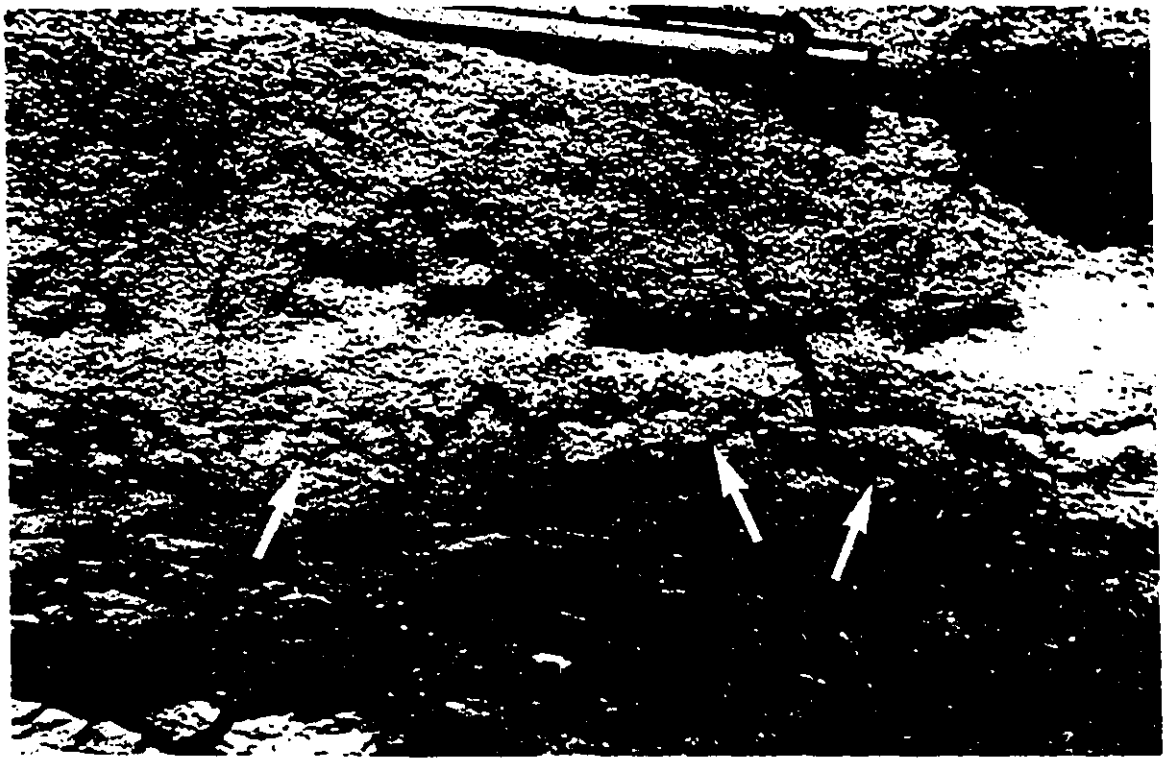

environment (Pemberton et al., 1992).

Like the unconformities, the disconformities are also interpreted as erosional surfaces. The Glossifungities ichnofacies along the disconformities is typically associated with erosive omission surfaces or firmgrounds formed in a high energy marine environment (Pemberton et al., 1992). The disconformities separating the fining-upward successions mark a pronounced basinwards shift in facies, which is indicative of relative sea level fall. The calcareous sandstone and mudstone concretions within some of the pebbly lags were probably derived by erosion of the top of the underlying succession during sea level fall. The extraformational clasts within the transgressive lags overlying the disconformities could not have originated from erosion of the top of the underlying successions, which usually consist of very-fine grained silty sandstone or silty mudstone. The extraformational clasts therefore had to have been transported into the basin sometime during the course of the relative sea level fall.

4.10.6. Generic depositional sequence

In the generic depositional sequence, strata of the DFA and TFA represent contemporaneous slope and submarine fan deposits respectively, while strata of the MFA and SFA represent contemporaneous offshore and shoreface deposits

(Fig. 4.57). The deposits of these two groups of facies are not contemporaneous, as observed by the erosive surfaces separating them (eg. the erosive contacts between deposits of the MFA and TFA, MFA and DFA). The deposits of the TFA do however grade upwards into those of the MFA. Contemporaneous deposits of the MFA and SFA of each sequence are separated from those of an older or younger sequence by an erosive surface.

The deposits of the DFA and TFA were probably emplaced during a period of relative sea level fall, which resulted in mass wasting of the deposits of the underlying sequence to the northeast. The products were redeposited in the form of the DFA within a slope environment to the southwest (Fig. 4.57). This process was also in part responsible for the creation of the erosional surface capping the deposits of the SFA and MFA within each sequence to the northeast.

Relative sea level fall also triggered the onset of submarine deposition to the southwest, represented by the deposits of the TFA. The initiation of submarine fan sedimentation in general is believed to be linked to periods of relative sea level fall (Mutti, 1988; Walker, 1992). The erosional surface underlying successions of the TFA may be attributed to the scouring accompanying the initiation of submarine channel incision.

Fig. 4.57 Model of a generic depositional sequence within the Longarm, Haida, and Skidegate Formations. Equivalant sequence stratigraphic terminology is included. The large scale fining-upward succession would corrrespond to a transgressive systems tract.

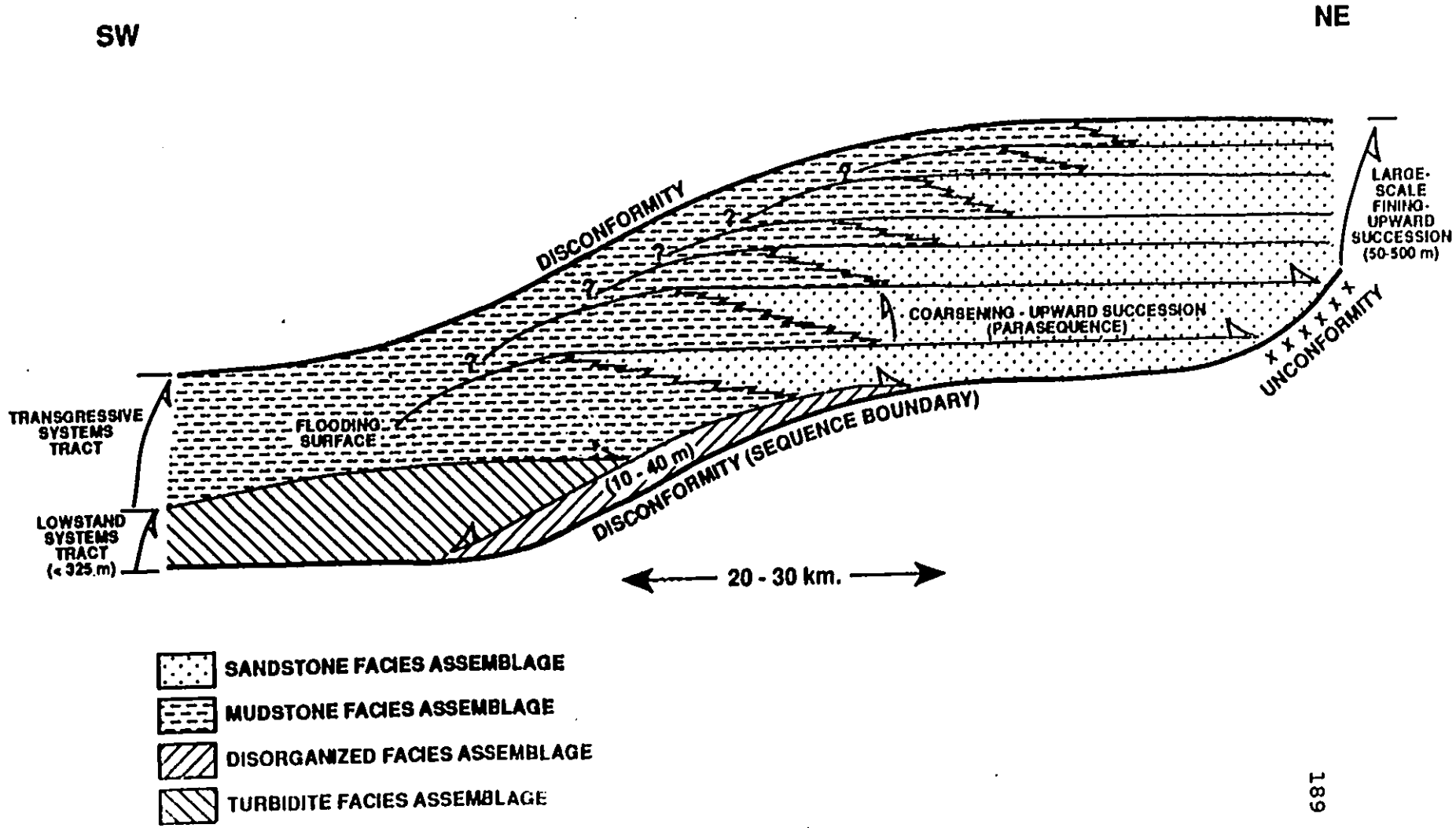
SW
NE
DISCONFORMITY
LARGE-SCALE FINING-UPWARD SUCCESSION (50-500 m)
COARSENING - UPWARD SUCCESSION (PARASEQUENCE)
UNCONFORMITY
TRANSGRESSIVE SYSTEMS TRACT
FLOODING SURFACE
(10 - 40 m)
DISCONFORMITY (SEQUENCE BOUNDARY)
LOWSTAND SYSTEMS TRACT (< 325 m)
20 - 30 km.
SANDSTONE FACIES ASSEMBLAGE
MUDSTONE FACIES ASSEMBLAGE
DISORGANIZED FACIES ASSEMBLAGE
TURBIDITE FACIES ASSEMBLAGE
ARC MASSIF

The large scale fining-upward successions of the SFA and MFA within each sequence accumulated during an ensuing period of relative sea level rise. Superimposed upon this long term rise were fluctuations of shorter duration, during which time the smaller scale coarsening upward successions were deposited. Each of these were deposited during periods of stillstand or sea level fall which accompanied these subordinate fluctuations. As sea level rose over the long term, these progradational successions backstepped towards the basin margin to the northeast, resulting in the accumulation of a fining-upward succession. Rising sea level also resulted in transgressive erosion of the rocky coastline along the northeastern basin margin.

As most sediment was trapped upon the shelf during these transgressive periods, the general thinning and fining upward trend within successions of the TFA reflect the progressive abandonment of the submarine fan system. Transgression was followed by another fall in relative sea level, during which time the deposits of the TFA and DFA of the overlying sequence was deposited.

In the context of this model the erosional surfaces are related to erosion accompanying both sea level fall and rise. The deposits within the confines of these surfaces represent the product of a single cycle of sea level fluctuation.

4.10.7. Comparison to sequence stratigraphic paradigm

The generic depositional sequence proposed above is similar in terms of scale and significance to the sequence of the sequence stratigraphic paradigm (van Wagoner et al., 1989). The deposits of the DFA and TFA within the generic depositional sequence correspond to the lowstand systems tract (Fig. 4.57). The deposits of the SFA and MFA within the generic depositional sequence correspond to the transgressive systems tract. The smaller coarsening-upward packages within the large scale fining-upward successions of the SFA and MFA correspond to progradational parasequences. These parasequences are stacked into retrogradational parasequence sets, forming thick fining-upward successions. The sequence boundaries represent erosional surfaces related to periods of significant relative sea level fall and rise. They bound a group of genetically related strata deposited during the course of a single cycle of sea level fall and rise. A point of major departure concerns the lack of a highstand systems tract within the generic depositional sequence.

4.11. STRATIGRAPHIC ANALYSIS

Using the generic depositional sequence as a base, the number and character of depositional sequences within

the Longarm, Haida, and Skidegate Formations will be determined. The first step will be to construct a strike and two dip sections (Figs. 4.58 to 4.63), each correlated on a lithostratgraphic and biostratigraphic basis. The molluscan biostratigraphic zonation used was that of McLearn (1972) and Haggart (1986). Biostratigraphic data for each of the measured sections was derived both from published reports by Sutherland Brown (1968), McLearn (1972), Haggart (1986, 1989, 1990, 1991, 1992), and from unpublished fossil reports of samples submitted by the author to J. Haggart.

Additional biostratigraphic data was derived from unpublished foraminiferal reports compiled by B. Cameron of the Pacific Geoscience Center in Sydney B.C. The age of measured sections, and the source of the age determination, is provided in Table 4.3.

McLearn (1972) and Haggart (1986) recognized up to 8 molluscan biozones and faunas within the Albian to Coniacian of the Queen Charlotte Island region. The average duration of each of the zones and faunas is approximately 3 Ma. Such coarse resolution is typical of the Cretaceous molluscan biostratigraphy of the west coast of North America (J. Haggart, pers. comm. 1993).

Identification of the various sequences will depend upon a variety of criteria. The first is the recognition and correlation of the erosional surfaces bounding the

Fig. 4.58 Dip section through the Longarm, Haida, and Skidegate Formations exposed in Skidegate Inlet. The numbers correspond to section locations on accompanying maps. Biostratigraphic zonation after Sutherland Brown (1968), McLearn (1972) and Haggart (1986).

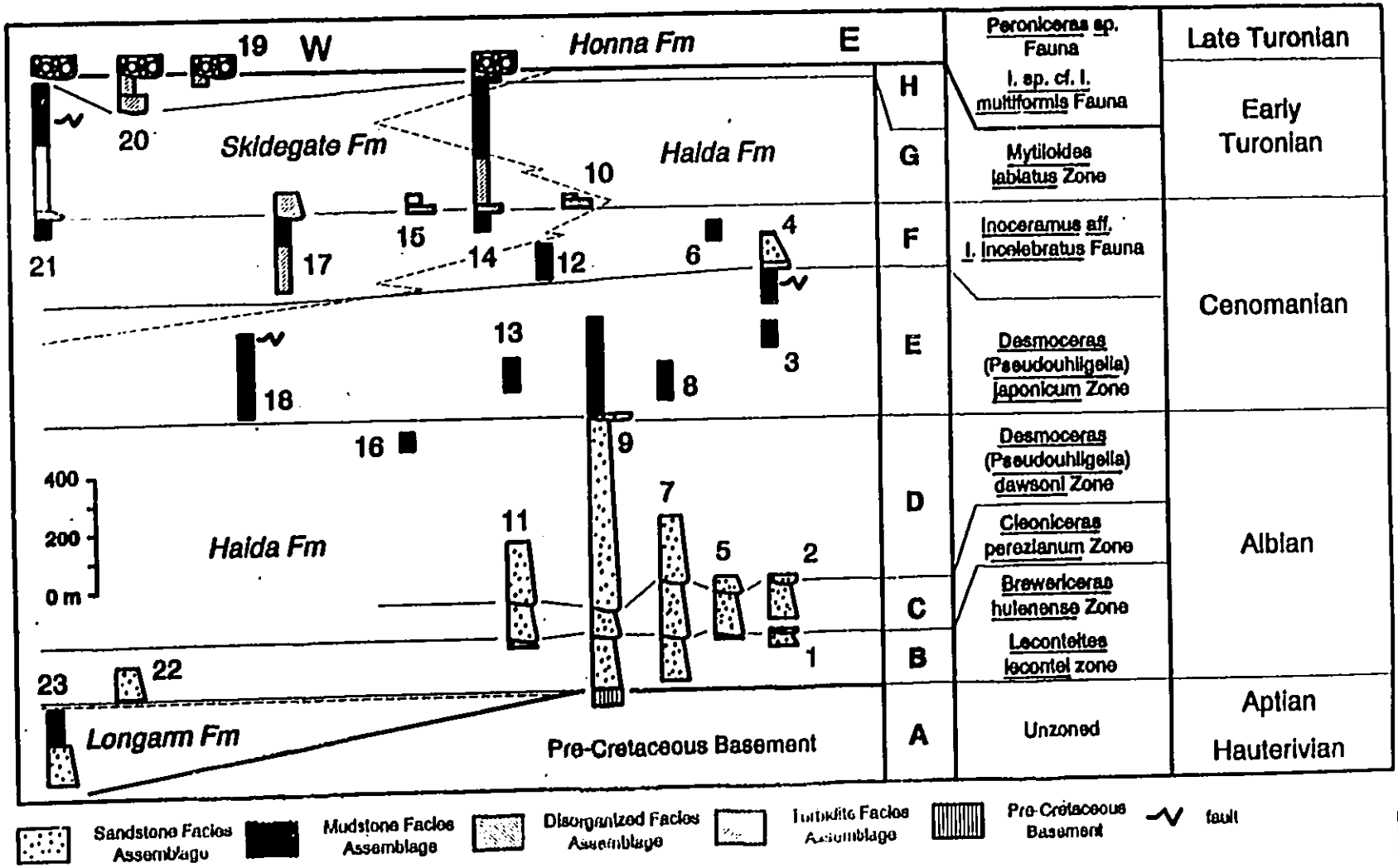
W
E
Honna Fm
Skidegate Fm
Halda Fm
Halda Fm
Longarm Fm
Pre-Cretaceous Basement
19
20
21
17
15
14
10
12
6
4
3
18
13
8
16
9
7
11
5
2
1
23
22
400
200
0 m
H
G
F
E
D
C
B
A
Peroniceras sp. Fauna
I. sp. cf. I. multiformis Fauna
Mytiloides labiatus Zone
Inoceramus aff. I. incelebratus Fauna
Desmoceras (Pseudouhligella) japonicum Zone
Desmoceras (Pseudouhligella) dawsoni Zone
Cleoniceras perezianum Zone
Brewericeras hulenense Zone
Lecontelites lecontei zone
Unzoned
Late Turonian
Early Turonian
Cenomanian
Albian
Aptian
Hauterivian
Sandstone Facies Assemblage
Mudstone Facies Assemblage
Disorganized Facies Assemblage
Turbidite Facies Assemblage
Pre-Cretaceous Basement
fault

Fig. 4.59 Location of measured sections on dip section (Fig. 4.58) from Skidegate Inlet.

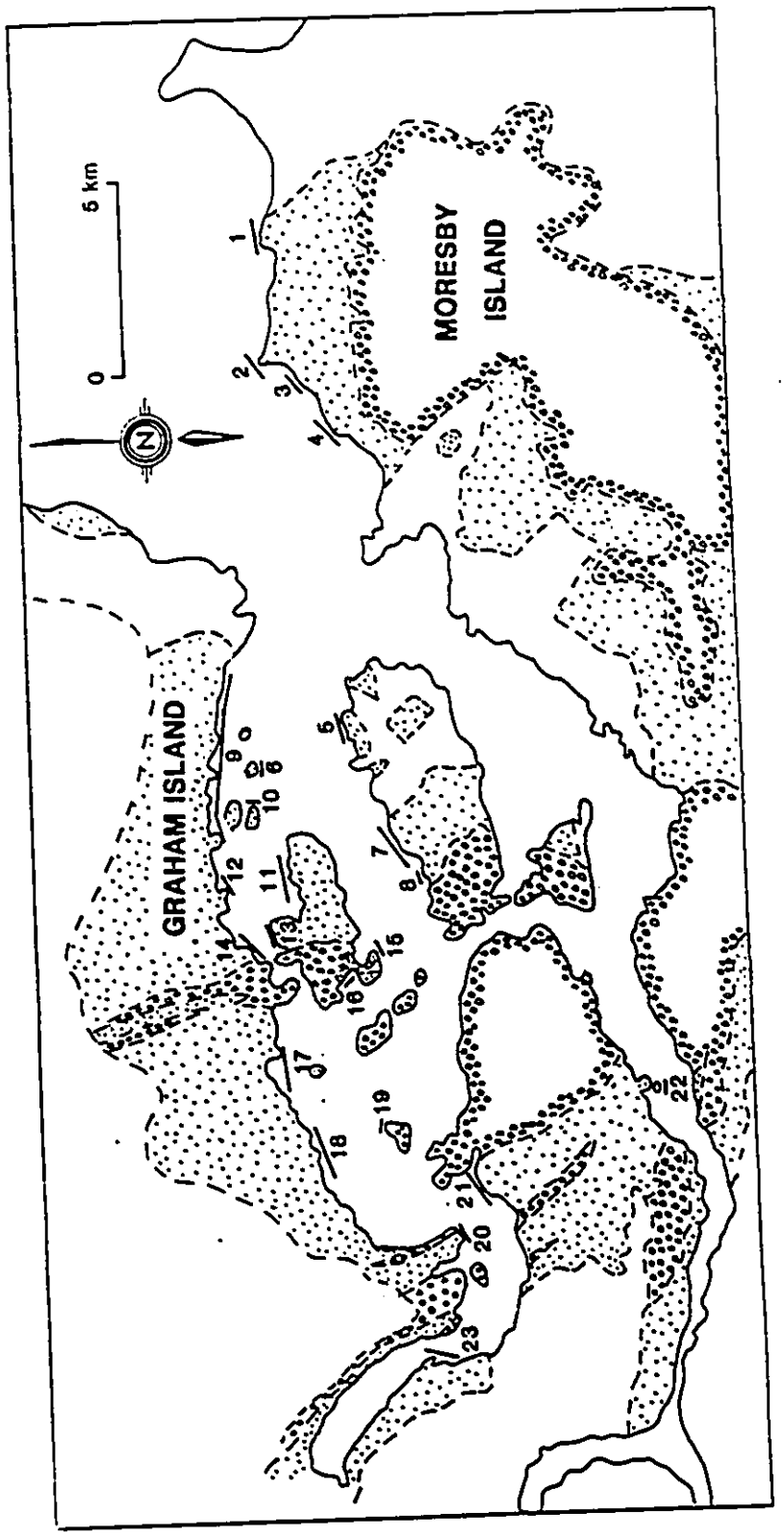
5 km
0
N
MORESBY ISLAND
GRAHAM ISLAND
1
2
3
4
5
6
7
8
9
10
11
12
13
14
15
16
17
18
19
20
21
22
23

Fig. 4.60 Dip section through the deposits of the Longarm, Haida, and Skidegate Formations exposed in Cumshewa Inlet.

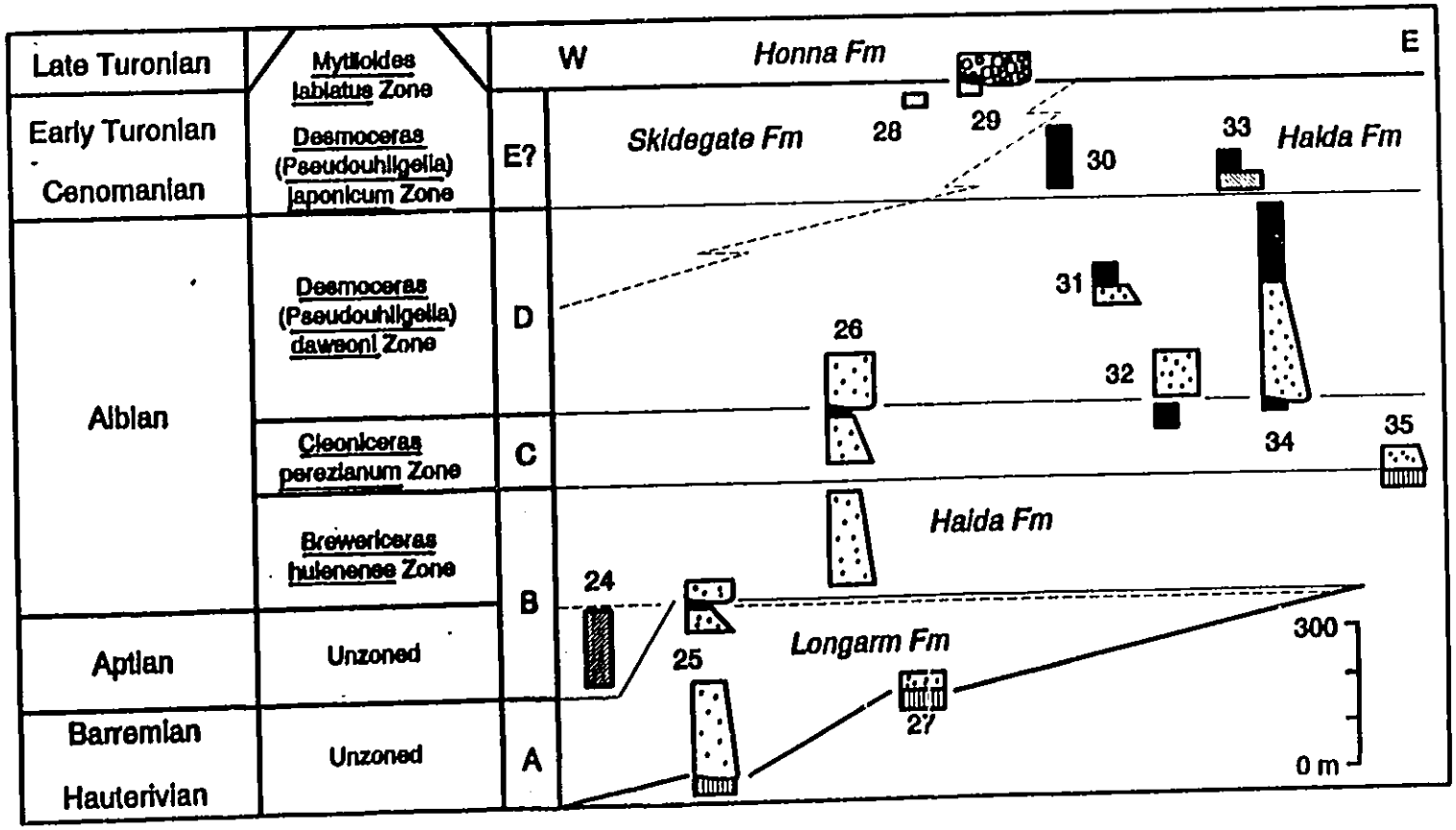
Late Turonian
Early Turonian
Cenomanian
Albian
Aptian
Barremian
Hauterivian
Mytiloides labiatus Zone
Desmoceras (Pseudouhligella) japonicum Zone
Desmoceras (Pseudouhligella) dawsoni Zone
Cleoniceras perezianum Zone
Brewericeras hulenense Zone
Unzoned
Unzoned
E?
D
C
B
A
W
E
Honna Fm
Skidegate Fm
Haida Fm
Haida Fm
Longarm Fm
24
25
26
27
28
29
30
31
32
33
34
35
300
0 m

Fig. 4.61 Location of measured section on the dip section (Fig. 4.60) from Cumshewa Inlet.

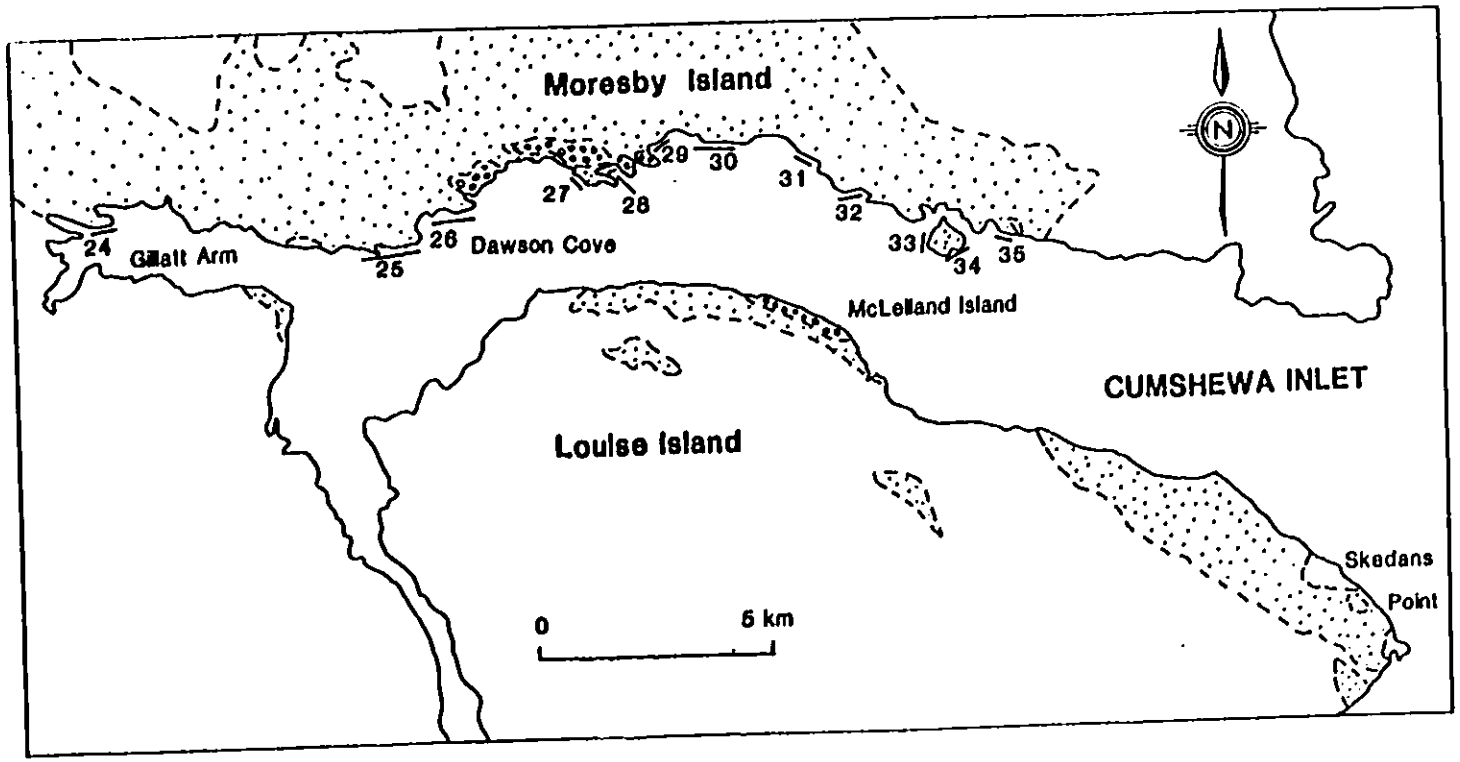
Moresby Island
N
24
Gillatt Arm
25
26
Dawson Cove
27
28
29
30
31
32
33
34
35
McLelland Island
CUMSHEWA INLET
Louise Island
Skedans
Point
0
5 km

Fig. 4.62 Strike section through the deposits of the Longarm, Haida, and Skidegate Formations.

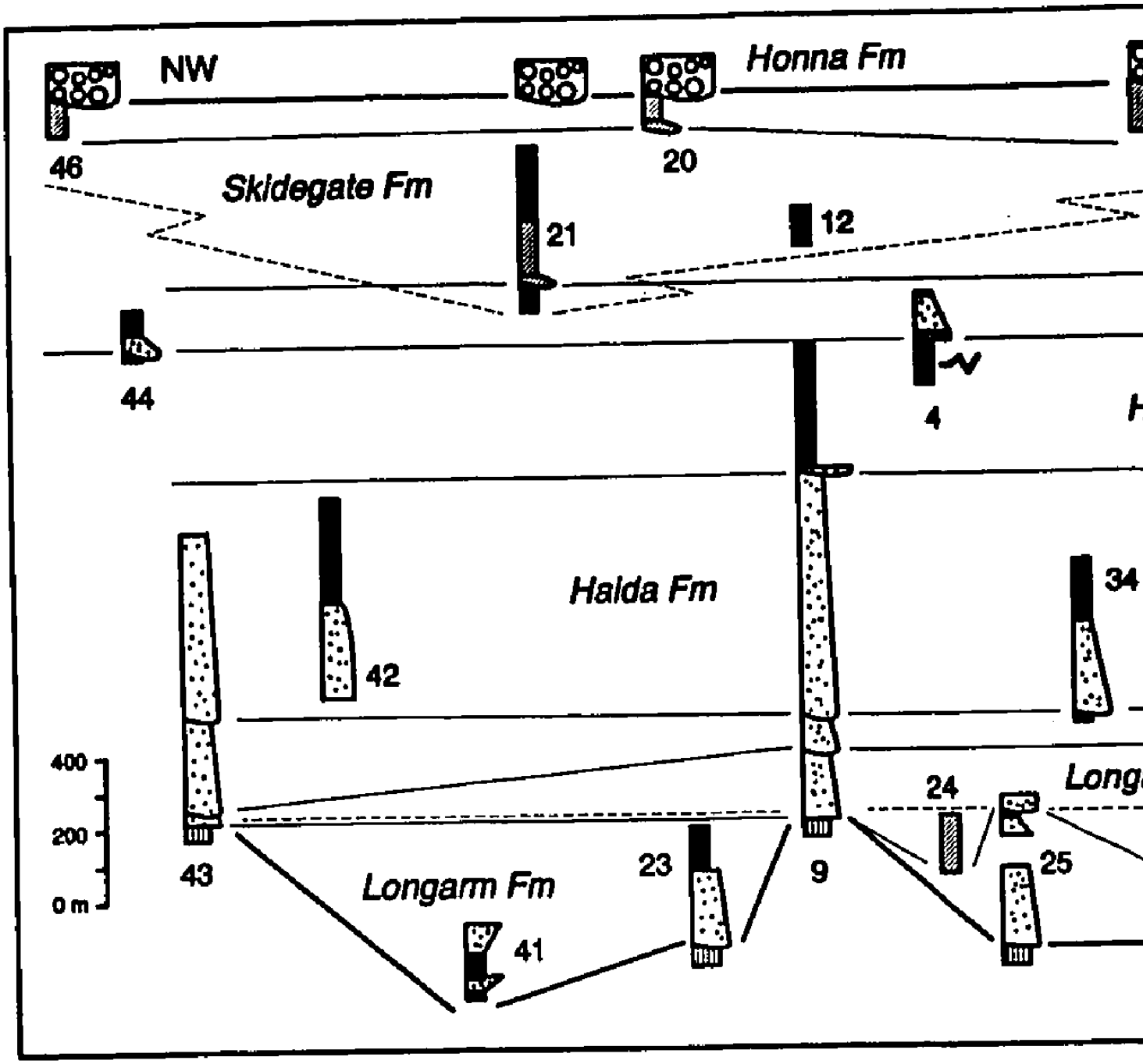
NW
Honna Fm
46
20
Skidegate Fm
21
12
44
4
Halda Fm
34
42
400
200
0 m
24
43
Longarm Fm
23
9
25
41

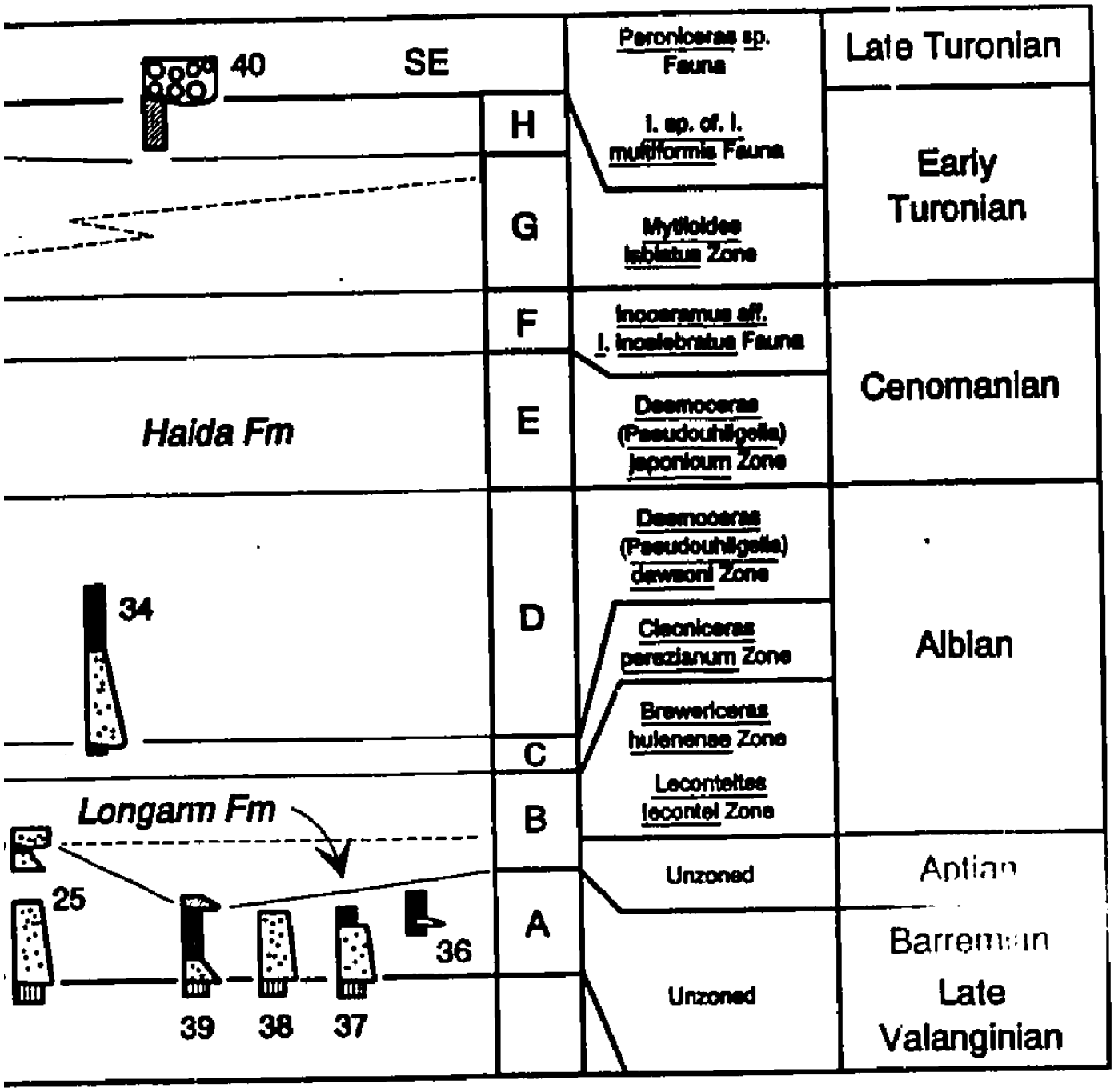
SE
40
Halda Fm
34
Longarm Fm
25
39
38
37
36
H
G
F
E
D
C
B
A
Peroniceras sp. Fauna
I. sp. of. I. multiformis Fauna
Mytiloides labiatus Zone
Inoceramus aff. I. inoelebratus Fauna
Desmoceras (Pseudouhligella) japonicum Zone
Desmoceras (Pseudouhligella) dawsoni Zone
Cleoniceras perezianum Zone
Brewericeras hulenense Zone
Lecontellas lecontei Zone
Unzoned
Unzoned
Late Turonian
Early Turonian
Cenomanian
Albian
Aptian
Barremian
Late Valanginian

Fig. 4.63 Location of measured sections on the strike section (Fig. 4.62).

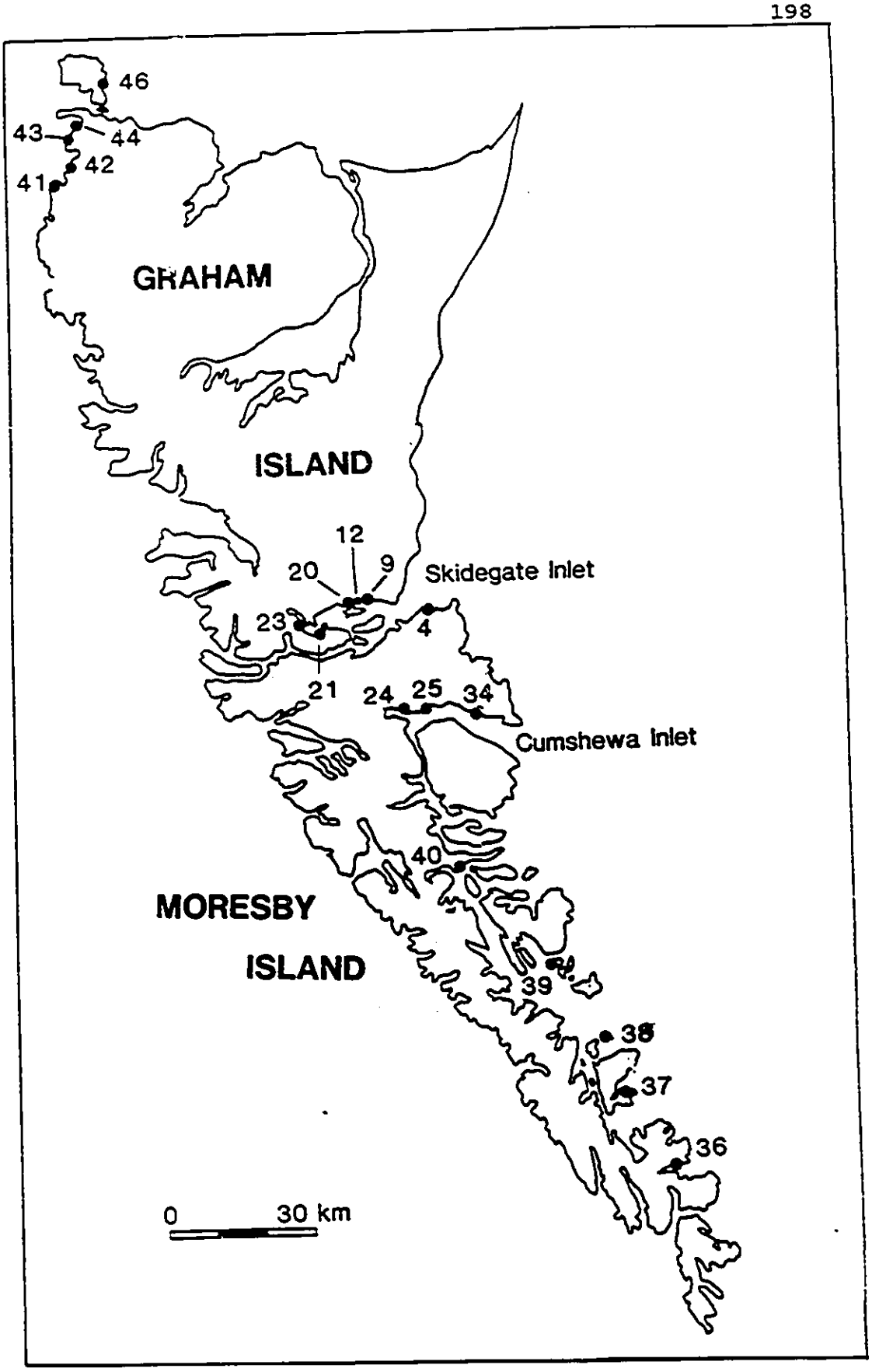
46
43
44
42
41
GRAHAM
ISLAND
12
20
9
Skidegate Inlet
23
4
21
24
25
34
Cumshewa Inlet
40
MORESBY
ISLAND
39
38
37
36
0
30 km

Table 4.3 Biostratigraphic references for the cross sections through the Longarm, Haida, and Skidegate Formations. Sources: 1) inferred from stratigraphic relations, 2) Sutherland Brown (1968), 3) McLearn (1972), 4) Haggart (1986), 5) fossil identification by Haggart, 6) Haggart (1989), 7) Haggart (1991), 8) Haggart and Gamba (1990), and 9) Haggart et al. (1993).

TABLE 4.3

SECTION	AGE	ZONE	SOURCE
1	Albian	?	1
2	Albian	?	1
3	Early Cenomanian	*Desmoceras (P) japonicum*	3
4	Late Cenomanian	?	1
5	Early to Middle Albian	*Brewericeras hulenense, Cleoniceras perezianum*	2,3,4
6	Cenomanian	?	1
7	Early to Late Albian	*B. hulenense, C. perezianum, D. (P) dawsoni*	2,3
8	Cenomanian	?	1
9	Early Albian to Cenomanian	*B. hulenense, C. perezianum, D. (P) dawsoni, D. (P). japonicum*	2,3
10	Early Turonian	*Mytiloides labiatus*	5
11	Middle to Late Albian	*C. perezianum, D. (P) dawsoni*	2,3
12	Cenomanian	*Inoceramus aff. I. incelebratus*	2,3
13	Cenomanian	?	1
14	Cenomanian to E. Turonian	?	1
15	Turonian	*M. labiatus*	5
16	Late Albian	*D. (P) dawsoni*	3,4
17	Late Cenomanian to E. Turonian	*I. aff. I. incelebratus, M. labiatus*	2,4
18	Early Cenomanian	?	1
19	Early Turonian	?	1
20	Early Turonian	?	1
21	Late Cenomanian to E. Turonian	?	1
22	Early Albian	*Leconteites lecontei, B. hulenense*	5
23	Late Valanginian to Aptian	unzoned	2,6,7
24	Late Aptian	unzoned	7
25	Hauterivian to Aptian	unzoned	2,6,7
26	Albian	*B. hulenense, C. perezianum*	2,4,5
27	Barremian	unzoned	7
28	Turonian	*M. labiatus*	4
29	Turonian	*M. labiatus*	4
30	Early Cenomanian	*D. (P) japonicum*	4
31	Late Albian	*D. (P) dawsoni*	4
32	Late Albian	*D. (P) dawsoni*	4
33	Cenomanian	?	1
34	Late Albian	*D. (P) dawsoni*	4,5
35	Middle Albian	*C. perezianum*	4
36	Hauterivian to Aptian	unzoned	8,9
37	Hauterivian	unzoned	8
38	Hauterivian	unzoned	8
39	Hauterivian to Aptian	unzoned	8,9
40	Early Turonian	?	1
41	Late Valanginian to Hauterivian	unzoned	6,7
42	Late Albian	*D. (P) dawsoni*	4
43	Albian	*L. lecontei*	2,5
44	Cenomanian	?	1
45	Early Turonian	?	1

sequences. The second will be the identification of large scale fining-upward successions composed of the SFA and MFA, as each represents the transgressive systems tract of a sequence. The final criteria will be the recognition of successions of the DFA and TFA, as each represents the deposits of the lowstand system tract of a sequence.

4.11.1. Depositional sequences within the Longarm, Haida, and Skidegate Formations

At least eight depositional sequences (A through H) are recognized within the deposits of the Longarm, Haida, and Skidegate Formations exposed in Skidegate Inlet (Fig. 4.58 and 4.59), Cumshewa Inlet (Fig. 4.60 and 4.61), and along strike (Fig. 4.62 and 4.63). A listing of the various attributes of each sequence is provided in Table 4.4.

Sequence A

Sequence A is composed entirely of Late Valanginian to Barremian and possibly Early Aptian deposits of the Longarm Formation. The base of the sequence is marked by an angular unconformity which separates the deposits of the SFA from the underlying pre-Cretaceous basement. The top of the sequence is marked by an erosional surface separating the deposits of the MFA from those of the TFA of sequence B exposed at Murchison Island (Fig. 4.61, # 39) and the

TABLE 4.4

SEQUENCE	AGE	THICKNESS	COMPOSITION
A	Late Valanginian to Aptian (17 Ma)	300 m	SFA, MFA
B	Late Aptian to Early Albian (8.2 Ma)	200 m	TFA, SFA
C	Middle Albian (5.2 Ma)	200 m	SFA, MFA
D	Late Albian (5.2 Ma)	600 m	SFA, MFA
E	Early Cenomanian (3.3 Ma)	350 m	SFA, MFA
F	Late Cenomanian (3.3 Ma)	300 m	TFA, DFA, MFA, SFA
G	Early Turonian (1 Ma)	500 m	TFA, DFA, MFA
H	Early Turonian (1 Ma)	150 m	TFA, DFA

deposits of the MFA from those of the SFA of sequence B exposed at Dawson Cove (Fig. 4.60, # 25). No deposits of the DFA or TFA were observed within this sequence.

Sequence B

Sequence B is Late Aptian to Early Albian in age (L. lecontei and B. hulenense zones of McLearn, 1972). As previously described, the base of the sequence in most areas is marked by an erosional surface separating Late Aptian to Early Albian strata from older strata of sequence A. In the western Cumshewa Inlet (Fig. 4.60, # 24) and Murchison Island (Fig. 4.62, # 39), sequence B consists of deposits of the TFA which are separated from underlying deposits of the MFA of sequence A by an erosional surface. In eastern Skidegate Inlet (Fig. 4.58, # 9) and at Lauder Point to the northwest (Fig. 4.62, # 43) the base of sequence B is marked by an angular unconformity. At both these locations, Early Albian deposits of the SFA of sequence B unconformably overlie pre-Cretaceous basement. As observed in the central Skidegate Inlet and Lauder Point regions, the deposits of sequence B are separated from the Middle Albian deposits of the SFA of sequence C by an erosional surface.

Sequence B therefore consists of Late Aptian deposits of the TFA in the western Cumshewa Inlet region, and Early Albian deposits of the SFA and MFA elsewhere.

Sequences C and D

Sequence C is of Middle Albian age (C. perezianum zone of McLearn, 1972), while sequence D is of Late Albian age (D. (P) dawsoni zone of McLearn, 1972). The tops of both sequences are marked by erosional surfaces separating the deposits of the SFA or MFA from younger deposits of the SFA belonging to the overlying sequence (Fig. 4.58, #'s 1, 2, 5, 7, 9, 11). Both sequences consist of the depcsits of the SFA and MFA, and lack exposed deposits of the TFA and DFA.

Sequence E

Sequence E is of Early Cenomanian age (D. (P) japonicum zone of McLearn, 1972). The base of the sequence is marked by an erosional surface separating the deposits of the SFA from those of the underlying sequence (Fig 4.58, # 9). In the Cumshewa Inlet region, the base of the sequence is marked by an erosional surface underlying the deposits of the DFA (Fig. 4.60, # 33). The top of the sequence is marked by an erosional surface underlying the deposits of the DFA of the overlying sequence (Fig. 4.58, # 4).

This sequence consists primarily of deposits of the MFA, with minor deposits of the SFA and DFA.

Sequence F

Sequence F is of Late Cenomanian age (I. aff. I. incelebratus zone of McLearn, 1972 and Haggart, 1986). In the Skidegate Inlet region, the top of the sequence is marked by an erosional surface overlain by deposits of the TFA and/or DFA of sequence G (Fig. 4.58, #'s 10, 14, 15, 17, 21). Deposits of all four facies assemblages are observed within this sequence in the Skidegate Inlet region. The lower part of the sequence consists of the deposits of the DFA, which are transitional to the west into those of the TFA. The deposits of the SFA abruptly overlie those of the DFA in eastern Skidegate Inlet (Fig. 4.58, # 4), and are in turn overlain by the deposits of the MFA. The deposits of the TFA to the west are gradationally overlain by those of the MFA.

Sequence G

The deposits of sequence G, though poorly constrained and exposed only in the Skidegate Inlet region, are of Early Turonian age (Mytiloides labiatus zone of Haggart, 1986). The top of the sequence is marked by an erosional surface which is abruptly overlain by deposits of the TFA belonging to sequence H (Fig. 4.58, #'s 14, 20). To the east, the lower part of the sequence consists of the deposits of the DFA (Fig. 4.58, #'s 10, 15). These deposits interfinger with those of the TFA (Fig. 4.58, #'s 14, 17). At these

locations, the deposits of the TFA and DFA are gradually overlain by those of the MFA.

Sequence H

Sequence H is of Early Turonian age (Mytiloides labiatus zone of Haggart, 1986), and is abruptly overlain by conglomerates of the Honna Formation (Fig. 4.58, #'s 14, 19, 20; 4.60, # 29; 4.62, #'s 40, 46). The sequence consists primarily of the deposits of the TFA.

4.11.2. Depositional history

As many as 8 sequences are recognized within the deposits of the three formations. It is however quite likely that the poor nature of exposure on the Queen Charlotte Islands masks the presence of additional sequences. The approximate duration of each sequence varies from a maximum of 17 Ma (sequence A) to 1 Ma (sequence G and H). This corresponds to the duration of the second (10 - 100 Ma) and third (1 - 10 Ma) order sea level cycles of Vail et al., (1977).

The poorly developed nature of the deposits of the SFA and better developed nature of the deposits of the TFA within the younger sequences (especially obvious within the Skidegate Inlet region; Fig. 4.58) reflects a long term net rise in sea level throughout Late Valanginian through Early

Turonian time. During the course of this long term rise, the nearshore depocenter progressively shifted northeastwards toward the basin margin. Deeper marine depocenters followed suit, which explains the better representation of the deposits of the TFA within younger sequences. The age of the deposits of the SFA unconformably overlying pre-Cretaceous basement of the arc massif decreases towards the east in both Cumshewa and Skidegate Inlets. In the western Dawson Cove area (Fig. 4.60, # 25), Hauterivian deposits of the SFA of sequence A unconformably overlie Early Jurassic strata of the Sandilands Formation. Approximately 4 km to the east (# 27), Barremian deposits of the SFA of sequence A unconformably overlie Late Triassic strata of the Peril Formation. Approximately 8 km further to the east (# 35), Middle Albian deposits of the SFA of sequence C unconformably overlie Middle Jurassic strata of the Yakoun Group. A similar northeastward onlapping trend is observed in the Skidegate Inlet region (Fig. 4.58). In Skidegate Channel to the west (# 23), Late Valanginian deposits of the SFA of sequence A unconformably overlie Middle Jurassic strata of the Yakoun Group. Approximately 20 km to the northeast at Bearskin Bay (# 9), Early Albian deposits of the SFA of sequence B unconformably overlie strata of the Yakoun Group.

The progressive eastward decrease in the age of the

SFA overlying the unconformity in Cumshewa and Skidegate Inlets indicates that the basal unconformity is diachronous, and that overlying strata progressively onlapped the eastern margin of the basin over time.

CHAPTER 5. SEDIMENTOLOGY AND STRATIGRAPHY OF THE LATE CRETACEOUS HONNA FORMATION AND UNNAMED UNITS

5.1. CHAPTER SUMMARY

Deposition of the Honna Formation was preceded by the progradation of muddy slope and sandy submarine fan systems preserved within the upper part of the Skidegate Formation. Slope progradation in the northwest led to the establishment of a muddy shelf environment. The Honna was deposited within an elongate, northwest - southeast trending basin supplied from an uplifted and dissected magmatic arc to the east. The Honna Formation consists primarily of turbiditic conglomerate and finer grained facies, most of which were deposited within deep marine environments. The onset of Honna deposition therefore accompanied an abrupt rise in relative sea level.

Two distinct types of gravelly submarine system are preserved within the Honna; a longitudinal linear northwest - southeast trending braided channel complex at least 20 km wide and 200 km long, and transverse radial fans sourced from the east, one of which is preserved in the Skidegate Inlet region. At least 4 stacked linear gravelly

braided channel complexes are preserved in the northwest Graham Island region. Each complex is separated from the overlying one by finer grained abandoned channel fill or levee deposits. The gravelly high density turbidity currents flowed primarily from southeast towards the northwest within the channel complexes.

The deposits of the fan system preserved within the Skidegate Inlet region are composed mainly of conglomerate in the east and sandstones in the west, reflecting a general proximal to distal relationship. Minor wave dominated shoreface deposits are also interstratified with the conglomerates to the east. Conglomerates on the fan were deposited within braided channel networks. The fans were probably fed by submarine canyons which bypassed the shelf. The transverse fans in turn fed sediment to the longitudinal channel complex. Provenance studies indicate that sediment was derived from an uplifted and dissected magmatic arc to the northeast, represented by the remnants of the Coast Plutonic Complex.

The longitudinal orientation of the linear channel complex system indicates that a northwest - southeast trending structural element may have defined the southwest margin of the basin. The onset of volcanism in Late Coniacian to Early Santonian time was accompanied by relative sea level fall and a transition to subaerial

environments. Muddy shelf conditions prevailed within the basin during Santonian to Maastrichtian time.

5.2. INTRODUCTION

The Honna Formation is exposed in a 20 km wide, 200 km long belt extending from Logan Inlet in the southeast to Langara Island in the northwest (Fig. 1.3), and consists of up to 2500 m of conglomerate with lesser sandstone and mudstone. Conglomeratic strata of the Honna abruptly and conformably overlie Early Turonian deposits of the Skidegate Formation within most of the Queen Charlotte Island region. In the northeast Moresby Island area however the Honna unconformably overlies Middle Jurassic volcanics of the Yakoun Group (Thompson et al., 1991). In the western Skidegate Inlet region, the Honna is overlain by 300 m of mafic volcanics (Haggart et al., 1989), which in turn are overlain by an Santonian to Maastrichtian mudstones (Haggart et al., 1989; Haggart and Higgs, 1989; Gamba, 1991). In the Pillar Bay region, the Honna is gradationally overlain by the unnamed mudstones (Gamba, 1991).

Six clastic sedimentary facies are recognized within the deposits of Honna (Table 5.1). In order to gain an appreciation of conditions prior to the onset of Honna deposition, the immediately underlying deposits of the

Table 5.1. Facies within the upper Skidegate and Honna Formation

FACIES	HONNA FM	SKIDEGATE FM
Conglomerate	X	—
Classical turbidite	X	X
Sandy turbidite	X	—
Swaley cross-stratified (SCS) sandstone	X	—
Hummocky cross-stratified (HCS) sandstone and sandy mudstone	X	X
Coherently deformed mudstone	X	X
Shale and silty mudstone	—	X
Intraclast breccia	—	X

Skidegate Formation must be analyzed. For this reason, two additional facies particular to the Skidegate Formation are recognized (Table 5.1).

5.3. FACIES DESCRIPTIONS AND INTERPRETATIONS

The swaley cross-stratified (SCS) sandstone, shale and silty mudstone, and the HCS sandstone and sandy mudstone facies are similar to those described from the previous chapter (sections 4.1.4, 4.2.1, and 4.2.3 respectively), and will not be described further.

5.3.1. Conglomeratic facies

Description

This facies is composed of beds of clast-supported pebble to boulder conglomerate and interstratified sandstone, and is by far the most common within the Honna Formation. Conglomerate beds are broadly lenticular and are 0.2 to 6 m thick. The beds are amalgamated and exhibit scoured basal contacts with up to 3 m of erosional relief (Fig. 5.1). Most of the conglomerates exhibit a framework texture; rarely was an openwork texture observed. Clasts are well rounded to angular, dependant on lithology, and consist primarily of granite and andesite with subordinate sedimentary lithologies and intraclasts. The largest

Fig. 5.1 Typical exposure of the conglomerate facies, with strata dipping gently towards upper left. Cliff is approximately 10 m high. Note the erosive basal contacts of the dark coloured conglomerate beds and the lenticular nature of the lighter coloured sandstone beds.

Fig. 5.2 Typical bed of massive, poorly sorted cobble conglomerate. Note the loads at the base of the conglomerate bed, and the flame protruding upwards from the underlying bed of massive sandstone. Stick 1.5 m long.

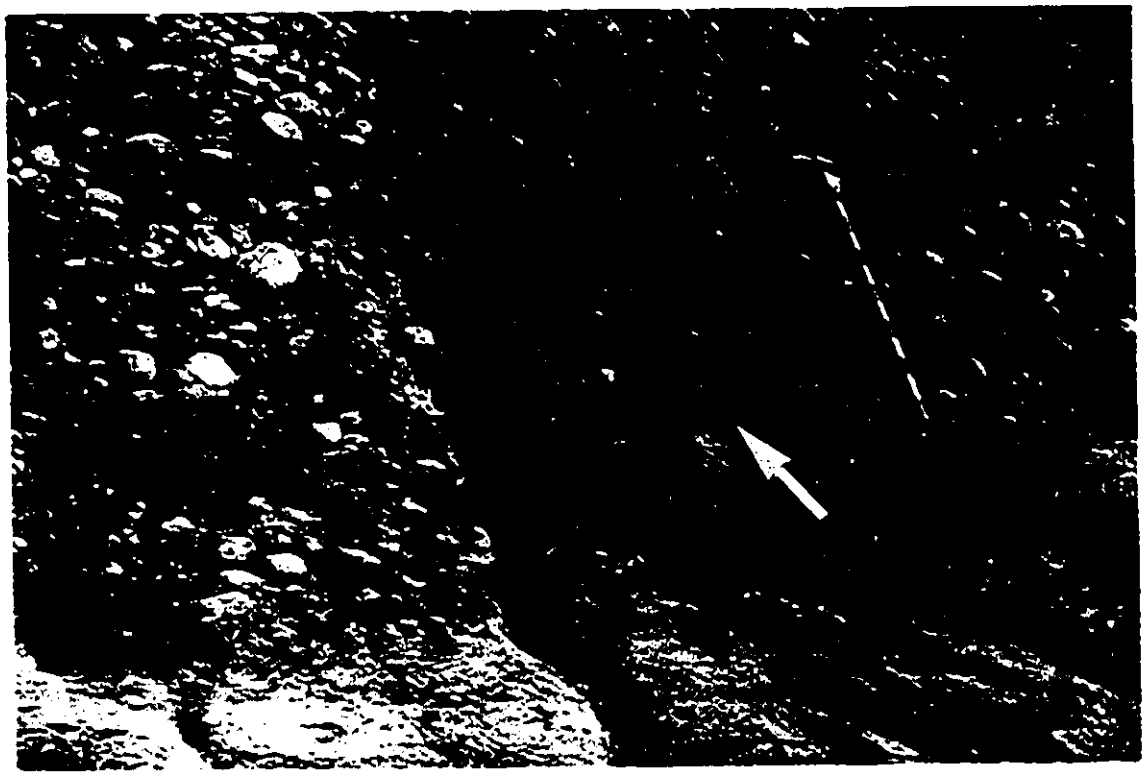

extraformational clast observed was a well rounded boulder of granite 3 m in diameter. The largest intraformational clast included an angular boulder composed of the thin bedded classical turbidite facies 6 m in diameter. Bedding within this facies is often difficult to discern, particularly in the absence of interstratified sandstones or marked changes in clast size.

Four different types of conglomerate were observed. In order of decreasing occurrence, they are: massive, graded, graded-stratified, and cross-stratified. Beds of massive conglomerate are up to 6 m thick and are generally poorly sorted and ungraded (Fig. 5.2). Clasts within many beds exhibit a very well developed a(i) a(p) imbricate fabric (Figs. 5.3 a and b). Some massive beds are no more than thin lags a couple of clasts thick (Fig. 5.4). These lags are very poorly sorted and usually contain outsized boulders.

Beds of graded conglomerate are up to 3 m thick, are poorly to moderately sorted, and display, in order of decreasing occurrence, inverse-to normal grading, inverse grading, or normal grading (Figs. 5.5, 5.6, and 5.7). Beds of inversely graded conglomerate may exhibit rafted boulders which protrude into overlying beds (Fig. 5.6). Some normally graded beds are transitional upwards into coarse grained pebbly sandstone (Fig. 5.7). The graded stratified

Fig. 5.3 a) Plan view of clast imbrication within a bed of graded pebble conglomerate. Flow from upper right to lower left in photo (arrow).
b) Plan view of a(p) a(i) clast imbrication within a bed of graded pebble conglomerate. Flow from bottom to top of photo.


A


B

Fig. 5.4 Poorly sorted lag of massive cobble conglomerate interstratified with massive sandstones. Note the rounded intraclast boulder composed of pebble conglomerate upon which the hammer rests.

Fig. 5.5 Typical bed of inverse- to normally graded pebble conglomerate. Bedding dips gently towards the upper left of the photo. Book 21 cm high.

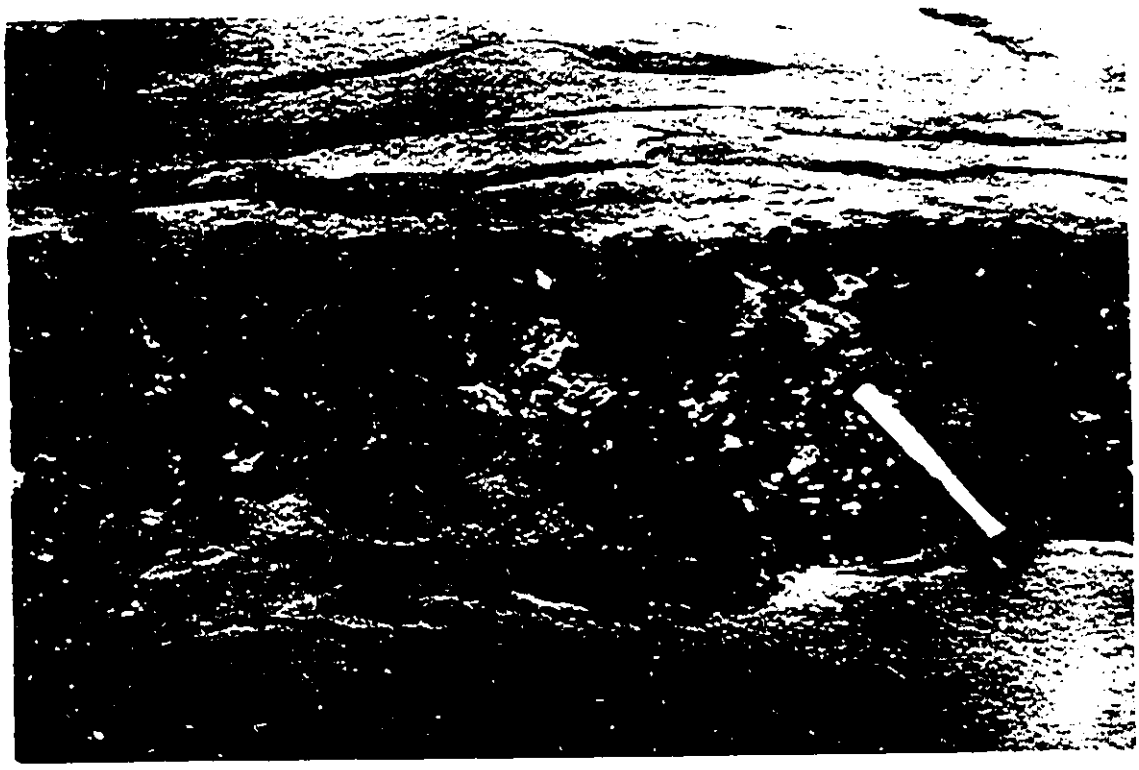

Fig. 5.6 Typical bed of inversely graded cobble conglomerate. Note the large rectangular boulder at the top of the bed protruding into the overlying massive sandstone. Note the amalgamated beds of conglomerate in the background. Ruler 15 cm long.

Fig. 5.7 Two amalgamated beds of normally graded conglomerate. Note the normal grading in the uppermost bed, with boulders at the base passing upward through cobbles into pebbly sandstone. Stick is 1.5 m long.

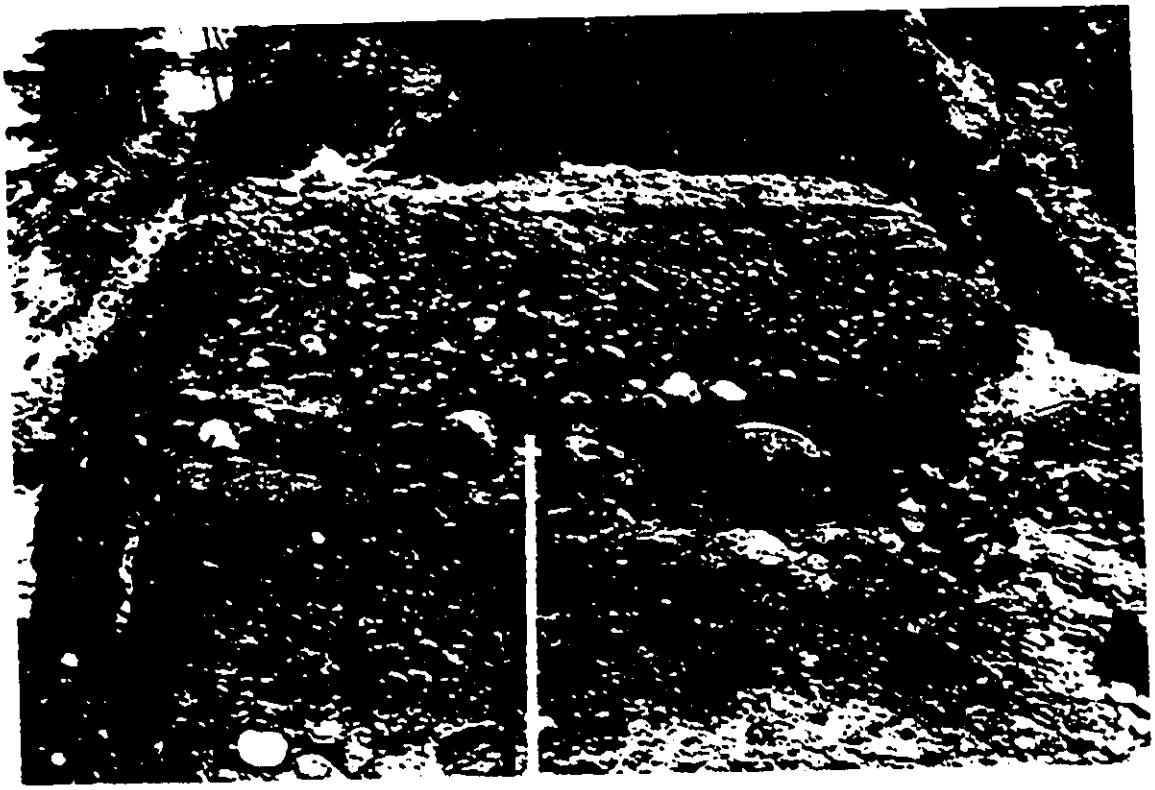

Fig. 5.8 Typical bed of graded stratified conglomerate. Note that the base of the bed consists of cobble conglomerates which grade upwards into pebble conglomerate and then into pebbly sandstone. The pebbly sandstone exhibits crude parallel bedding, with pebbly stringers alternating with well sorted sandstones.

beds are up to 2 m thick and consist of a massive to normally graded basal unit overlain by alternating layers of horizontally-stratified conglomerate and sandstone (Fig. 5.8). The layers tend to decrease in grain size and thickness upward. Clasts within all of the graded beds usually exhibit a well developed a(p) a(i) imbricate clast fabric.

Cross-stratification is rare within the conglomerates. Beds are solitary, exhibit sharp planar bases, and reach a maximum thickness of 3.5 m (Fig. 5.9). Individual cross-strata are up to 40 cm thick and consist of poorly sorted framework clast-supported pebble or cobble conglomerate with a poorly sorted sandstone matrix. The cross-strata are massive or inversely- to normally graded (Fig. 5.10), and are inclined at an angle up to 20 degrees. Clasts within some cross-strata display a well developed a(p) a(i) fabric. Stratification is defined by variations in clast size between adjacent strata. The cross-strata pinch out and interfinger down dip with beds of massive poorly sorted coarse grained sandstone. The inclination of the cross-strata decreases towards the horizontal down dip. Abundant pebble and cobble intraclasts of mudstone and sandstone occur within the conglomerate stringers at the down dip ends of cross-strata. No lateral changes in the thickness of cross-strata was observed, although the cross-

Fig. 5.9 Oblique view of a bed of trough cross-stratified conglomerate, with cross-strata dipping towards viewer. Bed is approximately 2.5 m thick. Note the inclined cross-strata (arrow).

Fig. 5.10 Detail of a single cross-strata within the bed featured in Fig. 5.9. Base and top of cross-strata marked by arrows. The cross-strata is inverse- to normally graded. Scale 8 cm long.

strata within one bed climb towards the north-northwest.

The conglomerates are interstratified with subordinate beds of fine to coarse grained pebbly sandstone and rare beds of mudstone. The sandstone beds are up to 6 m thick and are lenticular and amalgamated (Fig. 5.1). Some of the sandstone beds exhibit scoured bases up to 2 m deep. Beds are, in order of decreasing occurrence, massive, graded, parallel-laminated, ripple cross-stratified, trough cross-stratified or low-angle cross-stratified (Figs. 5.4, 5.11, and 5.12). Some massive sandstone beds are underlain by an intraclast pebble to cobble lag. The arrangement of sedimentary structures within most of the beds can be described in terms of the turbidite facies scheme proposed by Bouma (1962). Many of the massive and stratified sandstone beds contain outsized pebbles and cobbles which float within the sandy matrix (Figs. 5.13 and 5.14). Pebbly loads occur within the upper portions of many sandstone beds overlain by conglomerate. In addition, flame structures are observed along the bases of some conglomerates overlying sandstones beds (Fig. 5.2).

Interpretation

The grading and clast fabric within the graded and graded-stratified conglomerates is indicative of deposition from gravelly high density turbidity currents (Lowe, 1982).

Fig. 5.11 Bed of trough cross-stratified coarse grained sandstone interstratified with beds of conglomerate.

Fig. 5.12 Bed of low angle planar cross-stratified sandstone interbedded with massive pebbly sandstones. Note the flames along the upper surface of the cross-stratified sandstone bed, especially the one to left of the hammer head.

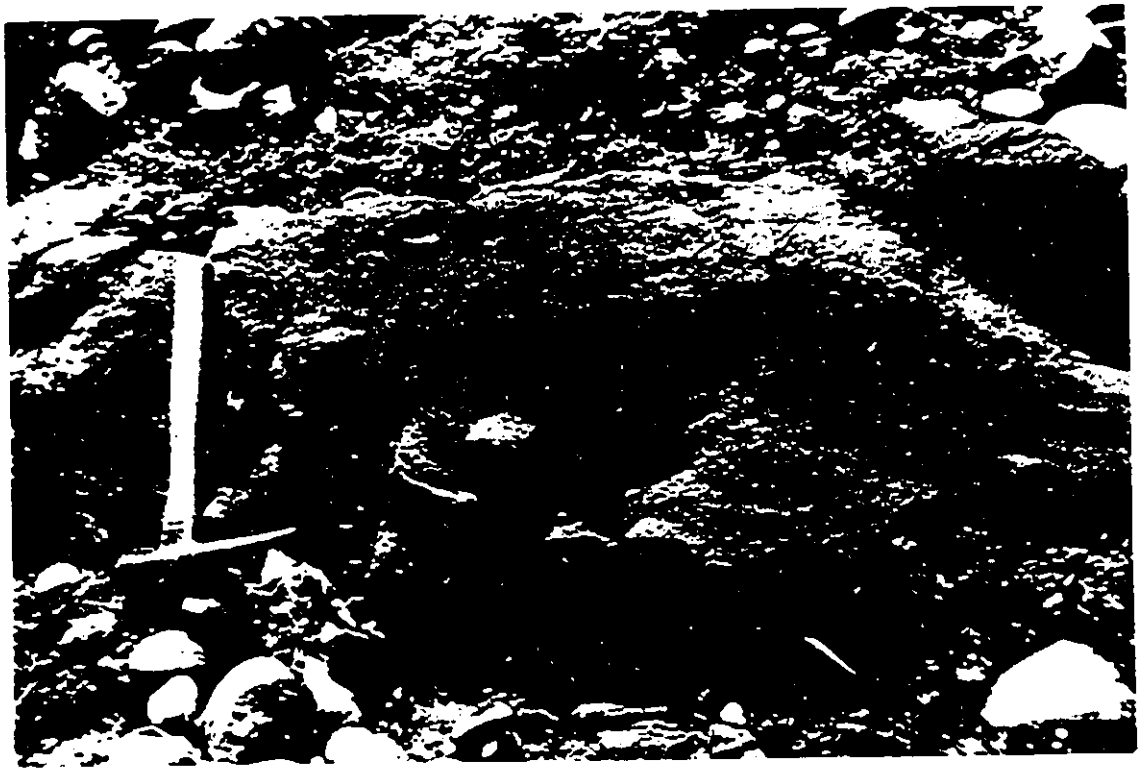

Fig. 5.13 Two separate beds of sandstone containing "floating" cobbles (arrows). The lower bed consists of massive medium grained sandstone and exhibits a solitary well rounded cobble at its centre. Immediately to the left of the cobble is a platy pebble, also floating midway within the bed. The overlying bed exhibits a pebbly base which grades upward into a well sorted medium grained massive sandstone containing a "floating" cobble at its centre (arrow).

Fig. 5.14 Three "floating" pebbles (arrows) within a parallel to ripple cross-laminated bed of sandstone. The pebbles occur within the cross-laminated upper part of the bed.

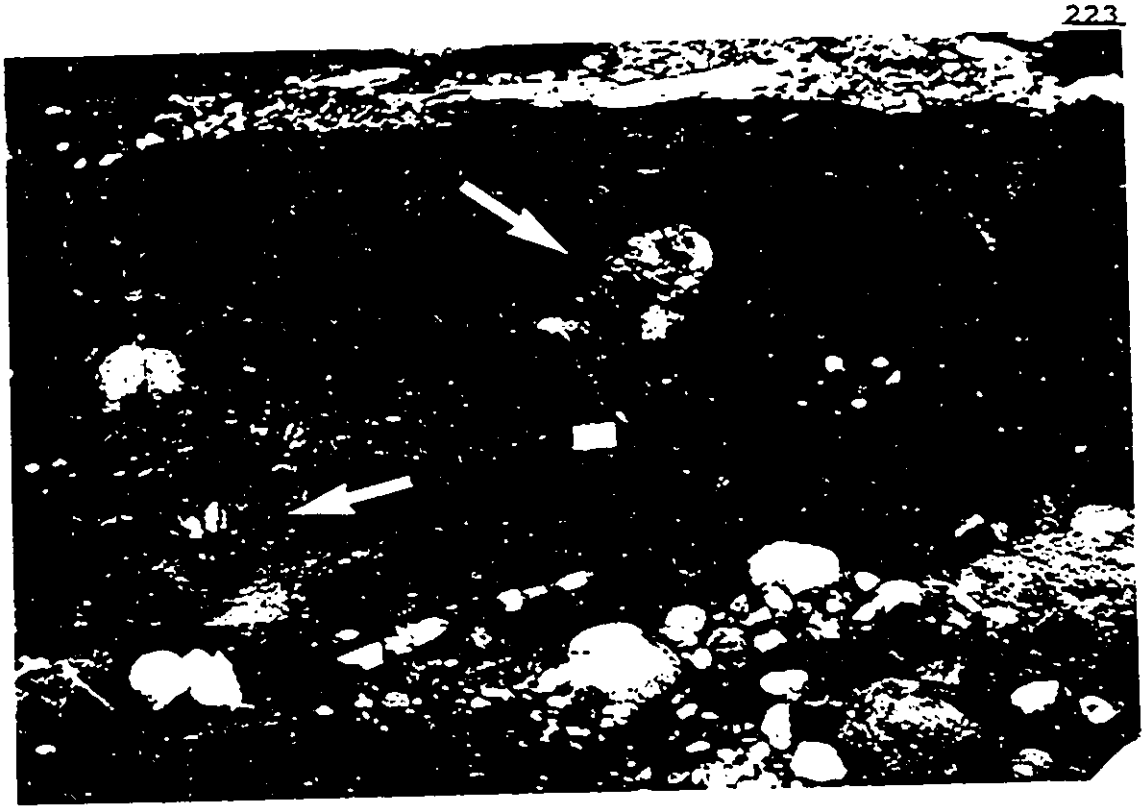

The a(p) a(i) clast fabric indicates that clasts were deposited directly from suspension without rolling on the bed (Walker, 1975 a, b). The inverse grading throughout or at the base of some of the beds reflects the freezing of a concentrated traction carpet at the base of the turbidity current. Clasts within the carpet are supported primarily by dispersive grain pressure, where larger clasts are buoyed towards the top. Deposition occurs instantly when the velocity of the turbidity current drops below that necessary to maintain the dispersive pressure in the traction carpet (Walker, 1975 a, b; Lowe, 1982), resulting in an inversely graded texture. The normal grading observed throughout or in the upper parts of some beds reflects deposition from decelerating gravelly high density turbidity currents, where successively smaller clasts were deposited directly from suspension (Walker, 1975 a and b, 1977; Hein, 1982; Lowe, 1982).

The texture and clast fabric of the massive conglomerates reflect deposition either from gravelly high density turbidity currents or from cohesionless debris flows. The well developed a(p) a(i) clast fabric within many massive beds would seem to favour deposition from turbidity currents, where clasts were deposited directly from turbulent suspension. The lack of grading within these beds may simply reflect a poorly developed lateral

Fig. 5.15 Plot of maximum particle size (MPS) versus bed thickness (BTh) for 39 beds of conglomerate. According to Nemec and Steel (1984), the lack of a good correlation indicates that the conglomerates were deposited by flows which lacked cohesive strength. The real explanation for the correlation however is likely related to the amalgamated nature of bedding.

Fig. 5.16 Typical exposure of the thin bedded classical turbidite facies illustrating both the tabular nature of bedding and the monotonous nature of the facies.

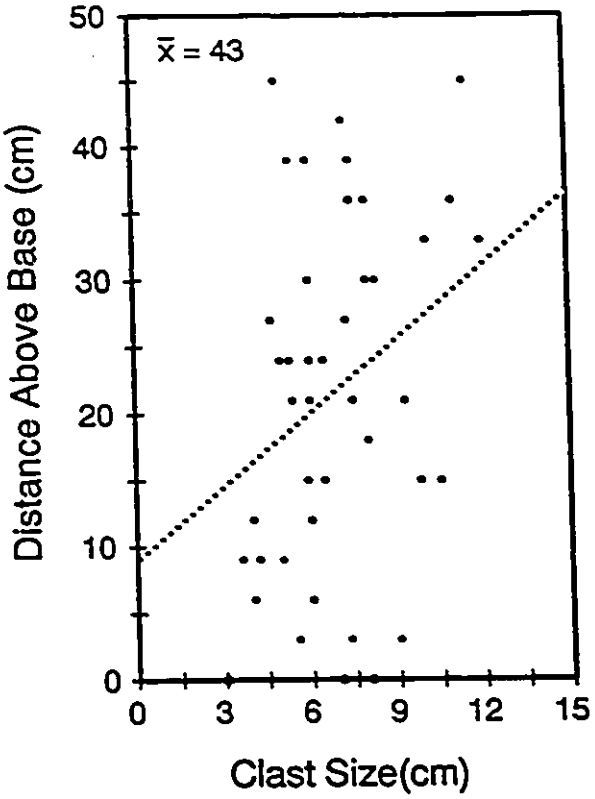
50
40
30
20
10
0
$\bar{x}$ = 43
Distance Above Base (cm)
0
3
6
9
12
15
Clast Size(cm)

segregation of clasts within the flow. The large outsized clasts within the thin massive gravelly lags were probably too large to be carried by the flows and hence were deposited out of suspension and left behind as the flow proceeded downslope.

The weak correlation ($r = 0.21$) between bed thickness and maximum particle size (Fig. 5.15) suggests that the conglomerates were not deposited by sediment gravity flows (Nemec and Steel, 1984). Plots of this sort are however not applicable to the conglomerates of the Honna, as the tops of most beds are clearly eroded. In addition, some of the beds (ie. the thin gravelly lags) appear to be the product of flow bypassing. The cross-stratified conglomerates may represent either lateral accretion deposits or the forsets of large gravelly dunes.

The textures associated with the interstratified massive, massive to parallel laminated, and ripple cross-laminated sandstones is indicative of deposition from sandy high density turbidity currents (Lowe, 1982). These sandstones correspond respectively to the T_a, T_{ab}, and T_c turbidite divisions of Bouma (1962). The dish and pillar structures associated with many of the T_a sandstones is indicative of rapid deposition from suspension followed by dewatering. The low angle and trough cross-stratified pebbly sandstones represent the deposits of low amplitude

and three dimensional dunes respectively. Both types were deposited by tractional processes operating within the turbidity currents.

The presence of outsized floating clasts within many of the T_a sandstone beds is difficult to explain. It is unlikely that the clasts could have been supported for any great distance within the same turbidity current that deposited the sand itself. The clasts may have been loaded into the sandstone following the emplacement of an overlying conglomerate lag. This may in part account for the massive texture of many of the beds, which may be the product of liquification. Judging by the abundance of gravelly balls and flame structures within the sandstone beds, loading was common. A similar mechanism was used by Crowell (1957) to explain the origin of massive pebbly mudstones in California.

The deeply scoured nature of many of the sandstone beds indicates that the turbidity currents were highly erosive. The lenticular and discontinuous nature of all of the sandstone beds is attributed in part to the scour fill nature of the beds, and to erosion by subsequent turbidity currents.

5.3.2. Classical turbidite facies

Description

This facies consists of monotonously interstratified fine to coarse grained sandstone and mudstone beds, and is similar in character to the classical turbidite facies described from the deposits of the Longarm, Haida, and Skidegate Formations (section 4.4.1). Two main varieties were identified: a thin bedded (< 10 cm; Fig. 5.16) variety and a thick bedded (> 10 cm; Fig. 5.17) variety. Sandstone beds within the latter typically exhibit well developed framework lags consisting of intra- and extraformational pebbles and cobbles. In addition, some coarse grained pebbly sandstone beds are trough cross-stratified.

A third variety of classical turbidite facies was also observed. Sandstone beds within this variety are generally thin (< 10 cm) and, besides displaying a vertical arrangement of sedimentary structures which may be described in terms of Bouma's (1962) scheme for turbidites, exhibit intraclast lags, climbing ripples, and convolutions (Fig. 5.18).

Macrofossils within this facies are rare. Traces are common, and include Cosmoraphae, Chondrities and Rhizocorallium, as well as a variety of unidentified forms.

Fig. 5.17 Typical exposure of the thick bedded classical turbidite facies, with strata dipping vertically. Up is towards left of photo. The tabular beds of sandstone display the T_{ab}, T_a, or T_b divisions of Bouma (1962). Stick is 1.5 m long.

Fig. 5.18 Boulder of the CCC-type variety of classical turbidite. The turbidites are thin bedded, parallel to ripple cross-laminated, and contain muddy intraclasts (arrow). The base of the hammer rests upon a slumped unit of thin bedded classical turbidites which displays synsedimentary faulting.

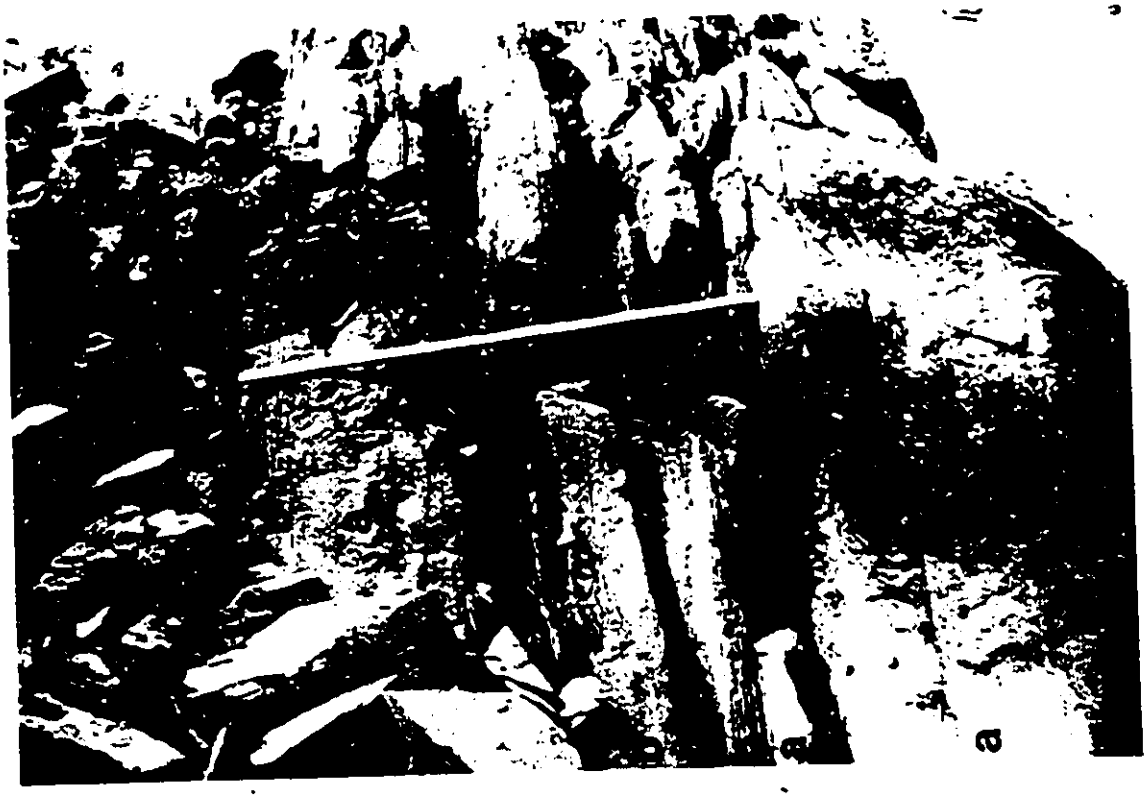
a

Interpretation

The characteristic arrangement of sedimentary structures within the sandstone beds of this facies reflects deposition from low density and sandy high density turbidity currents (Lowe, 1982). The thick bedded variety was obviously deposited from relatively more energetic currents than was the thin bedded variety. Although generally uncommon, trough cross-stratification has been reported from coarse grained turbiditic successions (Allen, 1980; Lowe, 1982). Its presence suggests that flow within at least some of the turbidity currents was steady enough to allow the formation and migration of three dimensional dunes.

The third variety of classical turbidite corresponds to the CCC type (for clasts, climbing ripples, and convolutions) of turbidite facies described by Walker (1985, 1992). The climbing ripples and convolutions reflect relatively high rates of deposition from suspension, while the intraclasts indicate that the turbidity currents were erosive. These types of turbidites were therefore deposited by somewhat more energetic currents than were the regular thin bedded classical turbidites.

The absence of wave formed sedimentary structures indicates that the turbidites were deposited within environments situated below storm wave base (greater than 200 m water depth). The traces observed within the deposits

of this facies belong to the Nereites ichnofacies of Pemberton et al. (1992), which is typically associated with ancient turbiditic successions deposited in submarine fan environments.

5.3.3. Thick bedded sandy turbidite facies

Description

This facies is similar in almost all respects to the thick bedded sandy turbidite facies described from the Longarm, Haida, and Skidegate Formations (section 4.4.2). Sandstones within this facies are medium to coarse grained and pebbly, forming erosively based amalgamated beds up to 4.5 m thick (Fig. 5.19). Flute and tool marks were observed on the sole of some beds. The basal contacts of many beds are overlain by a framework pebble conglomerate or breccia consisting of well rounded extraformational clasts or angular intraformational clasts. Most sandstone beds are completely massive, although some grade upwards into a thin unit of parallel laminated sandstone. Coarse-tail normal grading is evident within many pebbly sandstone beds. Dish and pillar structures were observed within massive part of beds. Interstratified mudstones are rare.

Interpretation

The massive and massive to parallel-laminated

Fig. 5.19 Typical exposure of the sandy turbidite facies, with stratification dipping vertically, up to left. Exposed (right) are amalgamated beds of massive sandstone, which are overlain by thick bedded classical turbidites. Stick is 1.5 m long.

Fig. 5.20 Amalgamated beds of massive intraclast breccia. The beds infill a deep, steep-walled scour (arrows), and are interstratified with and overlain by beds of hummocky cross-stratified sandstone and sandy mudstones. Scale 8 cm long.

sandstones of this facies correspond to the Ta and Tab divisions respectively of Bouma's (1962) scheme for turbidite facies. The massive texture, normal grading, water escape features and sole marks observed within the beds is indicative of deposition from sandy high density turbidity currents (Lowe, 1982). The paucity of interstratified mudstone beds, amalgamation, and the abundance of intraclasts testifies to the erosive nature of the turbidity currents responsible for emplacing beds of this facies.

5.3.4. Intraclast breccia facies

Description

This facies consists of amalgamated beds of framework clast-supported intraclast pebble to cobble breccia. The breccias are interstratified with deposits of the classical and sandy turbidite facies, as well as the HCS sandstone and sandy mudstone facies. Beds are 0.5 to 2.2 m thick and exhibit deeply scoured basal contacts (Fig. 5.20). The breccias are poorly sorted, massive, ungraded, and contain a fine to medium grained sandstone matrix. Clasts are angular to subrounded and are composed almost exclusively of fine grained sandstone and mudstone, as well as minor granite and andesite. Platy clasts within some beds exhibit a well developed subhorizontal fabric.

Interpretation

The massive clast-supported texture and fabric of the breccias indicate that the beds were deposited by high density turbidity currents or cohesionless debris flows. The composition of the beds indicates that partly lithified turbidites were eroded and incorporated into the flow. Given the deeply scoured basal contacts associated with the beds, the currents were very energetic and erosive.

5.3.5. Coherently deformed facies

Description

Beds of this facies are interstratified with the deposits of the thin bedded classical turbidite facies exposed at Egeria Bay on Langara Island. This facies consists of irregular, heavily deformed beds of the thin bedded classical turbidite facies 0.4 to 23 m thick. The internal structure of the beds is complex and variable. Stratification within most beds is folded and contorted but is usually coherent (Fig. 5.21), although some beds are cut by internal faults. In some thin beds stratification is thrown into simple overturned folds. Strata within parts of other beds are brecciated into irregularly-shaped blocks. Each coherently deformed bed is separated from the regional deposits below by a smooth glide plane (Fig. 5.22). Stratification within the regional deposits immediately

Fig. 5.21 Single bed of coherently deformed thin bedded classical turbidites. Strata within the bed are overturned towards the right. Scale (arrow) 15 cm long.

Fig. 5.22 Glide plane (arrows) separating regional thinly bedded classical turbidites (R) from the coherently deformed strata of the slide (S).


S
R

underlying the glide plane may also be somewhat deformed. Overlying deposits of the regional thin bedded classical turbidite facies onlap the irregular upper surface of the deformed beds.

Interpretation

The coherently deformed nature of this facies is indicative of sliding and rotational slumping, a process whereby partially lithified strata are detached from the sea floor and slid en masse downslope along a basal glide plane for a relatively short distance (Allen, 1980; Pickering et al. 1989). If the slides had continued downslope for any great distance, the beds would have been completely brecciated.

5.4. FACIES SUCCESSIONS

Four different types of facies succession are recognized within the deposits of the Honna Formation (Figs. 5.23 and 5.24). These include, in order of decreasing abundance, conglomerate, sandy to classical turbidite, sandy turbidite, and swaley cross-stratified facies successions. Two additional types of facies succession are recognized within the deposits of the Skidegate Formation immediately underlying the Honna. These include the chaotic and the classical turbidite facies.

Fig. 5.23 Northwest - southeast trending strike section through the Honna and upper Skidegate Formations extending from Egeria Bay on Langara Island to Logan Inlet on Moresby Island. Light dashed lines show inferred correlations.

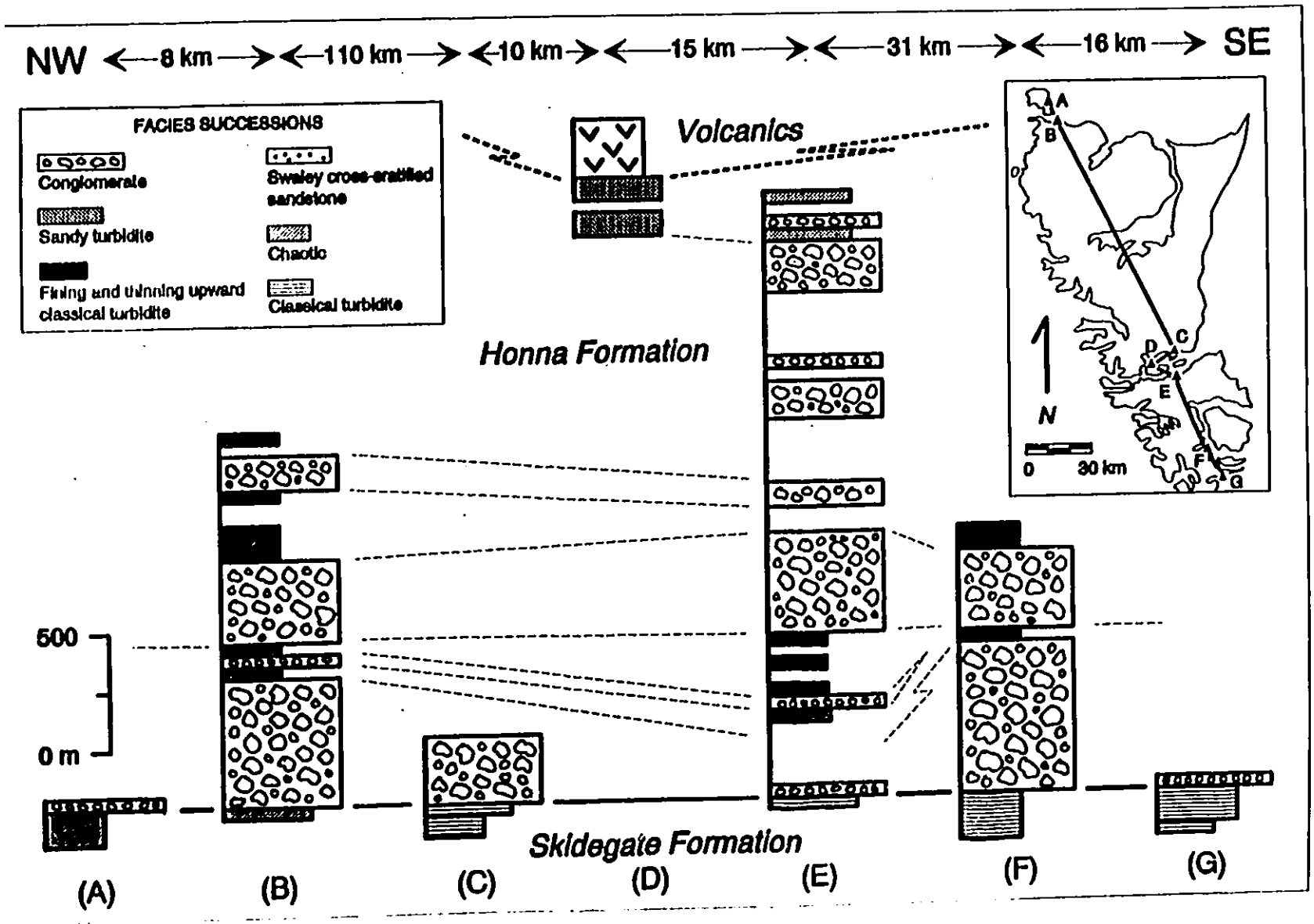
NW
8 km
110 km
10 km
15 km
31 km
16 km
SE
FACIES SUCCESSIONS
Conglomerate
Sandy turbidite
Fining and thinning upward classical turbidite
Swaley cross-stratified sandstone
Chaotic
Classical turbidite
Volcanics
Honna Formation
Skidegate Formation
500
0 m
A
B
C
D
E
F
G
N
0
30 km
(A)
(B)
(C)
(D)
(E)
(F)
(G)

Fig. 5.24 Roughly east - west trending dip section through the Honna extending from northeastern Moresby Island to Gust Island. Light dashed lines show inferred correlations.

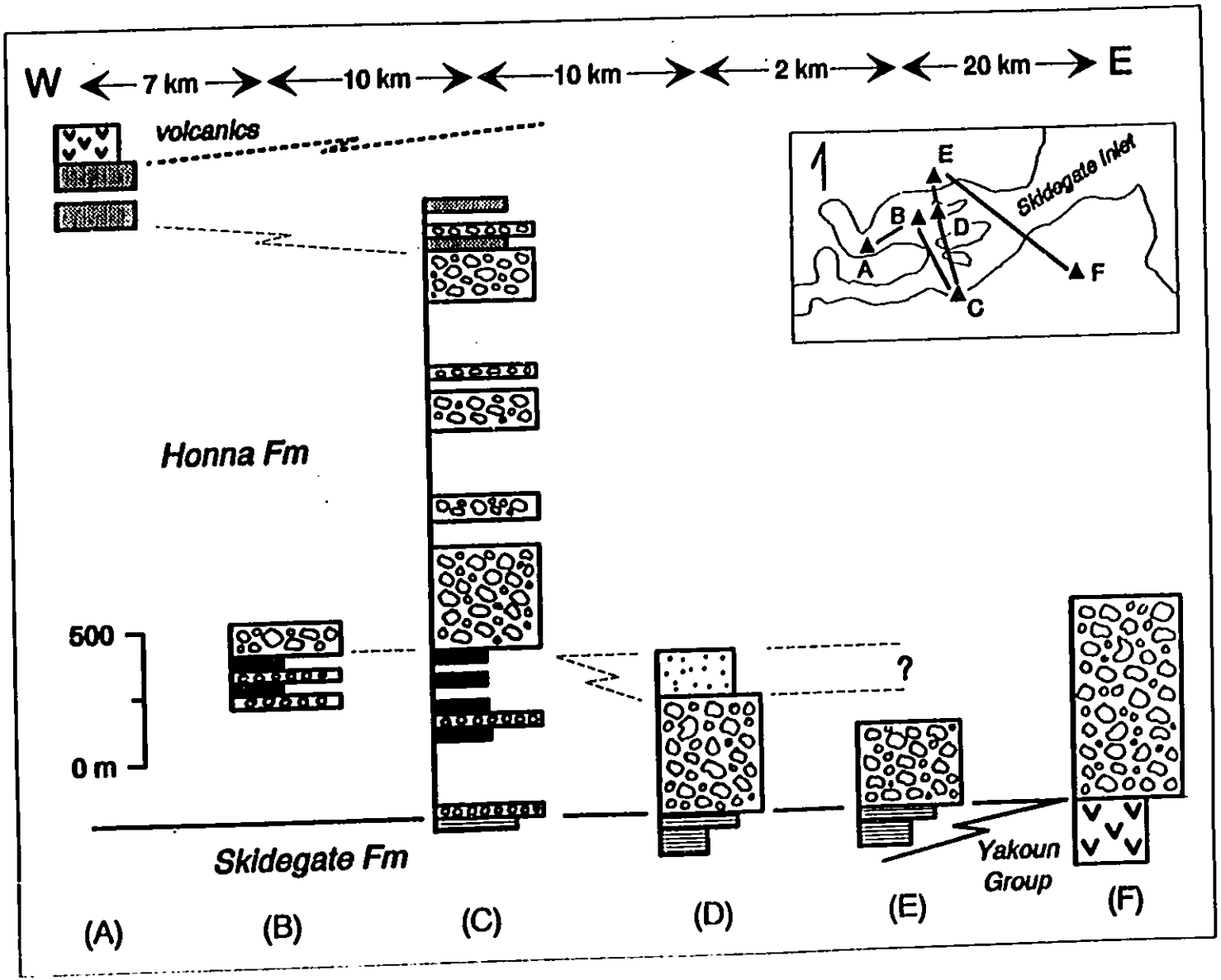
W
7 km
10 km
10 km
2 km
20 km
E
volcanics
1
E
Skidegate Inlet
B
D
A
F
C
Honna Fm
500
0 m
?
Skidegate Fm
Yakoun
Group
(A)
(B)
(C)
(D)
(E)
(F)

What follows is a brief description and interpretation of each type of succession observed within and immediately underlying the deposits of the Honna.

5.4.1. Chaotic facies succession within the upper Skidegate Formation

Description

This succession is exposed on the northern shore of Egeria Bay, located on eastern Langara Island (Figs. 5.25 and 5.26). The lower 125 m of the succession is composed primarily of the thin bedded classical turbidite facies with lesser interstratified beds of the coherently deformed mudstone facies. Beds of the latter are up to 23 m thick and are composed of deformed thin bedded classical turbidites identical in composition to the overlying and underlying deposits. The upper 25 m of the succession is composed primarily of the HCS sandstone and sandy mudstone facies, with lesser interstratified beds of the coherently deformed mudstone facies and the breccia facies. The breccias infill deep scours (Fig. 5.20), and are composed primarily of intraclast pebbles and cobbles, but also contain minor well rounded pebbles of granite and andesite.

The thickness of coherently deformed mudstone beds generally decreases upwards, from a maximum of 23 m within the lower part of the succession to 7 m in the upper part.

Fig. 5.25 Legend showing the various types of facies succession in the Honna used in the following cross sections. classical turbidite facies successions.

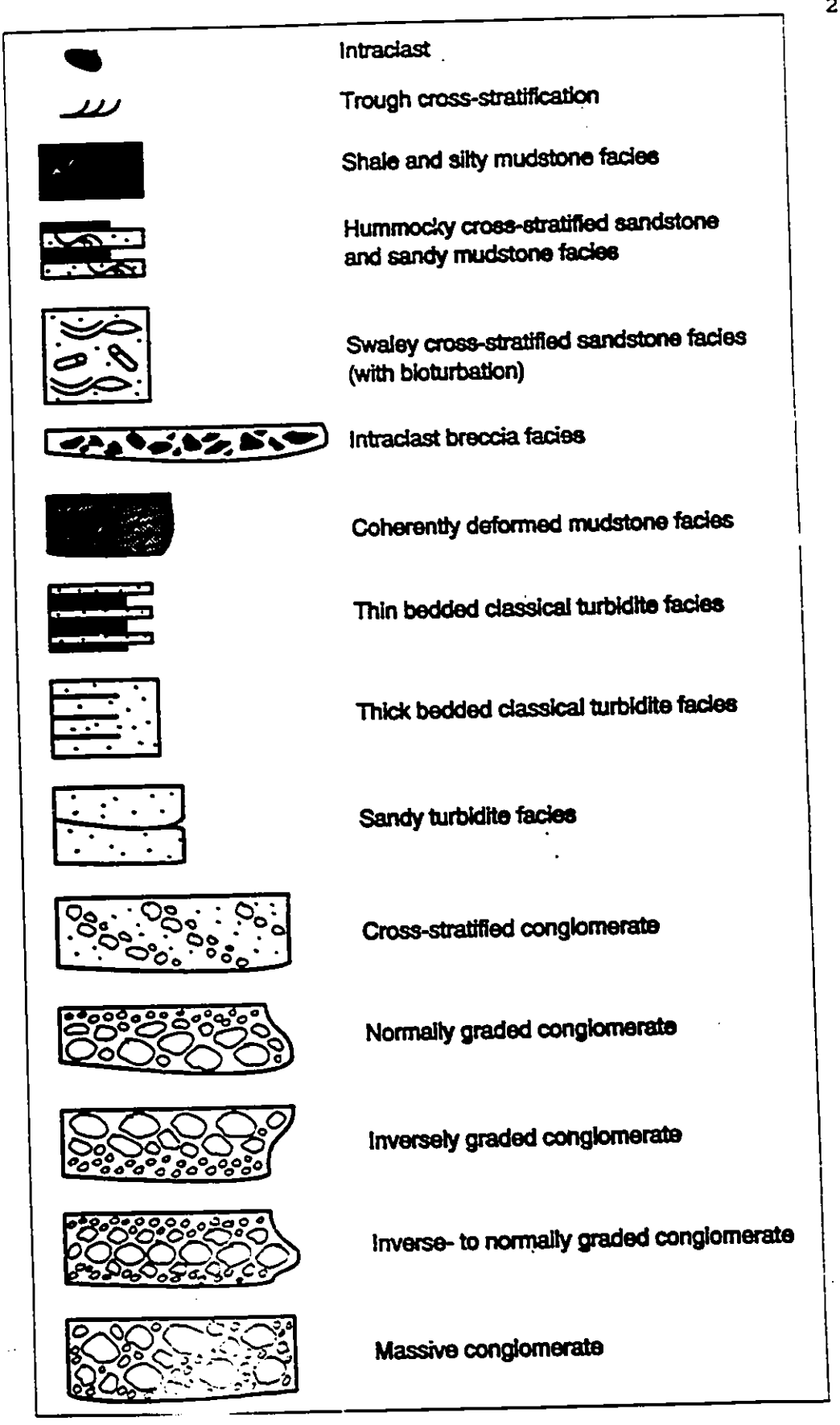
Intraclast
Trough cross-stratification
Shale and silty mudstone facies
Hummocky cross-stratified sandstone and sandy mudstone facies
Swaley cross-stratified sandstone facies (with bioturbation)
Intraclast breccia facies
Coherently deformed mudstone facies
Thin bedded classical turbidite facies
Thick bedded classical turbidite facies
Sandy turbidite facies
Cross-stratified conglomerate
Normally graded conglomerate
Inversely graded conglomerate
Inverse- to normally graded conglomerate
Massive conglomerate

Fig. 5.26 Measured section through the upper Skidegate and lower Honna Formations exposed in northern Egeria Bay, Langara Island (section A, Fig. 5.23).

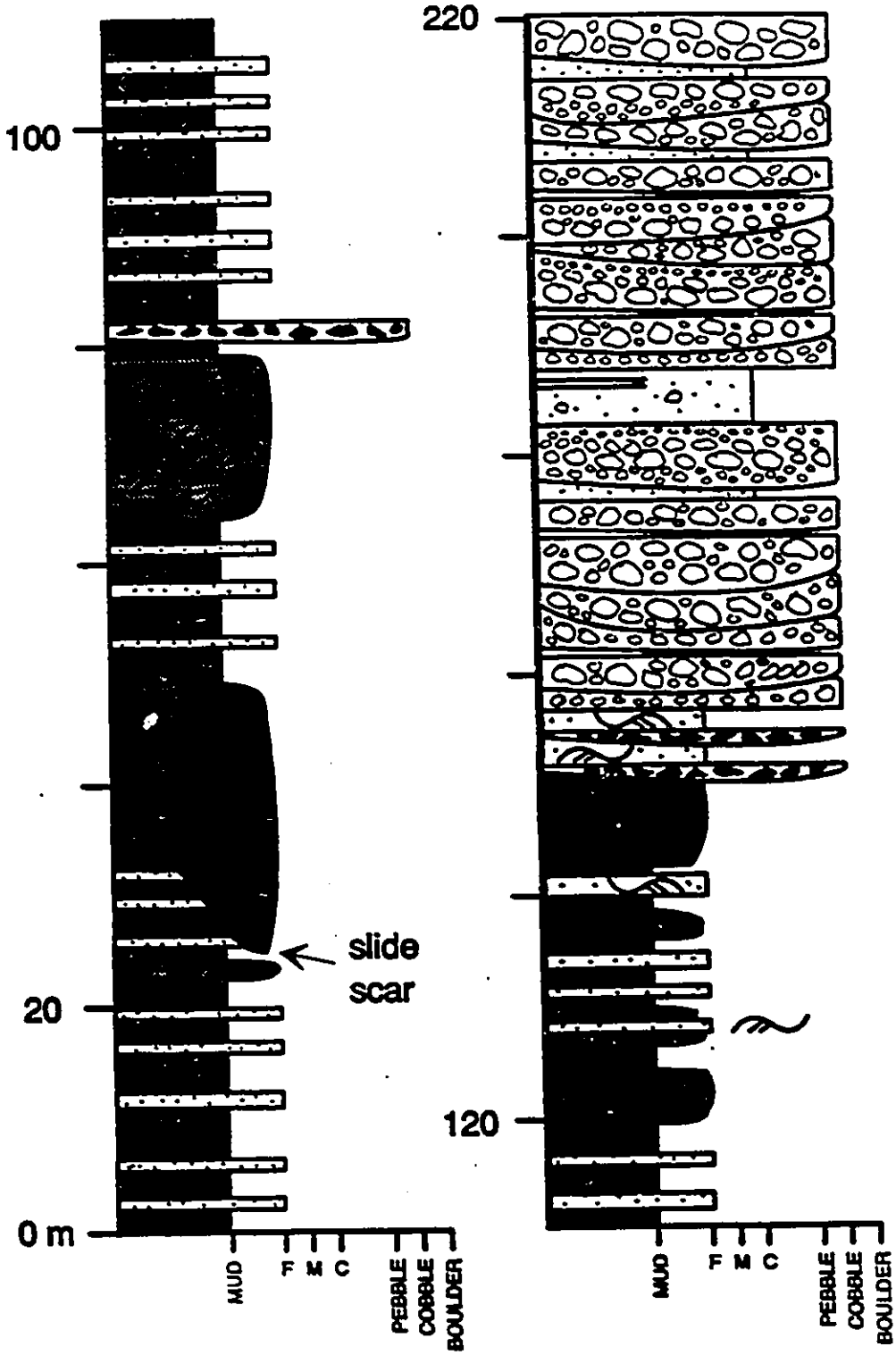
220
100
slide
scar
20
120
0 m
MUD
F M C
PEBBLE
COBBLE
BOULDER
MUD
F M C
PEBBLE
COBBLE
BOULDER

The abundance of interstratified sandstone beds tends to increase towards the top of the succession. The HCS sandstones and sandy mudstones are abruptly overlain by conglomerates of the Honna Formation.

Deposits of the HCS sandstone and sandy mudstone facies also underlie conglomerates of the Honna Formation exposed 4 km to the southwest at Hazardous Cove on Langara Island, as well as at Gunia Point 6 km directly to the south on northwestern Graham Island.

Interpretation

The vertical arrangement of facies within the succession exposed at Egeria Bay reflects a shoaling trend. The thin bedded classical turbidites forming most of the lower part of the succession were deposited within a low energy environment situated below storm wave base. Deposition within this environment was dominated primarily by the emplacement of sand by low density turbidity currents and mud from hemipelagic suspension. These sediments may have been deposited upon the distal lobes of a submarine fan system. The usual calm of this environment was sporadically punctuated by the emplacement of muddy slides represented by the thick coherently deformed mudstones.

The HCS sandstones and sandy mudstones forming much of the upper part of the succession were deposited within an

environment situated above storm wave base (< 200 m water depth). Deposition within this environment was dominated by the emplacement of sand during storm events. The presence of scour-fill breccias indicate that the sea floor within this environment was subject to periodic erosion. The erosion accompanying the emplacement of these breccias may have been related to storm events or perhaps to mass failure of the sea floor. Deposition within this environment was also affected by the emplacement of slides and slumps, though of smaller size than those emplaced within the deeper water turbiditic environment.

The slide deposits are thickest and best developed within the deeper water part of the succession and generally become thinner and more poorly developed within the shallower water part near the top. Slides are triggered by a variety of factors, most commonly oversteepening, seismic shock, rapid rates of sedimentation, and cyclic wave loading (Nardin et al., 1978; Allen, 1980). The slides progress downslope and come to rest when the gravitational forces acting upon the moving mass fall below the frictional force acting along the basal glide plane. This process usually occurs at a break in slope. It is not surprising that the thickest and best developed slides and slumps are encountered within the turbidites near the base of the succession, which was probably deposited in a base of slope

environment.

The vertical arrangement of facies within this succession therefore reflects the basinwards progradation of a muddy slope-apron. The superposition of high-energy shallow water deposits upon low-energy deeper water deposits is typical of other ancient examples of progradational clastic and carbonate slope-aprons (Stow, 1985; Pickering et al., 1989; and Coniglio and Dix, 1992). Ancient slope successions in general are characterized both by the presence of slump and slide deposits, and by a chaotic and diverse arrangement of facies.

5.4.2. Classical turbidite facies successions within the upper Skidegate Formation

Description

These successions occur within the uppermost part of the Skidegate Formation immediately underlying the deposits of the Honna Formation exposed at Logan Inlet (Figs. 5.23 g and 5.27) in the south, and at Lina Narrows (Figs. 5.23 c and 5.28), South Bay and Gosset Bay in Skidegate Inlet.

The lower 40 m of the succession exposed at Logan Inlet (Fig. 5.27) consists of a coarsening and thickening upward package of shales and thin bedded classical turbidites. This package is abruptly overlain by 100 m of thick bedded classical turbidites. Two fining and thinning

Fig. 5.27 Measured section through the upper Skidegate and lower Honna Formations exposed along northeastern shore at the mouth of Logan Inlet (section G, Fig. 5.23).

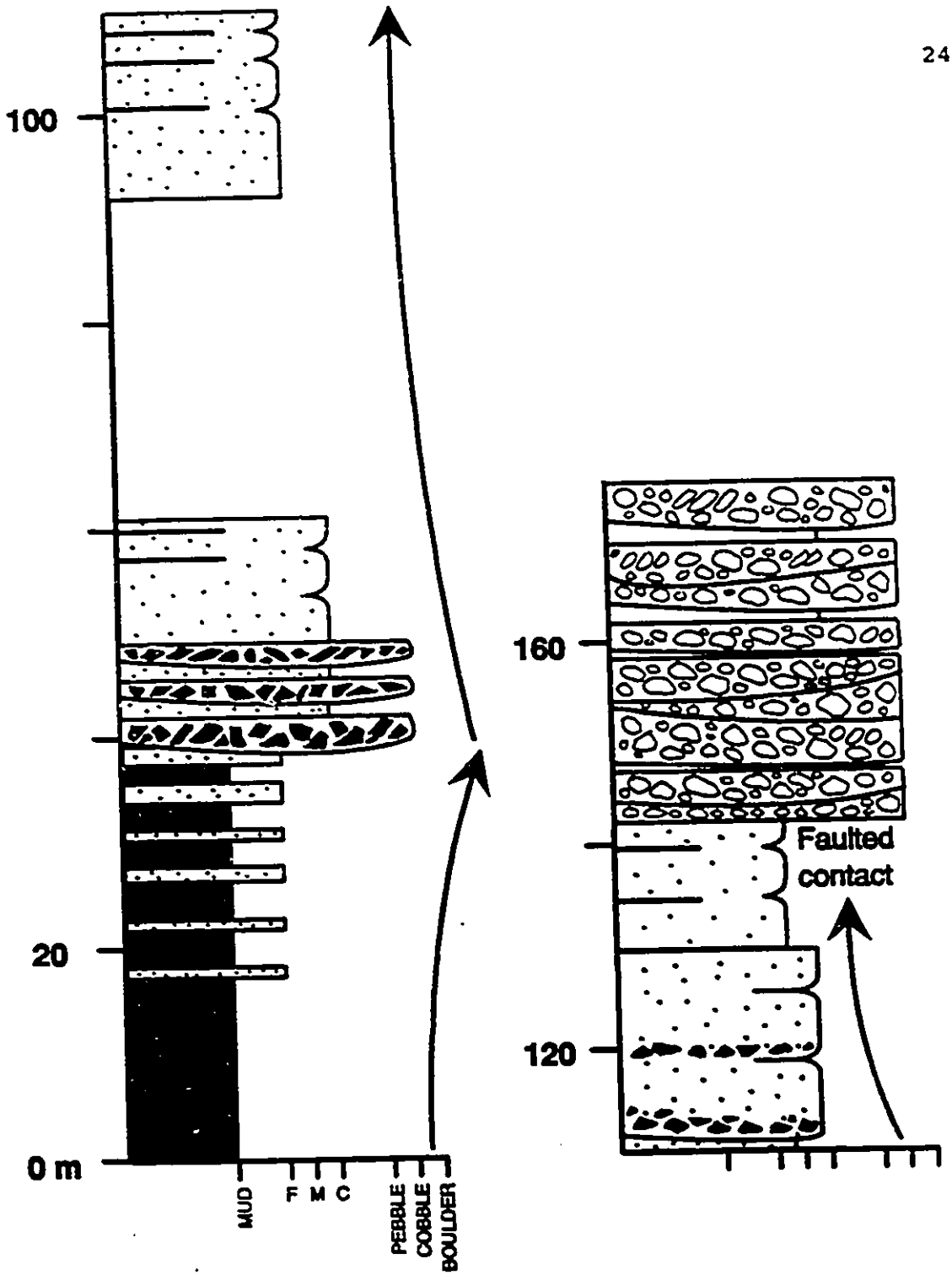
100
20
0 m
160
120
Faulted
contact
MUD
F
M
C
PEBBLE
COBBLE
BOULDER

Fig. 5.28 Measured section through the upper Skidegate and lower Honna Formations exposed in the northern Lina Narrows region of Skidegate Inlet (section C, Fig. 5.23).

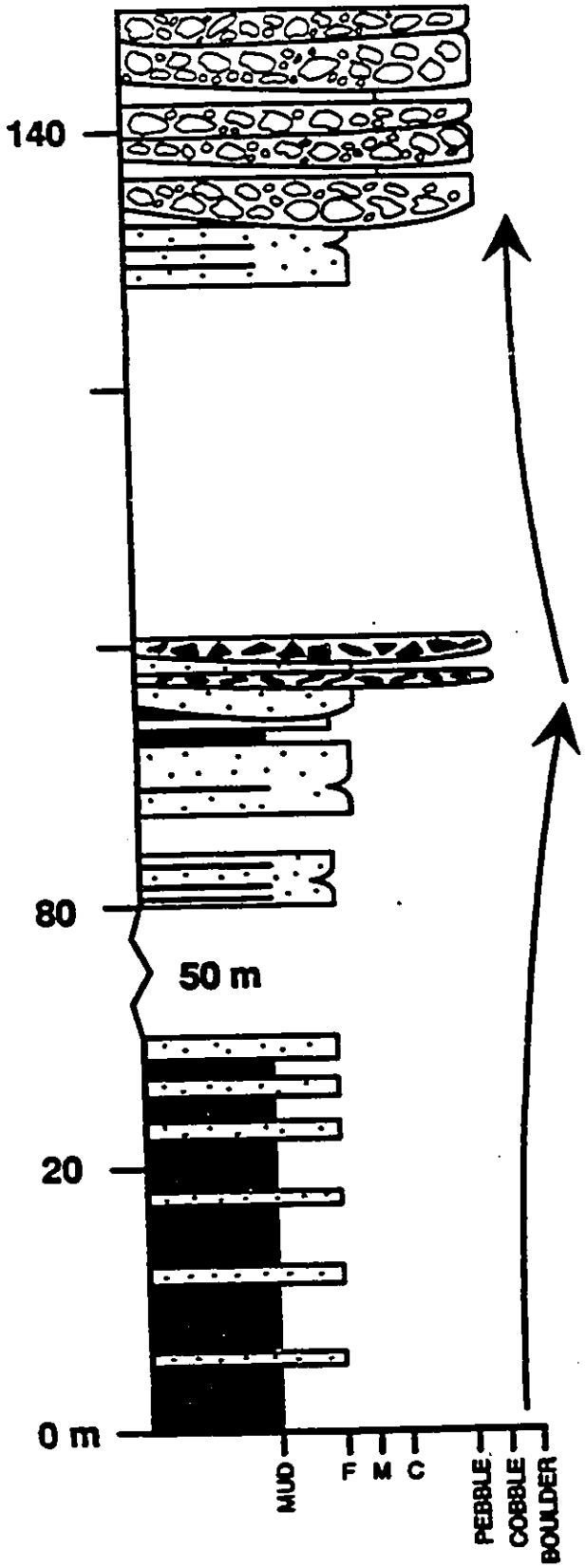
140
80
50 m
20
0 m
MUD
F
M
C
PEBBLE
COBBLE
BOULDER

upward packages 72 and 30 m thick may be distinguished within the upper part of the succession. The lower part of each package consists of coarse grained amalgamated beds of the thick bedded classical turbidite facies. Beds are up to 2.2 m thick, are predominantly massive (T_a), and contain abundant finer grained intraclasts. Beds of the breccia facies up to 2 m thick are interstratified with the thick bedded sandy turbidites of the lowermost package. Some of these breccias fill scours up to 1.7 m deep. Bed thickness and grain size decreases gradually upwards within each package. Sandstone beds within the upper part of each package are fine to medium grained, up to 1.2 m thick, and exhibit the T_{ae}, T_{abe}, and T_{be} divisions of Bouma (1962). The thick bedded classical turbidites of the uppermost package are overlain by conglomerates of the Honna Formation, although the contact at this particular section is faulted.

An identical succession immediately underlying the conglomerates of the Honna is exposed 60 km to the northwest at Lina Narrows in Skidegate Inlet (Fig. 5.28). This succession is approximately 140 m thick and consists of a lower 95 m thick coarsening and thickening upwards package overlain by at least one partially exposed 37 m thick fining and thinning upward package. Minor well rounded granitic and andesitic pebbles are also observed within the intraclast breccias interstratified with the thick bedded

classical turbidites at the base of the fining and thinning upward package. The succession is conformably overlain by conglomerates of the Honna.

Interpretation

The coarsening and thickening upward packages forming the lower part of each of the two successions are interpreted as the deposits of a prograding or laterally migrating submarine fan lobe(s). The lack of scouring at the base of the beds and their sheetlike nature indicate that the turbidites were emplacement by unconfined low density turbidity currents. The gradual upward increase in the occurrence and thickness of sandstone beds may reflect lobe progradation and a transition towards somewhat more proximal and energetic environments.

The overlying fining and thinning upward packages are interpreted as submarine channel fills. The channelized nature of these packages may be inferred from the amalgamated nature of bedding and the occurrence of intraclast breccias within the lower parts of these packages. The breccias may represent gravelly lags deposited by highly erosive turbidity currents. Alternatively, the breccias may have been emplaced by debris flows related to the slumping of channel walls. The amalgamated nature of bedding within the overlying massive

sandstones is typical of channelized turbidites (Walker, 1978, 1984, and 1992; Pickering et al., 1989), and reflects the erosive nature of confined high density turbidity currents. The upward decrease in grain size and bed thickness and the vertical arrangement of facies observed within each of the fining and thinning upward packages reflects a gradual transition towards deposition by less energetic turbidity currents as the channel fills (Mutti and Ricci Lucchi, 1972; Walker, 1978, 1984, 1992).

The arrangement of facies within these two successions may therefore reflect the progradation of a submarine channel complex over a submarine fan lobe.

5.4.3. Conglomerate facies successions

Description

These types of successions form the bulk of the Honna Formation (Figs. 5.23 and 5.24). The conglomerates form successions 10's to 100's of meters thick consisting entirely of amalgamated beds of massive, graded, and cross-stratified conglomerate interstratified with minor beds of coarse grained sandstone (Figs. 5.29 to 5.32). Individual beds of conglomerate could not be traced any great distance across the wide tidal benches exposed at Pillar Bay before being truncated by an overlying bed of conglomerate or

Fig. 5.29 Measured section through the upper part of the Honna Formation exposed along the south shore of Pillar Bay on northwestern Graham Island (section B, Fig. 5.23).

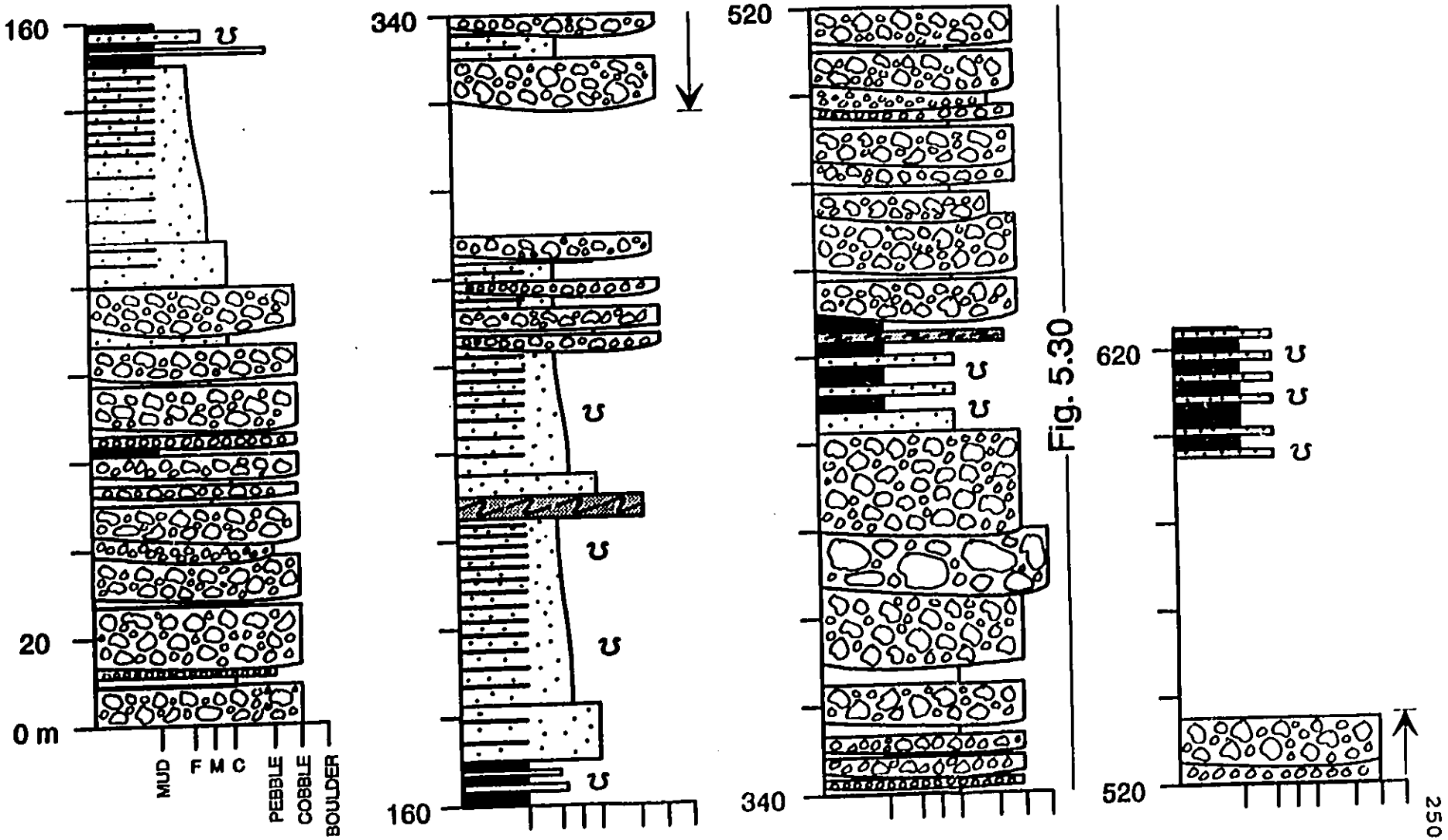
160
20
0 m
MUD
F M C
PEBBLE
COBBLE
BOULDER
340
160
520
340
620
520
250

Fig. 5.30

Fig. 5.30 Detailed section from the uppermost part of the Honna Formation exposed in Pillar Bay (upper part of Fig. 5.29).

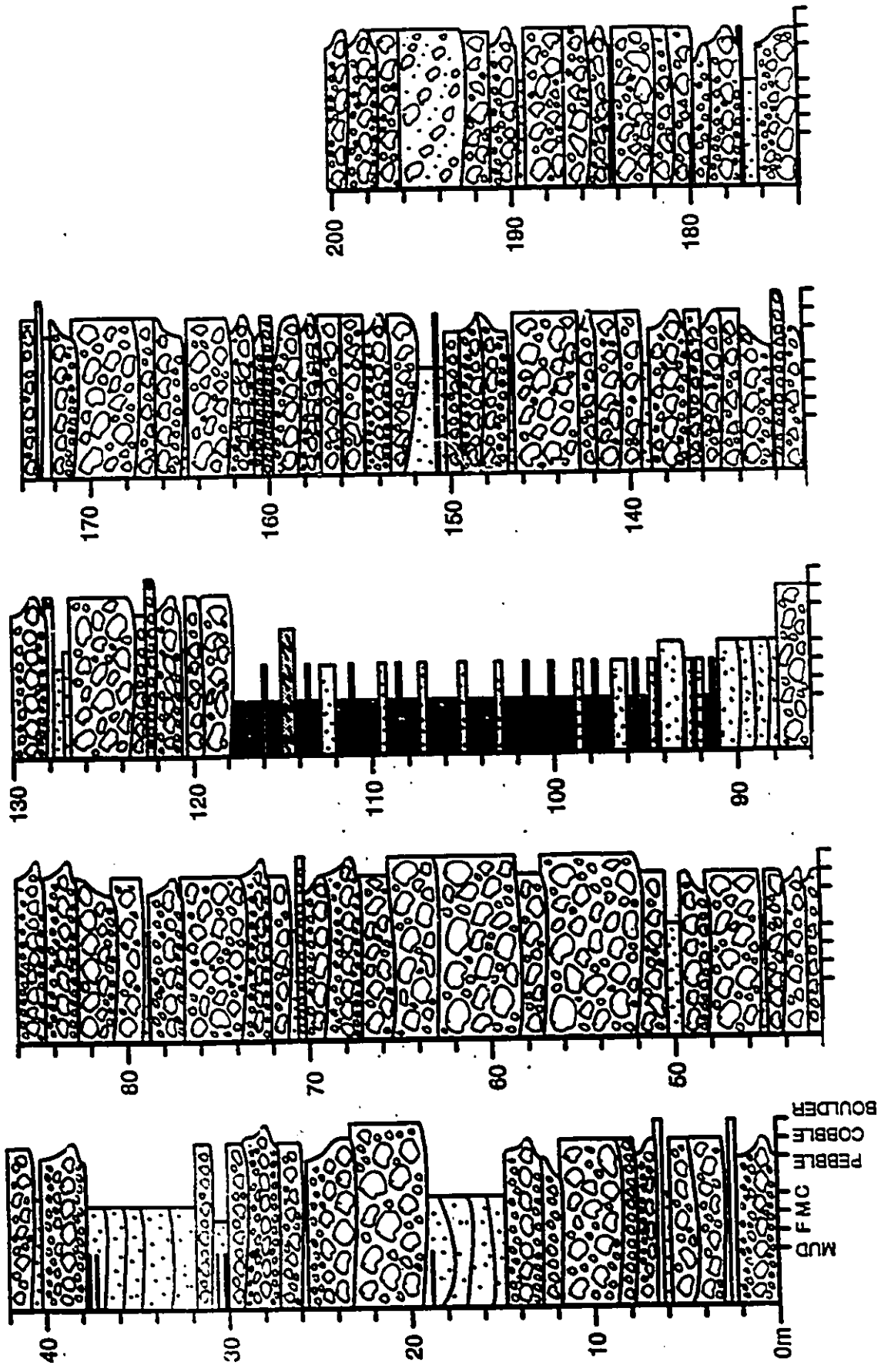
BOULDER
COBBLE
PEBBLE
FMC
MUD
0m
10
20
30
40
50
60
70
80
90
100
110
120
130
140
150
160
170
180
190
200

Fig. 5.31 Measured section of the Honna Formation exposed along the shoreline at Holland Point, southwestern Langara Island.

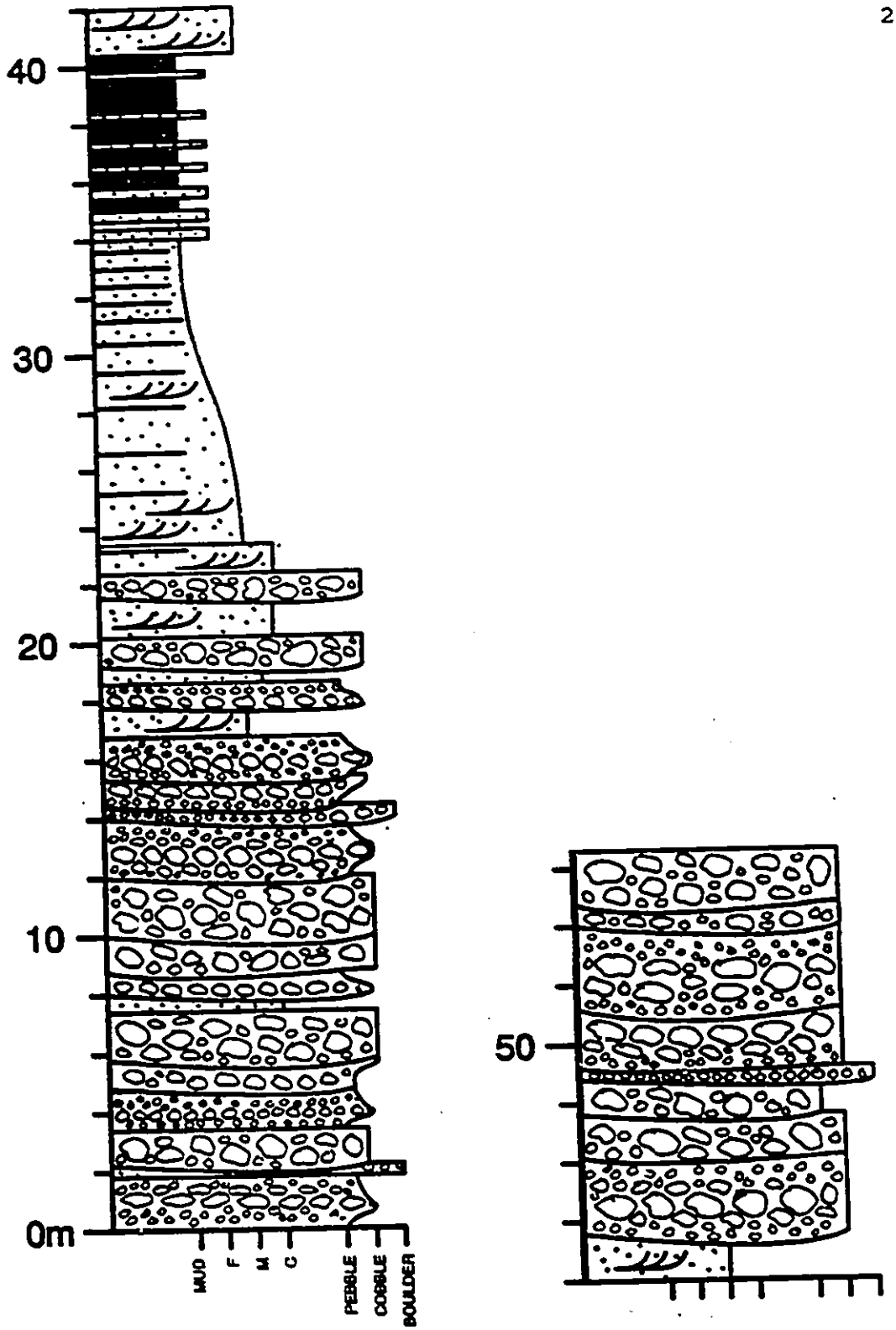
40
30
20
10
0m
MUD
F
M
C
PEBBLE
COBBLE
BOULDER
50

Fig. 5.32 Measured section of the Honna Formation exposed along the western shore of Burnt Island in central Skidegate Inlet (section B, Fig. 5.24).

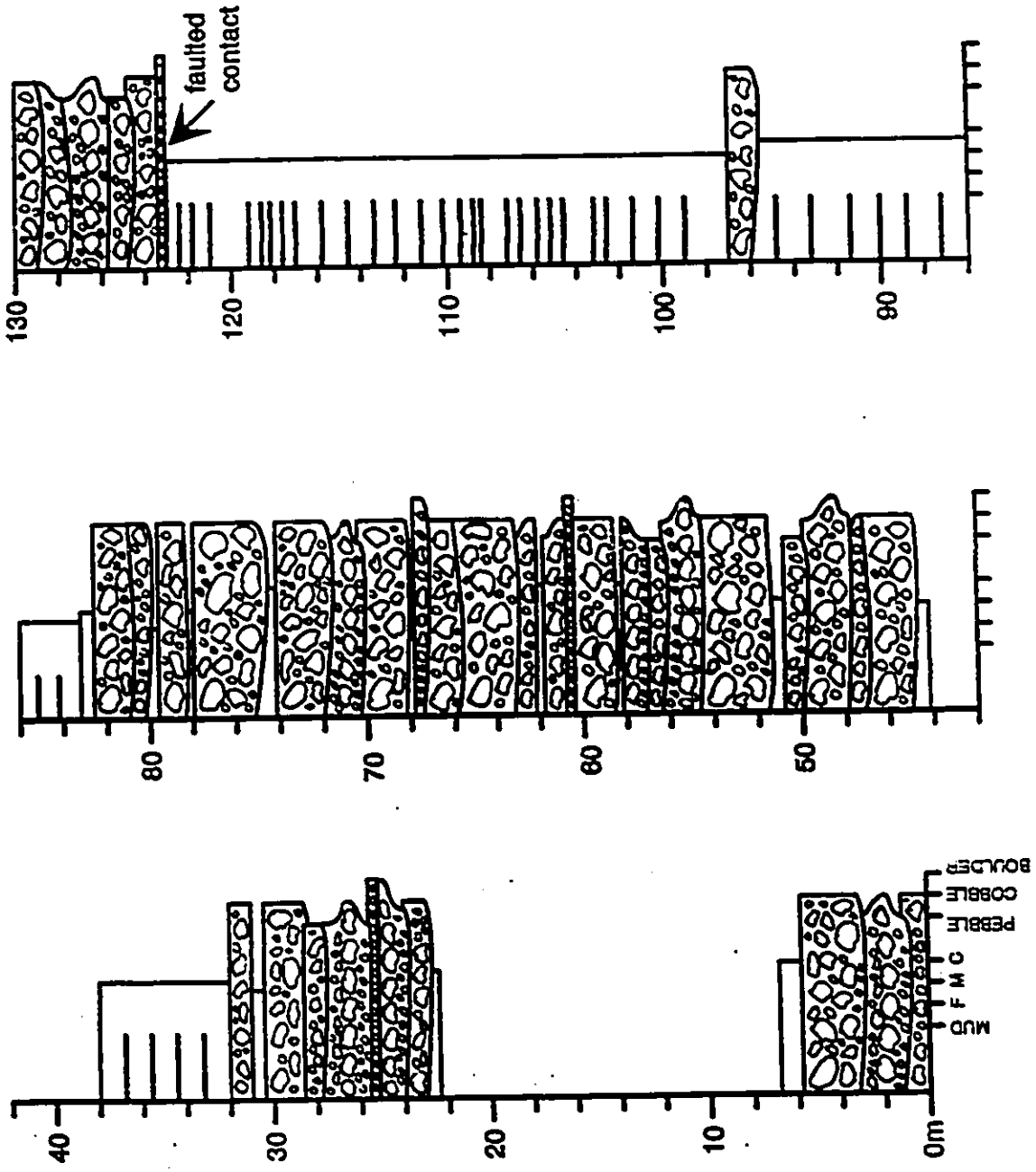
faulted
contact
130
120
110
100
90
80
70
60
50
40
30
20
10
0m
MUD
F M C
PEBBLE
COBBLE
BOULDER

sandstone. No well defined vertical changes in conglomerate type or clast size was discerned within any of the measured sections. Beds of the massive conglomerate facies form more than 50 % of the measured conglomeratic succession. This facies was also by far the most common within exposures not measured in detail. Beds of inversely to normally graded conglomerate are the next most common, followed by inversely and normally graded beds. Beds of cross-stratified conglomerate are rare.

Beds of interstratified sandstone were always medium to coarse grained, and almost invariably exhibited the Ta or Tab divisions of Bouma (1962). No solitary beds of interstratified mudstone were observed within the conglomeratic successions. Beds of conglomerate containing abundant mudstone rip up clasts were however observed within many of the sections (eg. section BuI 1; Fig. 5.32). The most characteristic features of these conglomeratic successions are therefore the amalgamated nature of bedding, the apparently random vertical arrangement of different types of conglomerate, and the lack of interstratified mudstone.

Interpretation

The conglomerates were deposited within a deep water marine environment. This may be inferred by the turbiditic

nature of the conglomerates themselves, and by the fact that they are interstratified with successions of the classical turbidite facies. The presence of rare ammonites and bivalves within the conglomerates themselves (Sutherland Brown, 1968) is also indicative of a marine environment, as is the presence of a benthic foraminifera fauna within the interstratified classical turbidites (F. Clark, pers. comm. 1993). The poorly preserved nature of the foram fauna, the almost complete lack of pelagic forms, and the presence of agglutinated forms, all may be indicative of restricted basin conditions or of deposition within a very deep marine environment almost below the calcium compensation depth (F. Clark, pers. comm. 1993). The paucity of macrofossils may therefore reflect similar conditions.

The conglomerates were probably deposited within braided gravelly submarine channels, as suggested by Yagishita (1985a). This accounts for the amalgamated and lenticular nature of the conglomerate beds. The relatively minor amount of relief associated with the basal scours (less than 3 m) of most beds indicate that the channels were relatively shallow, small scale features. Given the nature of the exposure, which consists of narrow tidal benches and low sea cliffs, it is quite probable that evidence of larger scale submarine channelling (i.e. greater than 10 m) would

be very difficult to discern.

The cross-stratified conglomerates within some of these successions (Fig. 5.9) are similar to those described from the Ordovician Cap Enrage Formation of southern Quebec by Hein and Walker (1982), and to those described from the Cretaceous Cerro Formation of southern Chile by Winn and Dott (1977). The former represent the lateral accretion deposits of point bars, and are composed of graded beds deposited by turbidity currents forming successions 1 to 10 m thick. The latter represent traction structures produced by grain-by-grain deposition from suspension and then traction transport as bed-load, forming dunes up to 4 m thick. Similar large dune-like features have also been documented from the modern feeder channel of the Laurentian fan by Piper et al. (1985), and within the Lower Var Canyon of southern France (Malinverno et al., 1988). The very poorly sorted and heterolithic nature of the cross-stratified conglomerates within the Honna stand in stark contrast to the well sorted pebble conglomerates forming the dunes described by Winn and Dott (1977). In addition, imbrication measurements from individual strata within one of the cross-stratified conglomerates exposed in Pillar Bay indicate paleoflow from east to west (Fig. 5.33). Cross-strata within this bed are inclined towards the north at right angles to the paleoflow direction inferred from clast

Fig. 5.33 Paleocurrent trend derived from clast imbrication from a bed of cross-stratified conglomerate. The mean paleocurrent trend is towards the west (274°), while the cross-strata within the bed dips almost due north.

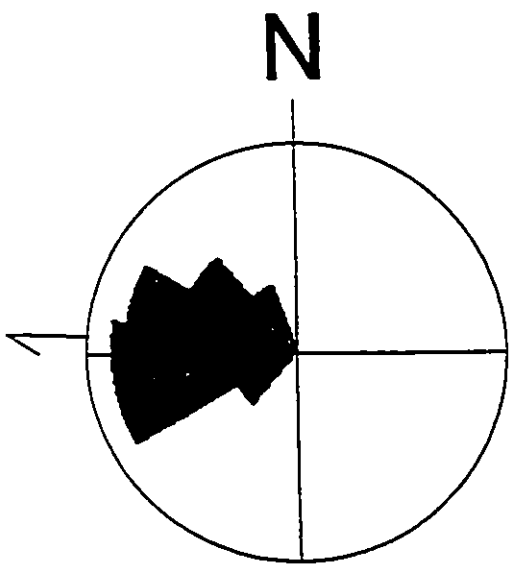
N

imbrication. These observations indicate that the cross-stratified conglomerates probably represent lateral accretion deposits emplaced by turbidity currents against the flank of a gravelly bar or the margin of a channel.

The deeply scoured basal contacts associated with the interstratified coarse grained sandy turbidites likewise indicates that they were deposited within small scale channels. The solitary floating clasts within the interstratified coarse grained Ta and Tbc turbidites (Figs. 5.13 and 5.14) may have been dislodged from a nearby channel wall as a turbidity current passed, and simply rolled onto the bed as it was being deposited. As outlined previously, it is unlikely that the clasts could have been maintained in suspension within the same flow which emplaced the sand. It is also unlikely that the lone clasts could have been loaded into the bed from above, especially in the case of the Tbc turbidites (Fig. 5.14) where stratification is clearly not deformed.

Finer grained sediments were probably deposited from hemipelagic suspension within the channels inbetween the influx of gravelly and sandy high density turbidity currents. These deposits were reworked by subsequent currents, to be redeposited in the form of intraclast lags. Deposition of conglomerates within the channel systems periodically halted rather suddenly, as indicated by the

abrupt manner with which the conglomeratic successions are interstratified with successions of the classical turbidite facies.

5.4.4. Fining and thinning upward classical turbidite facies successions

Description

The conglomeratic successions are interstratified with thick successions composed of the classical turbidite facies (Figs. 5.23, 5.24, and 5.29 to 5.32). These successions are up to 160 m thick, and usually display a fining and thinning upward (FTU) motif reminiscent of those described from the deposits of the Skidegate Formation immediately underlying the Honna (section 5.4.2).

Three stacked successions 40 to 70 m thick are observed within the lower part of the section exposed at Pillar Bay (Fig. 5.29). The lower part of each succession consists of thick bedded coarse grained classical turbidites. Beds are up to 4 m thick and usually display the T_a or T_{ab} divisions of Bouma (1962). Beds are typically amalgamated and exhibit basal lags composed of mudstone and siltstone intraclasts. The thickness and grain size of the sandstone beds decrease gradually upwards, while the number and thickness of interstratified mudstones increases. Sandstone beds within the upper part of each succession are

finer grained and thin bedded (generally less than 10 cm thick), and exhibit the T_{bce}, T_{be}, or T_{ce} divisions described by Bouma (1962). Solitary beds of the coherently deformed mudstone facies occur within the uppermost parts of two successions exposed within the lower part of the succession exposed at Pillar Bay (Fig. 5.29). The successions are abruptly overlain either by thick bedded turbidites of the overlying succession or by successions of the conglomerate facies.

A very similar 29 m thick FTU succession is exposed within the upper part of the section exposed at Pillar Bay (Figs. 5.29 and 5.30). The coarse grained thick bedded classical sandstones at the base of this succession contain thick, well developed basal intraclast lags. A bed of coherently deformed mudstone also occurs within the upper part of this particular succession.

A similar 24 m thick FTU succession was observed within the section exposed at Holland Point on southeastern Langara Island (Fig. 5.31). This succession differs from those exposed at Pillar Bay in two important respects. Firstly, beds of massive or normally graded cobble conglomerate are interstratified with thick bedded coarse grained sandstones at the base of the succession. Secondly, the interstratified sandstones are predominantly trough cross-stratified. The deposits of this succession are

abruptly overlain by 4 m of medium grained trough cross-stratified sandstone, which are abruptly overlain by 13 m of the conglomerate facies.

A poorly developed 30 m thick FTU succession also occurs interstratified with the conglomerates of the Honna at Burnt Island in central Skidegate Inlet (Fig. 5.32). The base of the succession consists of relatively thick bedded classical turbidites. Sandstones beds within this part of the succession are medium to coarse grained, and display the T_{ae}, T_{abe}, T_{bce}, and T_{ce} divisions of Bouma (1962). Many beds contain a well developed intraclast lag. A single bed of massive cobble conglomerate occurs within the middle of the succession, which in turn is overlain by 26 m of relatively thinner bedded, fine grained classical turbidites. The top of the succession is in fault contact with a succession of the conglomerate facies.

Interpretation

The amalgamated sandy turbidite beds forming the lower part of each of the FTU successions probably represent sandy channel deposits. This may be inferred frcm the high degree of scouring along the base of each bed, and the abundance of intraclasts within most of the beds. Both of these features indicate that the turbidity currents emplacing the sandstones were highly erosive. This may have

been the result of the current being partially confined to channels. In the case of the succession exposed at Holland Point (Fig. 5.31), the underlying conglomeratic succession appears to grade upward into the thick bedded cross-stratified sandstones forming the lower part of the FTU succession. This again indicates that the thick bedded sandstones forming the lower part of the FTU succession were probably deposited within channels. In this case the channel was in the process of being gradually abandoned by gravelly high density turbidity currents.

The upward decrease in grain size and bed thickness within each FTU succession reflects an overall net decrease in the energy level as the channel was gradually infilled. Considering the absence of evidence for large scale channelling, it is also possible that the thin bedded classical turbidites forming the upper parts of the FTU successions may represent interchannel deposits. Indeed, the CCC-type classical turbidites observed within some of these successions may well represent levee deposits (Walker, 1992).

Alternatively, other allocyclic mechanisms such as relative sea level rise may also be invoked to explain the generation of these types of successions (Mutti, 1985; Walker, 1992).

5.4.5. Sandy turbidite facies successions

Description

Successions of this sort are found in the western Skidegate Inlet region. Two sections were measured; one at Gust Island (Fig. 5.34), the other at a small unnamed island situated immediately to the northwest (Fig. 5.35).

The lower 40 m of the succession exposed on Gust Island consist of a package of thick bedded pebbly medium to coarse grained sandy turbidites. Beds are massive (T_a), up to 4 m thick, and are amalgamated. Many of the beds exhibit intraclast breccia lags up to 30 cm thick. This package is overlain by a 26 m thick package consisting of thick bedded sandy and classical turbidites. The lower part of this package consists of amalgamated beds of sandy turbidites up to 3 m thick. These beds are identical in character to the sandy turbidites within the underlying package. The sandy turbidites are overlain by thick bedded classical turbidites. Beds are up to 2 m thick, are primarily massive (T_a), and are interstratified with thin beds of mudstone. Both types of turbidite within this package contain abundant extraformational and intraformational pebbles and cobbles, both within basal lags and scattered throughout the bed. A 1 m thick massive bed of mafic volcanics occurs within the middle of the package. The bed exhibits very prominent chilled margins.

Fig. 5.34 Measured section of the upper part of the Honna Formation exposed along the north shore of Gust Island in western Skidegate Inlet (section D, Fig. 5.23).

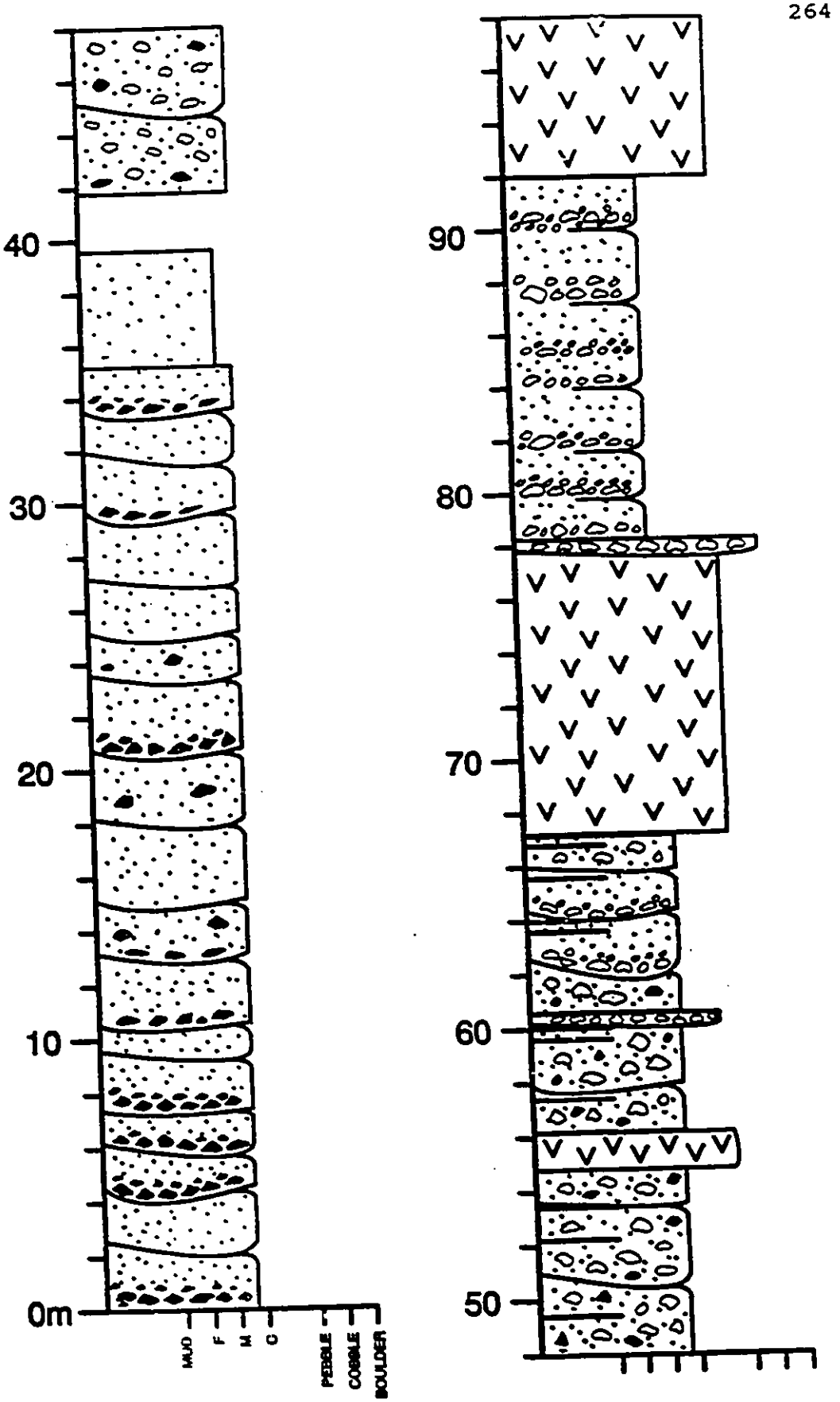
0m
10
20
30
40
50
60
70
80
90
MUD
F
M
C
PEBBLE
COBBLE
BOULDER

Fig. 5.35 Measured section of the upper part of the Honna Formation exposed along the northern shore of a small unnamed island in western Skidegate Inlet.

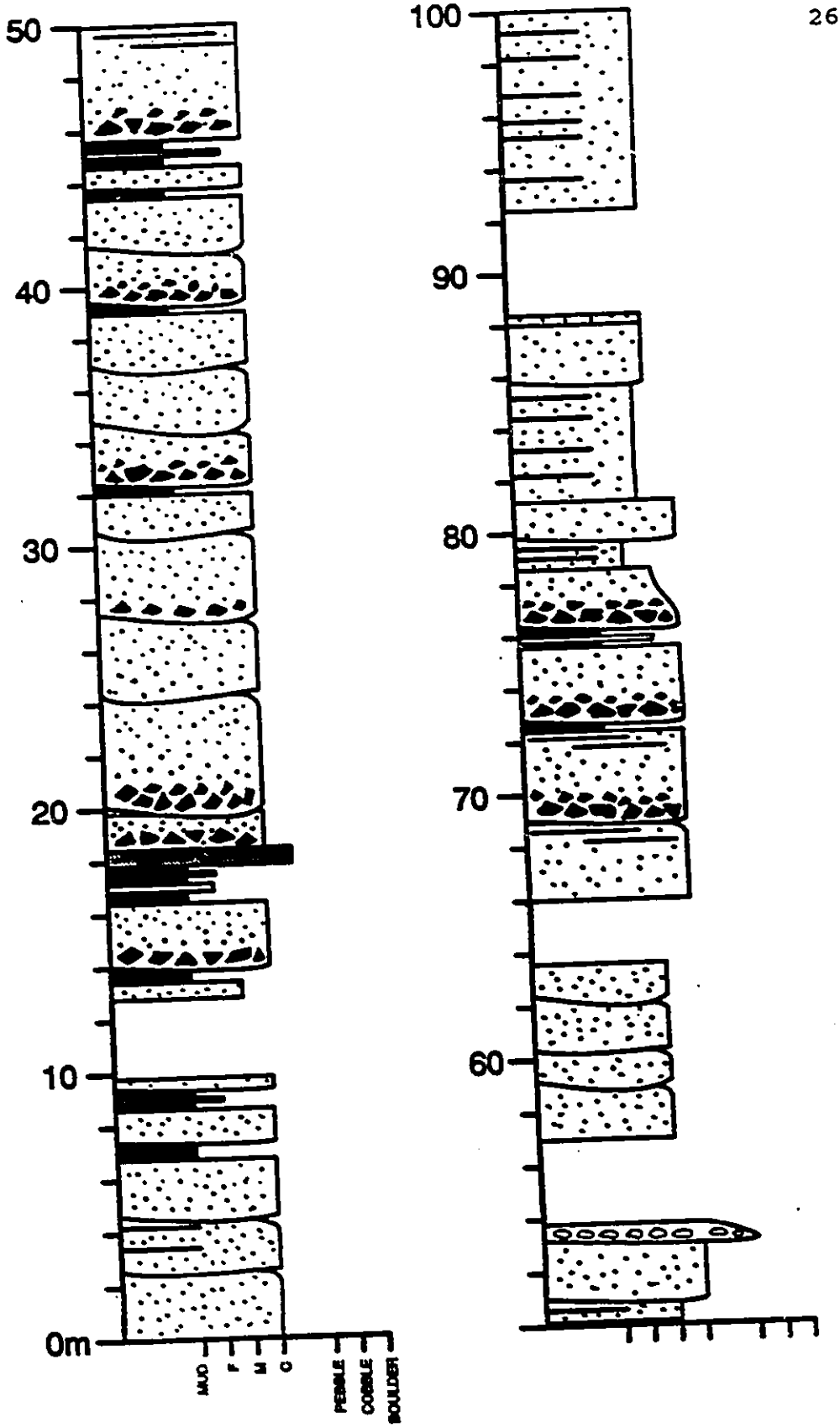
50
40
30
20
10
0m
100
90
80
70
60
MUD
F
M
C
PEBBLE
COBBLE
BOULDER

The middle package is abruptly overlain by 11 m of massive mafic volcanics. This unit is overlain by a 40 cm thick bed of poorly sorted massive cobble conglomerate. Clasts are angular to rounded, and are composed exclusively of mafic volcanics identical in composition to that of the underlying flow. the conglomerate is overlain by 14 m of interstratified pebble conglomerate and sandstone. The pebble conglomerates are up to 40 cm thick and occur as discontinuous lenses. Clasts within the conglomerate consist primarily of well rounded andesite with lesser granite. The interstratified sandstones are massive or graded. Contacts between the conglomerates and sandstones are very poorly defined. In many cases, it appears that the conglomerates grade normally into the overlying sandstones, and that the sandstones in turn grade inversely into the overlying conglomerate. Unlike the underlying turbidites, the sandstones and conglomerates of this package contain plant fragments. The succession is overlain by approximately 300 m of massive mafic volcanics with no interstratified sediments.

The succession exposed on the small island to the northeast consists of thick bedded sandy and classical turbidites (Fig. 5.35). The lower 18 m of the succession consists of a package of thick and thin bedded classical turbidites. Beds of the thick bedded turbidites are massive

(T_a) and amalgamated. Some of these beds exhibit well developed basal breccias. A 50 cm thick bed of coherently deformed mudstone occurs at the top of this package. No well defined vertical changes in bed thickness or grain size were observed within this package.

The middle part of the succession consists of packages of the sandy turbidite facies interstratified with thin beds of the classical turbidite facies. The sandy turbidites forming the base of each package consist of amalgamated beds of massive (T_a) coarse grained sandstone up to 4 m thick. Many of the beds contain well developed intraclast lags. The thickness of the lower part of each package appears to decrease somewhat up section.

The upper 48 m of the succession consists primarily thick bedded classical turbidites with lesser sandy turbidites and thin bedded classical turbidites. Classical sandstone beds are medium to coarse grained, are up to 3 m thick, and are massive (T_a) or massive to parallel laminated (T_{ab}). Some of the thicker beds contain intraclast lags.

Vertical changes in bed thickness or grain size are poorly defined within this particular succession. In a gross sense there is a change from coarse grained sandy turbidites within the lower part of the succession to medium grained thick bedded classical turbidites in the upper part.

Interpretation

The amalgamated and intraclast-rich nature of the sandy turbidites forming the lower part of the succession exposed on Gust Island (Fig. 5.34) is indicative of deposition in submarine channels (Walker, 1978, 1984, 1992; Pickering et al., 1989). The upward transition towards thinner bedded pebbly classical turbidites may reflect the gradual infilling of the channel system.

Haggart et al. (1989) suggested that the lack of quenching features and the scoriaceous nature of the mafic volcanics capping the succession on Gust Island indicate that they were emplaced subaerially. Given the turbiditic nature of the sediments immediately underlying the volcanics, this appears most unlikely, unless the volcanics are separated from the turbidites by a discontinuity related to uplift. The 11 m thick sequence of mafic volcanics within the upper part of the succession is overlain by a poorly sorted cobble conglomerate. It is possible that this conglomerate could be associated with a period of uplift and erosion. The overlying sandstones and conglomerates are quite different in character to those of the turbidites below. The poorly defined bedding within this package suggests that it may have been deposited all at once by a surging flow of some sort. This, and the occurrence of plant fragments within these sandstones, suggests that they

may have been deposited within an environment quite different than that in which the underlying turbidites were deposited.

The predominance of thick non-amalgamated classical turbidites within the succession exposed on the island to the northeast (Fig. 5.35) may be attributed to deposition upon a sandy submarine fan lobe. The thin packages of amalgamated sandstone within the middle part of the succession however may have been deposited within small channels incised into the lobe.

5.4.6. Swaley cross-stratified sandstone facies successions

Description

Successions of this sort are exposed only on northwestern Lina Island in Skidegate Inlet (Fig. 5.36). The two successions are situated approximately 450 m above the base of the Honna (Fig. 5.24), and are immediately underlain by a thick succession of the conglomerate facies. The succession exposed on western Lina island is 71 m thick (Fig. 5.36 a). The lower 40 m consists primarily of well sorted medium to coarse grained SCS sandstone (Fig. 5.37). The sandstones contain Ophiomorpha traces, as well as minor interstratified lenses of silty mudstone. A 4 m thick bed of horizontally to low angle stratified well sorted medium grained sandstone is interstratified with the SCS sandstones

Fig. 5.36 Measured section of the Honna Formation exposed at a) northwestern Lina Island and b) northern Lina Island (section D, Fig. 5.24).

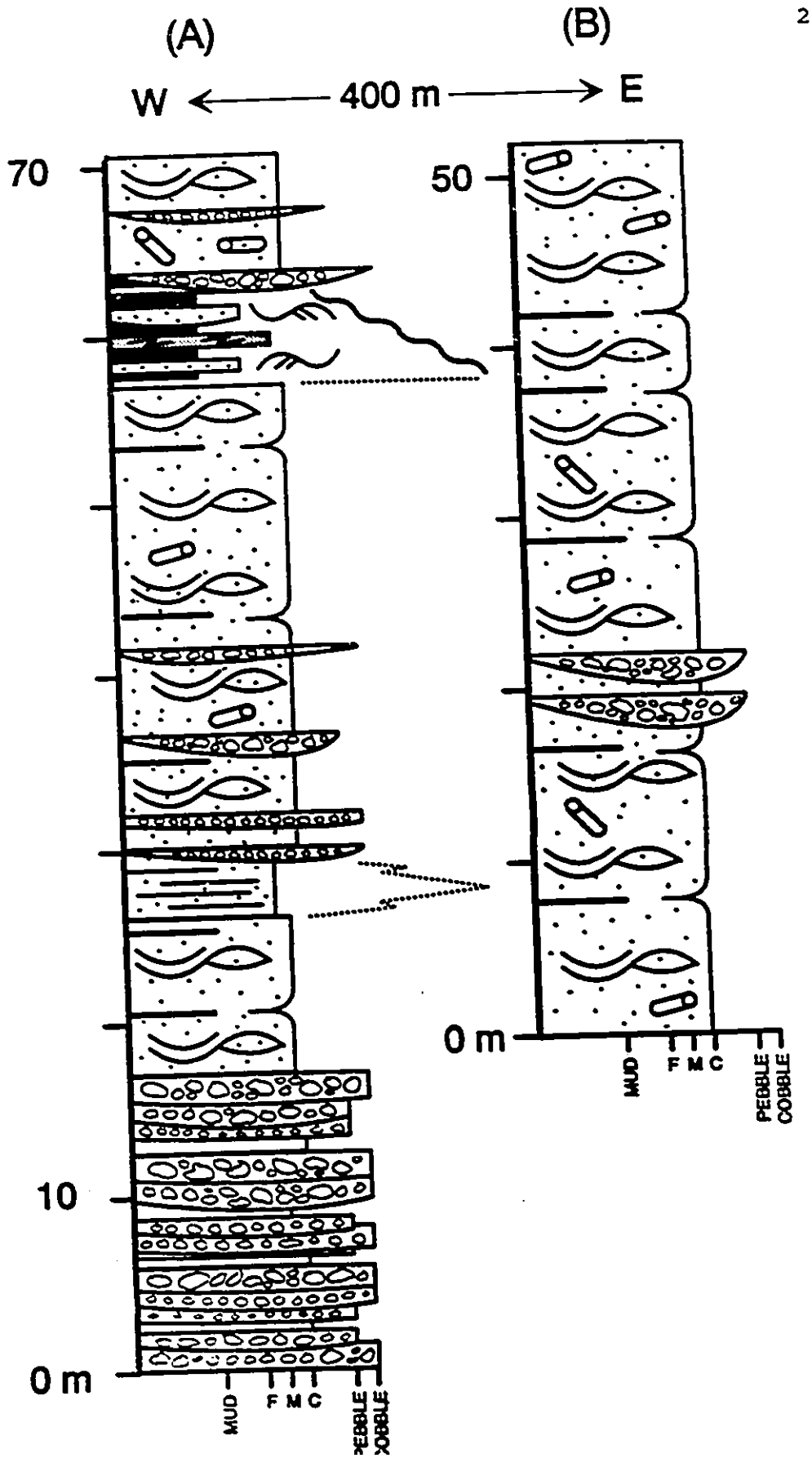
(A)
(B)
W
400 m
E
70
50
10
0 m
0 m
MUD
F M C
PEBBLE
COBBLE

Fig. 5.37 Swaley cross-stratified sandstones exposed within the lower part of the section of the Honna Formation exposed on northwestern Lina Island (Fig. 5.36 a).

Fig. 5.38 Hummocky cross-stratified sandstones and interstratified sandy mudstones within the upper part of the section of the Honna Formation exposed on northwestern Lina Island (Fig. 5.36 a).

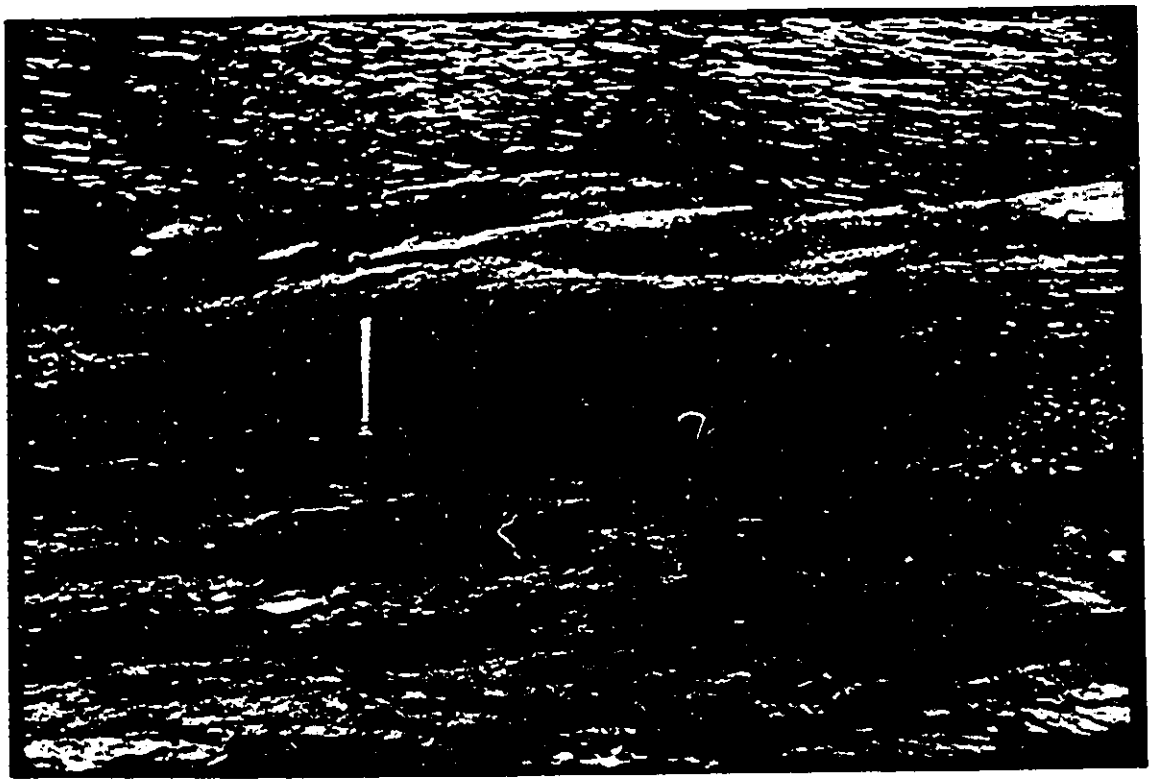

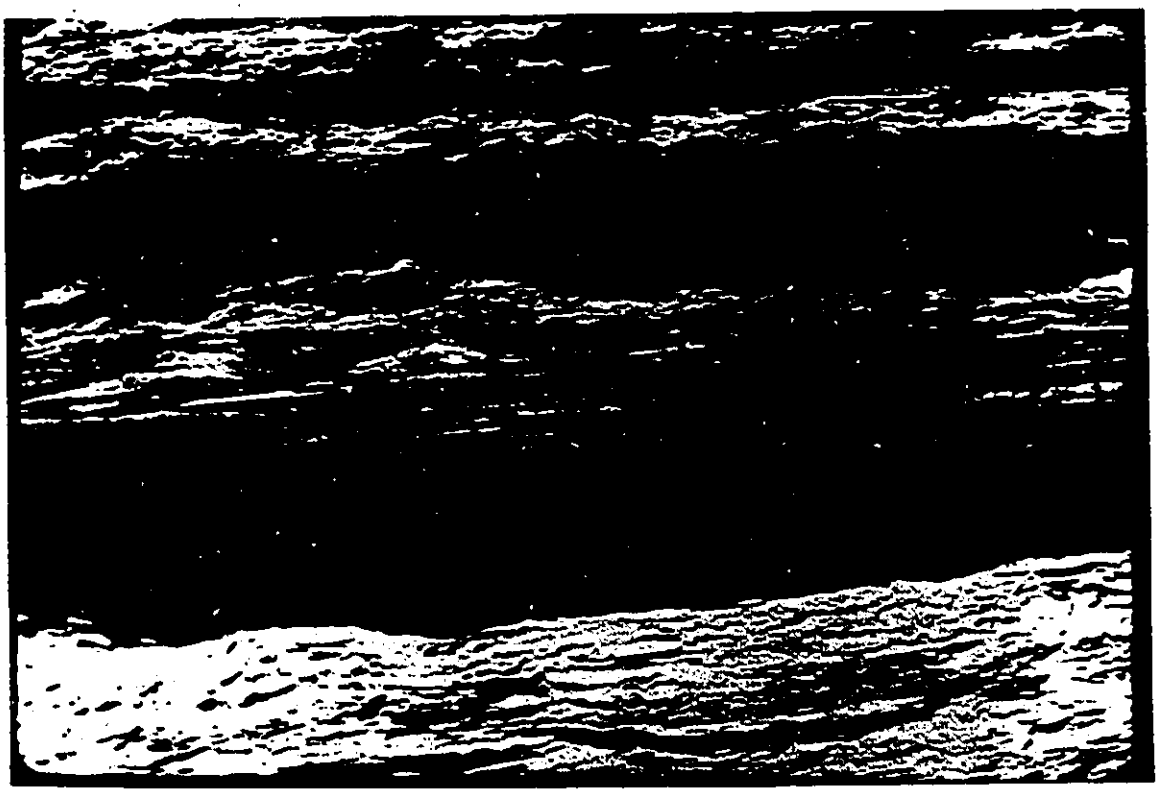

near the base. The overlying SCS sandstones contain several lenticular beds of massive, clast-supported pebble conglomerate up to 50 cm thick.

The upper part of the succession consists of 6 m of the HCS sandstone and sandy mudstone facies overlain by 7.5 m of coarse grained SCS sandstone. The mudstones contain fine grained beds of HCS and wave rippled sandstone up to 40 cm thick (Fig. 5.38). Some of these beds infill concave-up scours, and pinch out laterally against the scour margins. One bed of the coherently deformed mudstone facies was observed interstratified with the HCS sandstones and sandy mudstones. The sandstones contain a diverse collection of traces, the most common being Rhizocorallium and Thalassinoides. The contact between the mudstones and the overlying SCS sandstones is abrupt and exhibits up to 2 m of erosional relief. The contact is overlain by a poorly sorted lag consisting of angular cobbles of the underlying mudstone facies and lesser extraformational clasts. The overlying SCS sandstones contain thin lenses of massive clast supported pebble conglomerate near the base and abundant Ophiomorpha traces throughout.

The entire mudstone package near the top of section LiI2 is completely absent within a correlative section exposed 400 m to the east (Fig. 5.36 b). This 52 m thick succession is composed entirely of the SCS sandstones facies

with minor interstratified lenses of massive, clast-supported pebble and cobble conglomerate.

Interpretation

SCS sandstones typically reflect deposition within a wave dominated shoreface environment (Leckie and Walker, 1982; Walker, 1985; Rosenthal and Walker, 1987). The lenses of pebble conglomerate interstratified with the SCS sandstones may represent rip channel lags. Two separate shoreface packages are recognized within the succession to the west (Fig. 5.36 a); a lower 40 m thick package and an upper 13 m thick package. The gradual increase in grain size in the lowermost package suggests that it may represent a progradational, wave dominated shoreface succession.

The vertical arrangement of facies and ichnofacies within the uppermost package reflect the progradation of a wave dominated sandy shoreface into a muddy offshore environment. The presence of HCS and wave rippled beds of sandstones within the mudstones indicates that they were deposited within a wave dominated offshore environment. Rhizocorallium and Thalassinoides belong to the Cruziana ichnofacies of Pemberton et al. (1992), and are commonly associated with ancient muddy storm dominated offshore successions. The interstratified bed of deformed mudstone probably represent a slide deposit, and indicate that the

offshore environment was periodically subjected to mass failure and slumping. The concave up scours underlying some HCS sandstone beds may therefore represent slide scars which were subsequently infilled during later storm events. The erosive contact separating the sandstones and the underlying mudstones may be attributed to shoreface erosion accompanying a relative fall in sea level (a forced regression of Plint, 1991). The fact that the mudstones are truncated completely 400 m to the east (Fig. 5.36) indicates that erosion accompanying sea level fall was substantial. The Ophiomorpha traces observed within the overlying SCS sandstones are typical of ancient wave dominated shoreface successions (Pemberton et al., 1992).

No well developed progradational shoreface successions are observed within section exposed to the east (Fig. 5.36 b), despite the fact that it is correlative to section LiI2 where at least two are observed. This indicates that the shoreface packages within this succession are stacked and are separated by a subtle erosive surface. This, and the fact that any offshore mudstones separating them were removed by the effects of shoreface erosion accompanying progradation, makes individual shoreface packages difficult to discern within this succession.

5.5. PROVENANCE OF THE HONNA FORMATION

5.5.1. Paleocurrent analysis

Clast imbrication was measured at 81 stations within the Honna Formation. As the goal of the study was to obtain a regional paleogeographic reconstruction of paleoflow trends from the Honna, stations were chosen from the northwestern, central, and southern outcrop areas. Measurement of the a-b plane orientations of 25 flat (bladed or discoid) clasts was made at each station. Measurement at each station was restricted to beds of conglomerate representing a single depositional event. The measurements from each station were corrected for tectonic tilt (using SPLOT by Darton Software) if the bed was dipping at an angle greater than 25 degrees. The results were plotted (using ROCKPIX version 5 by Petmar Trilobite) in the form of a rose diagram which illustrates the inferred direction of paleoflow. Paleocurrent measurements with a vector magnitude of less than 35 % were rejected, as this indicates that the probability is greater than 5 in 100 ($p = 0.05$) that the distribution is random (Curray, 1956).

The 19 stations on Langara Island yield a narrow distribution of paleoflow trends ranging from southwest (243°) to due north (358°; Fig. 5.39 and Table 5.2). The 44 stations measured from Gunia Point to Pillar Bay on Graham

Fig. 5.39 Paleocurrent trends from conglomerate beds of the Honna Formation exposed in the northwestern Graham - Langara Island region. Each arrow represents the average paleoflow direction derived from measuring 25 clasts per bed. Rose diagrams (equal area) generated for each station are presented in the accompanying Table 5.2. Some of the arrows represent the average collected from several separate but closely spaced stations. Distribution of Honna Fornation from Sutherland Brown (1968), Thompson et al. (1991), and Hesthammer and Indrelid (1991) and the authors own observations.

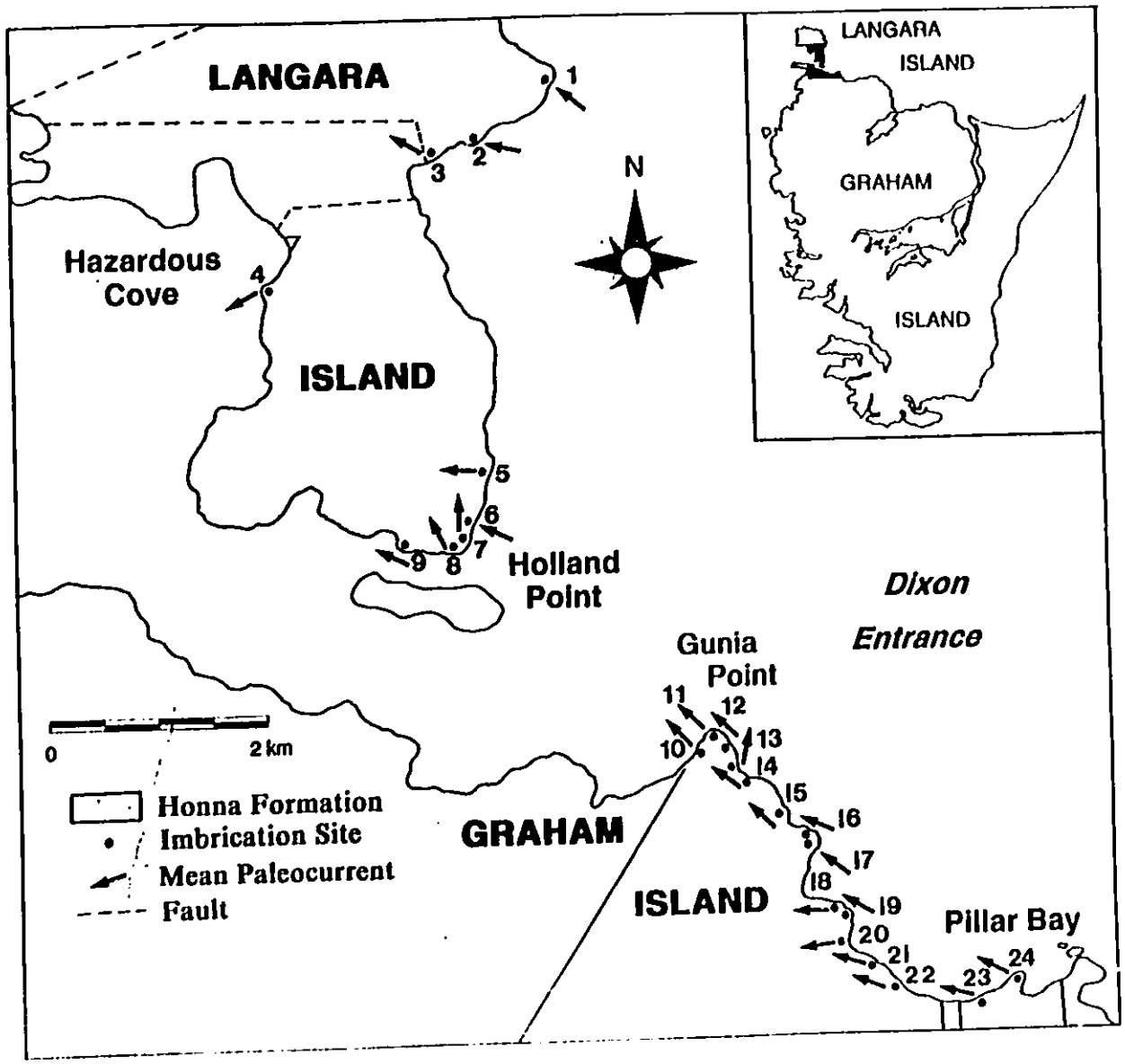
LANGARA
ISLAND
GRAHAM
ISLAND
N
Hazardous Cove
ISLAND
Holland Point
Dixon Entrance
Gunia Point
GRAHAM ISLAND
Pillar Bay
1
2
3
4
5
6
7
8
9
10
11
12
13
14
15
16
17
18
19
20
21
22
23
24
0
2 km
Honna Formation
Imbrication Site
Mean Paleocurrent
Fault

Table 5.2 Rose diagrams (equal area) collected from beds of conglomerate within the Honna Formation exposed in the northwestern Graham - Langara Island region. Each diagram represents the direction of flow derived from the direction of dip of the ab plane of 25 imbricate clasts per bed. Arrow represents the mean paleoflow direction for the station.

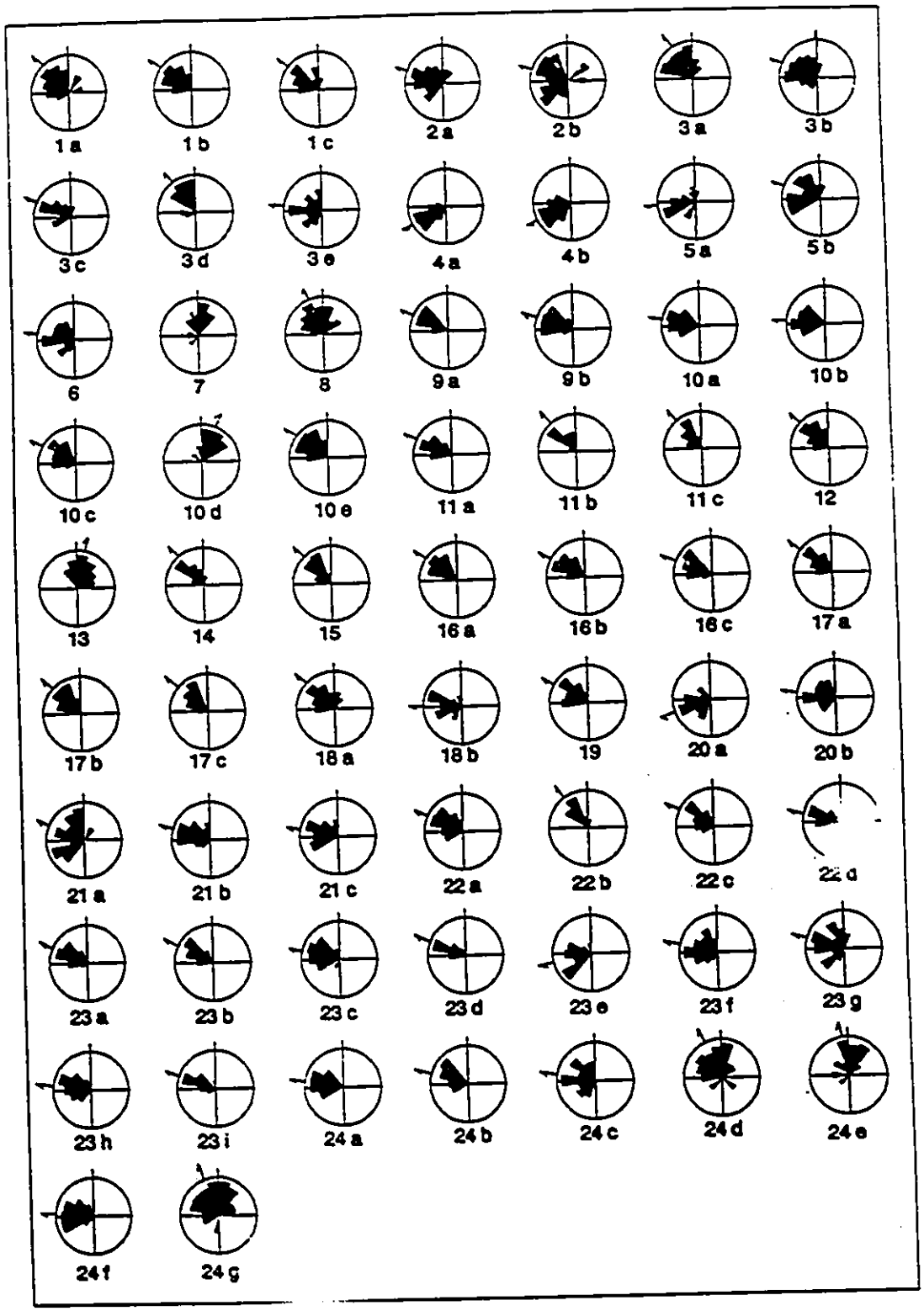
1a
1b
1c
2a
2b
3a
3b
3c
3d
3e
4a
4b
5a
5b
6
7
8
9a
9b
10a
10b
10c
10d
10e
11a
11b
11c
12
13
14
15
16a
16b
16c
17a
17b
17c
18a
18b
19
20a
20b
21a
21b
21c
22a
22b
22c
22d
23a
23b
23c
23d
23e
23f
23g
23h
23i
24a
24b
24c
24d
24e
24f
24g

Fig. 5.40 Plot of paleocurrent trend versus stratigraphic height within the section through the Honna Formation exposed at Pillar Bay. Note the slight shift in paleocurrent trend from the northwest towards the west over time.

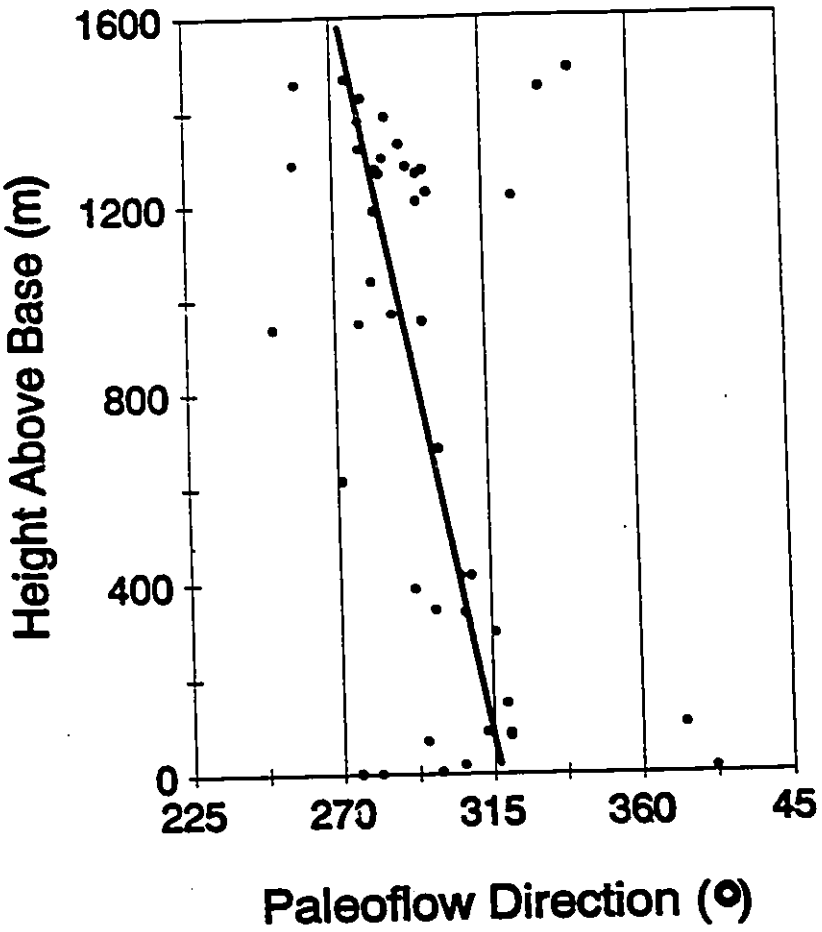
1600
1200
800
400
0
Height Above Base (m)
225
270
315
360
45
Paleoflow Direction (°)

Island yield a similar narrow distribution from west - southwest (251°) to north - northeast (21°; Fig. 5.39 and Table 5.2). Therefore, in the most general of terms, the turbidity currents supplying gravel to this region flowed mainly from the southeast towards the northwest throughout the deposition of the Honna.

A plot of paleoflow direction versus stratigraphic height of the station from the section exposed on northwestern Graham Island is presented in Fig. 5.40. It appears that there was a gross shift of flow from the northwest towards the west-northwest over time. It is also readily apparent, especially within the lowermost part of Fig. 5.40, that stations less than 10 m apart stratigraphically may exhibit paleoflow trends which diverge 180°.

Both Yagishita (1985a) and Higgs (1990) collected a large amount of paleocurrent data from the Honna in the Skidegate Inlet region. A compilation of Higgs (1990) and the authors own data is presented in Fig. 5.41 and Table 5.3 a. Although these measurements were collected from different stratigraphic levels, it is readily apparent that there is almost no consistent pattern in paleoflow. Flow was in general radially dispersed from the northeast counterclockwise to the south. The only paleoflow directions not represented span from the northeast clockwise

Fig. 5.41 Paleocurrent trends from the Honna exposed in the Skidegate Inlet region. Most of the data was derived from Higgs (1990). Supplemental data was also collected in the Lina Narrows area during the course of this study.

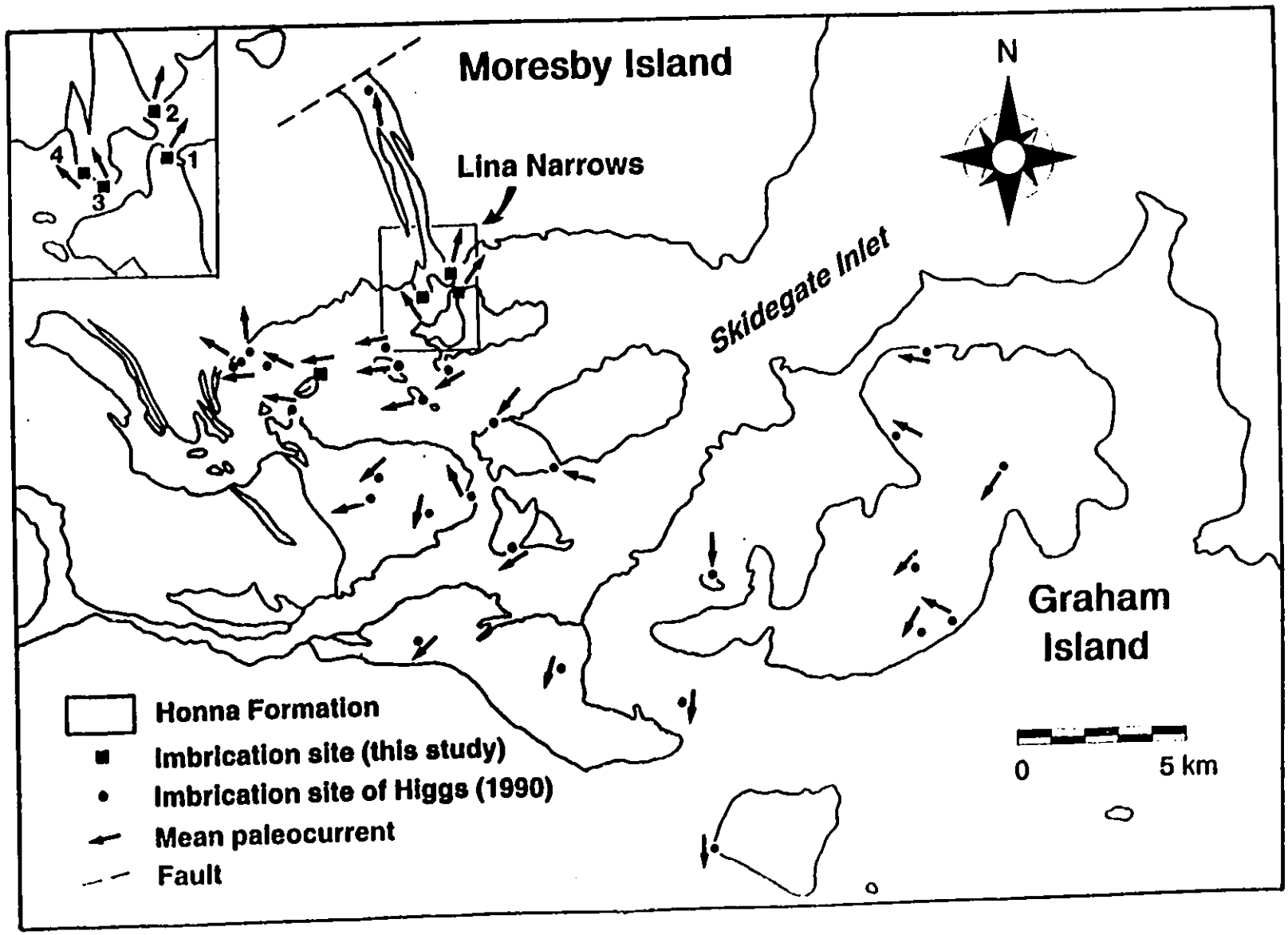
Moresby Island
Lina Narrows
Skidegate Inlet
N
Graham Island
0
5 km
Honna Formation
Imbrication site (this study)
Imbrication site of Higgs (1990)
Mean paleocurrent
Fault
1
2
3
4

Table 5.3 a) Rose diagrams (equal area) collected from the Honna in the Skidegate Inlet region, and b) from the Sewell Inlet region.

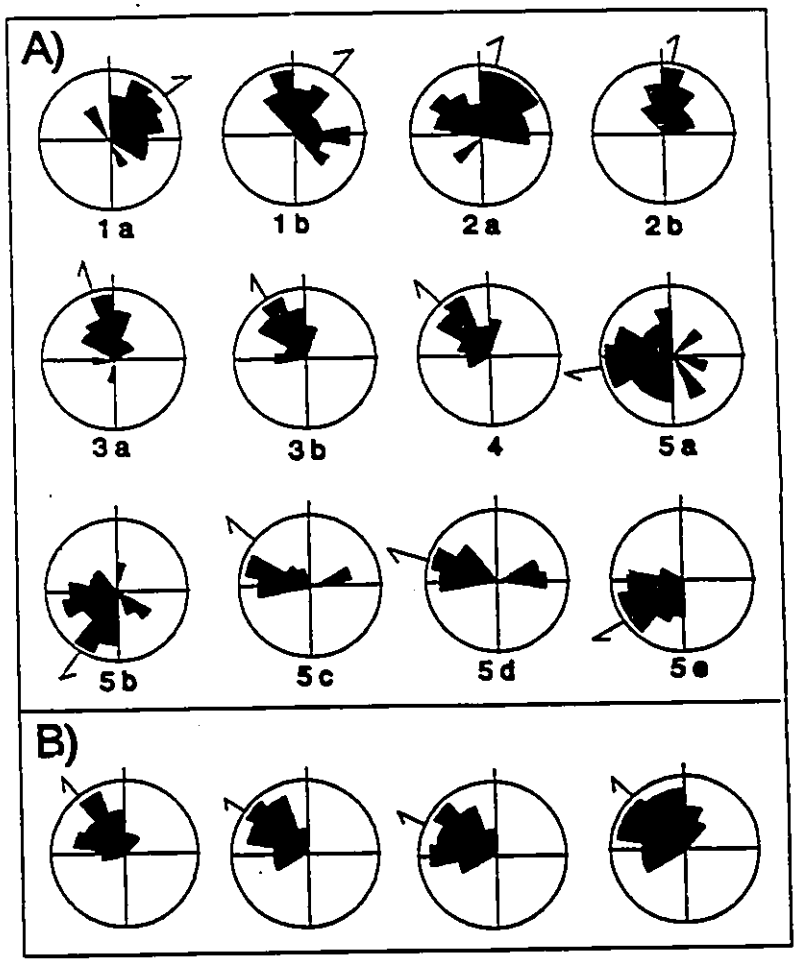
A)
1a
1b
2a
2b
3a
3b
4
5a
5b
5c
5d
5e
B)

round to the southeast. Form this apparently random pattern, both Yagishita (1985a) and Higgs (1990) concluded that paleoflow within the Skidegate Inlet region was generally from east to west. In this context, the northward paleoflow trends observed within the Lina Narrows region, and the southward trends observed at three stations on Moresby Island, are most interesting. Higgs (1990) suggested that the departures from the general east - west trend observed at Lina Narrows may reflect post depositional block rotation. This logic might also be invoked to explain the southward direction of paleoflow observed at the three stations indicating southward paleoflow. It is readily apparent from my work in the Lina Narrows region that the direction of paleoflow changes from northeastward at the base of the Honna to northwestwards approximately 200 m up section to the west (Fig. 5.41). This, aside from the structural evidence against block rotation presented by Thompson et al. (1991), indicates that the trends probably reflect variations in the geometry of the depositional system itself.

Paleocurrent measurements collected from four stations at the base of the Honna in the eastern Sewell Inlet region yield a consistent northwestward trend (Fig. 5.42 and Table 5.3 b).

With the proper stratigraphic control, it might well

Fig. 5.42 Regional map showing the average paleocurrent trend collected from clast imbrication from the basal conglomerate bed of the Honna at several different stations. Note the strong northwest trends in the northwestern Graham Island, Lina Narrows, and Sewell Inlet regions. Paleoflow in the western Skidegate Inlet region however is directed towards the west.

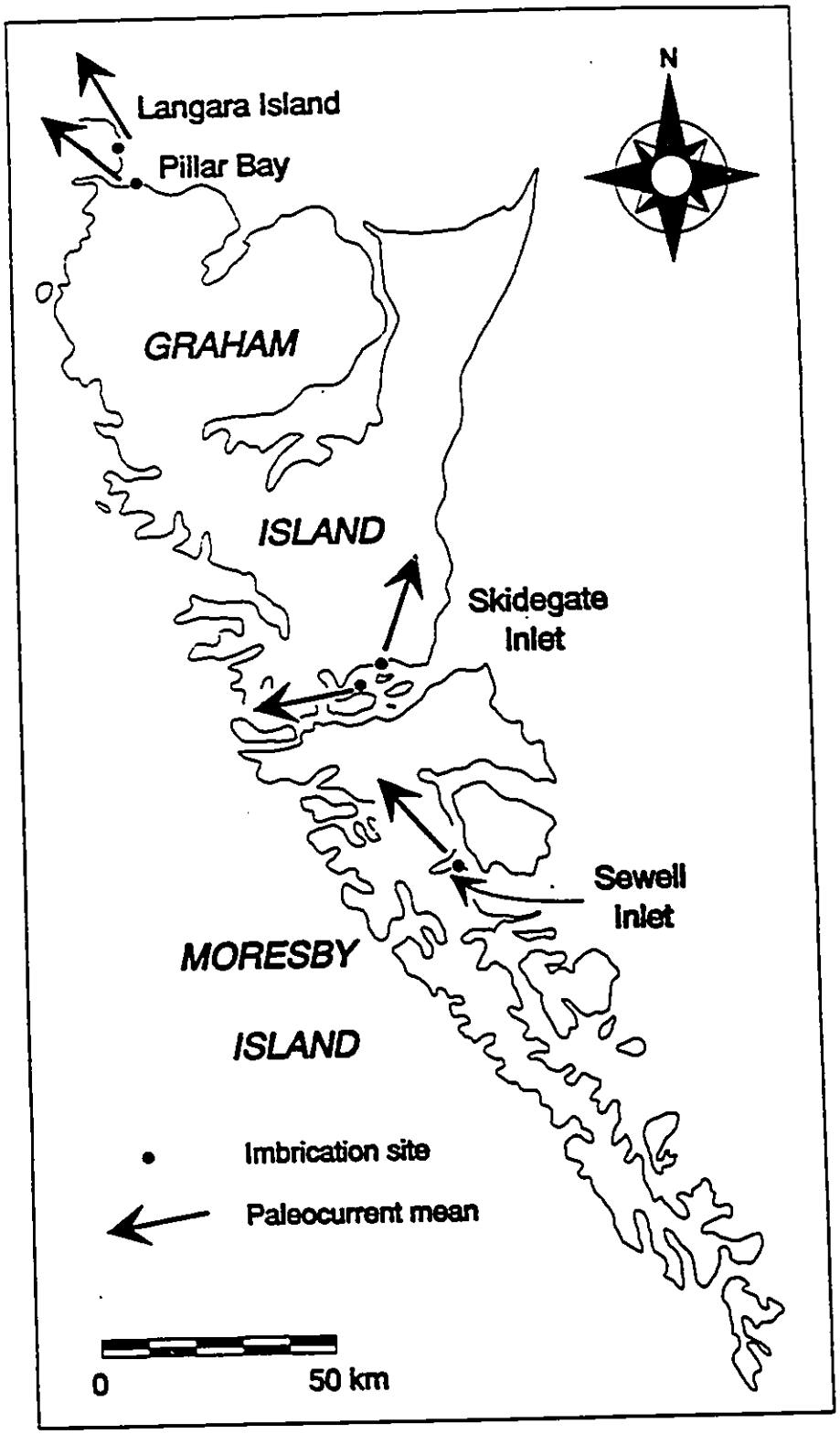
N
Langara Island
Pillar Bay
GRAHAM
ISLAND
Skidegate
Inlet
Sewell
Inlet
MORESBY
ISLAND
Imbrication site
Paleocurrent mean
0
50 km

be possible to accurately reconstruct the geometry of the system exposed in the Skidegate Inlet Region. Given the nature of both the formation and the exposure, this is not possible. It is possible however to construct a regional map exhibiting the paleoflow direction derived from the first occurrence of conglomerate at the base of the Honna at several different locations (Fig. 5.42). From this map, the predominant northwestward paleocurrent trend in the Pillar Bay - Langara Island and Sewell Inlet regions is obvious, as is the radial distribution in the Skidegate Inlet region.

5.5.2. Petrology

Petrographic examination of sandstones from the Honna reveal that they are mainly lithic and feldspathic arenites (Yagishita, 1985 a, b; Fogarassy, 1990, 1991). Yagishita (1985a, b) suggested that the composition of the sandstones, which plotted mainly within the centre of QLF diagrams, showed characteristics of a mature dissected magmatic arc provenance (Dickinson and Suzek, 1979). Yagishita (1985a, 1985b) also suggested that the nearly pure albite composition of the feldspar grains indicated derivation from the core of an uplifted and dissected arc, rather than from the extrusive volcanics of an active arc. Based upon this, Yagishita concluded that the source of the Honna lay to the east somewhere within the Coast Ranges.

5.5.3. Geochronology

In order to determine the provenance of the granitic clasts within the Honna, two samples were submitted to the Geochronology lab at the Geological Survey of Canada in Ottawa for U-Pb dating. One of the samples was collected from the uppermost part of the section exposed in Pillar Bay on northwestern Graham Island (section PiB 2; NTS 103 K/2 and K/7, UTM 600180N 63760E). The other sample was collected from the lower part of the Honna exposed on northeastern Moresby Island (NTS 103 G/4, UTM 589590N 30680E). The age of the granite cobble from northeastern Moresby Island is interpreted to be Early Cretaceous (123 + 0.2 Ma) based on the age of concordant fraction C which intersects concordia and the fractions A and B (Fig. 5.43). The age of the granite cobble from Pillar Bay is interpreted to be Early Silurian (435.9 + 0.9 Ma) based on the age of concordant fractions A and C which intersect concordia and each other (Fig. 5.44). Potential sources of the Early Silurian clast include plutonic suites exposed in the Coast Ranges of British Columbia and in southern Alaska (Fig. 5.45; Gehrels and Saleeby, 1987). Potential sources for the Early Cretaceous clast include plutonic suites identified in the McCauley Island Belt of the Coast Plutonic Complex (Fig. 5.45) which contain Early Cretaceous plutons (131 - 123 Ma; van der Hayden, 1992). Post-kinematic plutons of similar

Fig. 5.43 Concordia plot for granite clast collected from the base of the Honna Formation exposed at logging quarry in the northeastern Moresby Island region (NTS 103 G/4, UTM 589590N 30680E). The plot yields an age of 123 + 0.2 Ma (Early Cretaceous).

Fig. 5.44 Concordia plot for granite clast collected from the uppermost part of the Honna Formation exposed at Pillar Bay (NTS 103 K/2 and K/7, UTM 600180N 63760E). The plot yields an age of 435.9 + 0.9 Ma (Early Silurian).

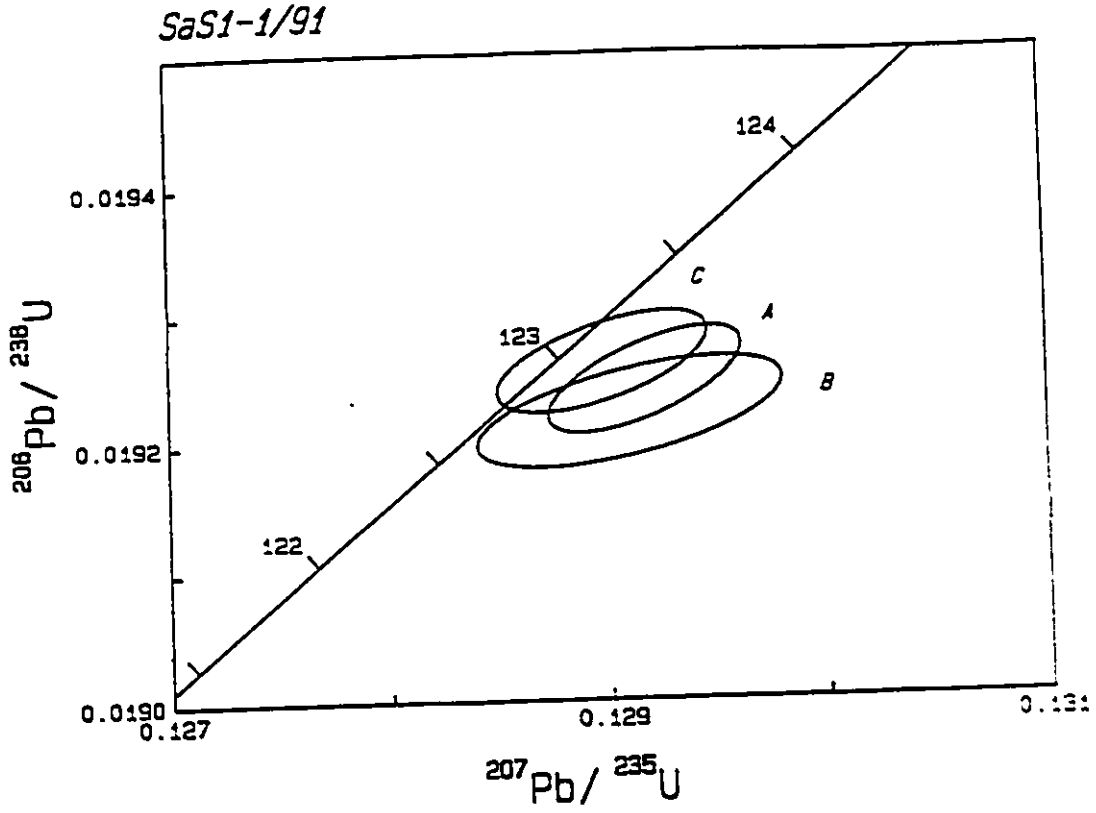
SaS1-1/91
124
123
122
A
B
C
0.0194
0.0192
0.0190
0.127
0.129
0.131
$^{206}Pb/^{238}U$
$^{207}Pb/^{235}U$

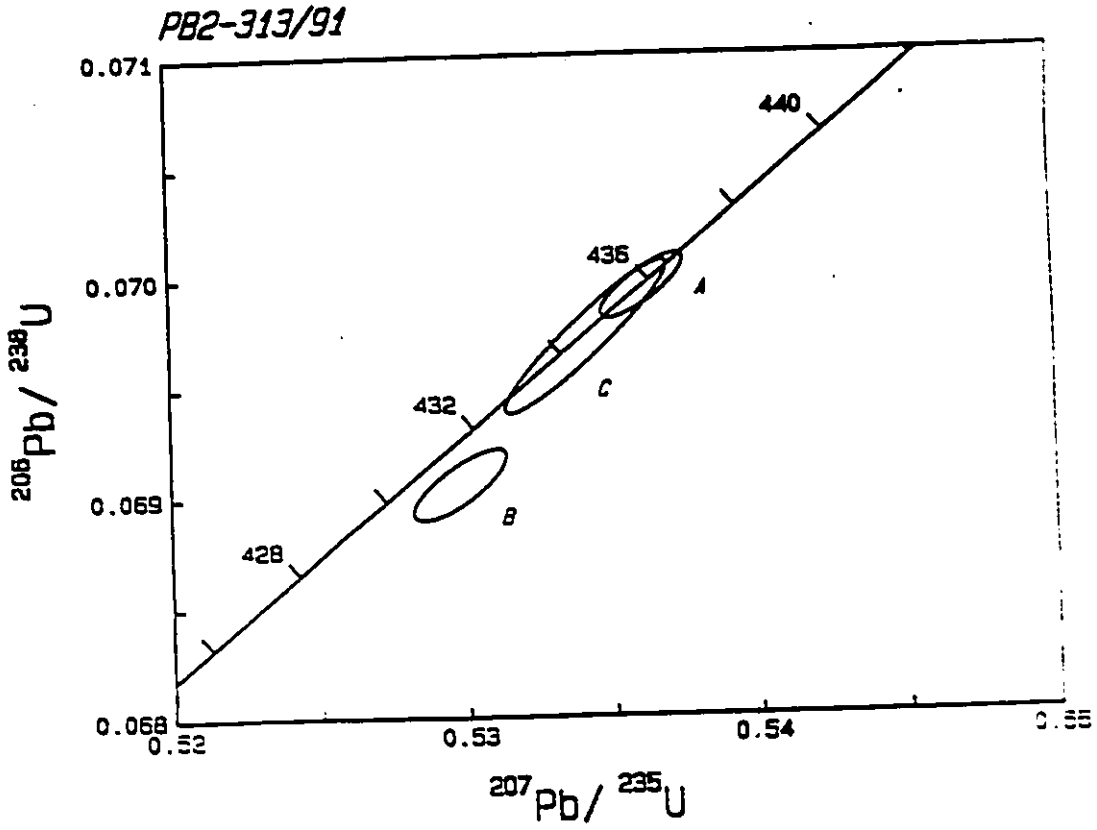
PB2-313/91
440
436
432
428
A
B
C
0.071
0.070
0.069
0.068
0.52
0.53
0.54
0.55
$^{206}Pb/^{238}U$
$^{207}Pb/^{235}U$

Fig. 5.45 Map showing the distribution Silurian and Early Cretaceous plutonic complexes within the Coast Plutonic Complex exposed in western British Columbia and southern Alaska. A - McCauley Island belt, B - Gamsby Complex, C -Upper Silurian trondhjemites and leucodiorites of the Alexander terrane. Location of thrusts from Rubin et al. (1990).

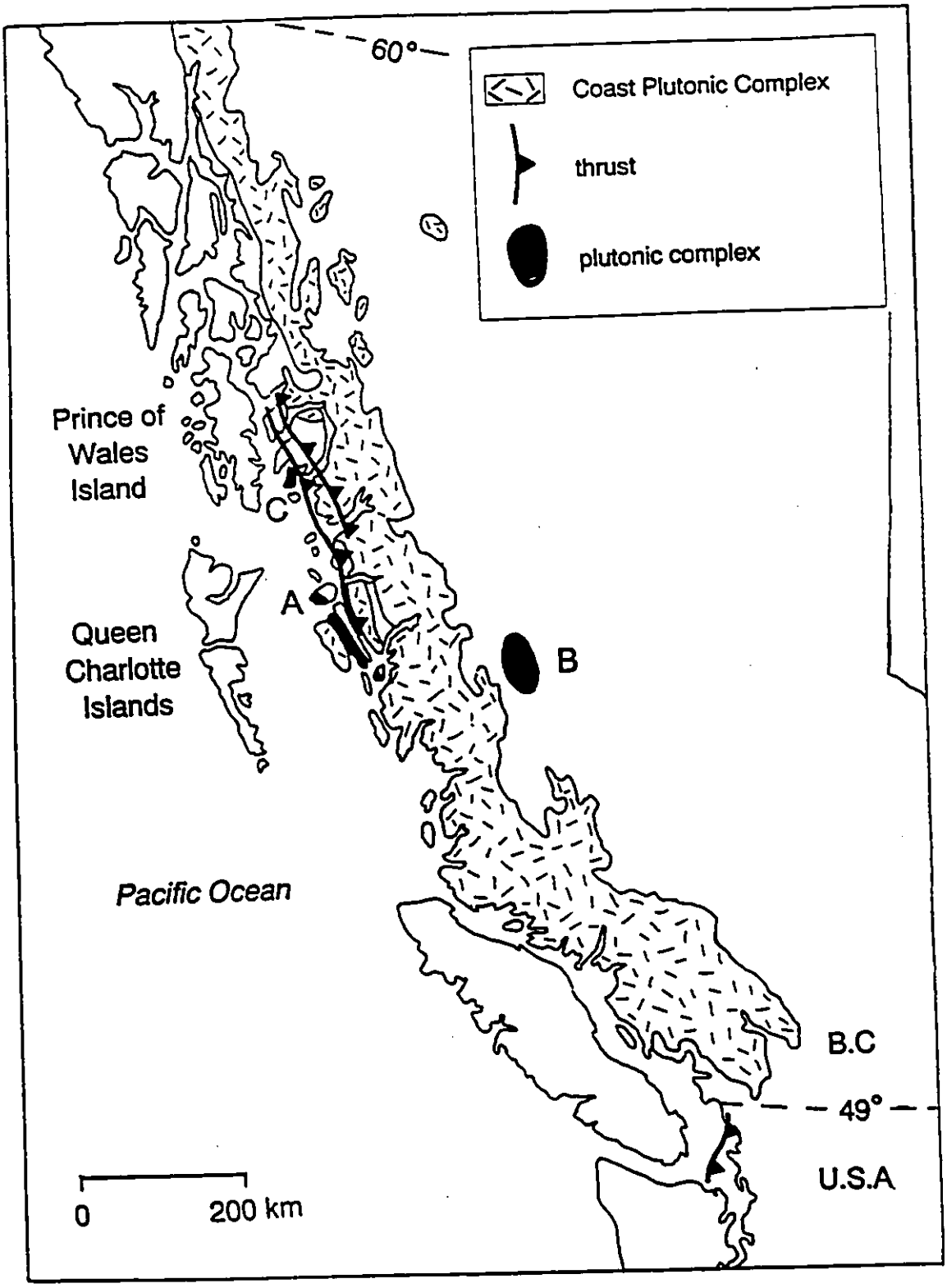
60°
Coast Plutonic Complex
thrust
plutonic complex
Prince of Wales Island
C
A
B
Queen Charlotte Islands
Pacific Ocean
B.C
49°
U.S.A
0
200 km

age (132 - 120) are also present within the Gamsby Complex in the eastern part of the Coast Plutonic Complex (van der Hayden, 1992).

5.5.4. Provenance summary

The paleocurrent analysis indicates that the turbidity currents supplying gravel to the basin flowed in a radial distribution oriented roughly east west in the Skidegate Inlet region, and generally towards the northwest in the Pillar Bay / Langara Island and Sewell Inlet regions. Paleoflow within the Skidegate Inlet region was however quite variable on a local basis, deviating from the east - west trend by more than 90° in some areas (eg. Lina Narrows).

The petrology of the Honna sandstones is indicative of a mature dissected arc provenance. Geochronology indicates that most if not all of the granitic clasts were derived from Early Cretaceous and Silurian plutonic complexes which lay within parts of the Coast Plutonic Complex situated immediately east of the Charlottes (McCaley Island and Gamsby Complexes). These geochronological results are consistent with the mature dissected arc provenance deduced by Yagishita (1985a, 1985b) from the petrology of the sandstones. The presence of Silurian-aged granitic clasts indicates however that rocks of an older

accreted Late Paleozoic terrane also acted as an important source of sediment. It is interesting to note that the Middle and Late Jurassic plutonic suites exposed on the Queen Charlotte Islands apparently did not act as a significant source of sediment.

5.6. STRATIGRAPHY AND DEPOSITIONAL MODEL

The rapid facies changes and lack of good biostratigraphic control within the Honna make it difficult to discern the lateral relationships between the various facies successions. Nevertheless, a few general along strike and down dip observations can be made, from which a depositional model of the Honna may be reconstructed.

5.6.1. Along strike relations

At least four 50 to 500 m thick conglomeratic successions are observed within the Honna at the section measured at Pillar Bay (Fig. 5.23 b). Eight are recognized within the section measured at South Bay (Fig. 5.23 e) in Skidegate Inlet by Yagishita (1985a). It should be kept in mind however that this last section is almost certainly faulted, making repetition highly probable. The thick successions at the base and in the middle of the formation may be correlated 200 km along the length of the outcrop

belt. The lowermost succession, which is 500 m thick at Pillar Bay, thins somewhat towards Skidegate Inlet, and then thickens to 600 m at Sewell Inlet in the southeast (Fig. 5.23 e). The middle succession, which is 400 m thick, maintains its thickness from Pillar Bay to Skidegate Inlet, and then thins somewhat towards Sewell Inlet.

At least four classical turbidite successions 50 to 250 m thick are recognized within the Honna exposed at Pillar Bay. Several are also recognized within the section exposed at South Bay. The recessive weathering style of these successions makes correlation difficult, but it appears they too extend a great distance along strike. The 250 m thick succession of classical turbidites in the lower part of the section exposed at South Bay thins towards the northwest at Pillar Bay and towards the southeast at Sewell Inlet. The conglomeratic succession at the top of the Honna is overlain by sandy turbidites and mafic volcanics in the western Skidegate Inlet region.

It is apparent therefore that the Honna is composed of several sheetlike successions of conglomerate interstratified with successions of classical turbidites. Both types of succession may be correlated 200 km along strike, although they may change dramatically in thickness.

5.6.2. Down dip relations

The Honna is a maximum of 2500 m thick in the Skidegate Inlet region (Fig. 5.24 c). Throughout most of this region, the Honna is underlain by deposits of the Skidegate Formation, except to the east, where the Honna unconformably overlies Jurassic volcanics of the Yakoun Group (Fig. 5.24 f). At least 8 conglomeratic successions are observed within the section exposed at South Bay (Fig. 5.24 c), though again this is probably a fault repeated section. The lowermost succession is approximately 500 m thick, and may be confidently correlated at least 15 km down dip from east to west. No down dip trends in the type of conglomerate (ie. massive, graded, etc) were noted within this particular succession.

The conglomerates are again interstratified with FTU classical turbidite successions (eg. Figs. 5.24 b and c), none of which may be confidently correlated down dip. At Lina Island (Fig. 5.24 d), a 90 m thick succession of the SCS sandstone facies overlies the lowermost conglomeratic succession. This is the only location at which shallow marine facies were observed within the Honna.

Successions of the sandy turbidite facies up to 200 m thick occur at the top of the Honna within the Gust Island and South Bay regions to the west and southwest (Figs. 5.24 a and c respectively). The sandy turbidites are overlain by

mafic volcanics, which Haggart et al. (1989) suggested were erupted subaerially. The volcanics are in turn are overlain, with uncertain stratigraphic relations, by Santonian to Maastrichtian shelf mudstones (Haggart and Higgs, 1989; Gamba, 1991).

At least 700 m of Honna strata are exposed on northeastern Moresby Island (Fig. 5.24 f). These strata are so poorly exposed as to preclude a detailed facies analysis. The exact nature of the strata within this region is unknown, although Higgs (1990; his Fig. 4) measured a 10 m thick section composed of the conglomerate facies at a small quarry in this area.

It appears that the Honna in the Skidegate Inlet region is again composed primarily of interstratified successions of the conglomerate and classical turbidite facies. A single succession of the SCS sandstone facies is interstratified with the conglomerates to the east, while successions of the sandy turbidite facies occur within the upper part of the Honna to the west.

5.6.3. Depositional model

The conglomeratic successions forming the bulk of the Honna represent the deposits of braided submarine channels, as originally suggested by Yagishita (1985a). This may be inferred by the amalgamated nature of bedding and the

presence of lateral accretion deposits, the latter not being recognized by Yagishita (1985a). The lack of well defined vertical facies successions within the conglomerates indicate that the channels were not gradually infilled, but were very rapidly abandoned.

At least four 50 to 500 m thick gravelly channel fills preserved within the Pillar Bay region (Fig. 5.23 b). The predominant northwestward paleocurrent trends (Fig. 5.39) and the orientation of the Honna outcrop belt indicate that the channels occupied a linear northwest - southwest trending belt at least 20 km in diameter (Fig. 5.46).

The FTU successions of classical turbidites interstratified with the channelized conglomerates in the northwest Graham Island region are interpreted as channel fill successions. This is based primarily upon the vertical arrangement of facies within the successions, which reflects a transition towards lower depositional energy levels as the channel filled (Mutti and Ricci Lucci, 1972; Walker, 1978, 1984, 1992). The presence of interstratified conglomerates within the lowermost part of one FTU succession (Fig. 5.31) indicates that the amalgamated sandstones within the lower part of the succession were deposited within the gravelly channel system. The overlying thin bedded classical turbidites may have also been deposited within the abandoned channel. Alternatively, they may have been deposited within

Fig. 5.46 Schematic stratigraphic diagram inferred from the deposits of the Honna Formation exposed in the northwestern Graham - Langara Island region. Paleoflow is directed into the page, from southeast to northwest. Presence of slope deposits to the northeast is inferred.

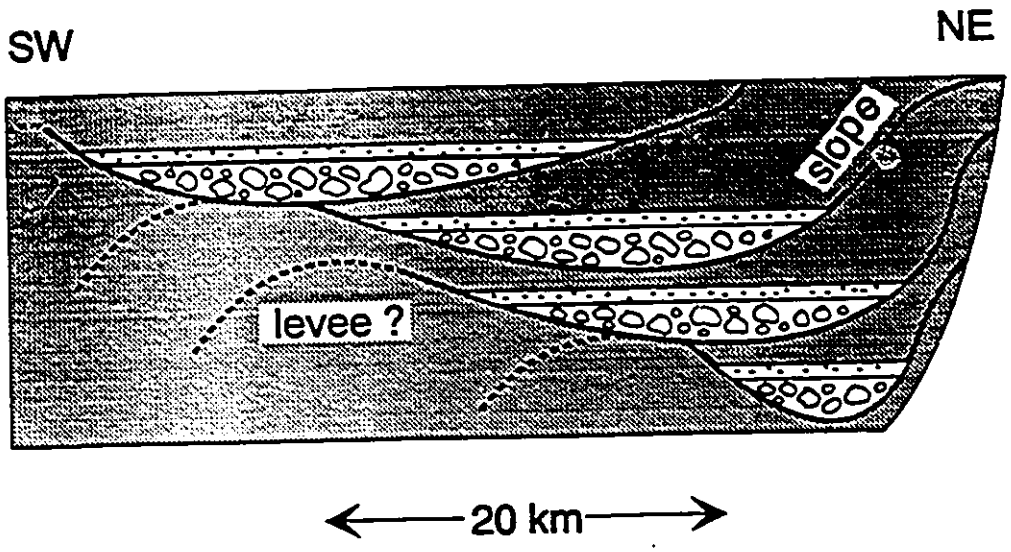
SW
NE
slope
levee ?
20 km

interchannel areas after the channel had been completely filled. The presence of CCC-type classical turbidites within some of these successions indicates that they may have been deposited upon levees (Walker, 1992; Fig. 5.46).

The lateral arrangement of the facies successions in the Skidegate Inlet region (Fig. 5.24) is indicative of a general westward deepening trend. The SCS sandstone succession exposed on Lina Island was deposited within wave dominated shoreface and muddy offshore environments. The fact that no SCS sandstones or other shallow marine strata are observed within the Honna exposed to the west of Lina Island suggests that these shallow marine environments were restricted to the eastern part of the basin.

In the central Skidegate Inlet region only conglomerate and interstratified classical turbidite successions are observed. The conglomeratic successions within this region are almost identical in character to those described from northwest Graham Island. No cross-stratified conglomerates were however observed within this region, neither during the course of this study nor by Yagishita (1985a) or Higgs (1990). Due to the similarity of the facies, it is probable that they too represent the deposits of braided submarine channels, as originally suggested by Yagishita (1985a).

As recognized by Yagishita (1985a) and Higgs (1990),

and as apparent from Fig. 5.41, the paleocurrent trends in this region are indicative of radial dispersion from a source to the east. This pattern indicates that the conglomerates were deposited upon a fan-shaped system (Fig. 5.47), with sediment likely being supplied from a point source to the east. This is quite unlike the situation in the northwest Graham Island region, where the Honna was deposited in a linear northwest - southeast trending channel system. The presence of northwards and northwestwards directed paleocurrent trends in the Lina Narrows area suggests that the radial system may have fed sediment to the channel system extending to the northwest.

The classical turbidites within this region do not display a well developed fining and thinning upwards arrangement of facies, as do those to the north. The classical turbidite successions here contain less interbedded mudstone and display only a poorly defined fining upward trends (eg. Fig. 5.32). For this reason, it is difficult to determine whether these successions represent channel fills or sandy lobe deposits.

Further west, and close to the top of the Honna, successions of the thick bedded classical and sandy turbidite facies are found on Gust Island. The thick bedded nature of the classical turbidites suggests that they represent proximal lobe deposits. The massive and

Fig. 5.47 Schematic diagram illustrating the environments inferred from the deposits of the Honna Formation exposed in the Skidegate Inlet region. This model is based upon the observed lateral relationships between the various facies assemblages and the distribution of paleocurrent trends. Width of the wave dominated shelf to the northeast is unknown, as is the width of the slope.

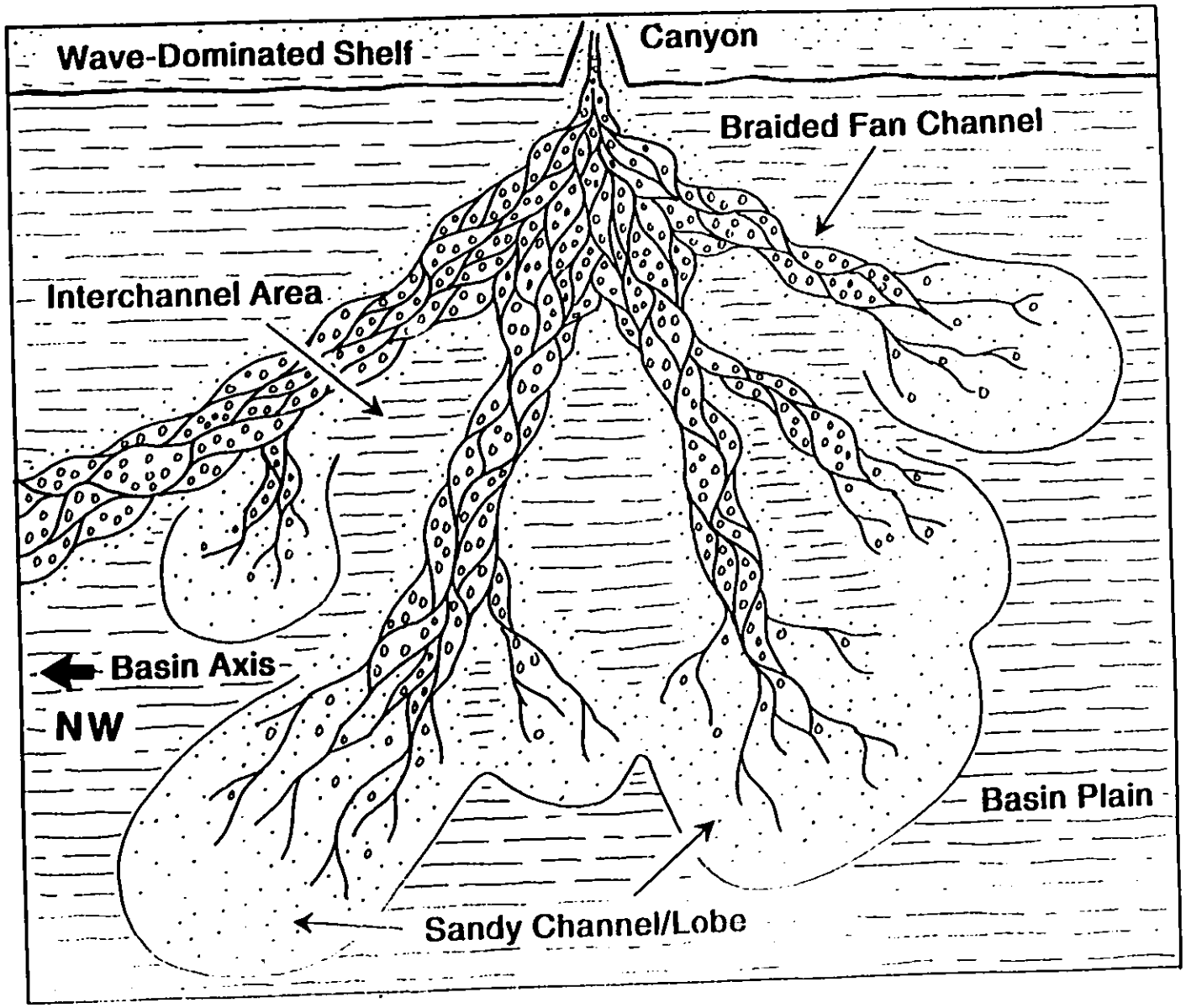
Wave-Dominated Shelf
Canyon
Braided Fan Channel
Interchannel Area
Basin Axis
NW
Basin Plain
Sandy Channel/Lobe

amalgamated nature of most of the sandstone beds within the overlying succession indicates that they were deposited within sandy submarine channels. The succession of thick bedded classical to sandy turbidites exposed in western Skidegate Inlet therefore may represent a progradational sandy lobe and channel system.

The lateral relationship between the facies successions and the inferred eastern provenance of the conglomerates indicates that the basin generally deepened towards the west, from shoreface and offshore environments in the Lina Island area, to gravelly submarine channel deposits in the centre, and finally to sandy submarine channel and lobe deposits in western Skidegate Inlet. It must be stressed however that this reflects only the most general of trends, as correlation within the Honna in this region is difficult. The entire submarine fan system was at least 20 km in length from east to west and at least 15 km in width from south to north. The poorly exposed nature of the strata exposed in the northeastern Moresby Island region precludes a reliable facies analysis, and it is entirely possible that the Honna in this region contain fluvial deposits.

The radial system may have been fed directly by a canyon or a fluvial system situated to the east. Higgs (1990), who recognized no shelf deposits within the Honna,

suggested that sediment was supplied directly to the submarine system by alluvial fans, despite the fact that no alluvial deposits have as yet been recognized from the Honna. The presence of SCS sandstones in the Lina Island area however indicates that the basin did possess a wave dominated sandy shelf. The shelf was clearly bypassed, perhaps by a submarine canyon which fed sediment directly from a deltaic source to the subaqueous fan.

The northwestward paleocurrent trends observed within the Honna exposed in the Sewell Inlet region indicate that the linear channel system extended beyond Skidegate Inlet towards the southeast. This portion of the longitudinal system was probably fed by another radial submarine fan located yet further to the southeast.

It is apparent that the Honna represents a submarine system possessing two distinct elements (Fig. 5.48): a northwest - southeast trending linear system of gravelly channels 20 km wide which extended at least 200 km along strike from Sewell Inlet to Langara Island, and radial east - west oriented gravelly submarine fans, one of which is exposed in the Skidegate Inlet region. These transverse systems supplied sediment to the linear system extending to the northwest.

Fig. 5.48 Schematic diagram illustrating the two components of the gravelly submarine system: a longitudinal northwest - southeast trending braided channel complex and the radial submarine fans supplying them. One of the latter is preserved within the Skidegate Inlet region. Model also shows the general tectonic setting of the Queen Charlotte region during Late Turonian to Coniacian time, with active thrust belt along the northeast margin of the basin (discussed in Chapter 6). The presence of canyons feeding the fans to the northeast is inferred.

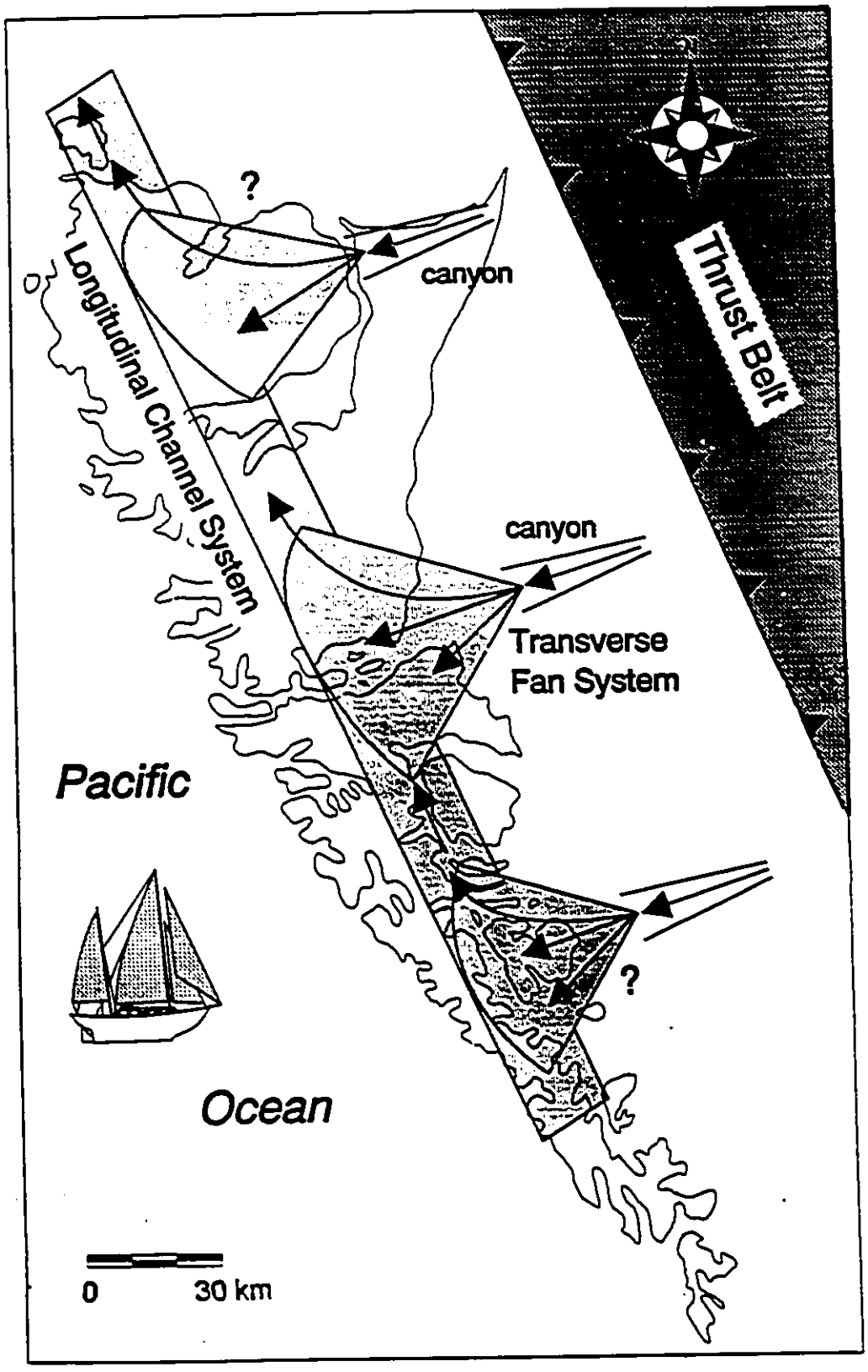
Thrust Belt
Longitudinal Channel System
canyon
canyon
Transverse
Fan System
Pacific
Ocean
?
?
0
30 km

5.7. DEPOSITIONAL HISTORY

Prior to Honna deposition, in latest Skidegate (Late Turonian) time, the Queen Charlotte Basin was the site of progradational muddy slope - apron deposition in the northwest and progradational sandy submarine fan deposition in the southeast. Progradation of both of these systems was probably related to a period of relative sea level fall, as was the case for similar successions described fromthe Longarm, Haida, and Skidegate Formations in chapter 4.

The onset of gravelly submarine fan deposition occurred immediately after a regional erosive event. The products of this event are represented by beds of intraclast breccia which can be correlated from Logan Inlet in the southeast to Egeria Bay in the northwest, a distance of some 200 km. The presence of extraformational clasts within these breccias effectively links the onset of conglomeratic Honna deposition to this regional erosive event. This erosional event is immediately followed by an abrupt period of deepening, evidence of which is observed within the section exposed at Egeria Bay, where deep marine conglomerates of the Honna abruptly overlie muddy shelf deposits of the Skidegate (Fig. 5.26). The abrupt transition between environments was probably related to a period of fault controlled basin subsidence, which resulted

in the establishment of a gravelly submarine fan system represented by the deposits of the Honna.

Two distinct components are recognized within the Honna: a northwest - southeast oriented longitudinal channel system and a transverse gravelly submarine fan system sourced from the east (Fig. 5.48). The longitudinal system was probably oriented parallel to the depositional axis of the basin. Gravelly submarine channel systems of this type tend to be oriented parallel to basin axes. Winn and Dott (1977) described a similar 20 km wide and 250 km long gravelly deep-marine fan-channel system from the Upper Cretaceous Cerro Toro Formation of Chile. The authors concluded that the system was oriented parallel to the depositional axis of the basin, which was confined between the rising (ie. faulted) cordillera to the west and the South American craton to the east.

Hein and Walker (1982) also described a similar gravelly submarine channel system from the Ordovician Cap Enrage Formation of Quebec. This particular system was at least 10 km wide and 70 km long, and was interpreted to have been deposited within a series of southwest - northeast trending braided channels oriented parallel to the Iapetus continental rise to the northwest.

The progressive westward shift of flow within the channel system over time (Fig. 5.40) may be attributed to

lateral migration of the channel belt away from the basin margin as the basin infilled and the basin slope prograded to the southwest (Fig. 5.46). The longitudinal channel system was probably fed by the transverse systems. The northerly paleocurrent trends observed within the Lina Narrows region of Skidegate Inlet may therefore reflect turbidity currents flowing down the fan being deflected to the northwest. In a similar fashion, the modern Var Canyon near Nice, France, is deflected approximately 45° to the east-southeast by a prominent bathyometric high to the southwest (Fig. 1 of Malinverno et al., 1988).

The vertical arrangement of facies successions exposed both at Pillar Bay (Fig. 5.23 b) and South Bay (Fig. 5.23 e) is not indicative of an overall shoaling trend associated with fan progradation. This indicates that the overall rate of basin subsidence exceeded that of sedimentation. The rate of basin subsidence throughout Late Turonian to Coniacian time appears to have been rapid; almost 2500 m of coarse clastics accumulated in a period of just 2 Ma. Submarine fan sedimentation was terminated abruptly by the onset of active volcanism. The rapid transition from deep marine sandy channel deposits to subaerial volcanics observed at Gust Island (Fig. 5.34) indicates that the onset of volcanism was accompanied by rapid uplift. This period of volcanism was followed by a

renewed period of subsidence resulting in the establishment of muddy shelf environments during Santonian to Maastrichtian time.

CHAPTER 6. LATE MESOZOIC DEPOSITIONAL HISTORY AND TECTONIC SETTING OF THE QUEEN CHARLOTTE BASIN

6.1. CHAPTER SUMMARY

The Late Mesozoic depositional history of the Queen Charlotte Basin (QCB) compares favourably to van der Hayden's (1992) model for the Late Mesozoic tectonic evolution of the Canadian Cordillera. The succession exposed on the Queen Charlotte Islands (QCI) was deposited in an elongate northwest - southeast trending continental forearc basin situated between an Andean-type magmatic arc (Coast Plutonic Complex) to the east and a subduction zone to the west. The Late Jurassic White Point Formation consists of gravelly fan delta successions deposited within a small westward deepening fault bounded intra-massif marine basin during an episode of regional block faulting. Following a brief hiatus spanning Berriasian to Early Valanginian time, deposition resumed within a much expanded northwest - southeast trending, southwest-deepening basin. The Late Valanginian to Early Turonian Longarm, Haida, and Skidegate Formations consist of eight sequences, each deposited during a single cycle of sea level fall and rise.

Local block faulting influenced the orientation of the shoreline, the location of deltas, and the thickness of progradational shoreface successions. The overall transgressive nature of the shelf deposits within each sequence reflects a high rate of basin subsidence relative to that of sediment supply. Deposition of the sequence was terminated by a new period of relative sea level fall, probably related to uplift of the basin margin. Block faulting during Late Jurassic to Early Turonian time was probably extensional in nature. The eight sequences progressively onlapped the arc massif to the northeast throughout this period. This onlap was probably related to thermal subsidence of the arc massif as the locus of active magmatism migrated east.

The Honna Formation consists primarily of gravelly deep marine submarine fan and channel deposits. The onset of Honna deposition coincided with an abrupt rise in relative sea level related to thrusting and crustal thickening along the basin margin to the northeast. Both sea level rise and fan progradation were related to crustal thickening within a northwest - southeast trending thrust belt situated along the northeastern margin of the basin. This change reflects a transition from Late Oxfordian - Early Turonian extension to Late Turonian - Coniacian compression.

Tectonic mechanims controlling the Late Mesozoic subsidence history of the QCB are discernable at both small scales (progradational shoreface successions) and large scales (transgressive onlap). The nature and evolution of the Late Mesozoic fill within the QCB is typical of both modern and ancient forearc basins. The progressive onlap of marine strata onto the flank of the arc massif appears to be particularly characteristic of modern and ancient forearc basins.

6.2. INTRODUCTION

The goal of this chapter is to determine which of the tectonic models describing the Late Mesozoic history of the Canadian Cordillera best fits the Late Jurassic to Late Cretaceous depositional history of the Queen Charlotte Basin (QCB). In order to do this, it is necessary to first discuss the nature of the mechanisms controlling deposition within the QCB during this period.

6.3. DEPOSITIONAL HISTORY OF THE WHITE POINT FORMATION

6.3.1. DEPOSITIONAL SUMMARY

Deposition within the Queen Charlotte island (QCI) region during this period was restricted to the northwestern Graham Island region (Fig. 6.1). Strata of the White Point

Fig. 6.1 Schematic Late Mesozoic stratigraphy and relative sea level history of the Queen Charlotte Basin, along with the major tectonic features active within the Queen Charlotte Islands region and the Coast Plutonic Complex. 1 - Armstrong, 1988; 2 - van der Hayden, 1992; 3 - Lewis et al., 1991; 4 - Thompson et al., 1991; 5 - Crawford et al., 1987; 6 - Rubin et al., 1990.

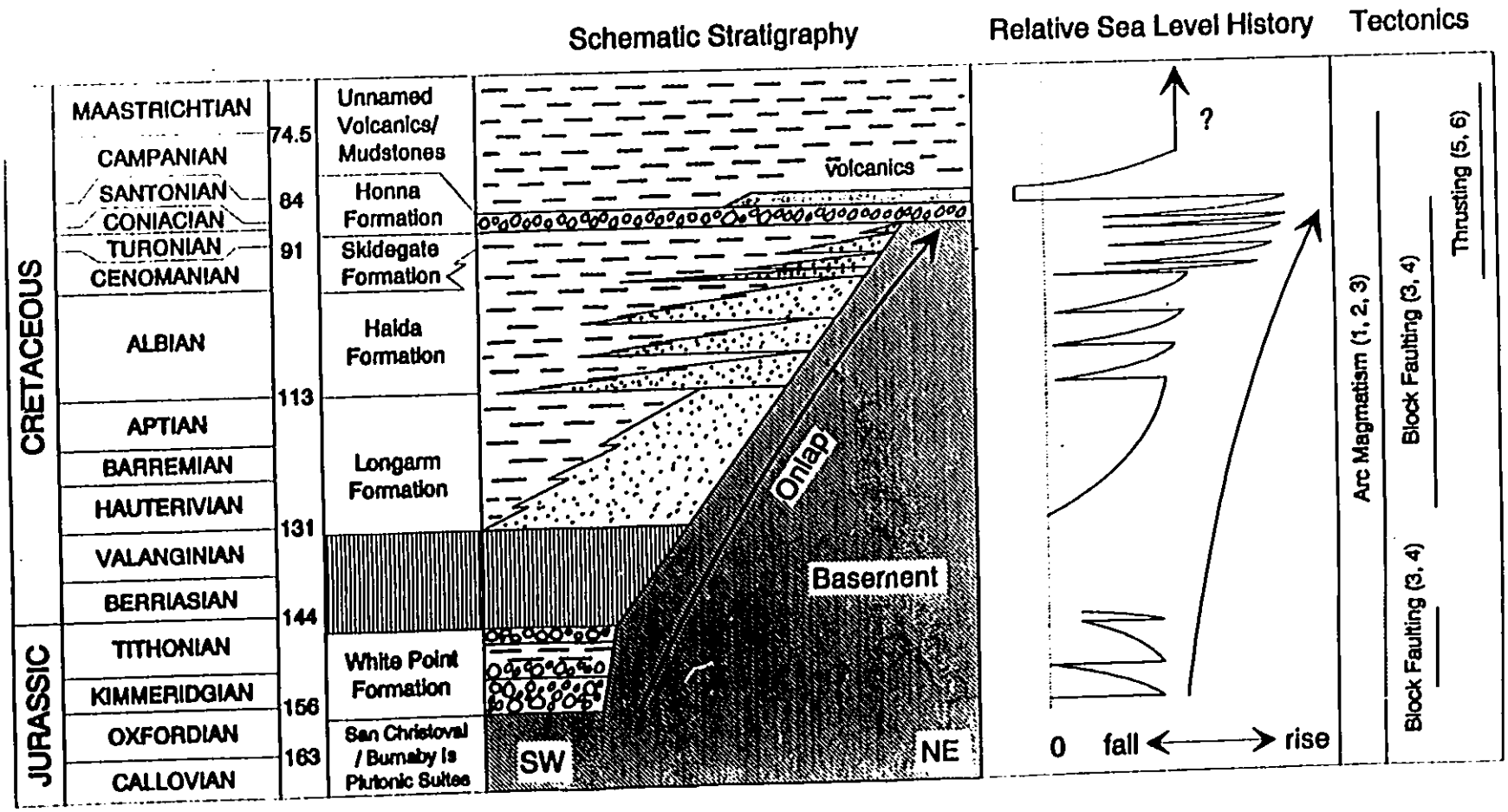
Schematic Stratigraphy
Relative Sea Level History
Tectonics
CRETACEOUS
JURASSIC
MAASTRICHTIAN
CAMPANIAN
SANTONIAN
CONIACIAN
TURONIAN
CENOMANIAN
ALBIAN
APTIAN
BARREMIAN
HAUTERIVIAN
VALANGINIAN
BERRIASIAN
TITHONIAN
KIMMERIDGIAN
OXFORDIAN
CALLOVIAN
74.5
84
91
113
131
144
156
163
Unnamed Volcanics/ Mudstones
Honna Formation
Skidegate Formation
Haida Formation
Longarm Formation
White Point Formation
San Christoval / Burnaby Is Plutonic Suites
volcanics
Onlap
Basement
SW
NE
?
0
fall
rise
Arc Magmatism (1, 2, 3)
Block Faulting (3, 4)
Block Faulting (3, 4)
Thrusting (5, 6)

Formation exposed here consist of gravelly fan delta deposits, with paleocurrent measurements and clast composition indicating derivation from an uplifted and partially dissected volcanic arc situated to the east. Each gravelly fan prograded westwards into storm dominated muddy offshore environments (Fig. 3.13). Gravelly deposition appears to have been switched on and off abruptly, as indicated by the abrupt vertical facies changes within each succession.

6.3.2. CONTROLS

The White Point Formation was deposited within a small fault bounded basin (Fig. 6.1) during a period of Late Jurassic faulting. Each of the successions was probably deposited in response to an episode of faulting. This resulted in both rapid basin subsidence and the progradation of a gravelly fan deltaic system westward into the basin.

6.4. DEPOSITIONAL HISTORY OF THE LONGARM, HAIDA, AND SKIDEGATE FORMATIONS

6.4.1. Depositional Summary

Deposition of the Longarm, Haida, and Skidegate Formations occurred within a marine basin which encompassed much of the QCI region. The lack of intervening Berriasian

to Early Valanginian strata indicates that this period of basin expansion followed a period of nondeposition (Fig. 6.1). At least eight sequences, each deposited during a cycle of relative sea level fall and rise, are recognized. Periods of sea level fall triggered regional erosion and the initiation of slope and submarine fan sedimentation. Periods of ensuing sea level rise led to the accumulation of thick transgressive successions composed of high energy sandy shoreface and muddy offshore deposits (Fig. 4.41). The coastline, which consisted of prominent headlands and bays, was generally oriented northwest - southeast throughout Late Valanginian to Early Turonian time. The basin deepened towards the southwest. The eight depositional sequences progressively onlapped the basin margin to the northeast throughout this period (Fig. 6.1).

Two scales of cyclicity are observed within the deposits of these three formations. The smallest is represented by the progradational shoreface successions within the deposits of the SFA and MFA of many of the sequence (Figs. 4.35 and 4.38). The larger scale cyclicity is represented by the sequences themselves (Fig. 6.1). The largest scale trend observed within the three formations is the overall transgressive nature in which the sequences are arranged (Fig. 6.1).

6.4.2. Controls influencing deposition of the progradational shoreface successions

The small scale progradational shoreface successions within the Longarm and Haida Formations are up to 110 m thick (Figs. 4.35 and 4.38). Six shoreface successions 5 to 45 m thick occur within the Hauterivian to Berriasian deposits of the Longarm Formation exposed on Arichika Island, a period of approximately 12 Ma. Although poorly constrained, the average time frame within which each succession was deposited is approximately 2 Ma.

The small scale cyclicity represented by the progradational shoreface succession within the Longarm and Haida Formations may be attributed to a variety of autocyclic or allocyclic mechanisms. One autocyclic mechanism includes the switching of shoreline position in response to deltaic avulsion. During this process, relative sea level remains constant. As the progradational successions are interpreted as shoreface deposits, this seems most unlikely. This leaves allocyclic mechanisms as the only viable control on the deposition of these successions. Allocyclic mechanisms induce changes in relative sea level to which the depositional systems are forced to respond. The relative sea level history of any basin is governed by three interdependent variables: subsidence, eustasy, and sedimentation. Because all three

variables interact, determining which is the main cause of sea level fluctuation is a tricky business at best. The mechanisms responsible for inducing sea level changes can be grouped into three main categories: tectonic, glacio-eustatic, and climatic. Discussions concerning the affect upon sea level of each mechanism are provided by Pitman (1978) and Hallam (1984).

Most progradational high energy shoreface successions are between 5 and 15 m thick (Walker, 1985). The unusually thick nature of the shoreface successions within the Longarm and Haida Formations is the key to determining which mechanism most influenced their deposition. The thickness of these shoreface successions may be attributed to two factors: 1) an unusually deep fairweather wave base, or 2) a high rate of accommodation space creation during deposition. The thickness of any particular shoreface succession is in part governed by the depth to which fairweather processes can operate. This depth depends upon the wave climate of the shoreface in question. For example, fairweather wave base for the modern Pacific coast of California is approximately 20 m (Walker, 1985), while that of the modern Atlantic coast is between 10 and 15 m (Dietz, 1963). The shorefaces in this study faced the open Pacific Ocean to the west during Late Valanginian to Early Turonian time. It is therefore reasonable to conclude that fairweather wave base

for these particular shorefaces was relatively deep. It is however impossible to see how fairweather wave base could have approached 44 m, which is the thickness of the trough cross-stratified sandstones within the uppermost progradational succession preserved within the Longarm Formation near White Point (Fig. 4.35). The unusual thickness of the shoreface deposits within these sequences therefore must reflect the relatively high rate at which accommodation space was created during the deposition of the successions. However, in order to generate a progradational succession, sedimentation rates must have been even higher than the rate at which accommodation space was created.

The 2 Ma average duration of the successions exposed on Arichika Island corresponds to the third order eustatic sea level cycle of Vail et al. (1977). It is however unlikely that eustatic sea level rise alone was the main force behind the relatively high rate at which accommodation space was created, because under conditions of rapidly rising sea level, sediment would be trapped in coastal plains and estuaries (Fisher, 1961; Swift, 1968). This would make it impossible for nearshore marine systems to prograde.

Another mechanism is therefore required to generate both a large amount of accommodation space and at the same time a high rate of sedimentation. Thompson et al. (1991)

and Lewis et al. (1991) mapped several northwest - southeast trending high angle Late Jurassic faults in the Skidegate Inlet and Cumshewa Inlet regions (Fig. 6.2). They proposed a number of stratigraphic arguments supporting the fact that these faults were reactivated throughout Early Cretaceous time. Most of the arguments centred around variations in the relative thickness of underlying pre-Cretaceous packages across the inferred faults (Fig. 6.3). Thick Cretaceous sandstone successions were believed to have accumulated upon the down-dropped fault block, while pre-Cretaceous strata on the uplifted block were eroded.

As Thompson et al. (1991) suggested, it is possible that movement along reactivated Late Jurassic faults influenced Early Cretaceous deposition within the QCB on a local scale. Minor offsets could have influenced the position of coarse grained deltaic sources. For example, in the Longarm Formation, gravelly shoreface deposits are found only in the Arichika Island and Dawson Cove areas. Similarly, the large boulders within the transgressive lag at Arichika Island reflect deposition adjacent to a coastal headland of high relief. The high relief of the headland in the vicinity of Arichika Island may be attributed to local block faulting. A localized fault control might also explain why the flooding surfaces bounding the progradational shoreface successions within the Longarm and

Fig. 6.2 Structure of the Skidegate and Cumshewa Inlet regions (from Thompson et al., 1991). Note the Late Jurassic faults (with the exception of the Sandspit Fault to the east) oriented primarily northwest - southeast.

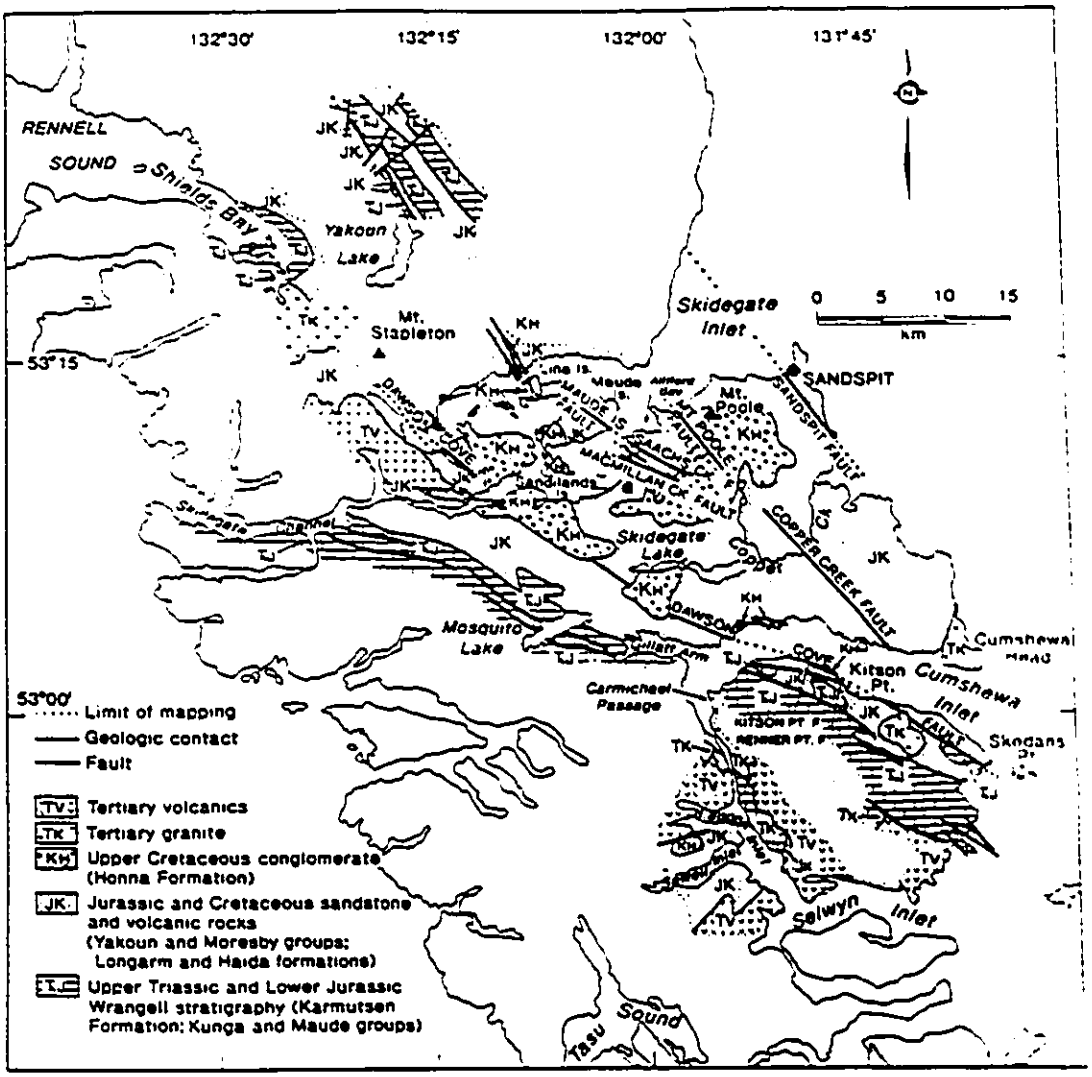
132°30'
132°15'
132°00'
131°45'
RENNELL SOUND
Shields Bay
Yakoun Lake
Mt. Stapleton
Skidegate Inlet
SANDSPIT
0 5 10 15
km
53°15'
Maude Is.
Alliford Bay
Mt. Poole
SANDSPIT FAULT
MAUDE FAULT
MACMILLAN CK FAULT
Sandilands
Skidegate Channel
Skidegate Lake
COPPER CREEK FAULT
Mosquito Lake
Cumshewa Head
Kitson Pt.
Cumshewa Inlet
Carmichael Passage
Skedans
Selwyn Inlet
Tasu Sound
53°00'
Limit of mapping
Geologic contact
Fault
TV Tertiary volcanics
TK Tertiary granite
KH Upper Cretaceous conglomerate (Honna Formation)
JK Jurassic and Cretaceous sandstone and volcanic rocks (Yakoun and Moresby groups; Longarm and Haida formations)
TrJ Upper Triassic and Lower Jurassic Wrangell stratigraphy (Karmutsen Formation; Kunga and Maude groups)

Fig. 6.3 Block faulting model of Thompson et al. (1991). The authors suggested that vertical displacement across these reactivated Late Jurassic faults accounts for the thinning of pre-Cretaceous units.

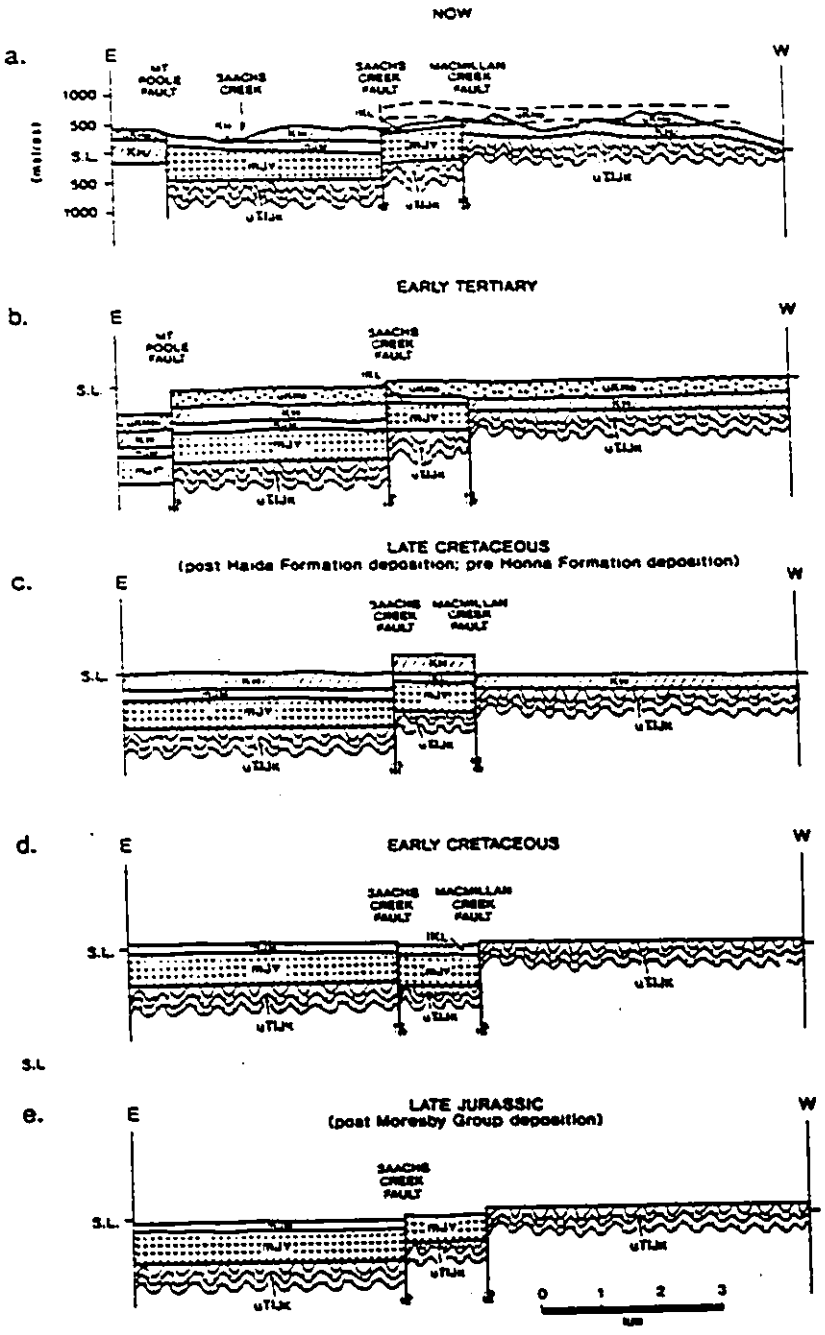
NOW
a.
E
W
1000
500
S.L.
500
1000
(metres)
EARLY TERTIARY
b.
E
W
S.L.
LATE CRETACEOUS
(post Haida Formation deposition; pre Honna Formation deposition)
c.
E
W
S.L.
d.
EARLY CRETACEOUS
E
W
S.L.
S.L.
e.
LATE JURASSIC
(post Moresby Group deposition)
E
W
S.L.
0
1
2
3

Haida Formations are not correlatable on a regional extent.

Thick progradational high energy shoreface and deltaic successions similar to those within the Longarm and Haida Formations have been documented in the Eocene Coaledo Formation of Oregon (Chan and Dott, 1986) and the Miocene of the southeastern Caliente Range in California (Clifton, 1981). The wave dominated deltaic successions within the Coaledo Formation are up to 115 m thick, while the high energy shoreface successions within the Miocene of the Caliente Range are up to 95 m thick. Chan and Dott (1986) attributed the thickness of the deltaic successions mainly to a high rate of basin subsidence or to a "combination" of unnamed factors. Clifton (1981) attributed the thickness of the shoreface successions, each deposited during a few tens of thousands of years, to eustatic sea level fluctuations related to climatic cycles produced by periodicity of the earth's solar orbit.

Both of these formations were deposited within an active margin setting dominated by faulting. It is likely that the thickness of the progradational successions within these formations reflects a high rate of basin subsidence coupled with a high rate of sedimentation, both of which could be facilitated by active faulting and vertical displacement of the sediment source relative to the basin.

In summary, the thick shoreface successions within

the Longarm and Haida Formations were probably deposited in response to high rates of localized fault-controlled subsidence accompanied by relatively higher rates of sedimentation. Third order eustatic sea level rise may however have contributed to the rate at which accommodation space was created.

6.4.3. Controls influencing deposition of the sequences

Eight sequences, each up to 600 m thick and each deposited over a period of 1 to 17 Ma are recognized within the Longarm, Haida, and Skidegate Formations (Figs. 4.0 and 6.1). The erosional surfaces bounding each sequence mark a distinct basinward change in facies and are correlatable on a regional scale, suggesting that they are related to periods of relative sea level fall. The regional aspect of these features, and of the sequences themselves, indicates that an allocyclic mechanism or mechanisms controlled their formation.

As the Cretaceous is generally believed to be a glacial free period, it is unlikely that the formation of the erosional surfaces and deposition of the sequences could have been controlled by a glacial-eustatic mechanism. The 1 to 17 Ma duration of the sequences fits the second and third order eustatic sea level cycles of Vail et al. (1977). Haq et al. (1989) documented 22 third order cycles and 5 second

order supercycles throughout Late Valanginian to Early Turonian time. The fact that 8 second or third order cycles are represented by the deposits of the Longarm, Haida, and Skidegate Formations may argue against eustatic sea level being the main mechanism controlling deposition. Alternatively, it is possible that several of the third order cycles documented by Haq et al. (1989) during this period are not represented within the three formations, or that second order eustatic cycles are over-represented.

One particularly unusual aspect of many of the sequences within the Longarm, Haida, and Skidegate Formations is the overall transgressive manner in which the progradational shoreface successions are stacked (Fig. 4.57). This indicates that over the long term, the rate of sedimentation was less that the rate at which accommodation space was created, a situation the reverse of that operating over shorter terms (ie. deposition of the progradational shoreface successions). The relatively high rate at which accommodation space was created may be attributed to a relatively high rate of basin subsidence compared to that of sedimentation over the long term. Aside from the relatively small scale faults described by Thompson et al. (1991), no regional fault systems active during the Early Cretaceous have been documented in the QCI area. Crawford et al. (1987) and Rubin et al. (1990) documented structural

evidence of a Late Cretaceous (Late Albian to Maastrichtian) west-vergent thrust belt in the Prince Rupert area approximately 100 km to the east of the QCI region. It is therefore possible that crustal thickening within this belt and the resulting flexure may have influenced the subsidence history of the QCB during the latter part of this period.

The transgressive nature of the shelf successions within many of the sequences may be attributed to relatively rapid rates of fault controlled basin subsidence that exceeded the rate of sedimentation over the long term. Formation of the erosional surfaces bounding the sequences may be related to periods of fault related uplift of the eastern margin of the basin. This would also have triggered progradation of the shoreface systems out into the rapidly subsiding basin.

Thick transgressive shelf successions similar to those within many of the sequences have been documented in the Cretaceous Cape Sebastian sandstone of southwestern Oregon (Bourgeois, 1982; Fig. 6.4) and the Miocene Sandstone of Floras Lake in southwestern Oregon (Leithold and Bourgeois, 1984). The deposits of the Cape Sebastian form a 200 m thick, apparently uninterrupted transgressive succession of high energy sandy shoreface to storm dominated offshore deposits, complete with a transgressive basal boulder lag. A similar 70 m thick overall transgressive

Fig. 6.4 Transgressive shoreface succession from the Late Cretaceous Cape Sebastian Sandstone of southwestern Oregon (from Bourgeois, 1982).

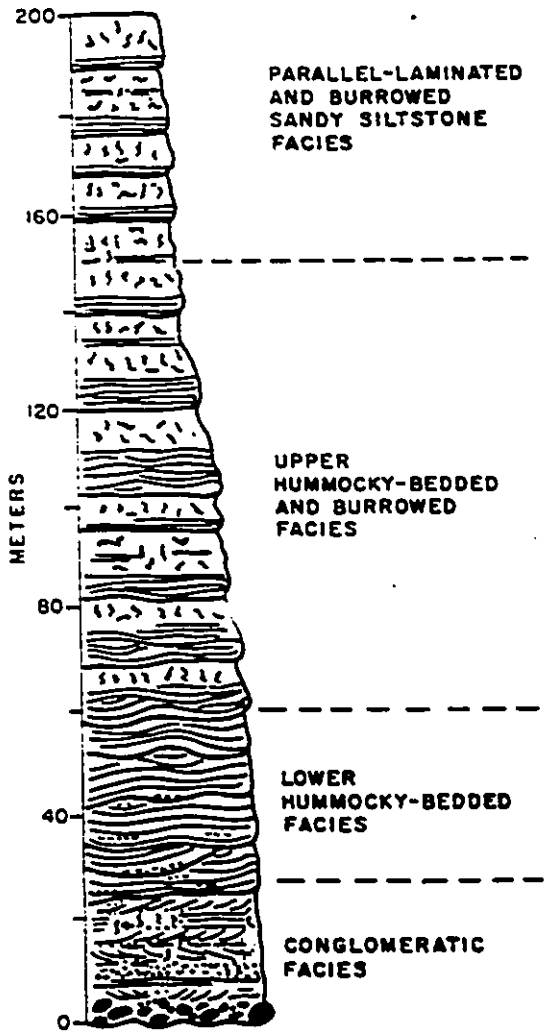
200
160
120
80
40
0
METERS
PARALLEL-LAMINATED AND BURROWED SANDY SILTSTONE FACIES
UPPER HUMMOCKY-BEDDED AND BURROWED FACIES
LOWER HUMMOCKY-BEDDED FACIES
CONGLOMERATIC FACIES

high energy shoreface succession is also preserved within the Sandstone of Floras Lake. These successions are identical to those observed within the Longarm Formation exposed on Murchison and Sea Pigeon Islands (Fig. 4.42 b and c). As previously discussed, the large scale transgressive successions preserved within the Early Cretaceous of the QCI are actually composed of smaller scale progradational shoreface successions. The same is probably true of the Cape Sebastian sandstone and the Sandstone of Floras Lake. Both of these were deposited within faulted forearc basin setting, with Bourgeois (1982) and Leithold and Bourgeois (1984) attributing the thickness and transgressive nature of the successions to high rates of fault controlled basin subsidence coupled with high rates of sedimentation related to an uplifted basin margin. In both cases, the long term rate of sediment supply, though voluminous, lagged behind that of subsidence, resulting in the accumulation of a thick transgressive succession.

6.5. DEPOSITIONAL HISTORY OF THE HONNA FORMATION AND THE UNNNAMED UNITS

6.5.1. Depositional summary

The uppermost deposits of the Skidegate Formation exposed on northwestern Graham Island and on Langara Island

document a shoaling trend from a mass flow dominated deep water slope environment to a muddy storm dominated shelf environment situated in less than 200 m water depth (Fig. 5.26). To the southeast, shoaling was accompanied by the progradation of a sandy submarine fan system. Both of these events likely occurred in response to a period of relative sea level fall (Fig. 6.1). The overlying deposits of the Honna Formation consist primarily of turbiditic gravels and sandstones emplaced within a deep marine environment. The change from shallow shelf to deep water gravelly turbidites observed within the sections exposed to the northeast reflect an abrupt rise in relative sea level (Fig. 6.1).

Two distinct types of gravelly submarine systems are recognized within the Honna: transverse gravelly fan(s) sourced from the east and a longitudinal braided channel complex within which currents flowed from southeast to northwest (Fig. 5.48). At least four different gravelly channel complexes, each separated by abandoned or interchannel mudstones, are exposed in the northwestern Graham Island - Langara Island region (Fig. 5.46).

The onset of volcanism in Late Coniacian - Early Santonian time was accompanied by rapid shoaling to subaerial environments in response to a relative sea level fall (Fig. 6.1). This was followed by conditions of rising relative sea level and a change to muddy shelf deposition

which persisted until Maastrichtian time.

6.5.2. Controls

The progradational slope and sandy submarine fan successions within the upper part of the Skidegate Formation probably reflect a period of relative sea level fall, as was the case for the initiation of slope and submarine fan deposition within the underlying sequences. The erosional breccia capping the slope succession exposed on Langara Island may be attributed to erosion and mass wasting at the shelf / slope break by wave process and gravity failure. Both processes operate at many modern shelf - slope breaks, which are commonly characterized by a series of erosional gullies (Pickering et al., 1989). Etheridge and Wescott (1984) also attributed the sharp erosional contact between many ancient progradational slope successions and overlying shallow shelf successions to erosion at the shelf edge. The cause of the relative sea level fall may be attributed to a eustatic fall in sea level, to fault related uplift, or to a combination of the two. Instead of being followed by the accumulation of a thick transgressive shelf succession, as was the case in many of the underlying sequences, the relative fall was followed by an abrupt rise in sea level and the emplacement of the turbiditic gravels of the Honna within a deep marine environment.

Haggart (1991, 1993) suggested that the Honna was deposited in response to a dramatic fall in base level related to the Late Turonian third order eustatic sea level drop documented elsewhere by Hancock and Kauffmann (1979) and Haq et al. (1987). Haq et al. (1987) calculated that sea level dropped approximately 120 m during this period. One observation serves to negate Haggart's (1991, 1993) interpretation. The sections exposed on Langara and northwest Graham Islands (Fig. 5.26) document an abrupt change from a storm dominated shelf environment during latest Skidegate time to a deep water turbiditic environments during earliest Honna time. This change is indicative of a rise in relative sea level, not a eustatic drop in sea level as suggested by Haggart (1991, 1993).

Thompson et al. (1991) suggested that deposition of the Honna was controlled by movement along several reactivated Late Jurassic high angle faults, many of which are presently exposed upon the islands. Their argument was based primarily upon the observation that the Honna rests with apparent unconformity upon Early Cretaceous and older strata at several locations in the eastern Cumshewa and Skidegate Inlet areas. Towards the west, strata of the Honna rest conformably upon those of the Skidegate and Haida Formations. This relationship suggests that localized uplift along these Late Jurassic faults led to uplift and

erosion of part or all of the underlying Cretaceous succession along the eastern margin of the basin, which is a maximum of 2 km thick within the central outcrop belt.

This interpretation has one rather important ramification, this being that faulting must have progressively backstepped towards the east throughout the deposition of the Honna. This is necessary to explain the fact that the Honna rests directly upon what had to have been at one time uplifted and eroded blocks. These blocks had to have been first uplifted, in order to shed their Early Cretaceous strata, and then down-dropped, in order to have reached the deep marine environments in which the overlying strata of the Honna was deposited. This scenario of localized fault-bounded blocks bouncing up and down during Late Turonian to Coniacian time seems highly improbable. An additional problem the interpretation of Thompson et al. (1991) is that it does not account for the presence of Early Cretaceous granitic clasts derived from plutonic suites exposed within the Coast Plutonic Complex more than 100 km to the east. If the Honna accumulated within localized, fault bounded basins, then surely sediment would have been derived from nearby uplifted basement block, and not from Early Cretaceous and Silurian plutonic complexes situated more than 100 km to the east and northeast respectively. The uplift and subsequent unroofing

of the Early Cretaceous plutonic complexes within the McCauley Island and Gamesby complexes to the east requires a regional tectonic mechanism, not localized block faulting.

Higgs (1989, 1990) suggested that the Honna was deposited within a foreland basin setting situated west of an active thrust belt (Fig. 6.5). In this model, the Sandspit fault is interpreted as a low angle west-vergent fault at the leading edge of a westward migrating thrust belt. Higgs (1989, 1990) suggested that the close proximity of the leading edge of the thrust belt to the basin, as well as its deep nature, implied that the submarine fans were supplied directly by alluvial fans. Hence he interpreted the Honna as the deposits of a "deep water" fan delta. There are two problems associated with Higgs (1989, 1990) interpretation. Firstly, on the basis of onland mapping and offshore seismic data, Thompson et al. (1991) interpreted the Sandspit fault as a high angle Cenozoic structure and not a Cretaceous low angle west vergent thrust. The Sandspit fault could not therefore have influenced the deposition of the Honna. Secondly, no alluvial deposits have been identified within the Honna (Higgs, 1989, 1990; Gamba, 1990, 1991). The lack of proximity to a thrust fault and the lack of alluvial deposits (let alone fan deposits) conspire against Higgs (1989, 1990) fan delta interpretation for the Honna.

Fig. 6.5 Late Cretaceous tectonic model of Higgs (1990) relating deposition of the deep water fan deltas of the Honna Formation to west-vergent thrusting along the Sandspit Fault (from Higgs, 1990).

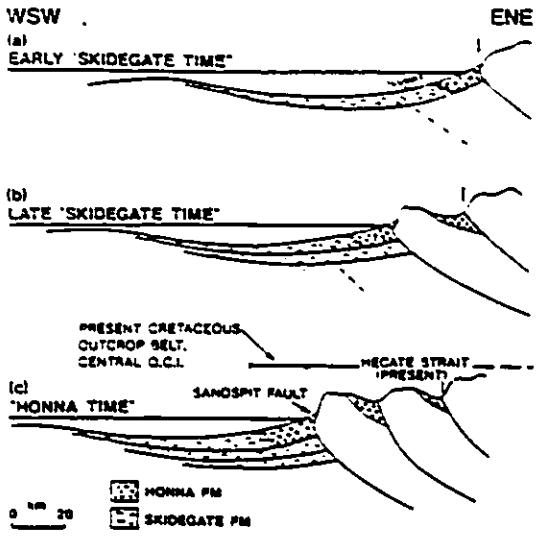
WSW
ENE
(a)
EARLY 'SKIDEGATE TIME"
(b)
LATE 'SKIDEGATE TIME"
PRESENT CRETACEOUS
OUTCROP BELT,
CENTRAL Q.C.I.
HECATE STRAIT
(PRESENT)
(c)
"HONNA TIME"
SANOSPIT FAULT
HONNA FM
SKIDEGATE FM
0 km 20

Regional structural features active within the QCI area during Late Turonian and Coniacian time include a series of northwest trending west-vergent thrust faults within the Coast Plutonic Complex 100 km to the east (Crawford et al., 1987; Rubin et al., 1990; Fig. 5.45 and 6.1). Crawford et al. (1987) suggested that the timing of crustal thickening was 100 - 70 Ma (Late Albian to Maastrichtian), while Rubin et al. (1990) suggested that 84 Ma (Late Santonian - Early Campanian) is the minimum age for the cessation of deformation. Magmatism within the Coast Plutonic Complex was also active throughout most of Late Turonian to Santonian time (van der Hayden, 1992; Fig. 6.1). Several observations suggest that crustal thickening within this thrust belt probably controlled the subsidence history of the QCB during this period. First, the orientation of the submarine systems within the Honna certainly seems to indicate that faults along the northeastern margin of the basin controlled deposition (Fig. 5.48). The nature and geometry of the submarine systems within the deposits of the Honna Formation are reminiscent of the geometry of fluvial systems within various types of fault controlled basins. The axes of these basins are generally oriented parallel to the major structures which control subsidence, such as high angle faults or thrust and fold belts (Miall, 1981). Fluvial systems within such basins tend to be oriented

normally and/or parallel to the structural grain. The normally (transversely) oriented systems flow away from the faulted or otherwise uplifted basin margins, while the axial (longitudinal) systems flow in a direction parallel to the basin margin, and in the direction in which the basin is tilted. The southeast - northwest orientation of the longitudinal submarine channel system parallels the orientation of the thrust belt forming the northeastern margin of the basin. The predominant southeast to northwest direction of flow within the longitudinal system indicates that the axis of the basin was tilted towards the northwest. The radial submarine fan system preserved within the Skidegate Inlet region is oriented roughly normal to the thrust belt, indicating that it represents a transverse system. These relationships suggest that crustal loading within the thrust belt likely controlled the structural grain and subsidence history of the basin during Late Turonian to Coniacian time.

Second, flexurally driven subsidence of the transitional continental crust underlying the basin in response to supracrustal loading may account for the dramatic rise in relative sea level observed at the Skidegate - Honna boundary (Fig. 6.1). Third, crustal thickening related to thrusting would also account for the rapid uplift and subsequent erosion of Early Cretaceous

plutons within the McCauley Island and Gamesby belts which supplied sediment to the basin situated to the west. Crawford et al. (1987) calculated rates of uplift as high as 1 mm/yr within this belt during Latest Albian to Maastrichtian time (98 to 70 Ma).

Finally, continued thrust loading along the northwestern margin of the basin throughout Coniacian time would have generated the subsidence required to maintain the depth of basin. This would have prevented shoaling within the basin, which seems to have been the case throughout Honna time.

This model differs from Higgs (1989, 1990) interpretation in two important respects. First, it places the leading edge of the thrust belt approximately 100 km farther to the east where low angle west-vergent thrusts have been documented. Second, due to the wide separation between source and the deep marine depositional site, it is unlikely that the submarine fans within the Honna were supplied directly by alluvial fans. This distance may however have been bridged by submarine canyons, as originally suggested by Yagishita (1985 a). As suggested by Thompson et al. (1991), block faulting within the immediate QCI area may have affected deposition locally, perhaps influencing the location of the transverse submarine fan systems feeding sediment to the longitudinal axial system.

At least four separate conglomerate-filled channel complexes are exposed in the northwestern Graham Island region (Fig. 5.46). Each period of channel fill and abandonment may reflect an autocyclic mechanism such as catastrophic channel avulsion where a levee is breached and the channel is re-established in an adjacent topographic low. The fact that individual conglomerate packages may be correlated 200 km alon_ strike however suggests a more regional, allocyclic control upon deposition. Channel incision and the onset of gravelly submarine fan deposition may have been in response to relative sea level fall, when sediment supply to the basin would increase in response to a drop in base level. Channel abandonment may have occurred in response to periods of relative sea level rise, when sediment was trapped upon the shelf and in the fluvial systems supplying the marine basin. These fluctuations may have been controlled by discrete episodes of thrusting, by changes in eustatic sea level, or perhaps by a combination of the two.

The onset of volcanism within the western Skidegate Inlet region was followed by a relative sea level fall resulting in a rapid transition from sandy submarine fan to subaerial environments (Fig. 6.1). This event was obviously associated with a renewed period of volcanic activity in the QCI area during Late Coniacian - Santonian time. This

volcanic period was followed by a relative rise in sea level (Fig. 6.1) leading to the establishment of a storm dominated muddy shelf environment which persisted well in Maastrichtian time (Haggart and Higgs, 1989; Gamba, 1991).

In summary, crustal thickening along the western part of the Coast Plutonic Complex appears to have exerted the main control on the deposition of the Honna Formation during Late Turonian to Coniacian time, and perhaps beyond as well.

6.6. TECTONIC MODELS

In this section, the tectonic models of Yorath and Chase (1981), Monger et al. (1982), and van der Hayden (1989, 1992; Fig. 6.6) will be reviewed to see which best compares to the Late Mesozoic depositional history of the QCB.

6.6.1. Yorath and Chase (1981)

These authors proposed that the Wrangel and Alexander terannes amalgamated during Early Cretaceous time (Fig. 6.6 a). During this period, the deposits of the White Point and Longarm Formations would have accumulated within a narrow northwest - southeast trending compressional "suture type" basin confined to the northeast by the Alexander terrane and to the southwest by the Wrangel terrane. The axis of this

Fig. 6.6 Models for the Late Mesozoic evolution of the western Cordillera: a) Yorath and Chase (1981), b) Monger et al. (1982), and c) van der Hayden (1989, 1992). I - Intermontane superterrane, II - Insular superterrane, NA - North America (including Omineca and Fold and Thrust Belts), CPC - Coast Plutonic Complex, W - Wrangel terrane, A - Alexander terrane, SWA - combined Stikine - Wrangellia - Alexander superterrane, SZ - subduction zone.

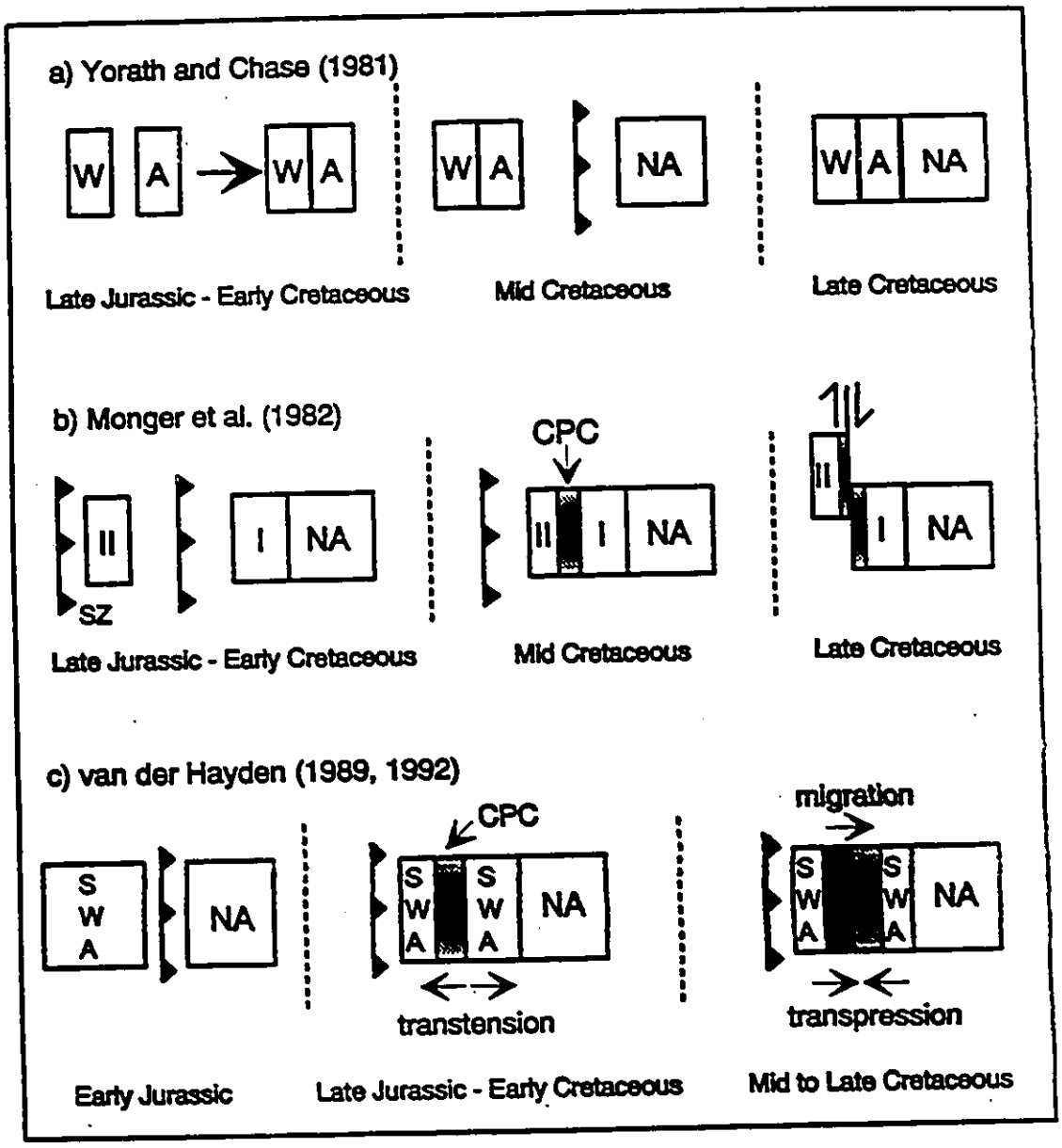
a) Yorath and Chase (1981)
W
A
W A
W A
NA
W A NA
Late Jurassic - Early Cretaceous
Mid Cretaceous
Late Cretaceous
b) Monger et al. (1982)
II
SZ
I NA
CPC
II I NA
II
I NA
Late Jurassic - Early Cretaceous
Mid Cretaceous
Late Cretaceous
c) van der Hayden (1989, 1992)
S W A
NA
CPC
S W A
S W A
NA
transtension
migration
S W A
S W A
NA
transpression
Early Jurassic
Late Jurassic - Early Cretaceous
Mid to Late Cretaceous

graben-like basin paralleled the suture between the two terranes, which the authors suggested ran northwest - southeast through Graham Island (Fig. 6.6 a). The authors cited a general decrease of grain size from southeast to northwest in the Longarm Formation as indicative of a proximal to distal relationship.

During mid Cretaceous time, the amalgamated superterrane moved eastward towards the North American margin, from which it was separated by an unknown expanse of the Panthalassian Ocean. According to this model, the deposits of the Haida, Skidegate, and Honna Formations represent a "post suture" assemblage which unconformably overlie the deposits of the "suture" assemblage (White Point and Longarm Formations). The post-suture assemblage accumulated without major interruption in a quiescent epicontinental setting as the superterrane drifted towards the North American margin. The authors suggested that the basin deepened towards the west, and was divided locally into three main depocenters (Fig. 6.6 b). Estuarine and low energy shelf deposits, represented by the Haida Formation, accumulated along the eastern part of the basin, while turbidites, represented by the deposits of the Skidegate and Honna Formations, accumulated within a deeper trough to the west. Sometime during the course of this Late Cretaceous "quiescent" period the superterrane was accreted to the

North American margin (Fig. 6.6 a).

Several features associated with the Late Mesozoic depositional history of QCB outlined in the previous section conflict with the model proposed by Yorath and Chase (1991). First, the stratigraphy and provenance of the White Point and Longarm Formations indicate that the shoreline, and hence the basin margin, was oriented southeast - northwest during Late Jurassic - Early Cretaceous time. Also, the basin deepened towards the southwest, not the northwest as maintained by Yorath and Chase (1981; Fig. 6.6 a). Furthermore, there is no sedimentological or stratigraphic evidence of a southwestern basin margin. Second, as indicated by the results of this study, and as correctly pointed out by Haggart (1991, 1993), both the style of deposition and the geometry of the QCB was continuous throughout Longarm, Haida, and Skidegate time. There is no evidence of a major change in the type or geometry of the depositional systems nor the geometry of the basin resulting from an Early Cretaceous suturing event, which is supposedly marked by an unconformity separating the deposits of the Longarm Formation from those of the Haida Formation. Third, the along strike continuity of the sequences within the Haida Formation negates the suggestion that it accumulated within three separate sub-basins. Finally, the deposits of the Haida, Skidegate, and Honna do not represent continuous

and uninterrupted deposition within a relatively quiescent epicontinental setting. As indicated by the results of this study, the onset of Honna deposition marks a fundamental change in the nature and geometry of the basin as well as the nature of the depositional systems within it.

Other lines of evidence also do not support the model proposed by Yorath and Chase (1981). First, the actual location of the boundary between the Alexander and Wrangel terranes lies at least 80 km to the east of the QCI's, where Triassic volcanics of the Wrangel terrane are exposed at Bonilla Island situated immediately off the mainland (Woodsworth, 1988; Lewis et al., 1991). The "suture" assemblage exposed on the QCI therefore lies not between two terranes, but entirely upon the Wrangel terrane. Second, both the Wrangel and Alexander terranes are unconformably overlain by Late Jurassic deposits of the Gravina - Nutzotin belts in southeastern Alaska (Monger et al., 1982). This indicates that the two terranes were amalgamated prior to the Late Jurassic, and not the Early Cretaceous as Yorath and Chase (1981) suggested.

6.6.2. Monger et al. (1982)

These authors proposed that superterrane I (the Intermontane superterrane) accreted to the western margin of North America in Middle Jurassic time (Fig. 6.6 b). The

Wrangel and Alexander terranes amalgamated somewhere in the Pacific Ocean to form superterrane II by Late Jurassic time. From Late Jurassic to mid Cretaceous time, superterrane II approached the accreted western margin of North America across an eastward dipping subduction zone (Fig. 6.6 b). This model also places an eastward dipping subduction zone to the west of superterrane II to account for the presence of Late Jurassic and Early Cretaceous plutonic suites presently situated within the Coast Plutonic Complex. The Late Jurassic to mid Cretaceous succession (the White Point, Longarm, Haida, and Skidegate Formations) is therefore placed within a forearc basin setting situated between an active magmatic arc to the east and a subduction zone to the west (Fig. 6.7). To the east, separating superterrane II from North America, was the Gravina - Tyaughton trough, an oceanic foredeep basin.

Monger et al. (1982) suggested that superterrane II collided with the margin of North America in mid Cretaceous time (Fig. 6.6 b) approximately 1000 km south of its present position. This resulted in the formation of the Coast Plutonic Complex (CPC) along the suture zone (Fig. 6.7). The CPC consists mainly of Cretaceous and Tertiary granitic rocks as well as high grade metamorphic rocks and intrusions. The presence of metamorphics within the CPC led the authors to suggest that the CPC was a collisional welt.

Fig. 6.7 a) Paleogeography of the Early Cretaceous suture assemblage (from Yorath and Chase, 1981). Note the deepening trend from conglomerates in the southeast to turbidites in the northwest. Note also the location of the "suture" between the Alexander and Wrangel terranes.

b) Paleogeography of the Late Cretaceous "post suture" assemblage from Yorath and Chase (1981). Note the general westerward deepening trend of the basin, the presence of estuarine deposits to the east, and the three local sub-basins.

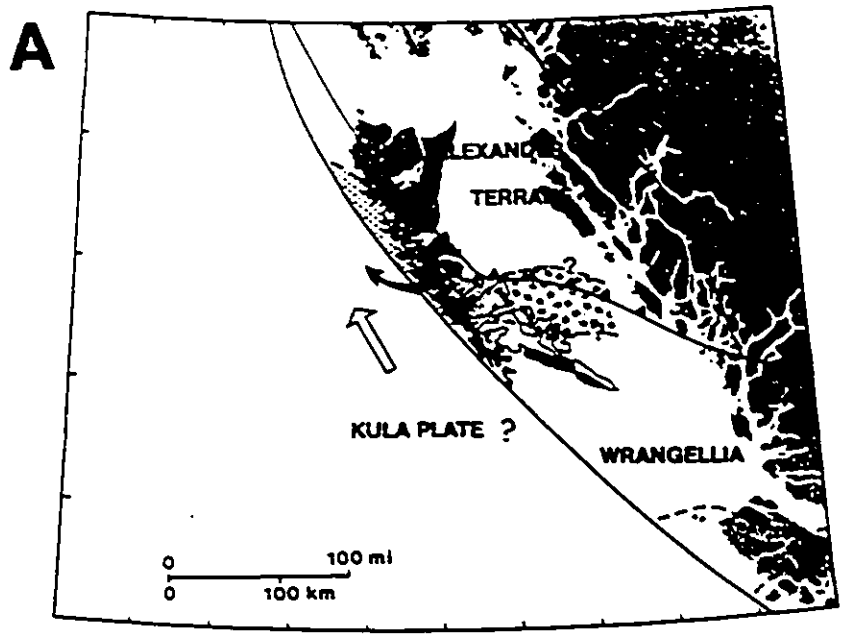

Conglomerate

Sandstone, graywacke

Siltstone, turbidites

Suture zone:
teeth on overriding terrane

Plutons

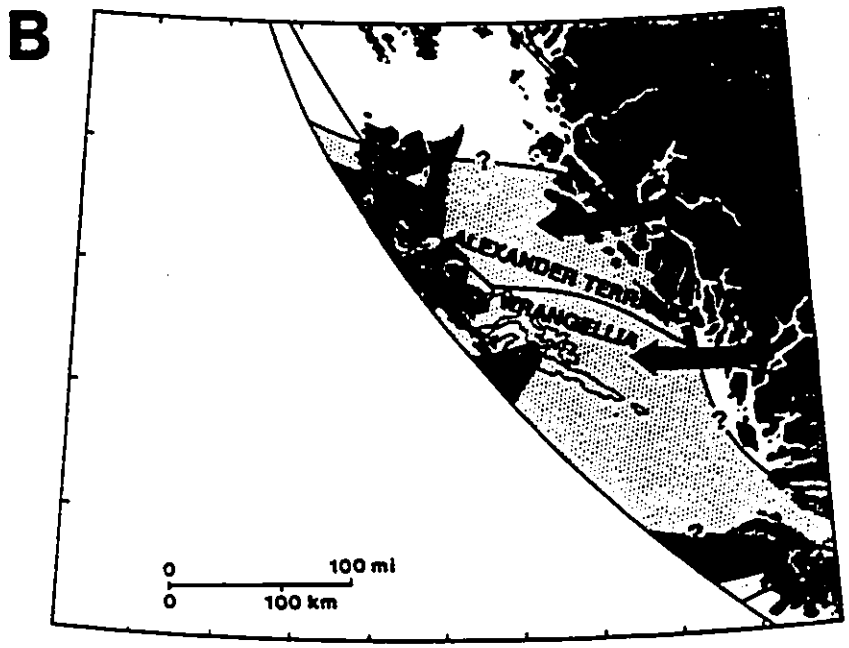

TROUGH FACIES:
siltstone, mudstone,
debris flow conglomerate

SHELF FACIES:
Estuarine to open shelf
sandstones, channel
conglomerate

From mid Cretaceous to Early Tertiary time, the CPC was the site of Andean-type arc magmatism related to the eastward subduction of Pacific Oceanic lithosphere beneath the accreted margin of North America. This model therefore places the Honna Formation within a forearc basin setting between a magmatic arc to the east (CPC) and a subduction zone to the west (Fig. 6.8). This model seems to fit the depositional history of the Late Mesozoic succession exposed on the QCI's. The White Point, Longarm, Haida, and Skidegate Formations were deposited within a westward-deepening, northwest - southeast trending basin which was the site of more or less continuous deposition from Late Jurassic to Early Turonian time. According to Monger et al. (1982), the arc - trench system was oriented roughly north - south, with the arc situated to the east of the basin. This orientation corresponds to the general northwest - southeast trend of the basin axis and southwest deepening trend inferred from the Late Mesozoic succession exposed on the QCI's. The Late Jurassic to mid Cretaceous succession would have accumulated in a relatively uninterrupted fashion within the basin as the superterrane drifted closer to the North American margin. The fundamental change in the nature and geometry of depositional systems within the basin in Late Turonian time may be attributed to compression related to collision of superterrane II with North America. The

Fig. 6.8 Tectonic model based on Monger et al. (1982). From van der Hayden (1992).

Fig. 6.9 Tectonic model of van der Hayden (1992). Modified from van der Hayden (1992).

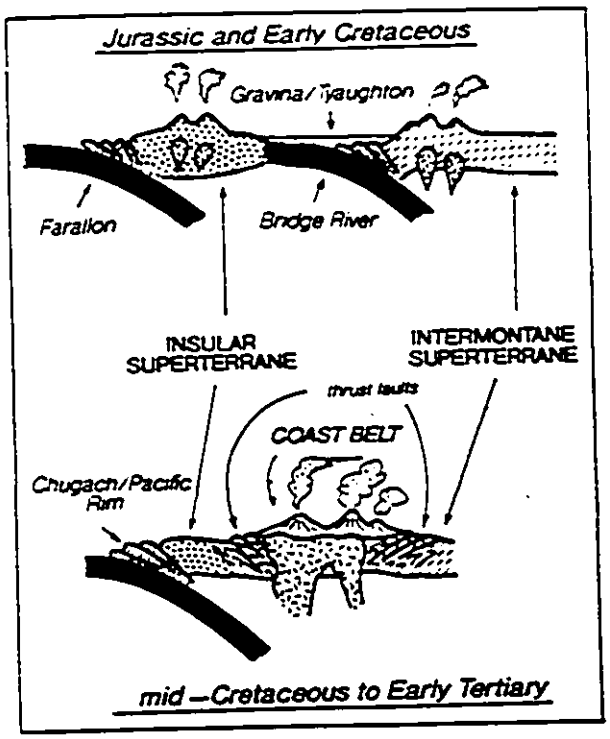
Jurassic and Early Cretaceous
Gravina/Tyaughton
Farallon
Bridge River
INSULAR SUPERTERRANE
INTERMONTANE SUPERTERRANE
thrust faults
COAST BELT
Chugach/Pacific Rim
mid–Cretaceous to Early Tertiary

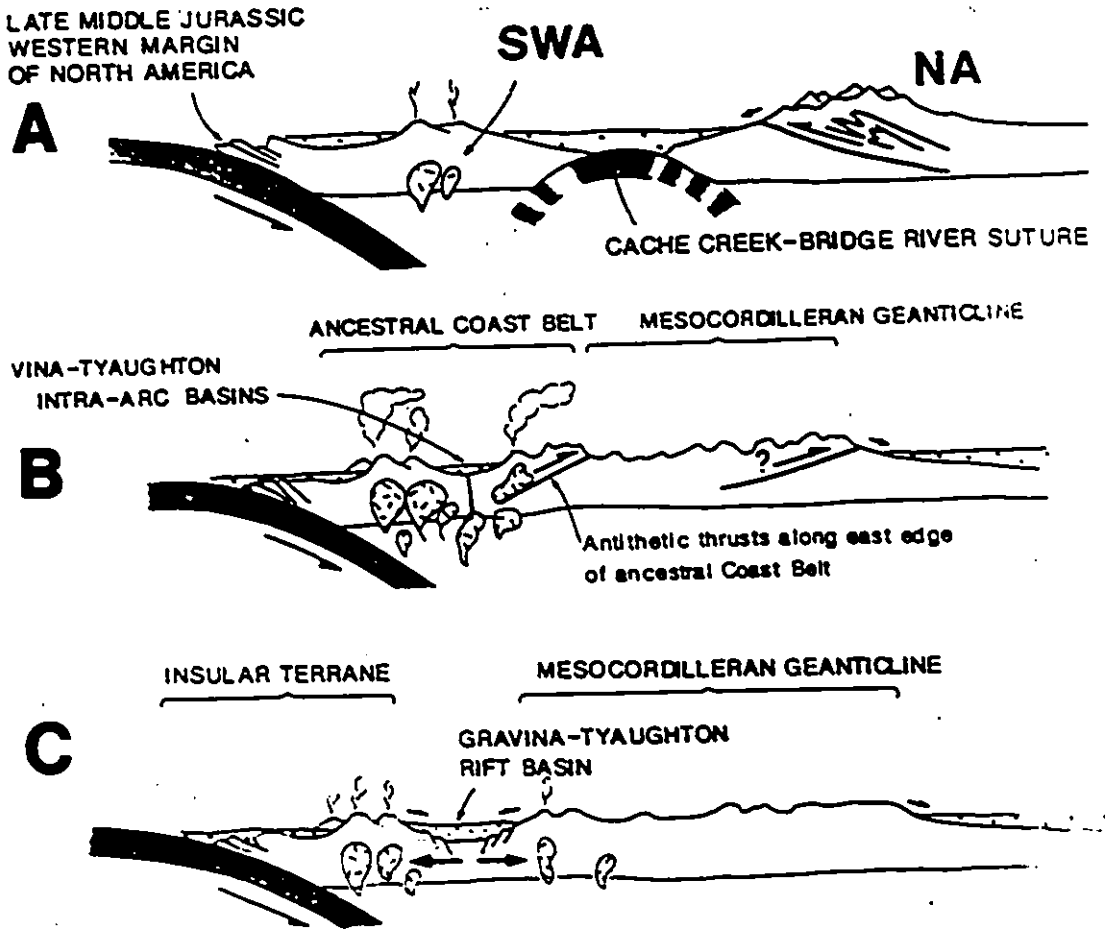
LATE MIDDLE JURASSIC
WESTERN MARGIN
OF NORTH AMERICA
SWA
NA
A
CACHE CREEK–BRIDGE RIVER SUTURE
ANCESTRAL COAST BELT
MESOCORDILLERAN GEANTICLINE
VINA–TYAUGHTON
INTRA–ARC BASINS
B
Antithetic thrusts along east edge
of ancestral Coast Belt
INSULAR TERRANE
MESOCORDILLERAN GEANTICLINE
C
GRAVINA–TYAUGHTON
RIFT BASIN

depositional axis of the basin during Late Turonian - Coniacian time also parallels the north - south trend of the arc - trench system.

6.6.3. van der Hayden (1992)

This author related the Late Mesozoic magmatic history of the CPC to the timing of superterrane accretion. He cited a growing body of evidence indicating that the Stikinia and Alexander terranes (the main components superterranes I and II respectively) were part of a combined superterrane (the Stikinia - Wrangel - Alexander superterrane) by Late Paleozoic time. Van der Hayden (1992) suggested that the combined superterrane was accreted during a single event to the western margin of North America in Middle Jurassic time (Fig. 6.6 c). He also suggested that the CPC represented not a plutonic welt related to mid Cretaceous collision, but rather the remnants of a Middle Jurassic to Early Tertiary Andean-type magmatic arc built upon the accreted basement of the combined superterrane (Fig. 6.9). Late Jurassic to Early Tertiary magmatism within the arc was related to the continuous eastward subduction of Pacific Oceanic lithosphere beneath the accreted margin of North America throughout this period. One of the critical bits of evidence supporting this hypothesis is the progressive eastward migration of

magmatism within the arc away from the trench throughout Middle Jurassic to Early Tertiary time (Armstrong, 1988; van der Hayden, 1989, 1992; Fig. 6.6 c).

Van der Hayden (1992) suggested that during Late Jurassic to Early Cretaceous time, the arc trench system was subjected to extension, resulting in the formation of a narrow rift basin to the east (Fig. 6.9). During Late Cretaceous time, the arc - trench system underwent a period of compression, resulting in closure of the rift basin and crustal thickening to both the east and west of the CPC.

Like the model of Monger et al. (1982), van der Hayden's (1992) model also places the Late Mesozoic succession exposed on the QCI's within an active forearc setting with a magmatic arc to the east and a subduction zone to the west. This again agrees with the geometry and evolution of the Late Jurassic to Late Cretaceous successions exposed on the QCI. The main difference is that in van der Hayden's (1992) model, the forearc basin was situated upon the accreted western margin of North America throughout Late Jurassic to Late Cretaceous time (Fig. 6.6 c and 6.9). In the model of Monger et al. (1982), the Late Jurassic to Late Cretaceous succession was deposited within a forearc basin situated upon superterrane II (Fig. 6.8), which until mid Cretaceous time had been separated from the North American margin by an oceanic basin and a subduction

zone (Fig. 6.6 b). Deposition of the Honna occurred in response to continental collision.

Both models place the Late Mesozoic succession within a forearc basin setting. There are however several specific features of the Late Mesozoic succession which seem to favour van der Hayden's (1992) model.

6.7. LATE MESOZOIC TECTONIC SETTING OF THE QUEEN CHARLOTTE BASIN

Two attributes concerning the depositional history of the Late Mesozoic succession within the QCB support van der Hayden's (1992) model. The first concerns the progressive northeastward onlap and transgression of Late Jurassic to Late Cretaceous (Early Turonian) marine strata onto the magmatic arc to the east. This trend appears to have tracked the progressive eastward migration of the locus of active magmatism within the arc documented by van der Hayden (1992) throughout this period. The second attribute concerns the conformity between the nature of the structural controls governing deposition within the QCB during the Late Mesozoic and those which van der Hayden (1992) suggested controlled the evolution of the magmatic arc.

6.6.1. Late Jurassic to Late Cretaceous (Early Turonian) transgression

As discussed in section 4.11.2, the vertical stacking of the eight sequences within the Longarm, Haida, and Skidegate Formations defines an overall transgressive trend related to progressive northeastward onlap of the basin margin throughout this period (Fig. 6.1). This trend also includes the Late Jurassic White Point Formation, which is exposed to the southwest of the Cretaceous outcrop belt. The rate of onlap within the QCB may be calculated from the Cretaceous stratigraphy observed in Skidegate and Cumshewa Inlets (Figs. 4.58 and 4.60). The rate of onlap from Late Valanginian (133 Ma) to Early Albian (111 Ma) time is 0.7 km/Ma. In Cumshewa Inlet, the rate of onlap from Early Hauterivian (128 Ma) to Early Albian (111 Ma) time is 0.8 km/Ma.

As suggested by Haggart (1991, 1993), the transgressive trend may be related to the long term first order rise in eustatic sea level which occurred throughout the Mesozoic, peaking in the Turonian (Vail et al., 1977; Hallam, 1984; Haq et al., 1989). Hallam (1984) and Haq et al. (1989) calculated that the absolute magnitude of eustatic sea level rise from Berriasian to Turonian time was on the order of 200 m. This mechanism alone however cannot possibly account for the creation of the 2500 m of

accommodation space necessary to deposit the White Point, Longarm, Haida, and Skidegate Formations. Nor does it account for the gross change from primarily shoreface sandstones at the base (Longarm and Haida Formations) to submarine fan deposits at the top (Skidegate Formation).

Alternatively, the overall transgressive nature of the Late Jurassic to Early Turonian succession may be related to a more localized tectonic control affecting the long term subsidence history of the basin. The progressive onlap of strata onto the flank of the magmatic arc is observed in many modern and ancient forearc basins. Seismic profiles across modern forearc basins feature a number of lens shaped seismic sequences (Fig. 6.10). These sequences are generally tilted towards and onlap the arc massif away from the accretionary wedge on the seaward side of the basin. Isopachs of seismic sequences within the West Luzon Basin of the Philippines (Lewis and Hayes, 1984: Fig. 6.11), the Atka Basin of Alaska (Ryan and Scholl, 1989; Fig. 6.12) and the Lima basin of Peru (Ballesteros et al., 1988; Fig. 6.13) indicate that the depocenters of successively younger sequences migrate arcwards over time.

Lewis and Hayes (1984) recognized 12 seismic sequences within the 4.5 km of Late Oligocene to Quaternary fill of the West Luzon Basin (Fig. 6.14). Each sequence is composed of continuous, high amplitude reflectors

Fig. 6.10 Seismic profile of Cenozoic fill within the West Luzon forearc basin, Philippines (from Lewis and Hayes, 1984). Note the lense-shaped seismic sequences which are tilted towards and onlap the arc massif to the east (left).

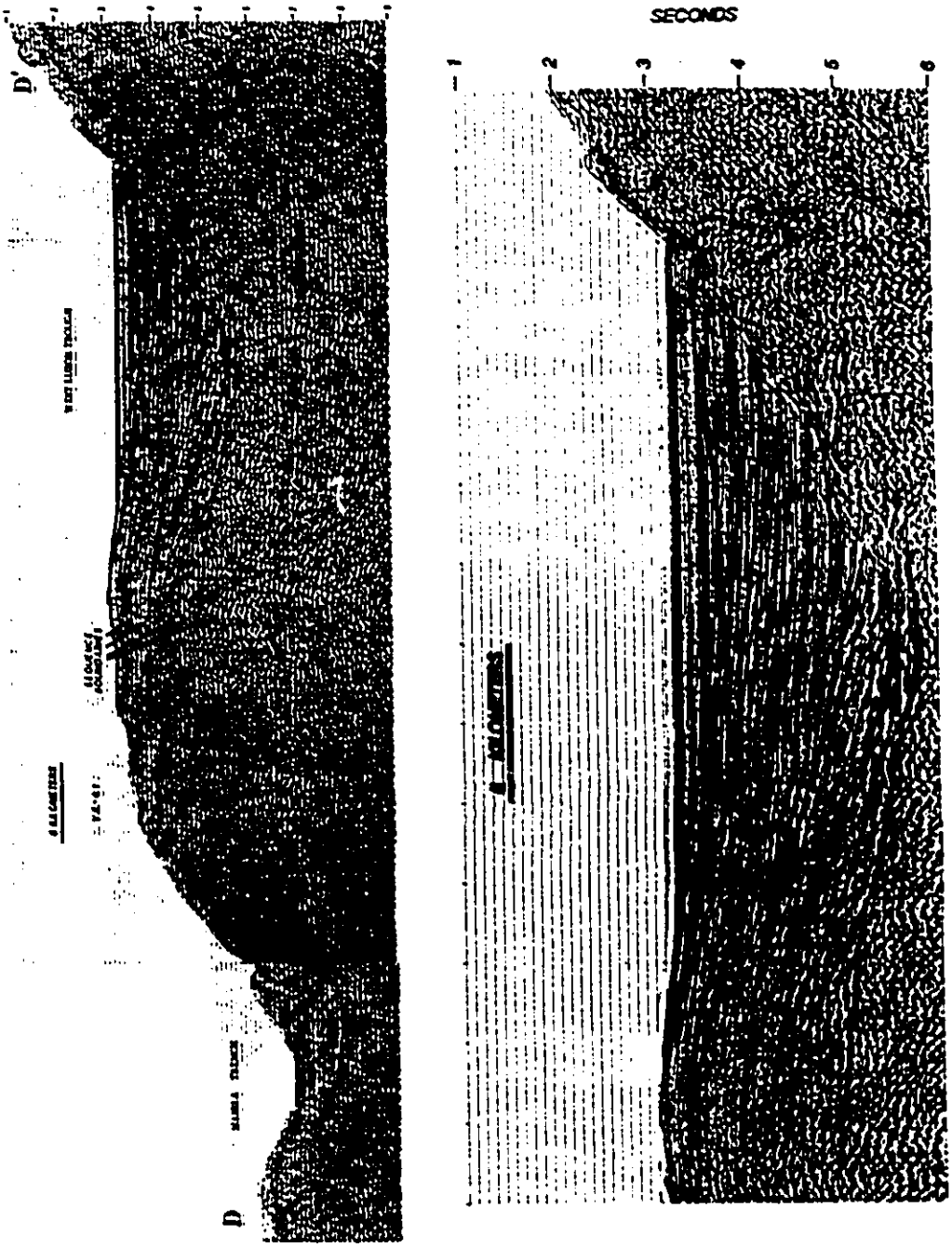
D'
D
SECONDS
1
2
3
4
5
6

Fig. 6.11 Isopaches of seismic sequences from the Cenozoic West Luzon Basin, Philippines (from Lewis and Hayes, 1984). Note the progressive eastward migration of the isopach thick (depocenter) towards the magmatic arc.

BASEMENT-BASE UNIT 6 SEDIMENT ISOPACH

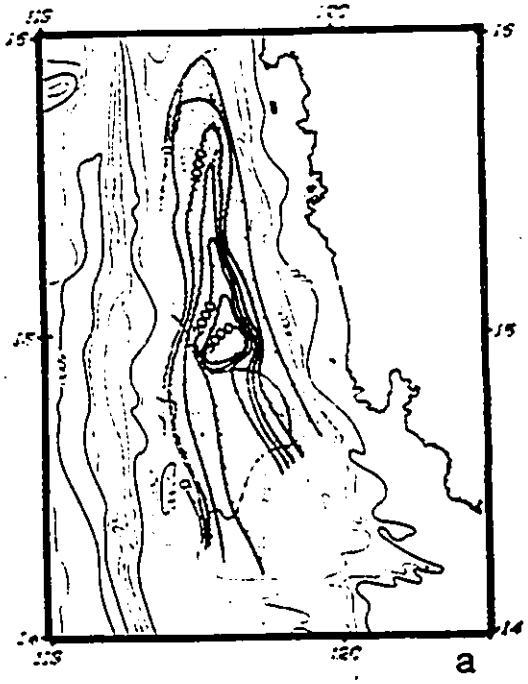

BASEMENT-BASE UNIT 2 SEDIMENT ISOPACH

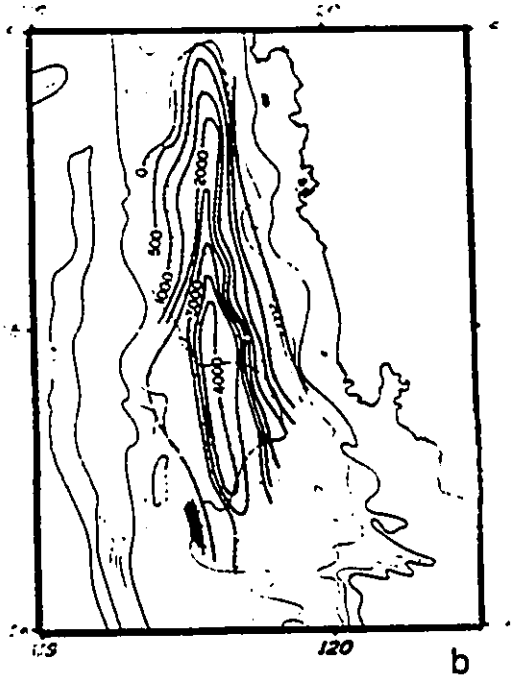

TOTAL SEDIMENT ISOPACH

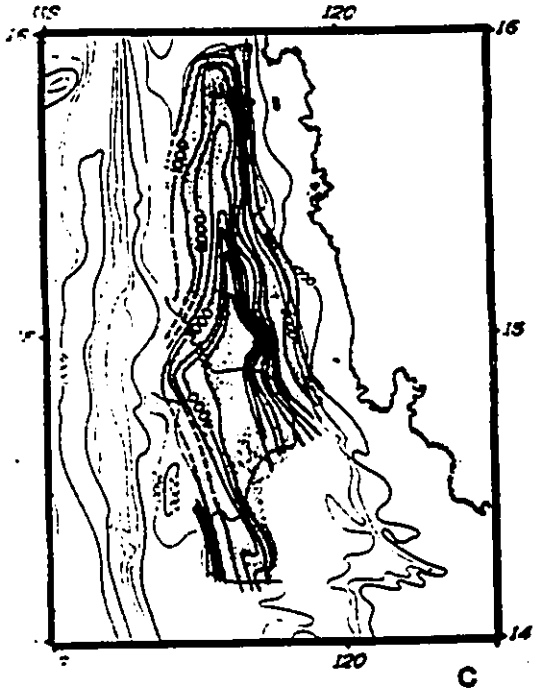

Fig. 6.12 Isopachs of seismic sequences within the Late Miocene to Recent Atka Basin, Alaska (from Ryan and Scholl, 1989). Note the progressive northwestward migration of younger isopach thicks (A - oldest, C - youngest) obliquely towards the magmatic arc to the north.

Fig. 6.13 Isopachs of seismic sequences from the Cenozoic Lima Basin of Peru (from Ballesteros et al., 1988). Note the eastward migration of progresssively younger isopach thicks towards the arc (L3 - oldest, L9 - youngest).

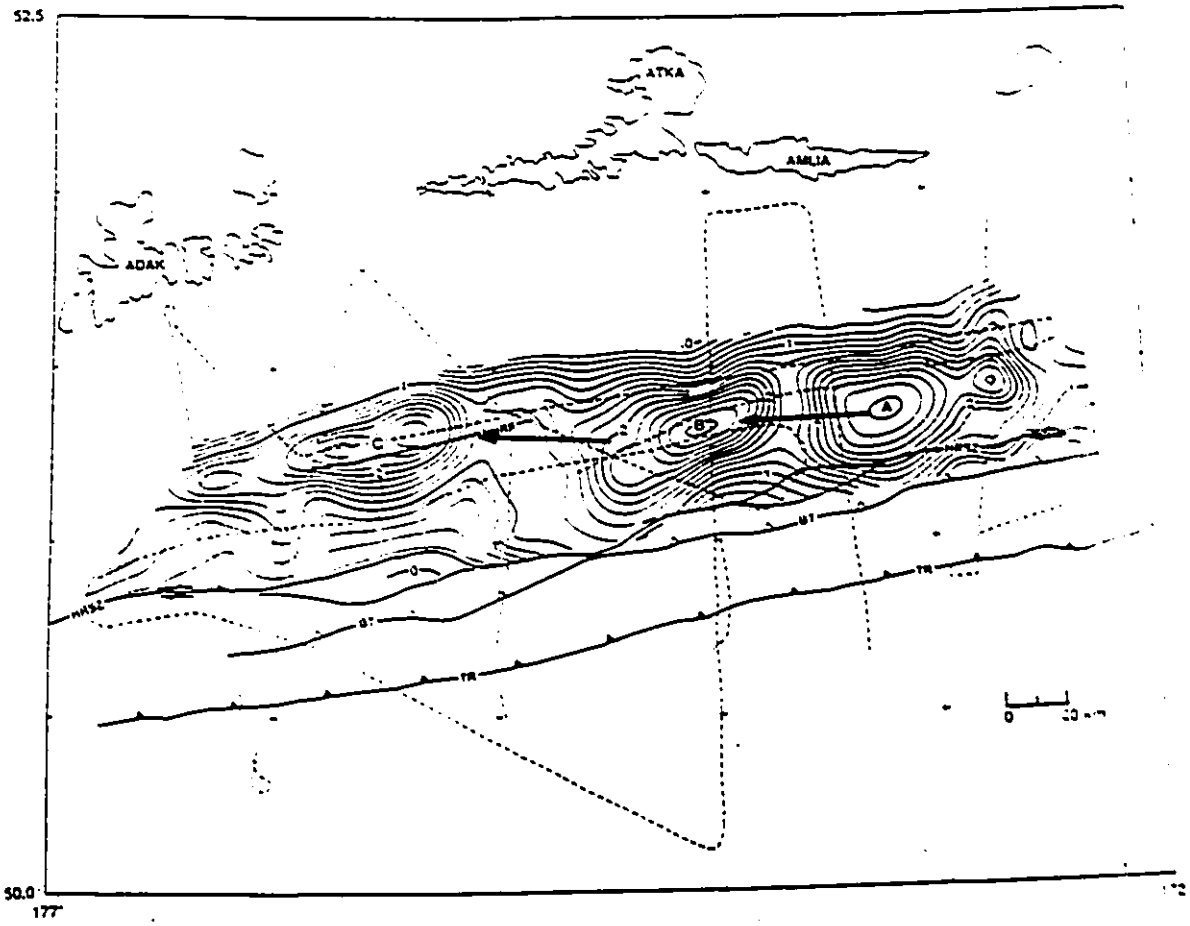
52.5
50.0
177°
ATKA
AMLIA
ADAK
0
0
10 km

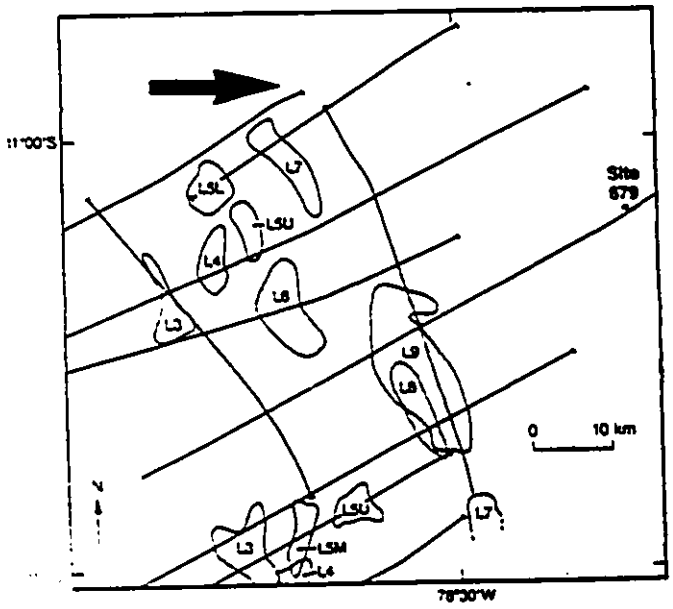
11°00'S
78°30'W
Site
679
L7
L5L
L5U
L4
L6
L3
L9
L8
0
10 km
N
L5U
L7
L3
L5M
L4

interpreted as interbedded turbidite and hemipelagic/pelagic deposits. Assuming the sequences to have been deposited along a paleohorizontal surface, the authors restored the tilted sequences to horizontal, determining that the outer structural high of the accretionary wedge has been uplifted a minimum of 1800 m. The degree of tilt is observed to increase steadily down-section, suggesting that uplift of the accretionary prism occurred continuously during forearc basin deposition. Isopachs of the sequences reveal that the depocenter migrated approximately 10-15 km landwards during the Cenozoic (Fig. 6.11). Seismic sections reveal approximately 21 km of onlap onto the arc massif over a maximum period of approximately 30 Ma, yielding an average onlap rate of 0.7 km/Ma. In addition to the onlapping sequences, two regressive offlapping sequences are observed (#'s 2 and 10, Fig. 6.14) which the authors attributed to progradation in response to the Late Miocene (6.8 Ma) and Late Pliocene to Early Pleistocene (2.9 Ma) eustatic lowstands of Vail et al. (1977).

Several seismic sequences are observed within the 2.5 km of fill within the Aleutian forearc (Ryan and Scholl, 1989; Fig. 6.15). Cores retrieved by the Deep Sea Drilling Project (DSDP sites 186 and 187) indicate that the sequences are of Late Miocene - Early Pliocene age. Isopaches of the sequences reveal that the depocenter migrated approximately

Fig. 6.14 Seismic sequences from the Cenozoic West Luzon Basin, Philippines (Fig. 6.10) expanded and restored to their original orientation. Note the progressive onlap of the sequences onto the arc massif to the east.

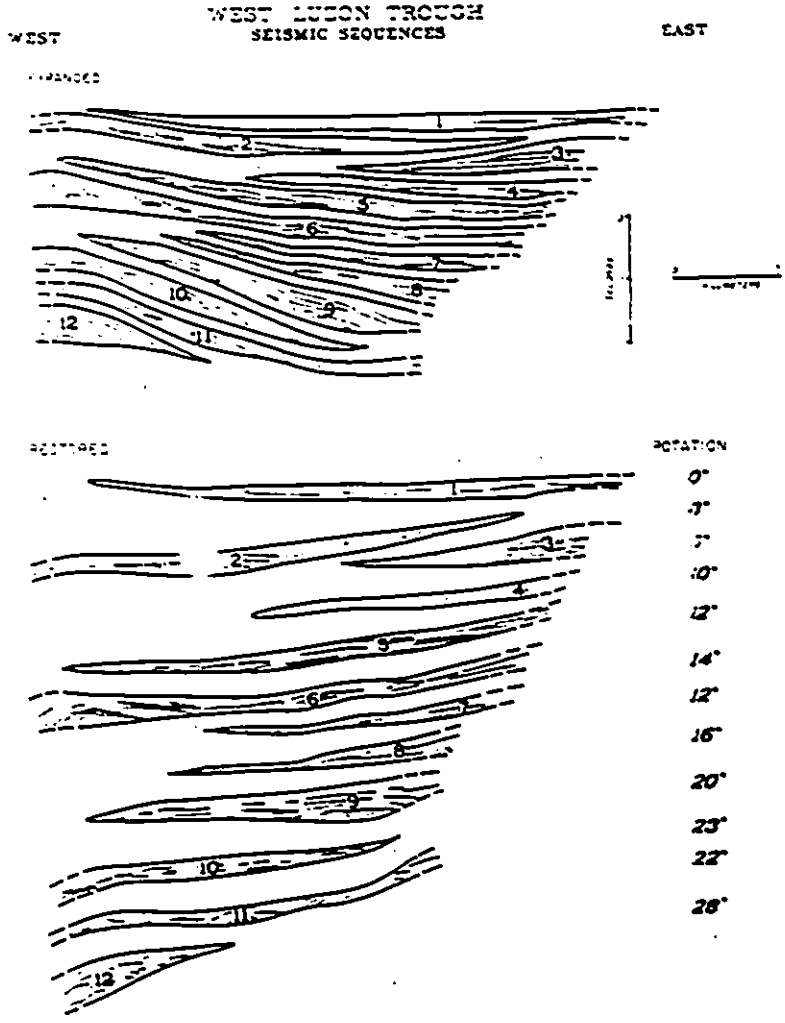
WEST LUZON TROUGH
SEISMIC SEQUENCES
WEST
EAST
ROTATION
0°
3°
7°
10°
12°
14°
12°
16°
20°
23°
22°
28°

Fig. 6.15 Seismic profile of the central Aleutian forearc, Alaska (from Ryan and Scholl, 1989). Forearc basin strata of the upper series (US; Late Miocene to Recent) progressively onlap the flank of the arc towards to north.

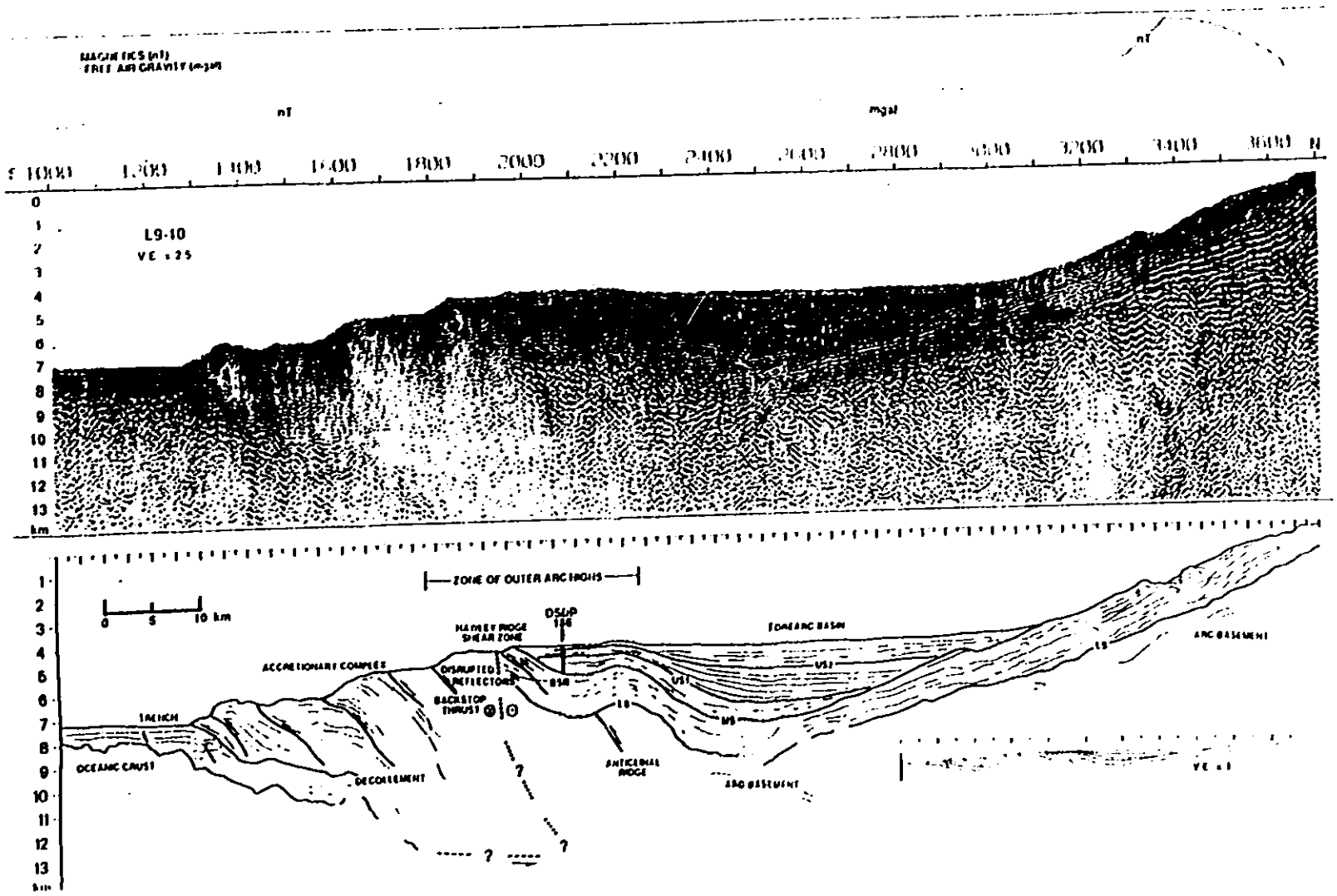
nT
mgal
L9-10
VE = 2:1
km
ZONE OF OUTER ARC HIGHS
0 5 10 km
DSDP 196
HAWKEY RIDGE SHEAR ZONE
FOREARC BASIN
ACCRETIONARY COMPLEX
DISRUPTED REFLECTORS
BACKSTOP THRUST
BSR
VS1
VS2
VS3
TRENCH
OCEANIC CRUST
DECOLLEMENT
ANTECEDENT RIDGE
ARC BASEMENT
VE = 1:1

20 km towards the arc during this period (Fig. 6.12). The sequences progressively onlapped the underlying slope deposits and the flank of the Aleutian arc to the north throughout this period. Seismic sections reveal up to 17 km of arcward onlap over a period of approximately 5 Ma, yielding an average onlap rate of 3.5 km/Ma.

A number of seismic sequences are also observed within the Iquique and Arica forearc basins of northern Chile and southern Peru (Coulbourne and Moberly, 1977; Fig. 6.16). These basins contain up to 3 km of Cenozoic fill. Drilling results from forearc basins located immediately to the north of the Iquique basin in Peru indicate that the basal strata are probably Eocene in age (Shipboard Scientific Party, ODP Leg 112, 1990). The sequences within both the Iquique and Arica basins progressively onlap the arc massif to the east throughout Eocene to Quaternary time. Seismic sections from the Iquique basin document 19 km of onlap over a period of approximately 50 Ma, yielding an average onlap rate of 0.4 km/Ma. The average rate of onlap within the Arica basin is 0.6 km/Ma. Progressive onlap of the arc is also observed on seismic sections from the Sunda forearc basin of Indonesia (Hamilton, 1988).

Deep and shallow marine strata within the Cretaceous to Early Tertiary fill of the Great Valley Basin in California are also observed to progressively onlap the

Fig. 6.16 Seismic profiles across the Cenozoic Iquique (upper) and Lima forearc basins (lower) of Peru (from Coulbourne and Moberly, 1977). Under each profile is a figure showing the expanded and restored sequences progressively onlapping the arc massif to the east.

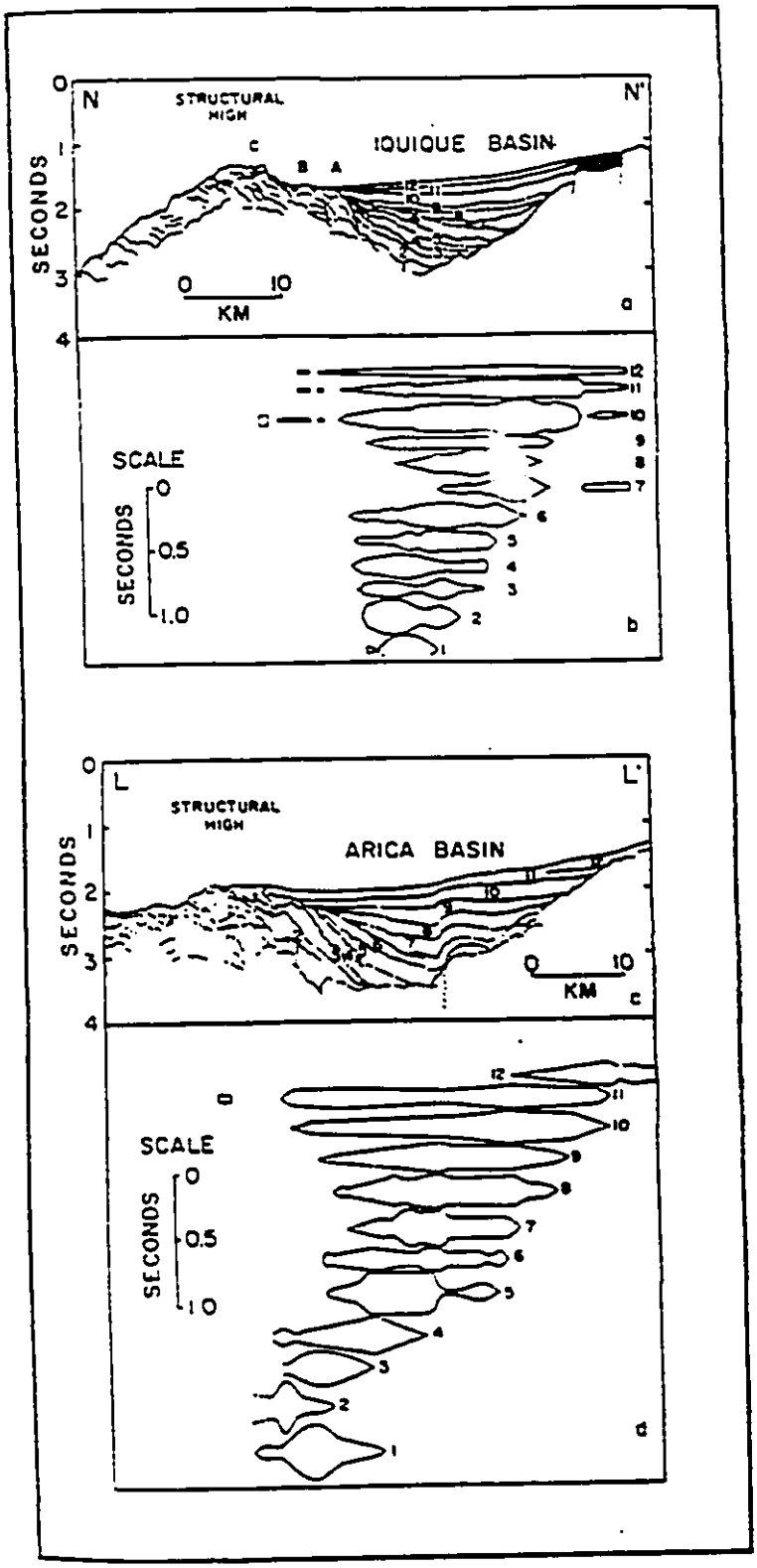
N
STRUCTURAL HIGH
N'
IQUIQUE BASIN
SECONDS
0
1
2
3
4
0 10
KM
a
SCALE
0
0.5
1.0
SECONDS
b
L
STRUCTURAL HIGH
L'
ARICA BASIN
SECONDS
0 10
KM
c
SCALE
0
0.5
1.0
SECONDS
d

margin of the Sierra Nevada arc to the east (Ingersoll, 1979; Dickinson and Seely, 1979). The average rate of onlap during Early to Late Cretaceous (125 - 75 Ma) time as deduced from Moxom and Graham (1987; their Fig. 4) is 1.2 km/Ma. A similar trend is observed within Late Cretaceous fill of the southern Alaska forearc basin (Deeter et al., 1983).

The arcward migration of the depocenter observed on the seismic sections from modern forearc basins was attributed to long term (10 Ma) uplift of the outer structural high (Luzon: Lewis and Hayes, 1984; Alaska: Ryan and Scholl, 1989; Peru-Chile: Coulbourne and Moberly, 1977; Moberly et al., 1982). This process resulted in progressive arcward tilting of the basin floor and the displacement of the basin axis (depocenter) away from the uplifted seaward margin. This mechanism however is unsatisfactory for explaining the progressive arcward onlap of strata onto the flank of the arc massif. While tilting can certainly result in the arcward migration of the depositional axis of the basin, it cannot possibly account for the progressive onlap of the arc itself. In order for strata to onlap, the margin of the arc must be subsiding. Nor can tilting of the basin floor affect the subsidence history of the magmatic arc. Some other mechanism controlling the subsidence history of both the basin and arc massif itself must be

responsible.

The progressive northeastward onlap of the sequences within the QCB tracked the general eastward migration of the locus of active magmatism documented within the Coast Plutonic Complex throughout Late Jurassic and Cretaceous time by Armstrong (1988) and van der Hayden (1992). The rate of eastward migration of magmatism within the CPC during Valanginian to Cenomanian time can be deduced from van der Hayden (1992; Fig. 6.17). The distance between the midpoints of the Early (136 - 120 Ma) and mid Cretaceous (110 - 94 Ma) plutonic belts exposed in the McCauley Island region is approximately 45 km, yielding an average migration rate of 1.1 km/Ma. This corresponds very closely to the 0.8 km/Ma rate of onlap within the QCB during this period.

The northeastward onlap and transgression of Late Jurassic to Late Cretaceous (Early Turonian) strata within the QCB may have been controlled by subsidence related to magmatic loading and subsequent thermal decay of the abandoned portions of the arc as the locus of active magmatism migrated eastwards (Fig. 6.18). The cessation of magmatic activity would initiate the decay of the thermal anomaly, resulting in thermal subsidence of the inactive portion of the arc massif. This would manifest itself in the form of extensionally and/or flexurally induced subsidence (McKenzie, 1978). Construction of volcanic

Fig. 6.17 Distribution of magmatic ages within the Coast Plutonic Complex located immediately east of the Queen Charlotte Islands in the McCauley Island region (from van der Hayden, 1992). Note the general eastward decrease in cooling ages.

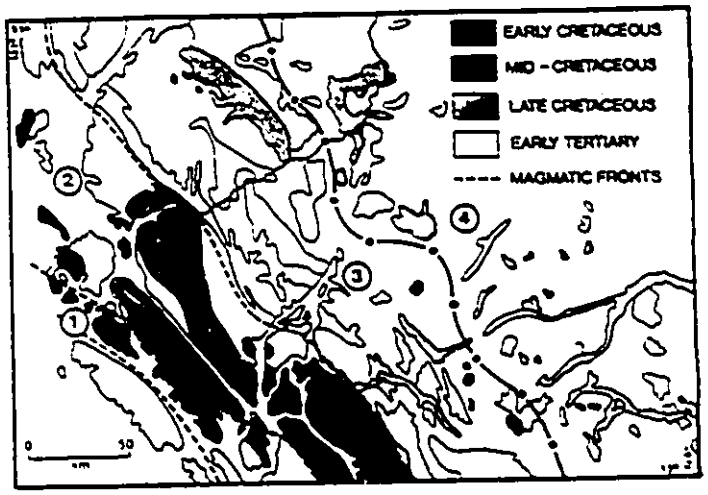
EARLY CRETACEOUS
MID - CRETACEOUS
LATE CRETACEOUS
EARLY TERTIARY
MAGMATIC FRONTS
1
2
3
4
0
30
km

Fig. 6.18 Model illustrating how the eastward onlap of marine strata onto the arc massif may have been driven by thermal subsidence as the locus of active magmatism migrated eastward within the Coast Plutonic Complex.

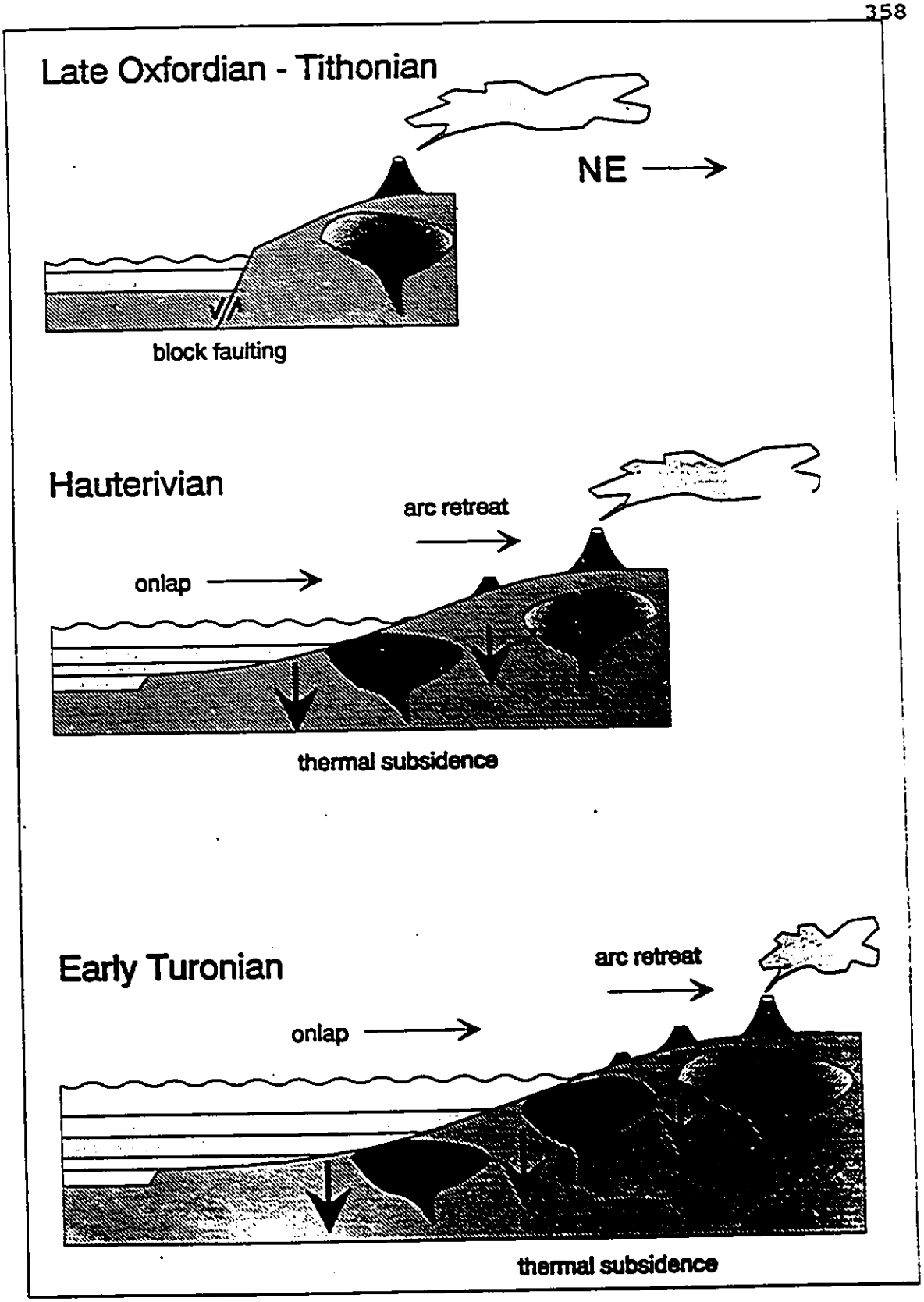
Late Oxfordian - Tithonian
NE
block faulting
Hauterivian
arc retreat
onlap
thermal subsidence
Early Turonian
arc retreat
onlap
thermal subsidence

edifices upon the arc massif would also result in flexure of the adjacent basement of the basin, a situation similar to that of the Hawaiian-Emperor seamount chain (Watts and Cochran, 1974), where seamounts are encircled by a deep moat.

It is unknown if magmatism within both the Philippine and Aleutian arcs migrated away from the basin over time. Magmatism within the central Andean arc however has been documented to have retreated landwards (eastwards) away from the forearc region throughout Late Cretaceous (Albian) to Tertiary (Neogene) time (Mukasa, 1986; Megard, 1989). It is quite probable that the progressive arcward onlap of strata within both the Andean, as well as the Philippine and Aleutian forearc basins, is controlled by subsidence related to the landward migration of the magmatic arc. Retreat of the modern and ancient magmatic arcs away from the forearc is common at rates of up to 1 km/Ma (Dickinson, 1973). This rate falls well within the range at which strata onlap the arc massifs of the basins described above.

Dickinson et al. (1987) and Moxom and Graham (1987) analyzed the subsidence history of the Great Valley sequence by backstripping outcrop and subsurface sections. Moxom and Graham's (1987) plots reveal a distinct change in subsidence histories across the magnetic anomaly located at the basement boundary separating oceanic crust to the west from

crust of the arc massif to the east (Fig. 6.19). The plots of residual tectonic subsidence for sections located in the western portion of the basin exhibit rapid subsidence during Late Mesozoic time (100-80 Ma) followed by uplift coinciding with the onset of Laramide deformation (80 Ma). This is followed by an irregular period of uplift and subsidence from 80-50 Ma, which in turn is followed by uniform subsidence. The subsidence history of sections located in the eastern portion of the basin exhibit an exponential decay which closely resembles the one-dimensional thermal subsidence curves generated by McKenzie (1978) for stretching values of 1.5-2.

This suggests that subsidence of the Great Valley forearc basin was controlled by two distinct mechanisms: 1) decay of the thermal anomaly of the arc massif driving subsidence along the eastern margin of the basin, and 2) in the western portion of the basin, an initial period (100-80 Ma) of rapid subsidence related to tectonic erosion of the California margin followed by compression and uplift of the outer structural high (80-50 Ma), presumably related to a period of accretion and underplating which coincided with the onset of Laramide deformation. Moxom and Graham (1987) suggested that thermally induced flexural subsidence controlled the progressive long term onlap of marine strata onto the eastern margin of the basin as the locus of active

Fig. 6.19 Tectonic subsidence curves from the eastern margin of the Great Valley Basin and a map of Californian showing how the approximate eastern limit of deposition tracked the eastward migration of magmatism within the Sierran arc throughout Cretaceous time (125 - 75 Ma; from Moxom and Graham, 1987). Note that the subsidence curves (heavy lines) derived from sections located along the eastern margin of the basin closely match thermal subsidence curves (light lines) for stretching values of 1.5 to 2.

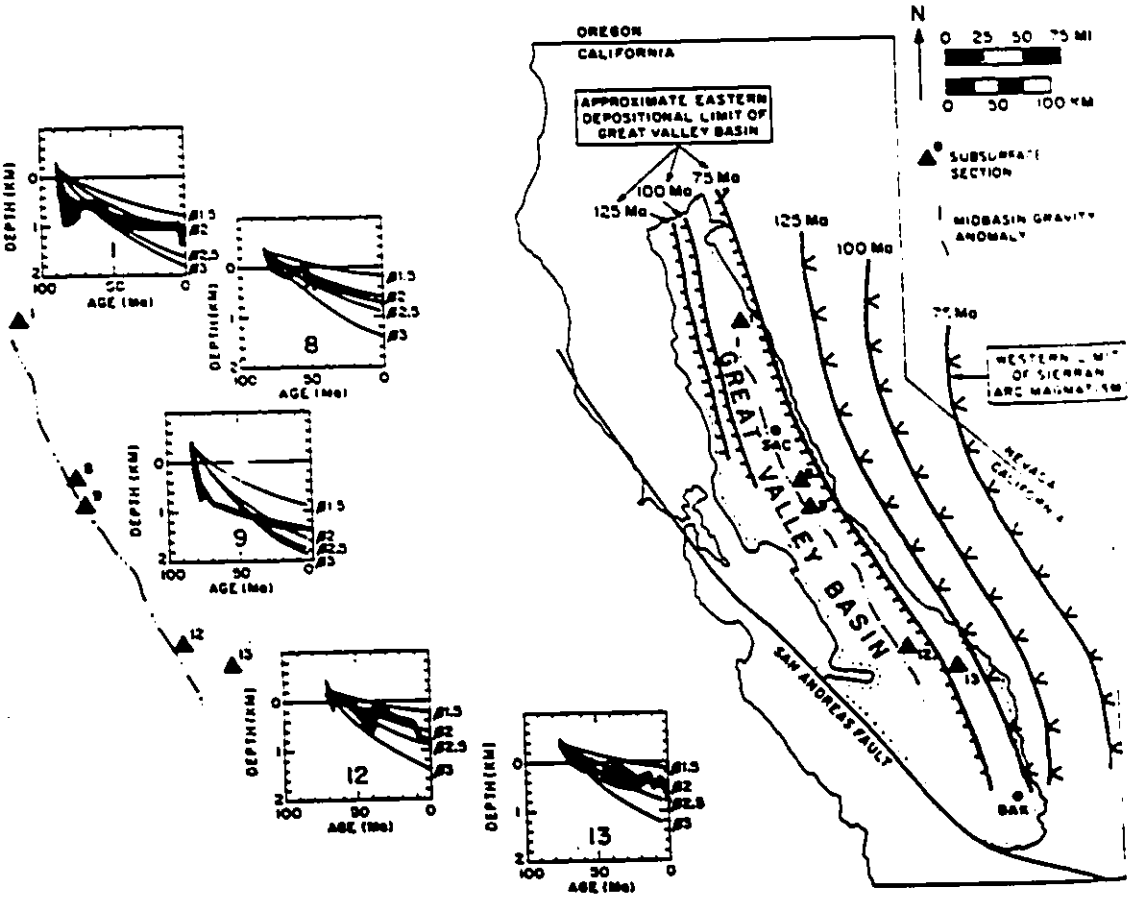
OREGON
CALIFORNIA
APPROXIMATE EASTERN DEPOSITIONAL LIMIT OF GREAT VALLEY BASIN
75 Ma
100 Ma
125 Ma
GREAT VALLEY BASIN
SAN ANDREAS FAULT
SAC
BAR
N
0 25 50 75 MI
0 50 100 KM
SUBSURFACE SECTION
MIDBASIN GRAVITY ANOMALY
DEPTH (KM)
AGE (Ma)

magmatism within the Sierra Nevada Ranges migrated landward during this period (Fig. 6.19). The average rate at which the active locus of magmatism migrated during Early to Late Cretaceous (125 - 75 Ma) time within the Sierra Nevada arc was 2.3 km/Ma. This rate compares rather favourably with the 1.2 km/Ma rate at which shallow marine strata onlapped the arc. Backstripping of Jurassic sections from the Cook Inlet forearc basin of southern Alaska (Caroll, 1987) also reveals a subsidence history governed by cooling of the batholiths within the Alaska - Aleutian arc to the north.

The progressive northeastward onlap of Late Jurassic to Late Cretaceous (Early Turonian) shallow marine strata onto the arc within the QCB is therefore typical of forearc basins. The rate of onlap within the QCB through Valanginian to Albian time is 0.8 km/Ma, which is fairly comparable to the 1.1 km/Ma rate at which the locus of active magmatism within the CPC retreated landwards. The rates of onlap are also comparable to the onlap rates observed within the modern and ancient forearc basins discussed above. This onlap appears to track the landward migration of the magmatic arc within both modern and ancient forearc basins. As tilting of the basin floor can in no way affect the subsidence history of the arc, this trend may best be attributed to a thermal mechanism associated with arc retreat.

The locus of active magmatism within the CPC could have migrated in response to a progressive decrease in the angle of subduction of Pacific oceanic lithosphere, progressive depletion of the overlying mantle wedge, subcrustal erosion by the subducting oceanic plate, intra-arc shortening, or to a combination of these processes (van der Hayden, 1992).

6.6.2. Comparison of controls influencing basin and arc

Deposition of the Late Jurassic to Late Cretaceous (Early Turonian) deposits of the White Point, Longarm, Haida, and Skidegate Formations was influenced by local block faulting. Evidence of this faulting comes not only from the recognition of reactivated Late Jurassic high angle faults within the QCI region (Thompson and Thorkelson 1989; Lewis et al., 1991: Thompson et al., 1991), but also from the sedimentology of the formations themselves (eg. the unusual thickness of the progradational shoreface successions, the inference of coastal cliffs at Arichika Island). Deposition of the Late Cretaceous (Late Turonian to Coniacian) Honna Formation was most likely a response to crustal thickening along the northeastern margin of the basin.

Van der Hayden (1992) suggested that during Late Jurassic to Early Cretaceous time the CPC underwent

extension, resulting in the opening of a narrow basin to the east of the arc (Fig. 6.9). Strata of the Late Jurassic to Early Cretaceous Gravina - Tyaughton assemblage were deposited within this basin. As no oceanic lithosphere has been recognized at the base of the assemblage, the basin does not represent a true back arc basin, but rather a narrow extensional rift basin. As summarized by van der Hayden (1992), evidence of this extensional event is supported by chemical data from the Gravina Basin (Ford and Brew, 1988) and from structural and stratigraphic observations in the southern part of the Coast Belt (Monger, 1991). Van der Hayden (1992) suggested that the extension was related to the rapid northward movement of the North American plate during this period, as documented by May and Butler (1986). This likely decreased the rate and increased the obliquity with which Pacific Oceanic lithosphere was subducted beneath North America. The destruction of this basin during mid to Late Cretaceous time coincided with crustal contraction to both the east and west of the arc, reflecting a change to a compressional stress regime (Fig. 6.9). Van der Hayden (1991) suggested that this change reflected an increase in the convergence rate related to rapid westward movement of the North American plate relative to the Pacific plate, as documented by Engebretson et al. (1985).

During Late Jurassic to Early Cretaceous time therefore the CPC was subjected to extension. It is therefore possible that the localized high angle block faulting documented by Thompson and Thorkelson (1989) and Thompson et al. (1991) within the QCI area during this period may also have been extensional in nature. This suggests that thermal subsidence and collapse of the magmatic arc may have been accommodated by extensional block faulting within the QCI region. In mid to Late Cretaceous time the CPC experienced compression which resulted in west-vergent thrust faulting and crustal thickening along the northeastern margin of the QCB. The resulting uplift of the thrust belt and subsidence of the basin led directly to deposition of the coarse clastics of the Honna Formation.

As outlined by Dewey (1980), the stress regime of any arc - trench system is controlled by the rate at which the hinge of the subducting plate rolls back from the subduction zone and the rate at which the overriding plate advances towards the subduction zone. Dewey (1980) identified three main types of arc - trench system: extensional (Marianas-type), neutral, and compressions (Peruvian-type). Where the overriding plate retreats from the subduction zone, or where it advances more slowly than roll back, the arc is extensional. These arcs are typically situated within intra-oceanic settings. Where the overriding plate advances

faster than roll back, then the arc is compressional. These arcs are typically situated within continental settings. Where the rate of advance of the overriding plate equals the rate of roll back, then the arc is neutral.

It would appear therefore that the Late Mesozoic structural history of the CPC as outlined by van der Hayden (1992) and that of the QCB as inferred from the depositional history of the succession exposed on the QCI conform rather well. Furthermore, the expansion of the QCB during Late Jurassic to Late Cretaceous (Early Turonian) time tracks the progressive eastward migration of magmatism within the CPC, lending further support to van der Hayden's (1992) model.

6.8. LATE MESOZOIC EVOLUTION OF THE QUEEN CHARLOTTE BASIN

It appears therefore that the QCB occupied a forearc setting located on the accreted western margin of North America throughout most of Late Mesozoic time. The basin was located between an Andean type magmatic arc to the east (CPC) and a subduction zone to the west. Like most other forearc basins, the QCB was elongate parallel to the arc - trench system, which was oriented northwest - southeast. The QCB represents but one of a series of forearc basins located along the subductive western margin of North America throughout the Late Mesozoic (Dickinson, 1976; Nilsen, 1986;

Fig. 6.20). The basin overlies Late Paleozoic to Early Jurassic strata of the Wrangel terrane, which consists primarily of volcanics and lesser sedimentary rocks. The thickness of the crust underlying the QCB, as determined seismically, is approximately 25 km (Sweeny and Seemann, 1991). This crust is of neither true continental nor oceanic affinity, but rather may be regarded as transitional continental crust.

The gravelly fan delta successions within the White Point Formation were deposited in a small fault-bounded basin located along the western edge of the QCI (Fig. 6.21). The gravelly fan deltas prograded westward into the basin away from a faulted highland to the east (Fig. 3.13). Sediment was supplied directly to the subaqueous deltas by alluvial fans, indicating that the basin had a very narrow coastal plain. The basin is underlain by Late Jurassic volcanics of the arc massif which extended to the east and southeast. The massif consists of andesitic volcanics of the Moresby Group and Late Jurassic plutonics of the San Christoval and Burnaby Island suites. Anderson and Reichenbach (1991) determined that these suites were emplaced between Bathonian and Middle Oxfordian time (172 - 158 Ma). The associated volcanics of the Moresby Group are probably comagmatic. Deposition of the White Point Formation therefore appears to have occurred during a lull

Fig. 6.20 Map showing the distribution of Mesozoic and Early Cenozoic forearc basin successions along the west coast of North America (from Nilsen, 1986).

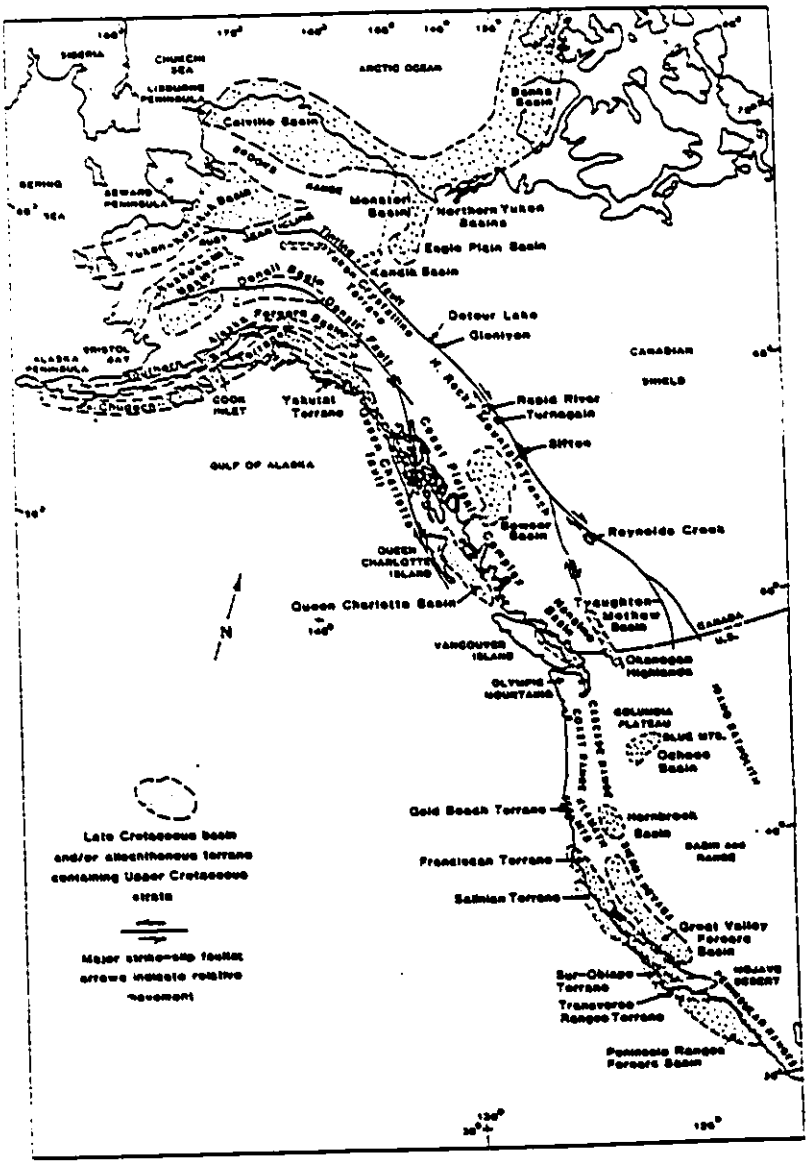
Colville Basin
Beaufort Basin
Mackenzie Basin
Northern Yukon Basins
Eagle Plain Basin
Tintina Trench
Kandik Basin
Denali Fault
Dextral Fault
Detour Lake
Glenlyon
Rapid River Turnagain
Sitlin
Yakutat Terrane
Queen Charlotte Fault
Queen Charlotte Basin
Sanak Basin
Reynolds Creek
Tofino Basin
Tyaughton-Methow Basin
Okanagan Highlands
Olympic Mountains
Columbia Plateau
Blue Mtns.
Ochoco Basin
Gold Beach Terrane
Hornbrook Basin
Franciscan Terrane
Salmon Terrane
Great Valley Forearc Basin
Sur-Obispo Terrane
Transverse Ranges Terrane
Peninsula Ranges Forearc Basin
Late Cretaceous basin and/or allochthonous terrane containing Upper Cretaceous strata
Major strike-slip faults; arrows indicate relative movement

Fig. 6.21 Schematic diagram illustrating the tectonic evolution of the preserved part of the Late Mesozoic Queen Charlotte Basin and related features in the Coast Plutonic Complex. Tectonic conditions to the west of the preserved part of the basin are unknown (Late Oxfordian to Early Turonian) or inferred (Late Turonian to Coniacian), as this part of the basin has been truncated by Tertiary dextral displacement across the Queen Charlotte Fault. Each diagram indicates the conditions within the basin at the end of the period indicated. No vertical or horizontal scale implied.

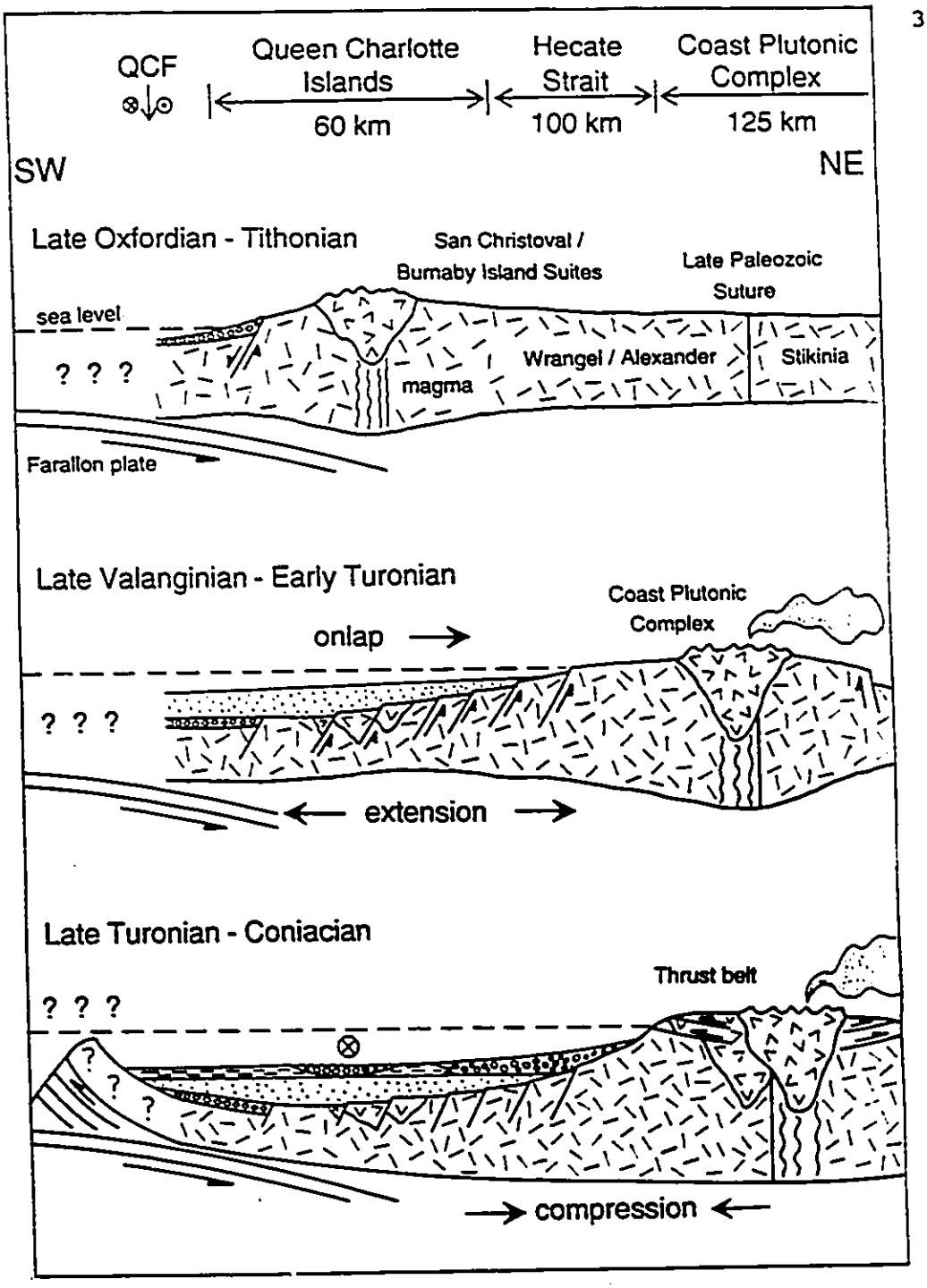
QCF
Queen Charlotte Islands
60 km
Hecate Strait
100 km
Coast Plutonic Complex
125 km
SW
NE
Late Oxfordian - Tithonian
San Christoval / Burnaby Island Suites
Late Paleozoic Suture
sea level
? ? ?
magma
Wrangel / Alexander
Stikinia
Farallon plate
Late Valanginian - Early Turonian
onlap
Coast Plutonic Complex
? ? ?
extension
Late Turonian - Coniacian
Thrust belt
? ? ?
? ? ?
compression

between Late Jurassic and Early Cretaceous arc magmatism. This basin corresponds to the intra-massif forearc basin classification of Dickinson and Seely (1979), as it is underlain by strata of the arc massif. The unpreserved western margin of the basin could have been an uplifted fault block of the arc massif, or the edge of an uplifted accretionary complex. The marine nature of the basin fill indicates that it was in communication with the Pacific Ocean.

Early to Late Cretaceous (Late Valanginian to Early Turonian) strata of the Longarm, Haida, and Skidegate Formations were deposited within a much enlarged forearc basin which encompassed most of the QCI region (Fig. 6.20). The axis of this basin was oriented approximately northwest - southeast, parallel to the trend of the magmatic arc. The basin extended at least 250 km along strike from Langara Island in the northwest to Carpenter Bay in the southeast. The minimum width of the preserved part of the basin is approximately 40 km, though it likely extended well into the Hecate Strait region in Early Turonian time. By Early Cretaceous (Valanginian) time, the magmatic arc had migrated from the QCI region to the McCauley Island region approximately 150 km to the northeast. From Valanginian to Campanian time, the locus of active magmatism within the arc continued to migrate further to the east.

This basin again corresponds to the intra-massif forearc basin classification of Dickinson and Seely (1979), as the preserved component is situated entirely upon basement of the arc massif. In the immediate QCI region, the massif consisted primarily of Middle Jurassic volcanics of the Yakoun Group and Late Jurassic plutonics of the San Christoval and Burnaby Island suites, both overlying and intruded into Wrangellian basement. Towards the northeast, the massif also included Early to Late Cretaceous plutonics and coeval extrusives. As suggested by Haggart (1993), it is possible that the basin was confined to the southwest by the uplifted margin of an accretionary complex. If this were indeed the case, it would be classified as a constructed forearc basin. Alternatively, the basin may have been confined to the southwest by an uplifted block of the arc massif.

Throughout this period, eight distinct shallow to deep marine sequences, each related to a single cycle of sea level fall and rise, were deposited within the basin. High energy shallow shelf to muddy offshore strata within each sequence were deposited along the northeastern margin of the basin (Fig. 4.41) during periods of sea level rise. Slope and submarine fan deposits were emplaced to the southwest during periods of sea level fall. Paleocurrent data indicate that the shorelines throughout this period were

generally oriented southeast - northwest. The position of the shorelines was likely controlled by reactivated Late Jurassic block faults. Sediment was probably supplied to the shelf by deltas along the northeast margin of the basin. The position of the deltas may have been influenced by basement faults. The deltas themselves were probably supplied by fluvial systems emanating from the active and partly dissected magmatic arc.

Shallow marine strata within each of the sequences progressively onlapped the eroded flanks of the arc massif. This onlap tracked the eastward migration of magmatism within the CPC. Deposition of each of the sequences may have been controlled partly by local (extensional ?) block faulting related to thermal subsidence of the arc massif, and partly by eustatic sea level fluctuations.

The Honna was deposited within a variety of deep marine turbiditic environments. The onset of Honna deposition accompanied an abrupt rise in relative sea level, which was most likely related to crustal loading by a northwest - southeast trending thrust belt situated along the northeastern margin of the basin (Fig. 6.21). The Honna consists primarily of gravelly submarine fan and channel conglomerates emplaced within deep marine environments. Petrographic and paleocurrent data indicate that it was sourced from the east. Two distinct gravelly submarine

systems are recognized; transverse submarine fans oriented orthogonally with respect to the basin margin, and a northwest - southeast oriented channel complex oriented parallel to the basin margin (Fig. 5.48). The fans were likely fed by canyons which bypassed the narrow wave dominated shelf. The channel complex was at least 20 km in width and 200 km long.

The general geometry of the Late Valanginian to Early Turonian basin was therefore maintained during Late Turonian and Coniacian time. As the preserved component of the basin rests entirely upon basement of the arc massif, it is still classified as an intra-massif forearc basin. The axial nature of the channel complex reflects the fact that the basin was confined to the northeast by the thrust front and to the southwest by some other structural element, wither the uplifted edge of the accretionary wedge or an uplifted block of the arc massif.

In Early Santonian time, the QCB was the site of a renewed episode of subaerial volcanism. Throughout the remainder of Santonian to Maastrichtian time, the QCB was the site of muddy offshore deposition. The poorly exposed nature of Santonian to Maastrichtian strata does not permit paleogeographic reconstruction of the QCB during this interval. As arc magmatism persisted well into Campanian time (70 Ma), the earlier geometry and extent of the QCB was

probably maintained.

6.9. COMPARISON TO OTHER FOREARC BASINS

While several aspects of the Late Mesozoic succession within the QCB are fairly typical of forearc basins, several aspects appear to be unique. These include the lack of an accretionary wedge, the abundance of shallow marine deposits within the Late Jurassic to Early Turonian succession, the overall transgressive nature of the Late Mesozoic succession, and the lack of volcanogenic deposits.

6.9.1. Where's the western margin of the Queen Charlotte Basin ?

Most arc-trench systems are composed of four distinct morphologic elements: a deep trench located at the site of subduction, an accretionary wedge consisting of sediments and other materials scraped off the descending plate and accreted snowplow fashion to the leading edge of the overriding plate, a volcanic or magmatic arc located approximately 100-150 km above the descending slab on the overriding plate, and an intervening forearc region. The largest and most typical forearc basins, corresponding to the constructed type of Dickinson and Seely (1979), are flanked seaward by an elevated ridge of the accretionary

prism or uplifted basement of the arc massif, commonly referred to as an outer structural high (Hayes and Lewis, 1984; Ryan and Scholl, 1989). The high forms a dam behind which sediments within the forearc basin accumulate.

Ancient onland exposures of accretionary prisms (eg. Franciscan Complex, California) consist of heavily tectonized high-pressure metamorphosed sequences of bedded and chaotic sedimentary and oceanic igneous rocks. Seismic profiles of modern prisms reveal a complex internal structure featuring prominent acoustic discontinuities attributed to low angle thrust faults dipping gently (7 to 9°) towards the arc massif (Seely, 1978). These thrusts merge at a basal decollement, the main detachment surface between the descending and overriding plates. Gravity surveys reveal that modern prisms are composed primarily of low density sedimentary rocks.

Strata belonging to a coeval accretionary wedge have not been identified from the QCI region. Seismic profiles show that basement rocks of the Wrangel terrane continue well west of the Cretaceous outcrop belt, and are truncated abruptly just offshore by the Queen Charlotte Fault. This lineament defines the western margin of the North American plate, and is interpreted as a dextral transform fault (Hyndman and Hamilton, 1991). It is quite possible therefore that the accretionary wedge, which Haggart (1993)

suggested defined the western margin of the QCB, was removed northwards along the Queen Charlotte Fault during the Tertiary. Haggart (1993) suggested that Late Cretaceous deep marine strata of the Yakutat terrane in southern Alaska represent the accretionary wedge associated within the QCB during Late Mesozoic time.

Aside from the axial orientation of the gravelly channel complex within the Honna Formation, there is no solid evidence that the QCB even possessed a western margin during late Mesozoic time, let alone one defined by the uplifted edge of an accretionary prism as suggested by Haggart (1993). Not all forearc basins are confined seawards by the uplifted edge of an accretionary prism. Moberly et al. (1982), Kulm et al. (1982) and the Shipboard Scientific Party, DSDP Leg 112 (1988) described the structure and fill of several forearc basins on the continental margin of Equador, Peru, and Chile. The Sechura, Salaverry, and East Pisco basins form a long network of basins separated from one another by uplifted horsts of continental crust. In the northwestern Peru region, metamorphic and igneous continental rocks are exposed only 80 km east of the trench axis. Subsurface mapping and seismic profiles of these basins reveal complex tensional fault patterns (Moberly et al., 1982; Ballesteros et al., 1988). Shelfal basins of the Mexican margin exhibit

an identical pattern (Moore and Watkins, 1979). The seaward margins of these basins are defined by structural highs, which both Moberly et al. (1982) and Kulm et al. (1982) suggested may be uplifted basement horsts.

The continental nature of the basement underlying many of the forearc basins along the Andean margin, as well as its block faulted nature, is reminiscent of the QCB in British Columbia. It is possible that, like the forearc basins of South America, the QCB was confined seawards by an uplifted horst of the arc massif, and not by an accretionary prism.

6.9.2. Where have all the deep marine deposits gone ?

Most modern forearc basins are deep (Table 6.1) and infilled primarily by turbidites. Intraoceanic basins are the deepest (e.g. Sunda - Banda, Japan, central Aleutian), while continental forearc basins are notably shallower (e.g. South America, Oregon).

The depth of forearc basins is governed primarily by the nature of the underlying crust. Oceanic crust, being thinner and weaker than continental crust, subsides much more rapidly when cooled, stretched, or loaded. It is no surprise therefore that those forearc basins underlain by oceanic crust or accretionary prisms overlying oceanic crust are generally deeper than those underlain by continental

Table 6.1. Evolution of ancient forearc basins

BASIN	TYPE *	AGE	THICKNESS	TREND	REFERENCE
Central Aleutian	Construc-ted	Late Cretaceous	2 000 m	Transgressive	Nilsen (1986) Dorter et al. (1983)
Cook Inlet Basin	Residual	Early Jurassic Pliocene	17 500 m	Regressive	Dickinson and Seely (1979); Magoon and Claypool (1980)
Queen Charlotte Basin	Intra Massif / Construc-ted ?	Late Jurassic Late Cretaceous	5 000 m	Transgressive	This study
Nanaimo Basin (B. C)	Intra massif	Late Cretaceous	2 000 m	None	Ward and Stanley (1982); England and Cowan (1991)
Ochocco Basin (Oregon)	Composite (?)	Late Cretaceous	4 300 m	Transgressive	Kleinhans et al. (1984)
Hornbrook Basin (Oregon)	Composite	Late Cretaceous	1 200 m	Transgressive	Nilsen (1984)
Great Valley Sequence	Composite	Late Jurassic Paleogene	20 000 m	Regressive	Dickinson and Seely (1979); Nilsen (1986)
Rosario Fm Peninsular Ranges (California)	Composite	Late Cretaceous	1 100 m	Transgressive to Regressive	Cunningham and Abbott (1986)
Alexander Island (Antarctica)	Construc-ted	Late Jurassic Late Cretaceous	7 000 m	Regressive	Butterworth (1991)
Mayo Trough (Ireland)	Residual	Early Ordovician	10 000 m	Regressive	Dewey and Ryan (1990)
Shimanto Belt (Kii Peninsula, Japan)	Construc-ted	Late Cretaceous Early Miocene	11 500 m	3 Regressive	Taira et al. (1982)

* After Dickinson and Seely (1979).

crust. The predominance of shallow marine deposits along the arcward margin of many ancient forearc basins can be attributed to the fact that this part of the basin is underlain by continental crust or thickened crust of the arc massif. Coeval deeper marine deposits generally predominate within that part of the basin underlain by oceanic crust.

The structure of the underlying crust is also important in controlling the local bathymetry of the basin. This is best illustrated in Central and South America, where the basement is complexly faulted. The forearc basins themselves are locally disrupted and separated by horsts and grabens, resulting in complicated bathymetries.

The abundance of shallow marine deposits within the Late Jurassic to Early Turonian succession within the QCB may therefore reflect the fact that the preserved portion of the basin is underlain by transitional continental crust.

6.9.3. Stratigraphic evolution of forearc basins

Dickinson and Seely (1979) suggested that most ancient forearc basin successions exhibited a general trend towards shallower bathymetries for successively younger strata. The authors based this remark primarily upon observations from the Great Valley Basin, probably one of the best studied ancient forearc basin successions. The

long term stratigraphic evolution of several ancient forearc basin successions are summarized in Table 6.2. It should be mentioned that the infill of all of these basins contain numerous unconformities, so the overall vertical trend is very general. While many of the basins have grossly regressive infills, several others, including the QCB, have grossly transgressive infills. Others, such as the Peninsular Basin of Baja California, are transgressive to regressive. Still others, such as the Nanaimo Basin of British Columbia, have successions which are consistently deep marine. There also appears to be no correlation between the type of forearc basins and the type of infill (transgressive or regressive). It is interesting to note however that the transgressive successions within the Ochoco, Hornbrook, and QCB overlie continental crust of the arc massif.

Several mechanisms may govern the long term stratigraphic evolution of forearc basins. Long term rise in eustatic sea level has been invoked as the mechanism responsible for the overall transgressive nature of the fill within the Ochoco Basin of Oregon (Kleinhans et al., 1984) and even the Early Cretaceous fill of the QCB (Haggart, 1991, 1993). Shorter term fluctuations may have controlled the distribution of seismic sequences within the West Luzon Basin of the Philippines (Lewis and Hayes, 1984).

Table 6.2. Circum-Pacific forearc basins
(based on Coulbourne and Moberly, 1977)

BASIN	WIDTH (km)	DEPTH (m)	REFERENCES
Mariana Trench	125	2600	Coulbourn and Moberly (1977)
Nankai Trough	20 - 50	750 - 2000	same
Japan Trench	25 - 50	1000 - 3000	same
Sunda - Banda	15 - 126	600 - 7500	Hamilton (1988)
West Luzon Trough	25 - 30	3570	Lewis and Hayes (1984)
Central Aleutian	40 - 60	4000 - 4600	Ryan and Scholl (1989)
Eastern Aleutian	10 - 15	0 - 3700	Coulbourn and Moberly (1977)
Oregon Margin	—	600	same
Northern California	13 - 35	750 - 1250	same
Middle America Trench	10 - 40	250 - 2000	same
Acequipa Basin, Peru	67	1700	Kulm et al. (1982); Moberly et al (1982)
Arica Basin, Peru - Chile	50	1500	same
Lima Basin, Peru	40	3000	same
Salaverry Basin, Peru	60	300	same
Iquique Basin, Chile	33	1700	same
Peru - Chile Trench (37°30' to 39° S)	15 - 80	subaerial - 800	Coulbourne and Moberly (1977)

Given the active plate margin setting of forearc basins, it is probable that tectonic mechanisms related to the subduction process control the long term stratigraphic evolution. Growth of the accretionary prism controls the subsidence history of the seaward part of the forearc basin. Underplating of the accretionary prism controls the rate at which the seaward margin of the basin is uplifted. For example, the formation of the Atka forearc basin in the central Aleutians is attributed to the influx of voluminous amounts of glacial sediments and the subduction of the aseismic Kula Ridge during the Late Miocene - Early Pliocene (Ryan and Scholl, 1989). Uplift of the seaward basin margin is countered by subsidence related to the load imposed by the prism on the underriding oceanic plate.

The magmatic history of the arc controls the subsidence history of the landward part of the forearc basin. Magmatism and the construction of volcanic edifices results in the general uplift of the landward basin margin. This uplift is countered by thermal subsidence of the arc massif.

Although data are sparse, calculated rates of subsidence from modern forearc basins are quite large. Using foraminiferal bathymetric data, Kulm et al. (1988) calculated rates of subsidence from 400-650 m/Ma within the Neogene Lima Basin of Peru. Subsidence rates of 400 m/Ma

were obtained from the central part of the Lima Basin (water depth 2600 m), while higher subsidence rates of 500 m/Ma were obtained at shallower depths (1000 m). A subsidence rate of 650 m/Ma was obtained from the outer structural high of the basin. These rates must however be treated with a degree of caution, as the samples were collected by a dredge and therefore may be resedimented. Drilling results from the Japan forearc off Honshu (von Huene et al., 1982) indicate at least 3 to 6 km of subsidence since Late Oligocene time, which translates to a rate of 120 to 240 m/Ma. Rates of uplift can be equally large. Moberly et al. (1982) noted that the forearc region of northwestern Peru and southern Chile has experienced up to 300 m of uplift during the Quaternary (150 m/Ma).

One of the best studied ancient forearc basin successions is the Late Mesozoic to Early Cenozoic Great Valley sequence of California. The Franciscan accretionary prism, central Great Valley sequence, and Sierra-Nevada massif form a Late Mesozoic to Early Cenozoic Andean-type arc-trench system related to eastward subduction of the Pacific plate (Ingersoll, 1978; Dickinson and Seely, 1979). The Great Valley forearc basin evolved from a residual to a composite forearc basin, and is infilled with up to 20 km of predominantly deep marine turbidites and lesser shallower marine deposits which onlap the arc massif to the east. An

abrupt westwards transition from continental rocks of the arc-trench massif to oceanic crust underlying the western portion of the basin is marked by a prominent gravity anomaly which parallels the axis of the basin (Moxom and Graham, 1987; Fig. 6.19). Two styles of subduction characterize the Late Mesozoic to Early Cenozoic evolution of the Californian margin: 1) a Late Mesozoic (100-80 Ma) phase characterized by steeply dipping subduction and voluminous arc volcanism, and 2) an Early Cenozoic (80-40 Ma) phase of shallow subduction and a lull in arc volcanism (Moxom and Graham, 1987). The transition from steep to shallow subduction coincided with onset of Laramide deformation (Dickinson and Seely, 1979).

Dickinson et al. (1987) and Moxom and Graham (1987) analyze the subsidence history of the Great Valley sequence by backstripping outcrop and subsurface sections. Moxom and Graham's (1987) plots reveal a distinct change in subsidence histories across the magnetic anomaly located at the basement boundary between oceanic crust and crust of the arc massif (Fig. 6.19). The plots of residual tectonic subsidence for sections located in the western portion of the basin exhibit rapid subsidence during Late Mesozoic time (100-80 Ma) followed by uplift coinciding with the onset of Laramide deformation (80 Ma). This is followed by an irregular period of uplift and subsidence from 80-50 Ma,

which in turn is followed by uniform subsidence. The subsidence history of sections located in the eastern portion of the basin exhibit an exponential decay which closely resembles the one-dimensional thermal subsidence curves generated by McKenzie (1978) for stretching values of 1.5-2. This suggests that subsidence of the Great Valley forearc basin was controlled by two distinct mechanisms: 1) decay of the thermal anomaly of the arc massif driving subsidence along the eastern margin of the basin, and 2) in the western portion of the basin, an initial period (100-80 Ma) of rapid subsidence related to tectonic erosion of the California margin followed by compression and uplift of the outer structural high (80-50 Ma), presumably related to a period of accretion and underplating which coincided with the onset of Laramide deformation.

It appears therefore that the regressive nature of the fill within the Great Valley Basin may be attributed to progressive underplating and uplift of the Franciscan Complex, which resulted in uplift of the basin.

The growth history of the accretionary prism is controlled by a variety of factors, which include rates of sedimentation in the trench, the subduction of aseismic ridges or other non-subductable features (ie. micro-continents), and subduction erosion. It is quite clear therefore that the stratigraphic evolution of a particular

forearc basin is dependant upon a number of factors unique to that arc-trench system. This no doubt explains the variety of fill patterns observed within other ancient forearc basins (Table 6.2).

6.9.4. Why no tuffs ?

The lack of tuffs and other direct evidence of volcanic activity within most of the Late Mesozoic to Late Cretaceous succession is puzzling given the evidence for continuous magmatic activity within the CPC to the east throughout this period. The petrology of the Cretaceous succession is however clearly indicative of a mature dissected arc provenance (Yagishita, 1985 a, b; Fogarassy and Barnes, 1991). Coarse ejecta as well as volcanic and pyroclastic flows may simply not have reached the preserved part of the basin, which was situated approximately 100 km to the west of the arc. The lack of tuffs may be attributed to the fact that the basin faced the open Pacific Ocean to the west. The prevailing westerly winds coming off of the Pacific may have transported most of the ejected material to the east.

CHAPTER 7. CONCLUSIONS

The following stratigraphic revisions are proposed for the Late Mesozoic succession exposed on the Queen Charlotte Islands (QCI):

1) A new stratigraphic unit, the White Point Formation (Table 1.1), is proposed for 300 m of polymictic conglomerate and mudstone strata of Late Oxfordian to Tithonian age exposed along the coast immediately south of White Point on northwest Graham Island (Fig. 2.1).

2) The Queen Charlotte Group is expanded to include Late Valanginian to Aptian strata of the Longarm Formation (Table 1.1).

The following conclusions can be made regarding the sedimentology of the Late Mesozoic succession exposed on the QCI:

3) The Late Jurassic White Point Formation consists of three gravelly fan delta successions deposited in a localized fault bounded basin (Figs. 3.13 and 6.1).

4) The overlying Late Valanginian to Early Turonian Longarm, Haida, and Skidegate Formations were deposited within an expanded northwest - southeast trending, southwest - deepening marine basin. At least eight sequences, each

deposited during a single cycle of sea level fluctuation, are recognized within the three formations (Figs. 4.57 and 6.1). Strata of the turbidite and disorganized facies assemblages (TFA and DFA respectively) were emplaced within submarine fan and slope environments during periods of relative sea level fall. Strata of the sandstone and mudstone facies assemblages (SFA and MFA respectively) within the sequences were deposited within high energy shoreface and muddy offshore environments during ensuing periods of relative sea level rise. The small scale progradational shoreface and mouth bar successions (Fig. 4.41) within the deposits of the SFA and MFA of the sequences are stacked retrogradationally into transgressive large scale fining-upward successions (Fig. 4.46). The sequences are bound by erosional surfaces representing a pronounced basinward shift in facies, and are related to relative sea level fall. The sequences progressively onlap the northeastern margin of the basin throughout Late Valanginian to Early Turonian time (Fig. 6.1).

5) Late Turonian to Coniacian strata of the Honna Formation were deposited within an elongate northwest - southeast trending southwest-deepening basin. Deposition of the Honna Formation coincided with an abrupt rise in relative sea level (Fig. 6.1). The conglomerates forming the bulk of the Honna were deposited within braided

submarine channels situated within a deep marine environment. Two distinct submarine systems are recognized (Fig. 5.48): a northwest - southeast trending linear system of gravelly channels 20 km wide which extended at least 200 km along strike from Sewell Inlet to Langara Island (Fig. 5.46), and radial east - west oriented gravelly submarine fans, one of which is exposed in the Skidegate Inlet region (Fig. 5.47). These transverse systems supplied sediment to the linear system extending to the northwest.

6) The unnamed Late Coniacian/Early Santonian volcanics overlying the Honna Formation were emplaced within a subaerial environment. Deposition of the overlying unnamed Santonian to Maastrichtian mudstones mark a return to deposition within shallow marine environments.

The main scientific problem addressed by this thesis concerned what the sedimentological and stratigraphic evolution of the Late Jurassic to Late Cretaceous succession exposed on the QCI can tell us about the Late Mesozoic tectonic evolution of the western Canadian Cordillera. It appears that the Late Mesozoic depositional history of the QCI region best fits the tectonic model proposed by van der Hayden (1992). This model places the succession within a forearc basin setting situated to the southwest of a northwest - southeast trending continental magmatic arc throughout Late Jurassic to Late Cretaceous time.

The sedimentological analysis also reveals that deposition in the QCI region during Late Mesozoic time was influenced by a variety of different tectonic controls acting on different scales. Block faulting appears to have influenced deposition on the local scale. The general fining-upward trend observed within the gravelly fan delta successions of the White Point Formation may be attributed to rapid, fault-related basin subsidence followed by progressive erosion of the uplifted basin margin. The unusual thickness of the progradational shoreface successions within the Longarm and Haida Formations may be attributed to rapid rates of fault-related basin subsidence and sediment supply. The northwest - southeast orientation of the Late Jurassic to Early Turonian paleocoastlines also reflects an underlying structural control.

Tectonic controls are also apparent on the large scale. The progressive northeastward onlap of marine strata throughout Late Jurassic to Early Turonian time was probably controlled by a thermal mechanism related to the eastward migration of active magmatism within the Coast Plutonic Complex. The abrupt rise in relative sea level and the onset of Honna deposition in Late Turonian time was probably related to crustal loading along the northeastern margin of the basin. This resulted in both rapid basin subsidence (relative sea level rise) and the progradation of gravelly

submarine fan(s) southwest into the basin away from the uplifted margin of the Coast Plutonic Complex. The strong influence of tectonic mechanisms on deposition at all scales reflects the active forearc setting of the QCI region throughout Late Mesozoic time.

REFERENCES

Aigner, T. 1982. Event-stratification in nummulite accumulations and in shell beds from the Eocene of Egypt. In G. Einsele and A. Seilacher (eds.), Cyclic and Event Stratification, New York, Springer, p. 248 - 262.

Allen, J. R. L. 1980. Sedimentary Structures: Their Character and Physical Basis, vols. I and II. Developments in Sedimentology 90, Elsevier, New York.

Anderson, R. G. and Reichenbach, I. 1991. U - Pb and K - Ar framework for Middle to Late Jurassic (172 - >158 Ma) and Tertiary (46 - 27 Ma) plutons in Queen Charlotte Islands, British Columbia. In G. J. Woodsworth, (ed.), Evolution and hydrocarbon potential of the Queen Charlotte Basin, British Columbia. Geological Survey of Canada Paper 90 - 10, p. 59 - 88.

Armstrong, R. L. 1988. Mesozoic and Cenozoic magmatic evolution of the Canadian Cordillera. Geological Society of America Special Paper 218, p. 55 - 91.

Ballesteros, M.W., Moore, G.F., Taylor, B., and Ruppert, S. 1988. Seismic stratigraphic framework of the Lima and Yaquina Basins, Peru. In Proceedings of the Ocean Drilling Program, Initial Reports 112: 77-90.

Berg, H. C., Jones, D. L. and Richter, D. H. 1972. Gravina - Nutzotin belt - tectonic significance of an upper Mesozoic sedimentary and volcanic sequence in southeastern Alaska. United States Geological Survey Professional Paper 800 D, p. 1-24.

Bhattacharya, J. P. and Walker, R. G. 1992. Deltas. In R. G. Walker and N. P. James (eds.), Facies Models; Response to Sea Level Change, Geological Association of Canada, p. 157 - 178.

Billings, E. 1873. On the Mesozoic fossils from British Columbia, collected by Mr. James Richardson in 1872. Geological Survey of Canada, Report of Progress for 1872 - 1873, p. 71 - 75.

Bluck, B. J. 1967. Sedimentation of beach gravels: examples from South Wales. Journal of Sedimentary Petrology 37: 128 - 156.

Bornhold, B. D. and Prior, D. B. 1990. Morphology and sedimentary processes on the subaqueous Noeick River delta, British Columbia. In A. Colella and D. B. Prior, (eds.), Coarse-grained deltas, International Association of Sedimentologists Special Publication 10, p. 169 - 183.

Bourgeois, J. 1980. A transgressive shelf sequence exhibiting hummocky cross-stratification: the Cape Sebastian Sandstone (Upper Cretaceous), southwestern Oregon. Journal of Sedimentary Petrology, 50: 681 - 702.

Brenchley, P. J. 1985. Storm influenced sandstone beds. Modern Geology, 9: 369 - 396.

Brenner, R. L. and Davis, D. K. 1973. Storm generated coquina sandstone: genesis of high energy marine sediments from the Upper Jurassic of Wyoming and Montana. Geological Society of America Bulletin, 84: 1685 - 1698.

Bouma, A. H. 1962. Sedimentology of some flysch deposits. Amsterdam, Elsevier, 186 p.

Busby - Spera, C. J. 1988. Development of fan-deltoid slope aprons in a convergent-margin tectonic setting: Mesozoic, Baja California, Mexico. In W. Nemec and R. J. Steel, (eds.), Fan deltas: sedimentology and tectonic settings, Blackie and Sons, p. 419 - 429.

----- and Boles, J. R. 1986. Sedimentation and subsidence styles in a Cretaceous forearc basin, southern Vizcaino Peninsula, Baja California, Mexico. In P.L. Abbott (ed.), Cretaceous Stratigraphy, Western North America, Special Publication Pacific Section, Society of Economic Mineralogists and Paleontologists, p. 79 - 90.

Caroll, A. R. 1987. Subsidence history of Cook Inlet Basin, southern Alaska: basement control on forearc basin devlopment. American Association of Petroleum Geologists Bulletin, 71: 536.

Chan, M. A. and Dott, R. H. Jr. 1986. Depositional facies and progradational sequences in Eocene wave-dominated deltaic complexes, southwestern Oregon. American Association of Petroleum Geologists Bulletin, 70: 415 - 429.

Clapp, C. H. 1914. A geological reconnaissance on Graham

Island, Queen Charlotte Group, British Columbia. Geological Survey of Canada, Summary Report for 1912, p. 12 - 40.

Clifton, H. E. 1981. Progradational sequences in Miocene shoreline deposits, southeastern Caliente Range, California. Journal of Sedimentary Petrology, 51: 165 - 184.

-----, Hunter, R. E. and Phillips, R. L. 1971. Depositional structures and processes in the non-barred high energy nearshore. Journal Sedimentary Petrology, 41: 651 - 670.

Colbourne, W.T. and Moberly, R. 1977. Structural evidence of the evolution of fore-arc basins off South America. Canadian Journal of Earth Sciences 14: 102-116.

Coniglio, M. and Dix. G. R. 1992. Carbonate slopes. In R. G. Walker and N. P. James (eds.), Facies models; response to sea level change, Geological Association of Canaa, p. 349 - 374.

Crawford, M. L., Hollister, L. S., and Woodsworth, G. J. 1987. Crustal deformation and regional metamorphism

across a terrane boundary, Coast Plutonic Complex, British Columbia. Tectonics 6: 343 - 361.

Crowell, J. C. 1957. Origin of pebbly mudstones. Bulletin, Geological Society of America, 68: 993 - 1010.

Curray, J. R. 1956. The analysis of two-dimensional orientation data. Journal of Geology, 64: 117 - 131.

Daly, R. A. 1926. Our Mobile Earth. Charles Scribner's Sons, New York and London.

Davidson-Arnott, R. G. D. and Greenwood, B. 1976. Facies relationships on a barred coast, Kouchibouguac Bay, New Brunswick, Canada. In R. A. Davis and R. L. Ethington, (eds.), Beach and nearshore sedimentation, Society of Economic Mineralogists and Paleontologists Special Publication 24, p. 149 - 168.

Dawson, G. M. 1880. Report on the Queen Charlotte Islands, 1878. Geological Survey of Canada, Report of Progress for 1878 - 1879, p. 1B - 239 B.

----- 1889. On the earlier Cretaceous rocks of the northwest portion of the Dominion of Canada. American Journal of

Science, 3rd Series, 38: 120 - 127.

Dawson J. W. 1873. Note on the fossil plants from British Columbia, collected by Mr. James Richardson in 1872. Geological Survey of Canada, Report of Progress for 1872 - 1873, p. 66 - 71.

Deeter, T. M., Wingate, F.H., and Mancini, E. A. 1983. Upper Cretaceous sedimentation on the Alaska Peninsula. Journal of the Alaska Geological Society, 3: 19 - 23.

Dercourt, J. 1970. L'expansion oceanique actualle et fossite; ses implications geotectoniques. Bulliten Society Geolog de France, 7: 261 - 317.

Dewey, J. F. 1980. Episodicity, sequence, and style at convergent plate boundaries. In D. W. Strangeway, (ed.), The continental crust and its mineral deposits, Geological Association of Canada, Special Paper 20, p. 553 - 573.

Dickinson, W. R. 1973. Widths of modern arc-trench gaps proportional to past duration of igneous activity in associated magmatic arcs. Journal of Geophysical Research, 78: 3376 - 3389.

----- 1976. Sedimentary basins developed during evolution of Mesozoic - Cenozoic arc trench system in western North America. Canadian Journal of Earth Sciences, 13: 1268 - 1287.

-----, and Seely, D.R., 1979. Structure and stratigraphy of forearc regions. American Association of Petroleum Geologists, 63: 2-31.

-----, Armin, R.A., Beckvar, N., Goodlin, T.C., Janecke, S.U., Mark, R.A., Norris, R.D., Radel, G., and Wortman, A.A. 1987. Geohistory analysis of rates of sediment accumulation and subsidence for selected California basins. In R. V. Ingersoll and W. G. Ernst (eds.), Cenozoic basin development of coastal California, Englewood Cliffs, N.J., p. 1-23.

Dietz, R. S. 1963. Wave base, marine profile of equilibrium and wave-built terraces - a critical appraisal. Geological Society of America Bulletin, 74: 971 - 990.

Dott, (Jr) R. H., and Bourgeois, J. 1982. Hummocky stratification: significance of its variable bedding sequences. Geological Society of America Bulletin, 93: 663 - 680.

Dickinson, W. R. and Suzek, C. A. 1979. Plate tectonics and sandstones composition. American Association of Petroleum Geologists Bulletin, 63: 2164 - 2182.

----- Armin, R.A., Beckvar, N., Goodlin, T.C., Janecke, S.U., Mark, R.A., Norris, R.D., Radel, G., and Wortman, A.A. 1987. Geohistory analysis of rates of sediment accumulation and subsidence for selected California basins. In R. V. Ingersoll and W. G. Ernst (eds.), Cenozoic basin development of coastal California, Englewood Cliffs, N.J., p. 1-23.

Duke, W. L. 1985. Hummocky cross-stratification, tropical hurricanes and intense winter storms. Sedimentology, 32: 167 - 194.

----- 1990. Geostrophic circulation or shallow marine turbidity currents ? The dilemma of paleoflow patterns in storm-influenced prograding shoreline systems. Journal of Sedimentary Petrology, 60: 870 - 883.

Dupre, W. R., Clifton, H. E., and Hunter, R. E. 1980. Modern sedimentary facies of the open Pacific coast and Pleistocene analog from Monterey Bay, California. In M. E. Field et al. (eds.), Quaternary Depositional

Environments of the Pacific Coast. Society of Economic Paleontologists and Mineralogists, Pacific Section, Pacific Coast Paleogeography v. 4, p. 105 - 120.

Engebretson, D. C., Cox, A., and Gordon, R. G. 1985. Relative motions between oceanic and continental plates in the Pacific Basin. Geological Society of America Special Paper 206, 54 p.

Enos, P. 1977. Flow regime in debris flows. Sedimentology, 24: 133 - 142.

Etheridge, F. G. and Wescott, W. A. 1984. Tectonic setting, recognition and hydrocarbon reservoir potential of fan delta deposits. In E. M. Koster and R. J. Steel (eds.), Sedimentology of gravel and conglomerates, Canadian Society of Petroleum Geologists Memoir 10, p. 217 - 236.

Fischer, A. G. 1961. Stratigraphic record of transgressing seas in the light of sedimentation on the Atlantic Coast of New Jersey. American Association of Petroleum Geologists Bulletin, 45: 1656 - 1666.

Fogarassy, J. A. S. 1989. Stratigraphy, diagenesis and

petroleum reservoir potential of the Cretaceous Haida, Skidegate and Honna Formations, Queen Charlotte Islands, British Columbia. Unpublished M. Sc. thesis, University of British Columbia, 177 p.

----- and Barnes, W. C. 1990. Stratigraphy and diagenesis of the middle to Upper Cretaceous Queen Charlotte Group, Queen Charlotte Islands, British Columbia. In G. J. Woodsworth (ed.), Evolution and hydrocarbon potential of the Queen Charlotte Basin, British Columbia, Geological Survey of Canada, Paper 90 - 10, p. 279 - 294.

Ford, A. B. and Brew, D. A. 1988. The Douglas Island volcanics: basaltic rift, not andesitic arc volcanism of the Gravina-Nutzotin belt, northern southeastern Alaska. Geological Society of America, Program with Abstracts 20, p. A111.

Gamba, C. A. 1991. An update on the Cretaceous sedimentology of the Queen Charlotte Islands, British Columbia. Geological Survey of Canada, Paper 91-1A, p. 373 - 382.

----- 1992. Lithofacies of the late Early to early Late

Cretaceous Queen Charlotte Group, Queen Charlotte Islands, British Columbia. Geological Survey of Canada, Paper 92-1A, p. 367-375.

----- 1993. Stratigraphy and sedimentology of the Late Jurassic to Early Cretaceous Longarm Formation, Queen Charlotte Islands, British Columbia. Geological Survey of Canada, Paper 93-1A, p. 139 - 148.

-----, Indrelid, J., and Taite, S. 1990. Sedimentology of the Upper Cretaceous Queen Charlotte Group, with special reference to the Honna Formation, Queen Charlotte Islands, British Columbia. Geological Survey of Canada, Paper 90 - 1F, p. 67 - 74.

Gehrels, G. E. and Saleeby, J. B. 1987. Geological framework, tectonic evolution, and displacement history of the Alexander terrane. Tectonics, 6: 151 - 173.

Haggart, J. W. 1986. Stratigraphic investigations of the Cretaceous Queen Charlotte Group, Queen Charlotte Islands, British Columbia. Geological Survey of Canada, Paper 86-20, p. 24.

----- 1987. On the age of the Queen Charlotte Group of

British Columbia. Canadian Journal of Earth Science, 24: 2470 - 2476.

----- 1989. Reconnaissance lithostratigraphy and biochronology of the Lower Cretaceous Longarm Formation, Queen Charlotte Islands, British Columbia, British Columbia. Geological Survey of Canada, Paper 89-1H, p. 39-46.

----- 1991. A synthesis of Cretaceous stratigraphy, Queen Charlotte Islands, British Columbia. In G. J. Woodsworth (ed.), Evolution and hydrocarbon potential of the Queen Charlotte Basin, British Columbia. Geological Survey of Canada, Paper 90-10, p. 253 - 277.

----- 1992. Progress in Jurassic and Cretaceous stratigraphy, Queen Charlotte Islands, British Columbia. Geological Survey of Canada, Paper 92-1A, p. 361-366.

----- and Carter, E. S. 1993. Cretaceous (Barremian - Aptian) Radiolara from the Queen Charlotte island, British Columbia: newly recognized faunas and stratigraphic implications. In Current Research, Part E, Geological Survey of Canada, Paper 93 - 1E, p. 55 -

65.

----- and Higgs, R. 1989. A new Late Cretaceous mollusc fauna from the Queen Charlotte Islands, British Columbia. Geological Survey of Canada, Paper 89 - 1H, p. 59 - 64.

-----, Lewis, P.D., and Hickson, C.J. 1989. Stratigraphy and structure of Cretaceous strata, Long Inlet, Queen Charlotte Islands, British Columbia. Geological Survey of Canada, Paper 89-1H, p. 65-72.

----- and Gamba, C.A. 1990. Stratigraphy and sedimentology of the Longarm Formation, southern Queen Charlotte Islands, British Columbia. Geological Survey of Canada, Paper 90-1F, p. 61-66.

-----, Taite, S., Indrelid, J., Hesthammer, J., and Lewis, P. D. 1991. A revision of stratigraphic nomenclature for the Cretaceous sedimentary rocks of the Queen Charlotte Islands, British Columbia. Geological Survey of Canada, Paper 91 - 1A, p. 367 - 372.

Hallam, A. 1984. Pre-Quaternary sea-level changes. Annual Reviews of Earth and Planetary Science, 12: 205 - 243.

Hamilton, W. B. 1988. Plate tectonics and island arcs. Geological Society of America Bulletin, 100: 1503 - 1527.

Hancock, J. M. and Kaufmann, E. G. 1979. The great transgressions of the Late Cretaceous. Journal of the Geological Society of London 136: 175 - 186.

Haq, B. U., Hardenbol, J., and Vail, P. R. 1988. Mesozoic and Cenozoic chronostratigraphy and cycles of sea level change. In C. K. Wilgus et als., eds. Sea-level change: an integrated approach. Society of Economic Paleontologists and Mineralogists, Special Publication 42, p. 71-108.

Hein, F. J. 1984. Deep-sea and braided fluvial channel conglomerates: a comparison of two case studies. In E. M. Koster and R. J. Steel, eds. Sedimentology of gravel and conglomerates. Canadian Society of Petroleum Geologists Memoir 10, p. 33 - 50.

----- and Walker, R. G. 1982. The Cambro-Ordovician Cap Enrage Formation, Quebec, Canada: conglomeratic deposits of a braided submarine channel with terraces. Sedimentology, 29: 309 - 329.

Hellwig, J. 1974. Eugeosynclinal basement and a collage concept for orogenic belts. In: Modern and ancient geosynclinal sedimentation. Society of Economic Mineralogists and Paleontologists, Special Publication 19, p. 359 - 376.

Hickson, C.J. and Lewis, P.D. 1990. Geology, Frederick Island (west half), British Columbia. Geological Survey of Canada, Map 8-1990, scale 1:50 000.

Higgs, R. 1989. Some aspects of the petroleum geology of the Queen Charlotte Islands. Field trip guidebook to sequences, stratigraphy, and sedimentology: surface and subsurface technical meeting, Canadian Society of Petroleum Geologists, 72 p.

----- 1990. Sedimentology and tectonic implications of Cretaceous fan delta conglomerates, Queen Charlotte Islands, Canada. Sedimentology, 37: 83-104.

Hill, M. L. and Dibble, T. W. Jr. 1953. San Andreas, Garlock and Big Pine faults, California. Geological Society of America Bulletin, 64: 443 - 458.

Howard, J. D. and Reineck, H-E. 1981. Depositional facies of

high-energy beach-to offshore sequence: comparison with low-energy sequence. American Association of Petroleum Geologists Bulletin, 65: 807 - 830.

Hunter, R. E., Clifton, H. E., and Phillips, R. L. 1979. Depositional processes, sedimentary structures, and predicted vertical sequences in barred nearshore systems, southern Oregon coast. Journal of Sedimentary Petrology, 49: 711 - 726.

Hyndman, R. D. and Hamilton, T. S. 1991. Cenozoic relative plate motions along the northeastern Pacific margin and their association with Queen Charlotte area tectonics and volcanism. In G.J. Woodsworth (ed.), Evolution and Hydrocarbon Potential of the Queen Charlotte Basin, British Columbia, Geological Survey of Canada, Paper 90-10, p. 107 - 126.

Indrelid, J. 1991. Stratigraphy, structural geology and petroleum potential of Cretaceous and Tertiary rocks in the central Graham Island area, Queen Charlotte Islands, British Columbia. Unpublished M. Sc. thesis, University of British Columbia, 192 p.

Ingersoll, R.V. 1979. Evolution of a Late Cretaceous forearc

basin, northern and central California. Geological Society of America Bulletin, 90: 813 - 826.

Jeletzky, J. A. 1976. Mesozoic and ?Tertiary rocks of Quatsino Sound, Vancouver Island, British Columbia. Geological Survey of Canada Bulletin 242, 243 p.

---- 1984. Jurassic-Cretaceous boundary beds of western and arctic Canada and the problem of the Tithonian - Berriasian stages in the Boreal Realm. In G. E. G. Westermann (ed.), Jurassic - Cretaceous Biochronology and Paleogeography of North America, Geological Association of Canada Special Paper 27, p. 175 - 255.

Kidwell, S. M. 1991. Condensed deposits in siliciclastic sequences: expected and observed features. In G. Einsele and A. Seilacher (eds.), Cycles and Events in Stratigraphy, New York, Springer, p. 682 - 695.

King, L. 1958. The origin and significance of the sub-oceanic ridges. In Continental Drift - a symposium. University of Tasmania, Hobart, p. 62 - 102.

Kleinhans, L. C., Balcells-Baldwin, E. A., and Jones, R. E. 1984. A paleogeographic reinterpretation of some

middle Cretaceous units, north-central Oregon: evidence for a submarine turbidite system. In T. H. Nilsen (ed.), Geology of the Upper Cretaceous Hornbrook Formation, Oregon and California. Pacific Section, Society of Economic Paleontologists and Mineralogists vol. 42, p. 239 - 257.

Kriesa, R. D. 1981. Storm-generated sedimentary structures in subtidal marine facies with examples from the Middle to Upper Ordovician of southwestern Virginia. Journal of Sedimentary Petrology, 51: 823 - 848.

----- and Bambach, R. K. 1982. The role of storm processes in generating shell beds in Paleozoic shelf environments. In G. Einsele and A. Seilacher (eds.), Cyclic and Event Stratification, New York, Springer, p. 200 - 207.

Kulm, L.D., Resig, J.M., Thornburg, T.M., and Schrader, H.J. 1982. Cenozoic structure, stratigraphy and tectonics of the central Peru forearc. In J. E. Leggett (ed.), Trench-Forearc Geology: Sedimentation and Tectonics of Ancient and Modern Active Plate Margins, Geological Society Special Publication No. 10, p. 151-170.

Thornburg, T.M., Suess, E., Resig, J., and Fryer, P. 1988. Clastic, diagenetic, and metamorphic lithologies of a subsiding continental block: Central Peru forearc. Proceedings of the Ocean Drilling Program, Initial Reports, v. 112, p. 91-108.

Komar, P. D. 1976. Beach processes and sedimentation. Englewood Cliffs, N. J., Prentice Hall, 429 p.

Kumar, N. and Sanders, J. E. 1976. Characteristics of shoreface storm deposits: modern and ancient examples. Journal of Sedimentary Petrology, 46:145 - 162.

Leckie, D. A., and Walker, R. G. 1982. Storm- and tide-dominated shorelines in Cretaceous Moosebar-Lower gates interval - outcrop equivalents of deep basin gas trap in western Canada. American Association of Petroleum Geologists Bulletin, 66: 138 - 157.

----- and Krystinik , L. F. 1990. Is there evidence for geostrophic currents preserved in the sedimentary record of inner to middle-shelf deposits. Journal of Sedimentary Petrology, 59: 862 - 870.

Leithold, E. L. and Bourgeois, J. 1984. Characteristics of

coarse-grained sequences in nearshore, wave-dominated environments - examples from the Miocene of south-west Oregon. Sedimentology, 31: 749 - 775.

Lewis, P. D., Haggart, J. W., Anderson, R. G., Hickson, C. J., Thompson, R. I., Dietrich, J. R., and Rohr, K.M.M. 1991. Triassic to Neogene geologic evolution of the Queen Charlotte region. Canadian Journal of Earth Sciences, 28: 854 - 869.

----- and Hickson, C. J. 1990a. Geology, Langara Island (west half), British Columbia. Geological Survey of Canada, Map 9-1990, scale 1:50 000.

----- and Hickson, C. J. 1990b. Geology, Frederick Island (west half), British Columbia. Geological Survey of Canada, Map 8-1990, scale 1:50 000.

Lewis, S.D., and Hayes, D.E. 1984. A geophysical study of the Manila Trench, Luzon, Philippines 2: Fore arc basin structural and stratigraphic evolution. Journal of Geophysical Research 89: [illegible]11, p. 9196-9214.

Lowe, D. R. 1976. Sediment gravity flows: their classification and some problems of application to

natural flows and deposits. Society of Economic Paleontologists and Mineralogists, Special Publication 27, p. 75 - 82.

----- 1979. Sediment gravity flows: their classification and some problems of application to natural flows and deposits. In L. J. Doyle and O. H.Pilkey (eds.), Geology of Continental Slopes, Special Publication Society of Economic Paleontologists and Mineralogists, vol 27, p. 75 - 82.

----- 1982. Sediment gravity flows 2: depositional models with special reference to the deposits of high density turbidity currents. Journal of Sedimentary Petrology, 52: 279 - 297.

McKenzie, D., 1978, Some remarks on the development of sedimentary basins: Earth and Planetary Science Letters 1: 25-32.

MacKenzie, J. D. 1916. Geology of Graham Island, British Columbia. Geological Survey of Canada, Memoir 88, 221 p.

Martinson, O. J. 1989. Styles of soft-sediment deformation

on a Namurian (Carboniferous) delta slope, western Irish Namurian basin, Ireland. In M. K. G. Whateley and K. T. Pickering (eds.), Deltas: sites and traps for fossil fuels. Geological Society Special Publication 41, Blackwell Scientific Publications, 167 - 177.

Massari, F. 1984. Resedimented conglomerates of a Miocene fan delta complex, southern Alps, Italy. In E. M. Koster and R. J. Steel (eds.), Sedimentology of gravel and conglomerates, Canadian Society of Petroleum Geologists Memoir 10, p. 259 - 278.

May, S. R. and Butler, R. F. 1986. North American Jurassic apparent polar wander: implications for plate motion, paleogeography and Cordilleran tectonics. Journal of Geophysical Research, 91: B11, p. 11519 - 11544.

McClelland, W. C., Gehrels, G. E., and Saleeby, J. B. 1992. Upper Jurassic - Lower Cretaceous basinal strata along the Cordilleran margin: implications for the accretionary history of the Alexander - Wrangellia - Peninsular terrane. Tectonics 11: 823 - 835.

McLearn, F. H. 1972. Ammonoids of the Lower Cretaceous Sandstone Member of the Haida Formation, Skidegate

Inlet, Queen Charlotte Islands, western British Columbia. Geological Survey of Canada, Bulletin 188, 78 p.

McPherson, J. G., Shanmugam, G., and Moiola, R. J. 1987. Fan deltas and braid deltas: varieties of coarse-grained deltas. Geological Society of America Bulletin, 99: 331 - 340.

-----, Shanmugam, G., and Moiola, R. J. 1988. Fan deltas and braid deltas: conceptual problems. In W. Nemec and R. J. Steel (eds.), Fan Deltas: Sedimentology and Tectonic Settings, Blackie and Sons, p. 14 - 22.

Megard, F. 1989. The evolution of the Pacific Ocean margin in South America north of Arica Elbow (18° S). In Z. Ben-Avraham (ed.), The Evolution of the Pacific Ocean Margins, Oxford University Press, New York, p. 208 - 230.

Miall, A. D. 1981. Alluvial sedimentary basins: tectonic setting and basin architecture. In A. D. Miall (ed.), Sedimentation and tectonics in alluvial basins, Geological Association of Canada, Special Paper 23, p. 1 - 34.

Middleton, G. V. and Hampton, M. A. 1973. Sediment gravity flows: mechanics of flow and deposition. In G. V. Middleton and A. H. Bouma (eds.), Turbidites and Deep-Water Sedimentation, Society of Economic Mineralogists and Paleontologists Short Course 1, p. 1 - 38.

----- 1976. Subaqueous sediment transport and deposition by sediment gravity flows. In D. J. Stanley and D. J. P. Swift (eds.), Marine sediment transport and environmental management, Wiley, New York, p. 197 - 218.

Moberly, R., Shepard, G.L., and Coulbourn, W.T. 1982. Forearc and other basins, continental margin of northern and southern Peru and adjacent Ecuador and Chile. In J. E. Leggett (ed.), Trench-Forearc Geology: Sedimentation and Tectonics of Ancient and Modern Active Plate Margins, Geological Society Special Publication No. 10, p. 171-190.

Monger, J. W. H. 1991. Georgia Basin Project: structural evolution of parts of southern Insular and southwestern Coast Belts, British Columbia. Current Research Part A, Geological Survey of Canada Paper 91-1A, p. 219 - 228.

Monger, J. W. H., Souther, J. G. and Gabrielese, H. 1972. Evolution of the Canadian Cordillera: a plate tectonic model. American Journal of Science, 272: 577 - 602.

------, Price, R. A., and Templeman-Kluit, D. J. 1982. Tectonic accretion and the origin of the two metamorphic and plutonic welts in the Canadian Cordillera. Geology, 10: 70 - 75.

Moore, G.F. and Watkins, J.S. 1979. Off Mexico: Middle American Trench. Geotimes, 24: 20-22.

Moxom, I.W., and Graham, S.A. 1987. History and controls of subsidence in the Late Cretaceous-Tertiary Great Valley forearc basin, California. Geology, 15: 626-629.

Mukasa, S. 1986. Zircon U-Pb ages of super-units in the Coastal batholith, Peru: implications for magmatic and tectonic processes. Geological Society of America Bulletin, 97: 241 - 254.

Mutti, E. 1985. Turbidite systems and their relations to depositional sequences. In G. G. Zuffa (ed.), Provenance of Arenites, NATO Advanced Scientific Institute, Dordrecht, Holland, D. Reidel, p. 65 - 93.

----- and Ricci Lucchi, F. 1972. Letorbiditi dell'appennino settentrionale: introduzuone all'analisi di facies. Mem. Soc. Geol. Italy, 11: 161 - 191 (1978 English translation by T. H. Nilsen, International Geological Reviews, 20: 125 - 166).

Myrow, P. M. and Hiscott, R. N. 1991. Shallow-water gravity-flow deposits, Chapel Island Formation, southeast Newfoundland, Canada. Sedimentology, 38: 935 - 959.

Nagle, J. S. 1967. Wave and current orientation of shells. Journal of Sedimentary Petrology, 37: 1124 - 1138.

Nardin, T. R., Hein, F. J., Gorsline, D. S., and Edwards, B. D. 1979. A review of mass movement processes, sediment acoustic characteristics, and contrasts in slope and base-of-slope systems versus canyon-fan-basin floor systems. In L. J. Doyle and O. H. Pilkey (eds.), Geology of continental slopes, Society of Economic Paleontologists and Mineralogists, Special Publication 27, p. 61 - 74.

Nemec, W. 1990. Deltas - remarks on terminology and classification. In A. Colella and D. B. Prior (eds.), Coarse-grained deltas, International Association of

Sedimentologists Special Publication 10, p. 3 - 12.

----- and Steel, R. J. 1984. Alluvial and coastal conglomerates: their significant features and some comments on gravelly mass-flow deposits. In E. M. Koster and R. J. Steel (eds.), Sedimentology of gravel and conglomerates. Canadian Society of Petroleum Geologists Memoir 10, p. 1 - 32.

Nilsen, T. H. 1986. Cretaceous paleogeography of western North America. In P. L. Abbott (ed.), Cretaceous stratigraphy of western North America. Pacific Section, Society of Economic Paleontologists and Mineralogists, 46: 1 - 40.

Pemberton, S. G., MacEachern, J. A., and Frey, R. W. 1992. Trace fossil facies models: environmental and allostratigraphic significance. In R. G. Walker and N. P. James (eds.), Facies models: response to sea level change, Geological Association of Canada, p. 47 - 72.

Pickering, K. T., Hiscott, R. N., and Hein, F. J. 1989. Deep Marine Environments: Clastic Sedimentation and Tectonics, Unwin Hyman, Boston, 416 p.

Piper, D. J. W., Shor, A. N., Farre, J. A., O'Connell, S., and Jacobi, R. 1985. Sediment slides and turbidity currents on the Laurentian Fan: sidescan sonar investigations near the epicentre of the 1929 Grand Banks earthquake. Geology 13: 538 - 541.

Pirrie, D. and Marshall, J. D. 1991. Field relationships and stable isotope geochemistry of concretions from James Ross Island, Antarctica. Sedimentary Geology, 71: 137 - 150.

Pitman, W. C. 1978. Relationship between eustasy and stratigraphic sequences of passive margins. Geological Society of America Bulletin, 89: 1389 - 1403.

Plint, A. G. 1988. Sharp-based shoreface sequences and "offshore bars" in the Cardium Formation of Alberta: their relationships to relative changes in sea level. In C. K. Wilgus et al. (eds.), Sea level changes, an integrated approach. Society of Economic Paleontologists and Mineralogists, Special Publication 42, p. 357 - 370.

----- 1991. High frequency relative sea level oscillations in Upper Cretaceous shelf clastics of the Alberta

foreland basin: possible evidence for glacial eustatic control ? In D. I. M. MacDonald (ed.), Sedimentation, tectonics, and eustasy. International Association of Sedimentologists, Special Publication 12, p. 409 - 428.

Prior, D. B. and Bornhold, B. D. 1990. The underwater development of Holocene fan deltas. In A. Colella and D. B. Prior (eds.), Coarse-grained deltas, International Association of Sedimentologists Special Publication 10, p. 75 - 90.

Pitcher, W. S., Atherton, M. P., Cobbins, E. J., and Beckinsale, R. B. 1985. Magmatism at a Plate Edge: the Peruvian Andes. Blackie, Glasgow/Halsted Press, New York.

Raiswell, R. 1971. The growth of Cambrian and Liassic concretions. Sedimentology, 17: 147 - 171.

Reineck, H. E. and Singh, I. B. 1980. Depositional sedimentary environments: with reference to terrigenous clastics, 2nd ed. Springer Verlag, New York. 551 p.

Rodine, J. D. and Johnson, A. D. 1976. The ability of debris, heavily freighted with coarse clastic

materials, to flow on gentle slopes. Sedimentology, 23: 213 - 234.

Rosenthal, L. R. P., and Walker, R. G. 1987. Lateral and vertical sequences in the Upper Cretaceous Chungo Member, Wapiabi Formation, southern Alberta. Canadian Journal of Earth Science, 24: 771 - 783.

Rubin, C. M., Saleeby, J. B., Cowan, D. S., Brandon, M. T. and McGroder, M. F. 1990. Regionally extensive mid-Cretaceous west - vergent thrust system in the northwestern Cordillera: implications for continent - margin tectonism. Geology, 18: 276 - 280.

Rust, B. R. 1972. Pebble orientation in fluvial sediments. Journal of Sedimentary Petrology 42: 384 - 388.

---- and Koster, E. M. 1984. Coarse alluvial deposits. In R. G. Walker (ed.) Facies Models, Geoscience Canada Reprint Series 1, p. 53 - 70.

Ryan, H. F. and Scholl, D. W. 1989. The evolution of forearc structures along an oblique convergent margin, central Aleutian arc. Tectonics, 8: 497 - 516.

Seely, D.R. 1978. The evolution of structural highs bordering major forearc basins. In Watkins, J.S. and Montadert, L. (eds.), Geology and Geophysical Investigations of Continental Margins, American Association of Petroleum Geologists Memoir 29, p. 245-260.

Shipboard Scientific Party, DSDP Leg 112, 1988. Introduction, objectives, and principal results, Leg 112, Peru continental margin In Proceedings of the Ocean Drilling Program, Initial Reports, 112: 5-24.

Short, A. D. 1984. Beach and nearshore facies: southeast Australia. Marine Geology, 60: 261 - 282.

Southard, J. B., Lambie, J. M., Federico, D. C., Pile, H. T., and Weidman, C. R. 1990. Experiments on bed configurations in fine sand under bidirectional purely oscillatory flow, and the origin of hummocky cross-stratification. Journal of Sedimentary Petrology, 60: 1 - 17.

Stow, D. A. V. 1996. Deep clastic seas. In H. G. Reading (ed.), Sedimentary Environments and Facies, second edition, Blackwell Scientific Publications, 399 - 444.

Surlyk, F. 1984. Fan delta to submarine fan conglomerates of the Volgian - Valanginian Wollaston Forland Group, east Greenland. In E. M. Koster and R. J. Steel (eds.), Sedimentology of gravel and conglomerates, Canadian Society of Petroleum Geologists Memoir 10, p. 359 - 382.

Sutherland Brown, A. 1968. Geology of the Queen Charlotte Islands, British Columbia. British Columbia Department of Mines and Petroleum Resources, Bulletin 54.

Sweeny, J. F. and Seemann, D. A. 1991. Crustal density structure of Queen Charlotte Island and Hecate Basin, British Columbia. In G.J. Woodsworth (ed.), Evolution and Hydrocarbon Potential of the Queen Charlotte Basin, British Columbia, Geological Survey of Canada, Paper 90-10, p. 89 - 96.

Swift, D. J. P. 1967. Coastal erosion and transgressive stratigraphy. Journal of Geology, 76: 444 - 456.

Taite, S. 1991. Geology of the Sewell Inlet - Tasu Sound area, Queen Charlotte Islands, British Columbia. Geological Survey of Canada, Paper 91-1A, p. 393 - 400.

Thompson, R. I. and Thorkelson, D. 1989. Regional mapping update, central Queen Charlotte Islands, British Columbia. Geological Survey of Canada, Paper 89 - 1H, p. 7 - 12.

--------, Haggart, J.W., and Lewis, P.D. 1991. Late Triassic through early Tertiary evolution of the Queen Charlotte Basin, British Columbia, with a perspective on hydrocarbon potential. In G.J. Woodsworth (ed.), Evolution and Hydrocarbon Potential of the Queen Charlotte Basin, British Columbia. Geological Survey of Canada, Paper 90-10, p.3-30.

Vail, P.R., Mitchum, R.M., Todd, R.G., Widmier, J.M., Thompson, S. III, Sangree, J.B., Bubb, .N., and Hattlelid, W.G., 1977. Seismic stratigraphy and global changes of sea level. American Association of Petroleum Geologists Memoir 26, p. 49-50.

van der Hayden, P. 1989. U - Pb and K - Ar geochronometry of the Coast Plutonic Complex, 53°N to 54°N, British Columbia. Unpublished Ph. D. thesis, University of British Columbia, British Columbia, Canada.

----- 1992. A Middle Jurassic to Early Tertiary Andean-

Sierran arc model for the Coast Belt of British Columbia. Tectonics, 11: 82 - 97.

van Wagoner, J. C., Mitchum, R. M., Campion, K. M., and Rahmanian, V. D. 1990. Siliclastic sequence stratigraphy in well logs, cores,and outcrops. American Association of Petroleum Geologists Methods in Exploration Series No. 7, 55 p.

von Huene, R., Langseth, M., Nasu, N., and Okada, M., 1982. A summary of the Cenozoic tectonic history along the IPOD Japan Trench transect. Geological Society of America Bulletin, 93: 829 - 846.

Walker, R. G. 1975a. Generalized facies models for resedimented conglomerates of turbidite association. Geological Society of America Bulletin, 86: 737 - 748.

------ 1975b. Upper Cretaceous resedimented conglomerates at wheeler Gorge, California: description and field guide. Journal of Sedimentary Petrology, 45: 105 - 112.

------ 1977. Deposition of Upper Mesozoic resedimented conglomerates and associated turbidites in southwestern Oregon. Geological Society of America Bulletin 88: 273

- 285.

------ 1985. Geological evidence for storm transportation and deposition on ancient shelves. In R. W. Tillman, D. J. P. Swift and R. G. Walker (eds.), Shelf sands and sandstone reservoirs, Society of Economic Paleontologists and Mineralogists, Short Course Notes 13, p. 243 - 302.

------ 1992. Turbidites and submarine fans. In R. G. Walker and N.P. James (eds.), Facies models: response to sea level change, Geological Association of Canada, p. 239 - 263.

------ Duke, W. E., and Leckie, D. A. 1983. Hummocky stratification: significance of its variable bedding sequences: discussion. Geological Society of America Bulletin, 94: 1245 - 1251.

------ and Plint, A. G. 1992. Wave- and storm-dominated shallow marine systems. In R. G. Walker and N. P. James (eds.), Facies models: response to sea level change, Geological Association of Canada, p. 219 - 238.

Watts, A.B., and Cochran, J.R. 1974. Gravity anomalies and

flexure of the lithosphere along the Hawaiian-Emperor seamount chain. Geophysical Journal of the Royal Astronomical Society, 38: 119-141.

Wescott, W. A. and Etheridge, F. G. 1980. Fan delta sedimentology and tectonic setting - Yallahs Fan Delta, southeast Jamaica. Bulletin American Association of Petroleum Geologists 64: 374 - 399.

------- 1983. Eocene fan delta - submarine fan deposition in the Wagwater Trough, east - central Jamaica. Sedimentology, 30: 235 - 247.

Wetzel, A. and Aigner, T. 1986. Stratigraphic completeness: tiered trace fossils provide a measuring stick. Geology, 14: 234 - 237.

Whiteaves, J. F. 1876. On some invertebrates from the coal bearing rocks of the Queen Charlotte Islands, collected by Mr. James Richardson in 1872. Geological Survey of Canada, Mesozoic Fossils, vol. 1, Part 1, 92 p.

Winn, R. D. and Dott, R. H. Jr. 1977. Large-scale traction produced structure in deep - water fan-channel conglomerates in southern Chile. Geology, 5: 41 - 44.

Woodsworth, G. J. 1988. Karmutsen Formation and the east boundary of Wrangellia, Queen Charlotte Basin, British Columbia. Current Research, Part E, Geological Survey of Canada, Paper 88-1E, p. 209 - 212.

Woodsworth, G. J. and Tercier, P. E. 1991. Evolution of the stratigraphic nomenclature of the Queen Charlotte Islands, British Columbia. In Woodsworth, G. J. (ed.), Evolution and hydrocarbon potential of the Queen Charlotte Basin, British Columbia. Geological Survey of Canada, Paper 90 - 10, p. 151 - 162.

Yagishita, K. 1985a. Mid- to Late-Cretaceous sedimentation in the Queen Charlotte Islands, British Columbia; lithofacies, paleocurrents and petrographic analysis of sediments. Unpublished Ph. D. Thesis, University of Toronto, Ontario.

-------- 1985b. Evolution of a provenance as revealed by petrographic analyses of Cretaceous formations in the Queen Charlotte Islands, British Columbia. Sedimentology, 32: 671 - 684.

Yorath, C. J. and Chase, R. L. 1981. Tectonic history of the Queen Charlotte Islands and adjacent areas - a model.

Canadian Journal of Earth Science, 18: 1717 - 1739.